Brunel UNIVERSITY LONDON

Sustainability of Water Abstraction by Hand Drilling in the Floodplain of River Benue of Yola, NE Nigeria

A thesis submitted to Brunel University London in fulfillment of the requirements for the degree of

Doctor of Philosophy

BY

Buba Apagu Ankidawa

B.Eng. Agric. and Environmental Engineering, University of Maiduguri, Nigeria

M.Sc. Water Resources and Environmental Engineering, Bayero University Kano, Nigeria

Supervised by:

Prof. Suzanne Leroy

Dr Philip Collins

March 2014

DECLARATION

The work described in this thesis is entirely my own work and was done independently, and has not been submitted for any other degree.

DEDICATION

To my mother **Ubumtu Thagai** and my lovely daughter **Surraiyatu Abubakar**

ABSTRACT

The aim of the research is to assess the sustainability of groundwater supply and the suitability of hand-drilling techniques for accessing groundwater for irrigation practices along the shallow alluvial floodplains of River Benue, NE Nigeria. Hand-drilling techniques are affordable means for the farmers to abstract water from these shallow aquifers. Determining the most sustainable hand-drilling techniques (taking into account the hydrology and sedimentology of the floodplain) will improve farming activities and food security in this region and the country at large. Hydrological data (obtained from fieldwork and modelling) demonstrate that the River Benue is the main source for recharge of the shallow alluvial aquifers of the floodplain during the dry season period. Water table heights were estimated by resistivity survey using ABEM Terrameter equipment and measured by automatic piezometer instruments. Floodplain sedimentology and hydrogeology were assessed at seventeen natural riverbank outcrops and twelve hand-drilled boreholes. At each location, sediment samples were collected from every exposed sedimentological unit. Locations and elevations were measured using a ProMark3 dual frequency GPS instrument, to create a detailed topographic map with updated contours. Twenty-four electrical resistivity sounding profiles and twelve-groundwater measurement were also obtained to explore the groundwater level of the floodplain. The resistivity results confirm the availability of water in the alluvial aquifers of the floodplain. In order to determine the most appropriate hand drilling techniques, a Field Shear Vane Tester was used to measure sediment shear strength at twelve different borehole locations. Shear strength forces were higher on clayey silt and sandy silt, and lower on sand formations. It appeared that in some areas of the floodplain, the farmers are already above the shear strengths that can be provided by human power. Hence, any increase of the hardness of

the surface of the sediment would make low-cost hand drilling impractical. Particle size analysis for the sediment samples showed that the samples were largely sandy in nature, which enables easy movement of water through the layers for aquifer recharge. Magnetic susceptibility (used to classify the source of sediment and the process of their formation) revealed that the main source of the sedimentary materials was upstream of the study site and varies little over time. The groundwater level of the study area decreased away from River Benue valley during the dry season period. One perched aquifer formations and possibly two others were observed in three different locations, which reflects a low-permeability stratigraphic unit (such as lens of clayey silt) within alluvial sands. These should be avoided by farmers, as they are likely to provide water only in the short-term. Finally, groundwater modelling was undertaken (with various scenarios) for the River Benue floodplain using acquired sedimentology and hydrology data integrated into MODFLOW software. The results revealed that low-cost hand-drilling techniques such as augering and jetting remain possible for abstracting the shallow alluvial aquifers on the floodplain for irrigation farming in the study area, unless the most likely low river water stages in River Benue, over-exploitation of the shallow alluvial floodplain groundwater and drought scenarios occur.

ACKNOWLEDGEMENTS

First of all, I thank Almighty Allah for given me the ability and strength to do this research work.

I want to express my deepest gratitude to my first supervisor Professor Suzanne Leroy for all her effort, support, help, guidance and enthusiasm throughout this PhD. I am also grateful to my second supervisor Dr Philip Collins for all his effort, help, guidance and enthusiasm throughout this PhD. Their supervision has greatly influenced and shaped my understanding of research. I highly appreciate their efforts for the successful completion of this PhD research.

I would like to express my great appreciation to my sponsor Petroleum Technology Development Fund (PTDF), Nigeria, for given me this great opportunity to study in London, United Kingdom, and their financial support to attend conference and to do the first fieldwork.

I am grateful to Dr Chris Bradley at University of Birmingham, United Kingdom, for his kind help and assistance in training me on how to use the MODFLOW software and for the modelling process. I really much appreciate his kind assistance.

I am grateful for financial support obtained from Professor Allan MacDonald, Principal Hydrogeologist at British Geological Survey Edinburgh, United Kingdom and the Institute for the Environment, Brunel University London, United Kingdom, that enabled me to do the second fieldwork campaign. The financial assistance from Quaternary Research Association, United Kingdom, is gratefully acknowledged. The financial assistance from Peter Hall, Hon Treasurer Water Conservation Trust, Reading, United Kingdom, is gratefully acknolwdged.

I wish to express my appreciation to Professor Ken Gregory a Council Member of Brunel University London, United Kingdom, for his useful and pertinent suggestions that help in guiding me to focus for achieving the goal of this research work.

I wish to thank Professor Richard Carter the Chair of the Rural Water Supply Network, at Water AID, United Kingdom for his guidance. Thanks to Mr Dotun Adekile a senior water resources consultant in Nigeria, for lending me a piezometer for my fieldwork. Thanks to

staff at Hydrological unit of Upper Benue River Basin Development Authority, Yola, for supplying me with the meteorological and hydrological data. I also wish to thank Peter Reading, Technical Director EQUIPEGROUP, UK.

I am grateful to all other staff at the Institute for the Environment, Brunel University London for their support and encouragement. I am grateful to Professor Susan Jobling, Head of the Institute for the Environment, Brunel University London, United Kingdom, for her support to me. I wish to thank Dr Edwin Routledge, Deputy Head of Research, Institute for the Environment at Brunel University London, United Kingdom, for his great encouragement, advice and support. I wish to thank Dr Mark Scrimshaw, Institute for the Environment at Brunel University London, United Kingdom, for his support.

I would like to thank Mal. Auwal Bappa at RWSN, Yola, Mr Ibrahim Inuwa at Girei, Faisal Gidado at Girei, Sale Baba, Wahab Hassan and Tanimu Garba Laboratory technologies from the Department of Agricultural and Environmental Engineering, MAUTECH, Yola, Nigeria for their assistance during the fieldwork survey. I thank Mr Papa and Mal. Garba Technologies from Department of Civil Engineering, Federal Polytechnic Mubi Adamawa State, Nigeria, for their assistance during my laboratory hydraulic conductivity analysis. I thank Paul Szadorski a technician from Brunel University, United Kingdom, workshops for his assistance on the CILAS instrument.

I wish to thank Dr Bashir Aliyu, the Deputy Vice Chancellor of Moddibo Adama University of Technology (MAUTECH), Yola, Nigeria, for his support and assistance whenever I approached him.

I wish to express my great appreciation to my senior brother Mr Peter Apagu Ankidawa and Mohammed Abana Girei for their effort and care they showed to my family during my study period.

Finally, a great thank to my family, especially my lovely wife and children, Suraiyatu, Abdul-razak, Ja'afar, Muhammed and Amina, who have supported me and who waited so patiently and eagerly for this research to be completed. A special thanks to my lovely daughter Suraiyatu. My sincere appreciation to my mother for her support, care and love towards my progress.

TABLE OF CONTENT

CHAPTER THREE – MATERIAL AND METHODS

CHAPTER FOUR - CLIMATE VARIABILITY AND RIVER BENUE DISCHARGE IN THE UPPER BENUE BASIN

CHAPTER FIVE - RESULTS AND INTERPRETATION

CHAPTER SIX - DISCUSSION

LIST OF FIGURES

LIST OF TABLES

LIST OF ABBREVIATIONS

AET:	Actual Evapotranspiration
BCF:	Block-Centered Flow
BH:	Borehole
BS:	British Standard
CILAS:	Particle Size Analyser
ET:	Evapotranspiration
FAO:	Food Agricultural Organisation
FSVT:	Field Shear Vane Tester
GHB:	General-Head Boundary
GPS:	Global Positioning System
HRP:	Horizontal Resistance Profiling
I:	Current
IPCC:	Intergovernmental Panel on Climate Change
ITCZ:	Inter-Tropical Convergence Zone
LGA:	Local Government Area
LOI:	Loss on Ignition
MAE:	Mean Absolute Error
MAlog:	Itmsoil Automatic Piezometer
MC:	Moisture Content
MODFLOW:	Software designed to manage groundwater resources
MS2:	Bartington instrument magnetometer
NCDC	National Climatic Data Center
OC:	Output Control

OPUS: Online Positioning User Service

P: Precipitation

PCA: Principal Component Analysis

PCG: Preconditioned Conjugate-Gradient

PDSI: Palmer Drought Severity Index

PSD: Particle Size Distribution

Q: Discharge

ρ_a: Apparent Resistivity

RMS: Root Mean Square

RWSN: Rural Water Supply Network

S: Storativity

SAS: Signal Averaging System

SEM: Scanning Electron Microscopy

SPI: Standardized Precipitation Index

SST: Sea-Surface Temperature

S_y: Specific Yield

T: Transmissivity

UBRBDA: Upper Benue River Basin Development Authority

UNICEF: United Nations International Children's Education Fund

V: Voltage

VES: Vertical Electrical Soundings

WFAI: Water For All International

CHAPTER ONE – INTRODUCTION

1.1 Introduction

This thesis draws together a novel interdisciplinary dataset to identify new ways of assessing, accessing and sustainably managing a shallow, alluvial floodplain aquifer where the principal extraction method is low-cost hand drilling. The focus here is on the floodplain of the River Benue in Sub-Sahelian eastern Nigeria.

Globally, in arid and semi-arid regions, shallow groundwaters on alluvial floodplains are the major source of water supply for irrigation, particularly during the dry season period. In, northeast Nigeria, the shallow alluvial groundwaters are being exploited by farmers for irrigation activities.

Methods for abstracting shallow groundwaters from floodplains for irrigation activities are of great importance to farmers. Low-cost hand-drilling methods are used for extracting groundwater along the floodplains of the Sahel because they are more affordable than machine drilling methods. The cost of a hand-drilled well can be less than half the cost of a machine drilled well to similar depth (RWSN, 2013).

Approximately 80% of Adamawa State's populations (NE Nigeria) are farmers (Sabo and Adeniji, 2007). Therefore, improving small hold farmers' agricultural productivity and access to groundwater by hand drilling can increase local incomes, improve food security, and provide much needed water for livestock and domestic needs.

Assessing and understanding the suitability of low-cost hand drilling for abstracting groundwater on the alluvial floodplains requires an understanding of floodplain sedimentology and floodplain water levels; both present and future. However, there is little knowledge of groundwater sustainability of the Sahel and sub-Sahelian floodplains in

Nigeria, and therefore the future application of low-cost hand drilling methods (with their economic benefits and operational shortcomings) is uncertain, leading to the present investigation.

In the global context, the importance of the research work includes the following:

i. Limited knowledge of African groundwater resources exists on how they might respond to climate change (MacDonald et al., 2005). This research work will assess the response of the floodplain groundwater to potential climatic change to inform the continued use of the low-cost hand-drilling techniques.

ii. UNICEF goal is to increase water supply in Africa by, for example identifying suitable zones for hand drilling. UNICEF has a programme in 12 countries in sub-Saharan Africa: Chad, Madagascar, Niger, Sierra Leone, Central African Republic, Mauritania, Togo, Senegal, Benin, Ivory Coast, Liberia, and Mali (Weight et al., 2012), but not in Nigeria. UNICEF is also paying special attention to cross-border problems that could result in a tragedy of the commons. This research is located in NE Nigeria (Figure 1.1), and focuses on the upper reaches of River Benue in Nigeria and Cameroon; therefore, it could serve as a means of introducing the UNICEF programme there.

iii. The Lagdo Dam (Figure 1.1) was built in Cameroon (a neighbouring country) upstream of the study site on the River Benue (Anderson and Brakenridge, 2007). It regulates the flow during the dry season and Nigeria has no control on the dam. Although the dam has so far had a positive impact on downstream users (Toro, 1997), this research will assess and quantify the impact of potential changes to the operation of the dam.

iv. Populations in sub-Sahelian countries are rapidly increasing (Sissoko et al., 2011) and consequently, food production is intensifying also. In the region of River Benue, this has resulted in an increase in the farming area requiring irrigation. This raises concerns

about whether this agricultural intensity can continue sustainably. This study will assess and quantify the future sustainability of the floodplain groundwater for improving irrigation activities along the River Benue floodplain.

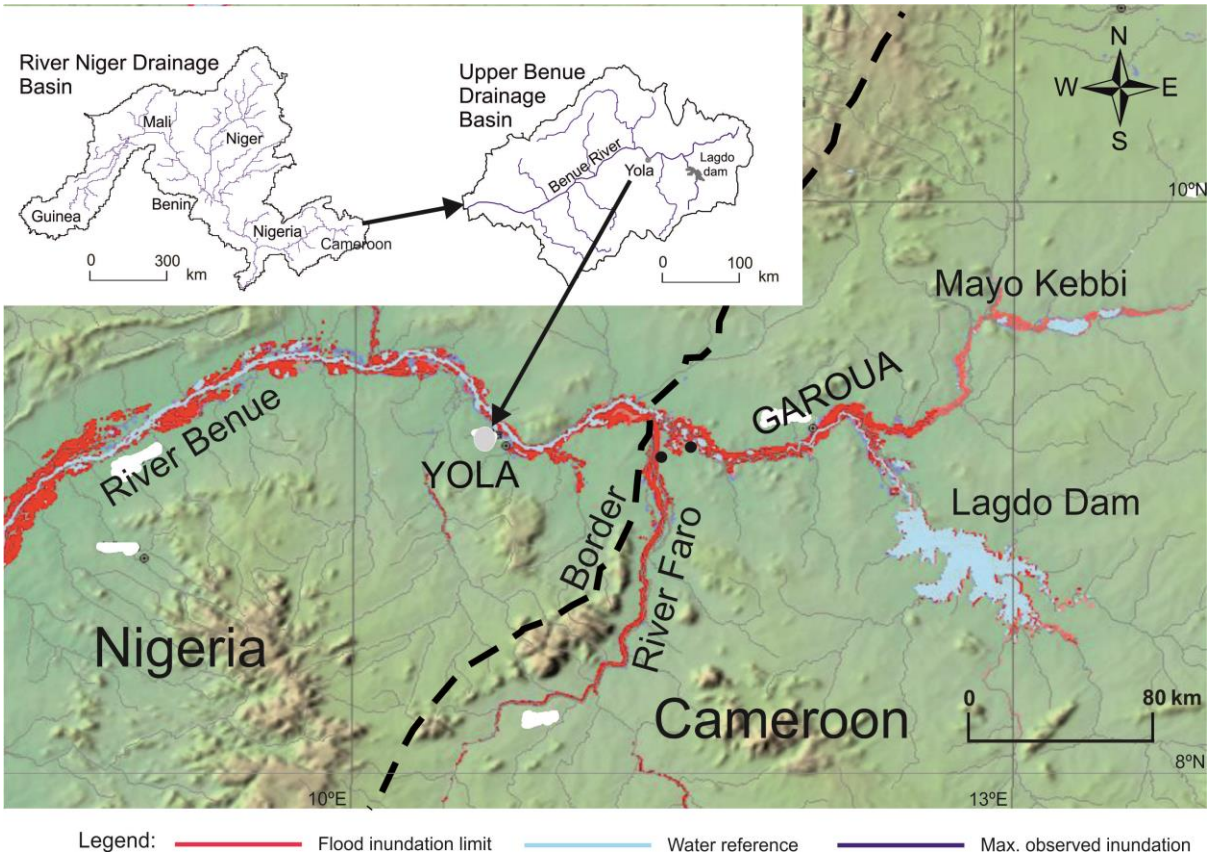

Figure 1.1: Map showing the River Benue valley and the study area in the NE Nigeria. The grey dot is the location of Yola. Black dots are sampling points on Benue and Faro River in Cameroon (Modified after Anderson and Brakenridge, 2007).

1.2 Groundwater availability

In semi-arid environments, the shallow alluvial floodplain aquifers are the main source of water supply for domestic purposes and irrigation (Zume and Tarhule, 2011; Taylor et al., 2013a). However, the sustainability of these shallow alluvial floodplain aquifers to continued abstraction, particularly during the dry season, is affected by high water demand for irrigation as well as increasing population (Zume and Tarhule, 2011; Passadore et al., 2012). Globally,

approximately 72% of water supplies for irrigation activities are derived from surface and groundwater sources and, in developing countries like Africa, agricultural water demand accounts for approximately 90% (Wisser et al., 2008). This emphasises the importance of water supply for irrigation in Africa, especially Sahel regions as the case of northern Nigeria.

Shallow groundwater in Sahelian areas occurs in the alluvial aquifers at depths of between 5 to 40 m below the floodplain surface (RWSN, 2010). Exploiting these water sources involves digging wells in the floodplains to intercept the water table. Despite a long history of exploitation of groundwater on the alluvial floodplain, very little research on the hydrological characteristics of these shallow aquifers exists.

Groundwater has always been considered to be a readily available source of water for domestic use, agriculture and industry. In many parts of the world, especially arid and semi-arid regions, groundwater extracted for a variety of purposes continues to make a major contribution to the social and economic wellbeing of human beings. Understanding the loss (abstraction/use) or gain (precipitation) relationship between aquifers and surface water is therefore important, especially where extraction of groundwater may result in severe lowering of nearby surface waters, threatening the overall water balance (Baalousha, 2012).

1.3 Sustainability of groundwater withdrawal on Fadama floodplain

Groundwater sustainability is defined as groundwater development in a manner that can be maintained for longer period without causing severe environmental impact and sustained loss of groundwater (Cao et al., 2013). Applying this definition in the context of the Fadama floodplain, groundwater sustainability can be defined as groundwater abstraction, which would not cause severe lowering of the shallow floodplain aquifers needed for irrigation of farmland crops. The term ‘Fadama’ is a Hausa word, which refers to small shallow depressions to the floodplain of major rivers but does not include permanently flooded or

waterlogged marshes or swamps. Fadama are important not only for irrigation potential but also as a major source of water for domestic consumption and livestock grazing (Tarhule and Woo, 1997). Sustainability of the shallow alluvial aquifers along the Fadama will require effective management of irrigation practices in order to preserve this important resource on long-term basis (Gupta and Onta, 1997; Alley et al., 1999).

Along the River Benue floodplain, shallow alluvial aquifers are available, where most of the farmers practice hand-drilling irrigation during the dry season to boost agricultural production at a low-cost. According to Sabo and Adeniji (2007), dry season vegetable production plays a key role in the economics of Adamawa State as a basic source of food, income and employment, especially for poor farmers. It would not be economical for them to use machine-drilling rigs for such formations because the farmers do not have the means to pay for equipment, maintenance and security. Accordingly, assessing hand-drilling techniques used in the River Benue floodplain by the farmers is important, in order to understand how best to improve their performance especially for the dry season farming.

1.4 Hand drilling and the Fadama

Water borehole drilling is an essential process for establishing safe, sustained, accessible water supplies in many poor rural regions of the world. Hand drilled boreholes can provide access to groundwater reserves, particularly for domestic and irrigation use. As pointed out by Sutton (2007), hand-dug wells offer similar access to groundwater supplies but often require strenuous and timely manual labour inputs, costly construction materials and potentially unsafe construction practices.

The application of hand drilling is limited to areas with soft unconsolidated geological formations such as the alluvial deposits, sufficiently shallow water tables and high permeability aquifers (Labas et al., 2010; Vuik et al., 2010; RWSN, 2012). Many suitable

areas of loose sediments, Quaternary alluvial deposits exist along the River Benue floodplain and shallow water table in lowland areas of Yola region. Low-cost hand drilling is therefore commonly practiced by farmers for extracting groundwater along the alluvial floodplain of River Benue for irrigation activities.

Hand drilled wells for water supply or irrigation purpose are more affordable than machine-drilled wells. They are also more productive than the hand-dug wells, thereby providing access to improved sustainable water points at a lower cost (Labas et al., 2010; Vuik et al., 2010). Water bore drilling encompasses a variety of techniques, ranging from simple hand auguring to the use of conventional, truck mounted and hydraulic drilling rigs. Hydraulic rigs require more operational maintenance expertise and more expensive component parts. Poor access routes to potential drill sites can prevent such large rigs reaching remote rural areas, while hand-drilling tools can easily reach these remote rural areas (Sutton, 2007).

In Nigeria and many other African countries, groundwater abstraction (for water supply and irrigation) has traditionally used hand dug wells and water holes where water is lifted from the well by a rope and bucket (Adekile and Olabode, 2009). In the northern parts of the country, water lifting for irrigation was done by the shadouf. This comprises a pole on a fulcrum with a rope and container at one end, and a counter-weight at the other end; these were brought to the Sahel by the Islamic culture (Adekile and Olabode, 2009). The Fadama (dry season farming) studies carried out by the World Bank in the 1980s evaluated the irrigation potential of the alluvial aquifers of the major rivers in northern Nigeria leading to the development of the low-cost hand drilling for irrigation boreholes (Adekile and Olabode, 2009).

The presence of a groundwater resource at the shallow alluvial depths (less than 40 m) in most of the Fadama regions of the northeast Nigeria, throughout the dry season plays a key

role for the low-cost hand-drilling methods (Adekile and Olabode, 2009). These aquifers are recharged annually with the onset of the rain and the river flow as the case for the River Benue. At Gurin, in Adamawa State, northeast Nigeria, the community depends on rainwater harvesting during the rainy season, because of groundwater salinity. During the dry season periods, hand drilling techniques are used to drill tube wells into the alluvium in the dry bed of the River Faro (Cameroon), which provide domestic and irrigation water to the community (Adekile and Olabode, 2009).

The use of the hand drilling techniques by farmers occurs in different drilling fields, all over the world. However, every drilling technology has a special range of conditions where the technique is most effective in dealing with the inherent hydrogeology conditions and in fulfilling the purpose of the intended drilling technique for the specified study location.

1.5 The research problem

Globally, food crises are on the increase (MacDonald et al., 2011) due to increasing population numbers and affected by climate change. Nigeria, in common with many developing countries, faces fundamental challenges concerning food security. Although, domestic food production is said to be on the increase, it is grossly inadequate in meeting the growing food demand in the country.

Nigeria is heavily dependent on imported food to meet its food deficit and the country's annual food import bill as of 2009 is US$3billion (Apata et al., 2009). In the first quarter of 2008, the Nigerian government approved the import of 500,000 tonnes of rice estimated to cost US$600 million to meet higher rice demand in the aftermath of the global crisis (Apata et al., 2009). This food import is disturbing, given that Nigeria is blessed with abundant fertile floodplain land resources suitable for food production, especially during the dry season farming. Assessment of the suitability of hand drilling techniques to abstract the shallow

alluvial aquifer along the floodplain is needed to boost agricultural production in the region and the country at large.

Irrigation plays a dominant role in Adamawa State, especially along the River Benue floodplain, because of the distinct dry season, starting November and lasting until May each year (Sabo and Adeniji, 2007). During this period, no rainfall occurs and irrigation along the riverbanks takes place by use of tube wells from shallow aquifers. Improving the hand-drilling methods for abstracting these shallow aquifers for irrigation activities is necessary.

In order to carry on abstracting the shallow alluvial aquifers with the low-cost hand-drilling methods along the floodplains, it is necessary to understand and quantify the floodplain groundwater resource and its sustainability. The alluvial floodplains of the Upper Benue Basin contain groundwater supplies of environmental significance. Competing demands occur on these groundwater systems have led to increased stress on the groundwater resources. These groundwater resources are finite and must be carefully managed for a number of reasons:

- The shallow groundwater system supports water supply for domestic use and irrigation. The irrigation activities along the floodplain solely rely on this shallow groundwater system.
- Population growth across the region has led to an increased demand for water for domestic and irrigation uses.
- Excessive groundwater extraction could lower the water table in the shallow alluvial aquifer on the floodplain. This would subsequently make it more difficult for farmers to access water for irrigation.

- Exploitation of groundwater resources has the potential to significantly alter groundwater levels and intrinsic processes.

The development of a groundwater model may assist with characterising the existing groundwater in the floodplain and developing a better understanding of the groundwater flow processes involved. It could also assist in determining the sustainability of the groundwater across the floodplain for future abstraction, especially using hand drilling techniques such as the augering and jetting methods.

1.6 The research question and objectives

In this research, I will address whether farmers will be able to continue to use the manual way of abstracting the shallow groundwater from the floodplain for irrigation use.

After a detailed review of the existing literature and consultation with experts, it was decided that my research would principally determine if water abstraction by hand-drilling techniques would be best method of accessing groundwater in Yola region on the shallow alluvial floodplain formations by understanding the mechanisms behind it in relation to the sedimentology and hydrology of the floodplain. Secondly, my research would seek to assess the sustainability of groundwater resources along the alluvial floodplain, under different climate, water abstraction and dam operation scenarios. These aims will be achieved through the following specific objectives:

i. To scientifically characterise the sedimentology of cores and of River Benue outcrops using laser granulometry and examine why they are suitable for the application of the low-cost hand drilling techniques.

ii. To quantify the maximum drilling depths required for irrigation at the peak period of the dry season for the application of hand drilling techniques.

iii. To critically compare the types of sediment in the floodplain to the aquifer potential for the application of hand drilling techniques.

iv. To establish the hydrogeology of the floodplain to improve the planning and effectiveness of abstraction sites for irrigation of the low-cost hand drilling techniques.

v. To develop a transient state model and calculate the water balance of the floodplain.

vi. To quantify the flux exchange between the groundwater and the river in the groundwater – surface water interaction.

vii. To critically examine long-term water level variations in the alluvial aquifer of the floodplain and their relationship to climate conditions.

viii. To critically assess how the operation of the Lagdo Dam in Cameroon upstream and abstraction rates will influence the water table of the floodplain.

The data gathered will help assess in a scientifically robust way if hand drilling techniques will continue to be a sustainable approach for water abstraction, and will assist with understanding the groundwater flow processes within the system, specifically during the dry season period (January to June) and to support the development of conceptual and numerical models of the floodplain.

1.7 Thesis structure

The thesis contains seven chapters:

The research problem, overall aims and specific objectives of the research are described in Chapter One (Background).

Chapter Two (literature review) provides a detailed account of the physical setting of Adamawa State (including the topography, geology and climate) details of the floodplain under consideration (including land use and agricultural development, type of irrigation techniques in the study area and typical surface water and river discharges), details of the structure and sedimentology of alluvial floodplains, including aquifer characteristics, perched aquifer systems) and the likely impacts of climate change on groundwater. This chapter also reviews the impact of dams, existing hand-drilling techniques, and reviews the methods used for characterising sedimentology, groundwater and groundwater modelling.

Chapter Three describes the actual methodology used for characterising the sediments and soils needed to develop a numerical conceptual groundwater model for the shallow alluvial floodplain.

Chapter Four describes River Benue in Yola and Garoua and analyses the hydrological and climatic variability in Yola and Garoua regions, River Benue and Lagdo Dam in Cameroon.

Chapter Five integrates of the results obtained from both the sedimentology and groundwater modelling of the floodplain in order to assess the suitability and sustainability of hand-drilling techniques.

Chapter Six presents discussions of the results following their interpretations.

Chapter Seven presents the overall conclusions about the contribution achieved from both the sedimentology and groundwater modelling of the floodplain and lists recommendations for further research.

CHAPTER TWO - LITERATURE REVIEW

2.1 Introduction

This chapter starts with a presentation of the background to the current study, including topography map of the study area, physical setting of Adamawa State, geology, hydrogeology, sedimentology of the floodplain, land use and agricultural development, type of irrigation techniques in the study area, surface water and river discharge, groundwater and impact of climate change on groundwater (section 2.2) from the more global to the more local. The second section reviews impact of dams in the neighbouring country upstream and highlights the downstream impact of Lagdo Dam (section 2.3). The third section reviews the criteria for assessing the suitability and sustainability of hand drilling techniques for abstracting the shallow floodplain alluvial aquifers (section 2.4). The fourth section reviews the existing hand drilling techniques, including drilling techniques used by irrigation farmers along the floodplain of River Benue (section 2.5). The fifth section presents what is presently known of the floodplain sediment as well as sampling and laboratory methods used for analysing the sediments (section 2.6). The sixth section presents an overview on the use of groundwater modelling for assessing the interaction between river and floodplain generally and for River Benue specifically, and for estimating the groundwater sustainability of the alluvial floodplain for the application of hand-drilling (section 2.7).

2.2 Physical background

2.2.1 Topographic map of the study area

Figure 2.1 shows the topographic map, which is currently available for the study area, which lies between latitudes 9° N and longitude 12° E. The available topographic map was found to be insufficient for the purpose of the present research because the contour lines provided

were limited in number and precision thus preventing any estimation of the role of relief on groundwater levels across the catchment area. Precise and sufficient contour lines are necessary for proper understanding the water levels along the floodplain.

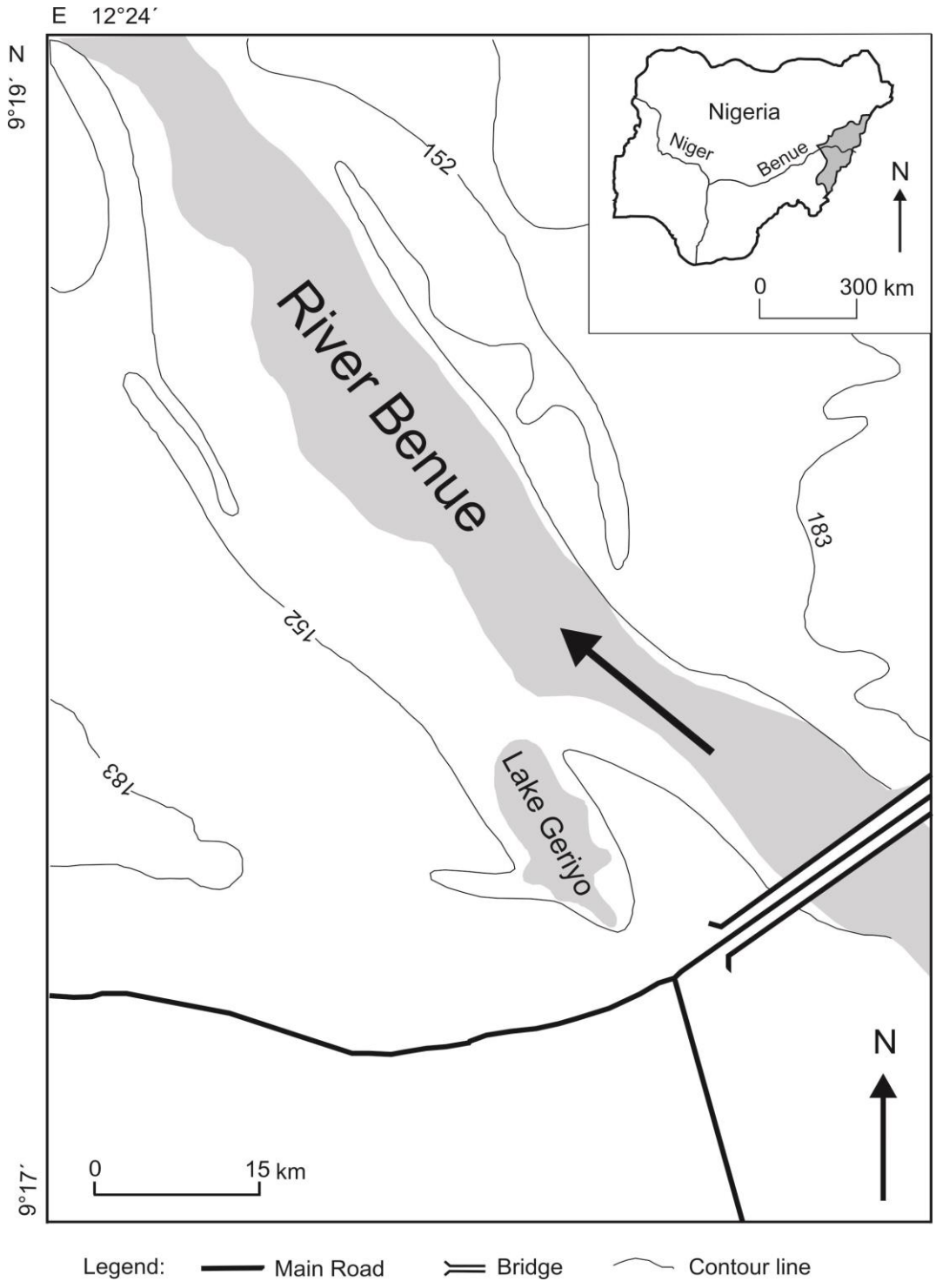

Figure 2.1: Simple topographic map of the study area (Modified after Federal Surveys of Nigeria Topographic sheet 48, 1974). Altitude in metres.

The elevation of the study area varies from 149 to 228 m above mean sea level and falls within the Upper Benue Basin, which has a catchment area of about 750 km^2.

The floodplain is drained by the River Benue, which is the largest and only perennial river in the area. The River Benue is fed by two major streams in Cameroon; Mayo Kebbi and River Faro (see Figure 1.1) and flows into River Niger 1400 km downstream.

2.2.2 The physical setting of Adamawa State and climate

The study area (Figure 2.1) is in Adamawa State which is located in the North Eastern part of Nigeria, between latitudes 7 and 11° N of the equator and longitude 11 and 14° E of the Greenwich meridian (Figure 2.2). It shares a boundary with Cameroon Republic along its eastern border. The state covers a land area of about 38,741 km^2 with a population of 3,168,101 people, and a population density of 82 persons per square kilometer (Census, 2006). Adamawa State is made up of twenty one local government areas (LGA) as shown in Figure 2.1.

Adamawa State has some of the longest mountain ranges and breath-taking landscape sceneries in the country with areas as low as 129 m and as high as 2042 m above sea level (Ashafa, 2009). The land rises from the low-lying Gongola and Benue valleys to the rugged hills to the northeast defining the Mandara Alantika Shebshi Mountain Ranges and the central portion, which is dotted with isolated uplift such as the Lamurde Longuda, Song-Bagale and Yardang hills (Ashafa, 2009).

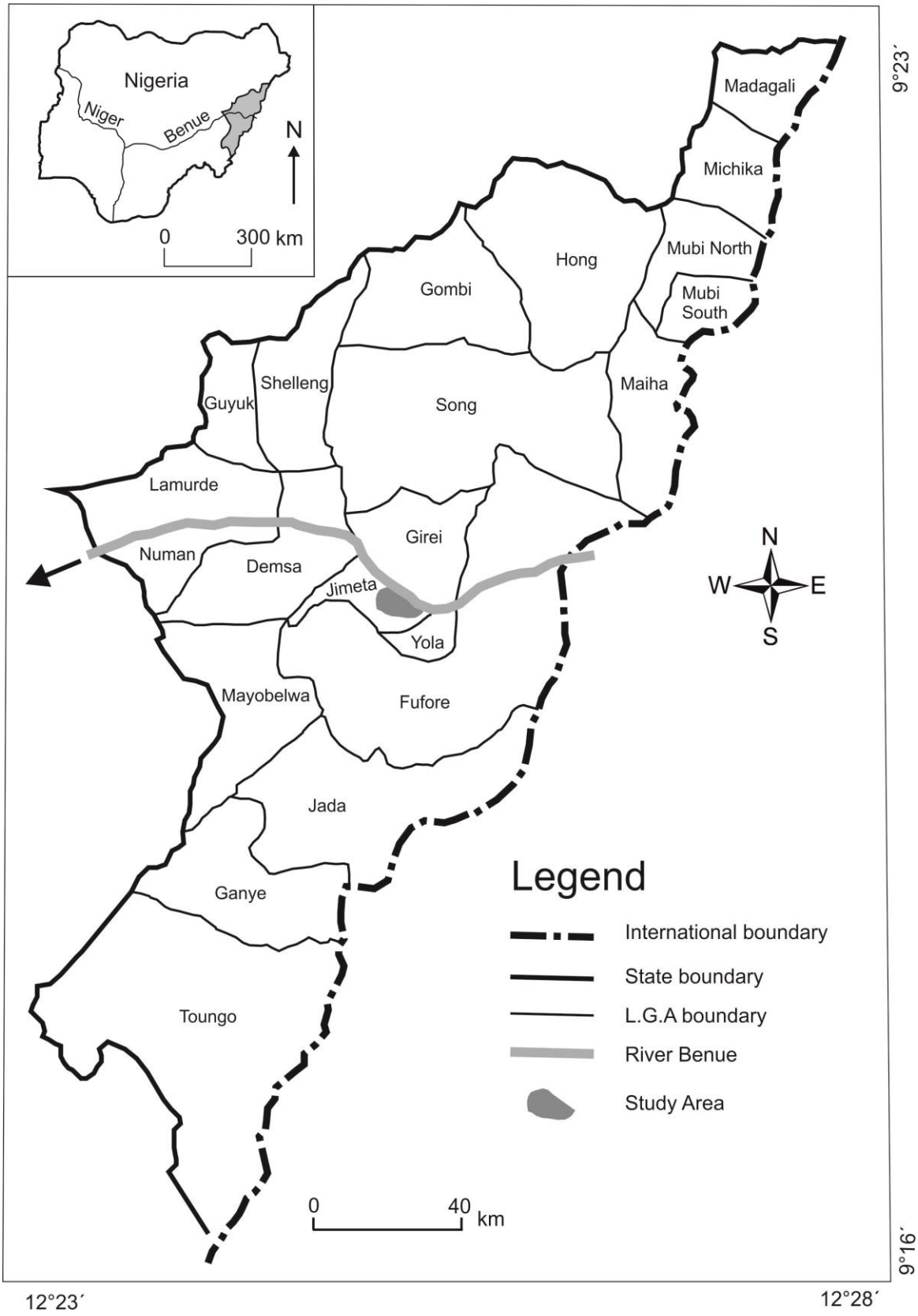

Figure 2.2: A map of Adamawa State showing the twenty one local government areas (LGA) and study area (Modified after Adebayo and Tukur, 1999).

Sahel regions are characterised by low rainfall variability (see Figure 2.3). As reported by Nicholson (2013), mean annual precipitation in the Sahel regions are in the range between 100 to 200 mm in the north and 500 to 600 mm in the southern limit of West Africa.

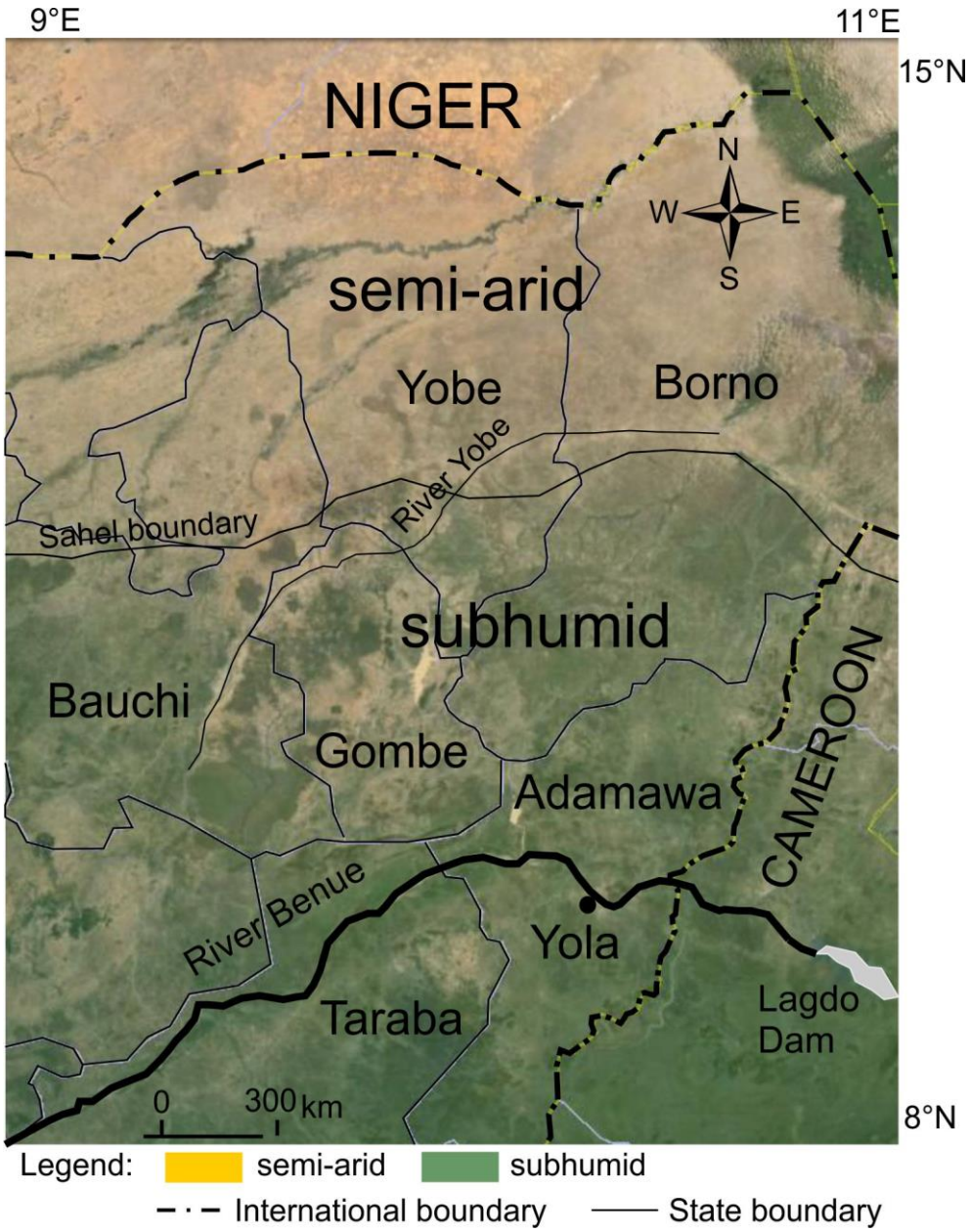

Figure 2.3: Map of north and south basins of Sahel in north-east Nigeria showing the study area and River Benue (Modified from Google Earth Image, 2013).

Although, Yola is not within true Sahel climatic zone (Figure 2.3), it still features broadly Sahelian characteristics such as a long dry season period, from November to May and it has only five months of wet season, from June to October. The annual mean rainfall for the

region is high (914 mm), but this is because of large storm events usually occurring in the months of August and September each year (Adebayo, 1999). During the dry season period, low-cost hand-drilling techniques are used to abstract the shallow alluvial aquifers of the floodplain for irrigation activities.

2.2.3 Geology

The Benue floodplain in the region of Yola is underlain by sedimentary rocks, which consist of two stratigraphic units (Barber and Jones, 1958; Carter et al., 1963; Reyment, 1956; Cratchley, 1960). The feldspathic Bima sandstone and the Yola sandstone (Figure 2.4) are found along the main course of the bank of the River Benue valley and its tributaries and consist of all grain size between clays and pebbly-sands (Obiefuna et al., 1999; Ishaku and Ezeigbo, 2000; Yenika et al., 2003). At the upstream sections, volcanic intrusions are found along Benue and Faro Rivers in Cameroon (see Figure 2.4) (Tamfuh et al., 2011).

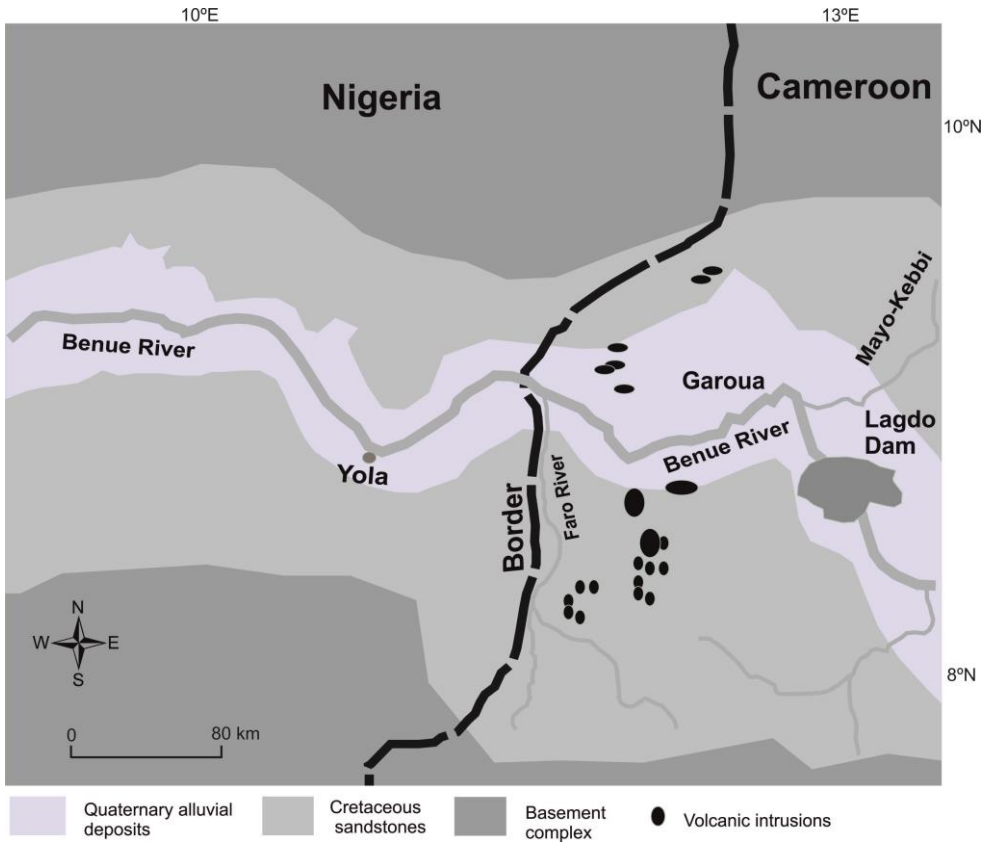

Figure 2.4: Geological map of River Benue in Cameroon and Nigeria (Modified after Nigeria Geological Society, 2006 and Tamfuh et al., 2011).

The detailed descriptions of the Bima sandstone were provided by Carter et al. (1963), Allix (1983), Popoff et al.(1986), Popoff (1988) and Guiraud (1990, 1991) with three major units B1, B2 and B3 collectively known as the Bima Group. The classifications for the Bima sandstone include the Lower Aptian/Albian (B1), the Middle Albian (B2) and the late Albian/Cenomanian Upper Benue (B3) (Carter et al., 1963 cited in Obiefuna and Orazulike, 2011b). The outcrops of the Bima Group belong to the Bima 2 and 3 in the Yola region (Braide, 1992). The Bima sandstone (B2) varies from fine to coarse grained sediment (Allix, 1983) and the deposits were regarded as of proximal braided river origin (Guiraud, 1990; 1991 in Ishaku, 2011). The Bima sandstone (B2) is widely distributed and is characterised by trough and tabular cross bedding. This sandstone ranges from 100 to 500 m thick. The upper Bima sandstone (B3) is fairly homogenous, relatively mature and fine to coarse-grained sandstone, characterised by tabular cross-bedding, convolute bedding and overturned cross-bedding (Zaborski et al., 1997). The thickness ranges from 500 to 1500 m.

According to Obiefuna and Orazulike (2011a), the Bima – Yola sandstones consist of layers, which range from poorly to moderately fine to coarse-grained sandstone, having an average thickness of 250 m. The Bima sandstone consists of feldspathic sandstone, grits, pebble beds and clay intercalations in some places (Eduvie, 2000). The sandstones are generally light brown, medium to coarse grained and distinctly feldspathic (Onugba and Aboh, 2009). The Yola Bima sandstone consists of quartz (65%), feldspars (14%), mica (9%), iron oxide (5%) and calcite (3%) (Obiefuna and Orazulike, 2011b).

2.2.4 Hydrogeology

The geology of the research area was classified according to the age of formations. These formations are the recent Quaternary river coarser alluvial at the top and the older Cretaceous Bima sandstone formation underneath. The upper alluvial aquifers constitute recent

Quaternary sediments; while the lower semi-confined aquifer system constitutes the Cretaceous sediments (Obiefuna and Orazulike, 2010). The alluvial deposits are composed of recent sediments that reach more than 80 m in thickness. Diagonally along the southeast-northwest part of the research area, the alluvial aquifer decreases in thickness as it moves away from the River Benue interfingering with some saturated sand lenses (Obiefuna and Orazulike, 2010). The hydrogeology, as described by Obiefuna and Orazulike (2010), indicates the occurrence of two aquifer systems, an upper unconfined alluvial aquifer and the lower semi-confined to confined aquifer, capable of yielding quantities of water. The upper unconfined alluvial aquifer is recharged through surface precipitation and River Benue during the dry season period, while the lower semi-confined to confined aquifer is recharged through precipitation and lateral groundwater volumes flowing through the sandstone formations bounding the aquifer.

The hydrogeology as discussed by Obiefuna and Orazulike (2010) is mainly focusing on deep boreholes in towns for obtaining drinking water supply. No available study in the area considered the hydrogeology of the alluvial floodplain shallow groundwater in the region. The present research study will be the first attempt to understand hydrogeology of the alluvial floodplain shallow groundwater in region for abstraction for the dry season farming system.

2.2.5 Sediment of the floodplain

Understanding the shallow sediment formations in the basin is another key aspect in any integrated study of catchment management for two reasons. First, the predominant activity of the area is agriculture and therefore, a good description of the sediment properties (e.g. texture, drainage) is needed prior to the formation of a land use and flood risk management strategy. Secondly and relevant to this investigation, infiltration and unsaturated zone storage parameters are a function of sediment properties and their values and spatial distribution will

assist in the selection of characteristic parameters for the hydrological system (Obiefuna and Orazulike, 2010). Figure 2.5 shows the alluvial formation in the floodplain along the left shore of River Benue.

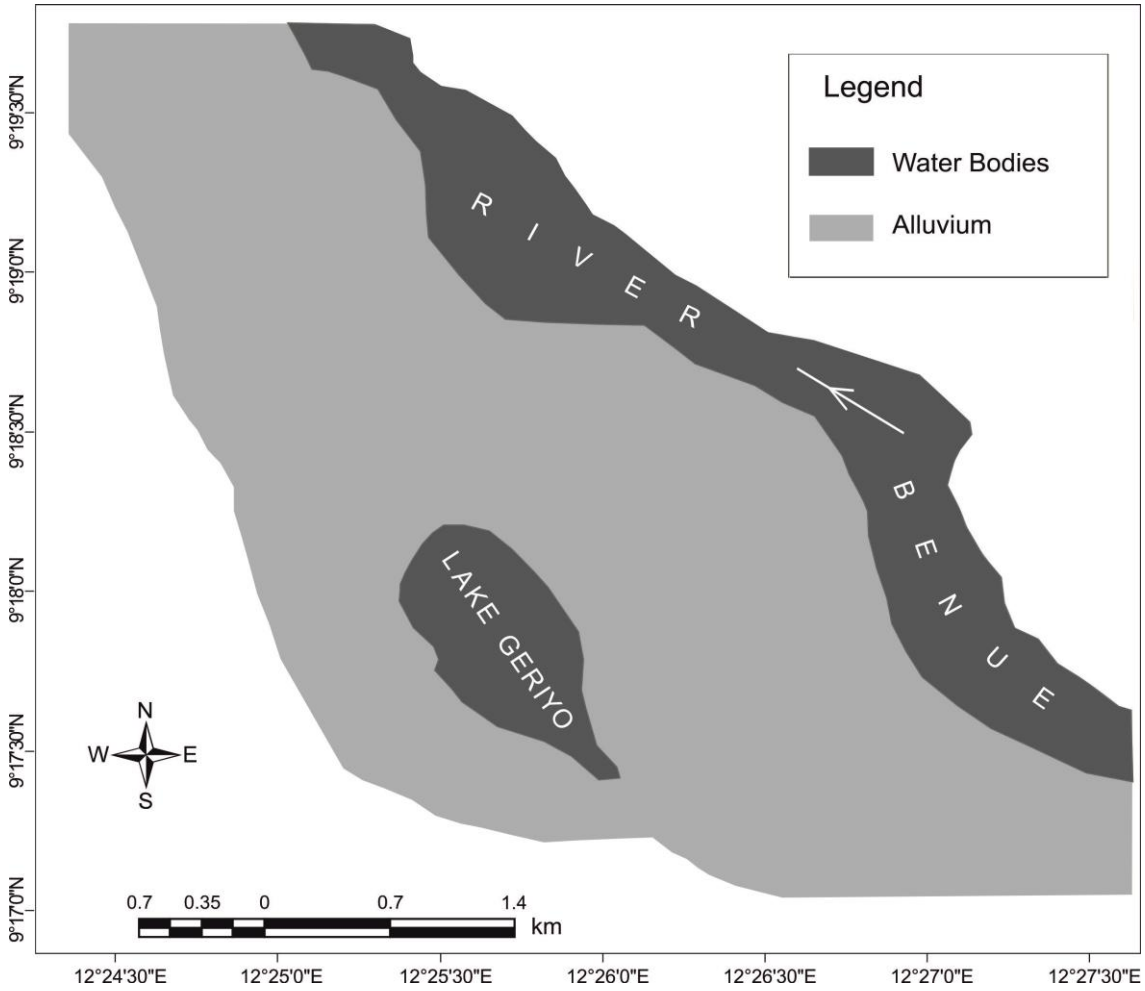

Figure 2.5: Alluvial formation along the floodplain of River Benue, Yola region (Modified after Nigeria Geological Society, 2006).

The Upper Benue River Basin Development Authority (UBRBDA), in charge for the management of the Upper Benue Basin, Yola, has drilled an extensive network of alluvial shallow tube wells 8 to 20 m depths throughout the floodplain for irrigation activities. The borehole logs made available to us reveal a typical fining upward sequence of alluvium sediments, immediately overlying sandstones bedrock. Part of the alluvial deposits is products of in-situ alteration caused by chemical and physical weathering of the rocks

(Adelana et al., 2008) and another part is the result of river transport and Aeolian transport. In the floodplain, sand is widespread and may overly some silt and clayey silt. Hence, sand is not always laterally continuous. The estimated thickness of the alluvial floodplain sediment is 80 m depth (Obiefuna and Orazulike, 2010).

In brief, no detailed sedimentological investigations have been made so far on the floodplain. This is a pre-requisite before any hydrological studies are undertaken.

2.2.6 Land use and agricultural development

Agriculture is the dominant activity among the people of Adamawa State, especially the rural dwellers who constitute about 85% of the state population. Adamawa State is endowed with a lot of floodplain suitable for irrigation farming using both surface and groundwater resources (Polycarp and Mustapha, 2001). It was estimated that such Fadama lands cover an area of about 350,000 ha that lies along the basins of major rivers and lakes in the state. About 260,000 ha of Fadama lands in the state could be exploited using the shallow aquifers located within the basins of both the perennial and seasonal rivers (Polycarp and Mustapha, 2001).

The Lake Geriyo Irrigation Project near Yola was established in 1976 by the Federal Government of Nigeria in order to promote irrigation activities in the State, which is still under expansion for irrigation. The project started with 24 hectares of land and 24 farmers in 1976. However, presently, the project has expanded to over 400 hectares of land with more than 1500 farmers, but at the peak period of operations, the number rises to over 1600 farmers. The present area under cultivation includes i) 150 hectares of rice with harvests of 750 tons, ii) 80 hectares of maize with harvests of 240 tons and iii) 120 hectares of assorted vegetables with harvests of 360 tons (D.D. Mamtso, Project Manager of Geriyo Irrigation Project, UBRBDA, Yola, Personal communication on 18th April 2012).

Figure 2.6 displays the main land uses on Lake Geriyo Irrigation Project, which include floodplain under production and under development, residential areas and fisheries. As stated by the project manager, Lake Geriyo Irrigation Project has a great impact on its immediate community and environs because it creates employment opportunities, economic empowerment and reduced youths restiveness at the time other areas of labour employment are less active. At harvest period, the prices of grain fall drastically for a period of one month or more because of flooding of grains into Yola main market from the project area. In addition, the vegetable farmers feed Yola market with assorted vegetables throughout the year at moderate prices.

Lake Geriyo Irrigation Project is faced with the following challenges: i) siltation of Lake Geriyo due to dumping of refuse, dirt and polythene bags, which contribute in lowering the groundwater level of the project area, ii) land encroachment as a result of persistent erosion and collapsing of River Benue bank, iii) quelea birds invasion, iv) high costs of agro-inputs, e.g. fertilizers, improved seeds, agro-chemicals, etc. (D.D. Mamtso, Project Manager of Geriyo Irrigation Project, UBRBDA, Yola, Personal communication on 18th April 2012). Understanding the condition of the groundwater in the floodplain will help in managing and planning for the future irrigation activities in the area. Especially the problem of siltation of the Lake Geriyo is one of the main factors contributing to the degradation of the groundwater level of the floodplain.

I had discussion with the local water managers regarding the problems facing water levels in Lake Geriyo during the dry season period. According to him, one of the possible reasons for lowering water in the lake is dumping of refuse, dirt and polythene bags that are dumped into the lake. Lake Geriyo has water all the year round and it contributes to recharging the floodplain groundwater during the dry season period. This polythene bags may possibly prevent infiltration of water from the lake to the alluvial floodplain groundwater.

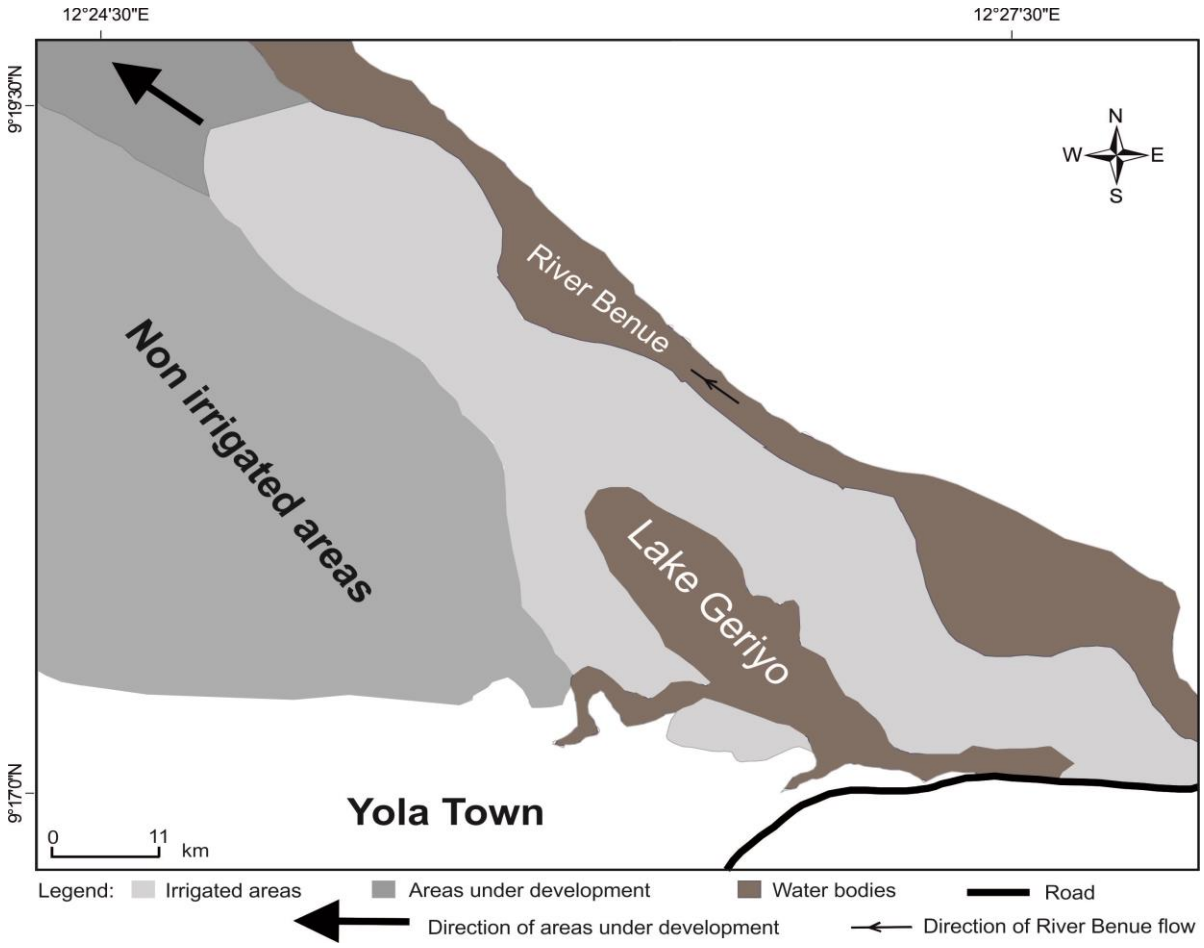

Figure 2.6: Land use map of Lake Geriyo Irrigation Project showing areas under cultivation and development (large arrow in north-west direction) along River Benue floodplain (Modified from Google Earth Image, 2011).

2.2.7 Type of irrigation techniques in the study area

Basin irrigation techniques are practiced in the floodplain of Lake Geriyo Irrigation Project, the study site. Figure 2.7 shows a farmer irrigating his farm using the basin irrigation system in the floodplain from water pumped from the well with a water pump. Basin irrigation system is a method of watering plants in which a level field area is surrounded by a ridge of earth, so that the applied water to the basin accumulates before it soaks into the sediment for uptake by crops.

Figure 2.7: Farmer irrigating using basin irrigation method in the floodplain (Photograph taken by Mohammed Abana Girei on 20th April, 2012).

Agricultural activity by irrigation in the state is a popular endeavour, especially among the riverbank communities along River Benue valley. The people practice irrigation during the dry season for food crops and fresh vegetables, which include cereals like maize, rice, wheat and vegetables like amarantus (alefo), okra, spinach, onions, lettuce, tomatoes.

Irrigation activities in the Lake Geriyo Irrigation Project Area are entirely dependent on the groundwater. Irrigated agriculture using groundwater through power-operated pumps was introduced by Upper Benue River Basin Development Authority (UBRBDA), Yola in 1976 in order to boost irrigation activities in the region. Upper Benue River Basin Development Authority installed various shallow irrigation wells across the floodplain for the irrigation activities. Groundwaters are abstracted using pumping machines and the abstracted groundwaters are applied directly to the crops in the basin. Understanding the sustainability

of abstracted groundwater for irrigation during the dry season period is the focus of this research work.

The locations for all the sediment-sampling points along River Benue floodplain both in outcrops and in cores are presented in Figure 2.8.

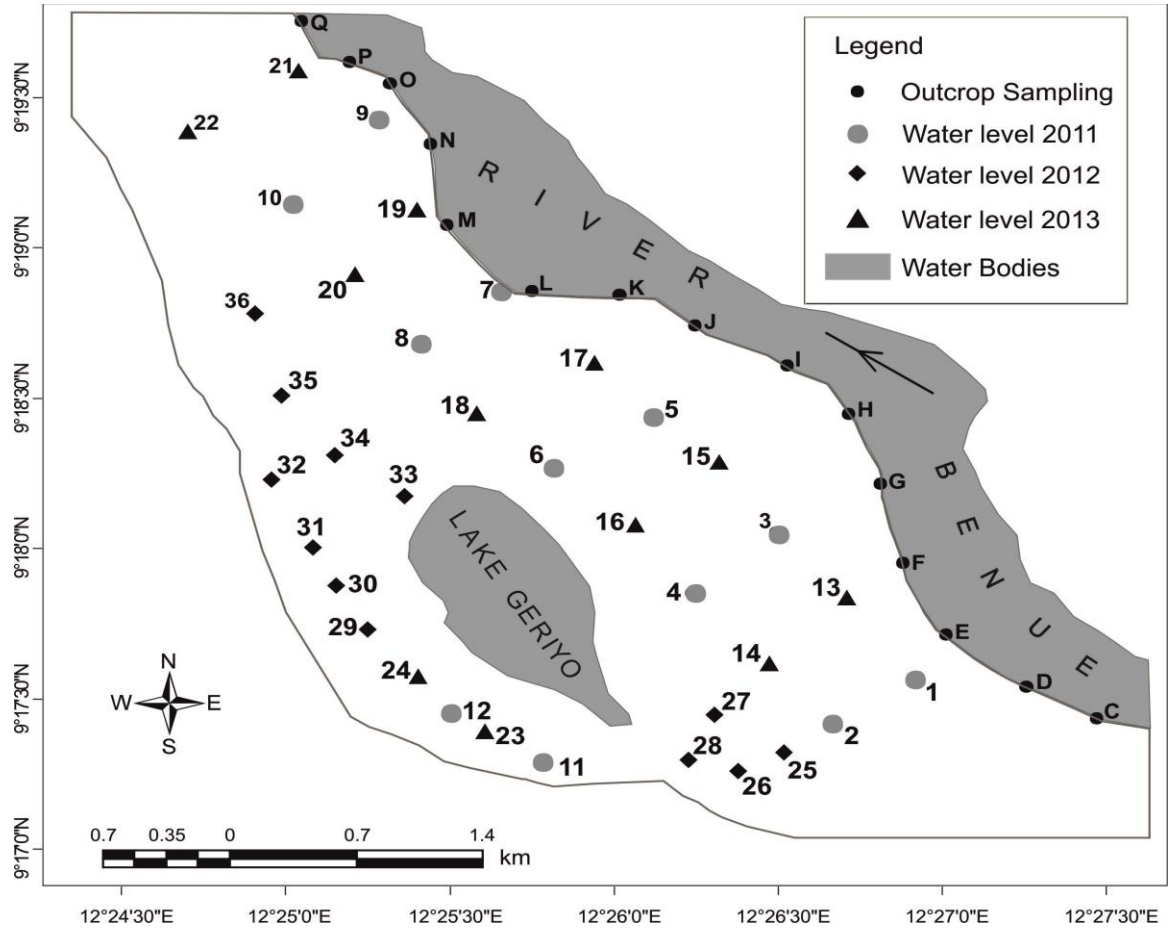

Figure 2.8: Map showing sampling location for both outcrops and sediment cores on the alluvial floodplain.

As mentioned before, land loss due to river erosion is one of the major problems facing the farmers. Every year farmers closer to the river loose approximately 10% of their land. Figure 2.9 shows an example of land loss due to persistent erosion during overbank flooding events, usually during the rainy season because of rising of river level due to excessive storm from precipitation and sudden water released from Lagdo Dam upstream.

Figure 2.9: Land loss as a result of persistent erosion and collapsing of River Benue bank, due to river flow and seasonal flooding at sampling location E, see Figure 2.8 (The photograph taken by the author on 24th April 2012.

2.2.8 Surface water and river discharge

Although the surface water resources of the region are enormous, they are unevenly distributed in time and space. Surface water is not available during the dry season, except in the few deep ponds, Lake Geriyo and River Benue itself (see Figure 1.1) that have water all the year round. Tributaries from surface water drainages coming from town and rainfall in the rainy season period seem to feed Lake Geriyo according to my own observation. The groundwater level in the basement complex structure falls rapidly during the dry season due to seepage and high evapotranspiration (Adebayo, 1997; Adebayo and Umar, 1999). The climate of the state controls the regime and other characteristics of the river (Adebayo and Umar, 1999). River Benue is the most important source of surface water. It discharges 345 m^3 of water per year. More analyses of its flows are provided in Chapter Four.

2.2.9 Groundwater

Groundwater is water found in the saturated zone below the ground (Bill, 2011). Groundwater is the largest storage of freshwater in Africa (MacDonald et al., 2012). The interplay between geology, geomorphology and climate gives rise to the hydrogeological environments (MacDonald et al., 2009; MacDonald et al., 2011). Globally groundwater storage constitutes approximately 97% of the world water resources (Holden, 2012). Most of arid and semi-arid environments depend more on groundwater than the surface water during the dry season period such as the research area (Scanlon et al., 2006). Aquifers of the floodplain are replenished by rainfall and River Benue flow. The region is underlain by Bima Yola sandstone, and the floodplain groundwater occurs from rainfall and bedrock (Nur and Kujir, 2006). Groundwater is the main source of water in the region in the form of wells and boreholes. Assessing the low-cost hand-drilling techniques requires an understanding of groundwater levels along the floodplain. Hand drilling can only abstract groundwater of up to 40 m depth from the floodplain ground surface due to operational power limitation.

2.2.9.1 Aquifers characteristics

An aquifer is an underground layer of water-bearing material from which groundwater can be usefully extracted through water well. Aquifers are generally found in porous types of rocks such as sandstone, conglomerate and alluvial sediments. Aquifer recharge is the water that crosses the lower limit of the non-saturated zone to reach the aquifer and produces measureable increases in the water table level (Quirez-Londono et al., 2012). As reported by MacDonald et al. (2011), most of the floodplain shallow aquifers in Africa come from alluvial formation, which represents approximately 25% of the land surface. These alluvial formations are permeable with high percolation during the rainy season that recharges the shallow floodplain groundwater (Nur and Kujir, 2006).

Alluvial aquifers along the floodplain of River Benue are the main source of water supply for irrigation. Good knowledge on floodplain alluvial aquifers such as understanding their depth, spatial distribution and the geology could improve the sustainability of the groundwater (Park et al., 2007). Therefore the study will focus on understanding the floodplain aquifer characteristics in order to improve its sustainability. Figure 2.10 shows the occurrence of groundwater flow in unconsolidated floodplains such as the present study site.

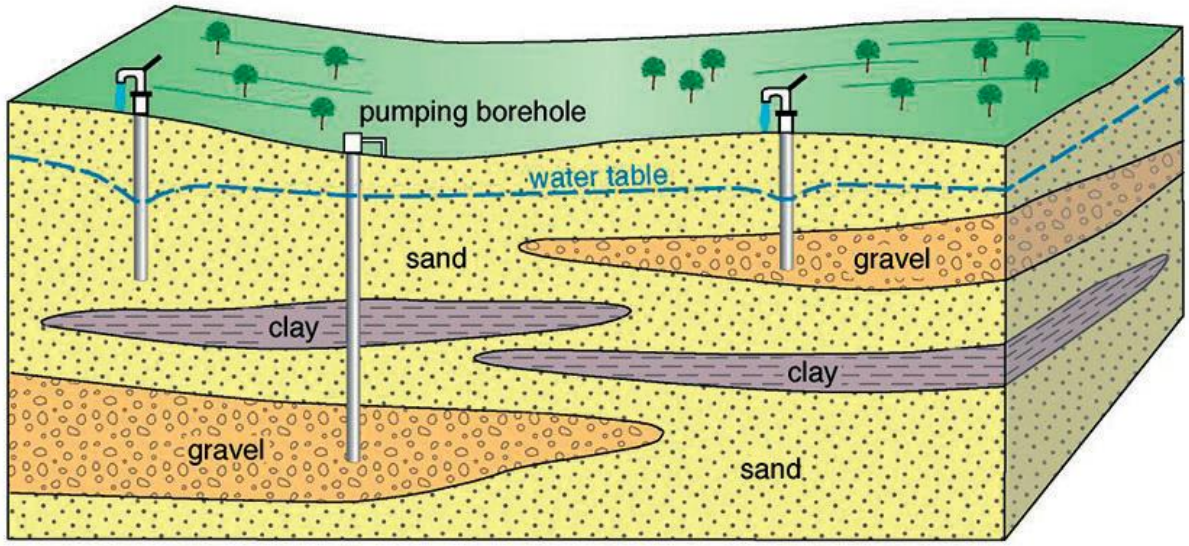

Figure 2.10: Diagram showing lenses of clay and groundwater occurrence on alluvial floodplain (From MacDonald et al., 2011).

Yobe floodplain is similar to the present study area and they are in the same climate region in northeastern Nigeria. The shallow groundwater resources of the extensive river floodplain alluvial aquifers of River Yobe (see Figure 2.3), arid zone of northeast Nigeria, was studied by Carter and Alkali (1996) to evaluate the recharge to the alluvial aquifers of the river. These authors suggested the development of shallow groundwater investigation through low-cost tube well construction in the floodplain of the river. In principle, recharge to the shallow alluvial aquifer which underlies the Yobe River floodplain could be by river channel seepage,

floodwater infiltration, or infiltration of excess rainfall or some combination of all three (Carter and Alkali, 1996).

A network of 20 piezometers was set up in the alluvial aquifers west of Gashua of Yobe State and was able to show aquifer response to river stage rise and recession through the flood of 1992 and up to June 1993 (Alkali, 1995). Similarly, a separate study on the floodplain of Yobe River showed a rapid alluvial groundwater rise in response to high river stage (Water Surveys, 1994). A thorough understanding of the mechanisms of recharge to the alluvial floodplain aquifer is essential, if groundwater development for small-scale irrigation is to continue in a sustainable manner (Carter and Alkali, 1996). Understanding the recharge of the alluvial floodplain aquifers is necessary in order to improve groundwater development for irrigation activities using low-cost hand-drilling techniques.

Aquifers can be confined and unconfined (Fetter, 1994), but this study focuses mainly on unconfined aquifer, since low-cost hand-drilling techniques are applicable only to shallow unconfined alluvial aquifers.

2.2.9.2 Perched aquifer system

The review of perched aquifer is useful to the present study, because perched aquifers are common features on the alluvial floodplains. Knowing the locations of perched aquifers in the floodplain is useful to the farmers to avoid them, because water in perched aquifers is limited in supply. If there are more perched aquifers in the floodplain could affects sustainability of wells, because yield of perched aquifers are limited. Perched water tables occur where lenses of impermeable material in alluvial sediment exist. An example of perched aquifers found along alluvial floodplain rivers are shown in Figure 2.11. Fetter (1994) defined perched aquifer as a limited areal extent which develops from surface water sources (e.g. streams, ponds) infiltrating through the vadose zone accumulating on a layer of

less permeable formations such as clay. Perched aquifers are of little importance for water supply, because perched aquifers do not have contact with the groundwater flow. Perched aquifers have been found to form above impermeable layers such as lenses of clays in a semi-arid region (Carter et al., 2011).

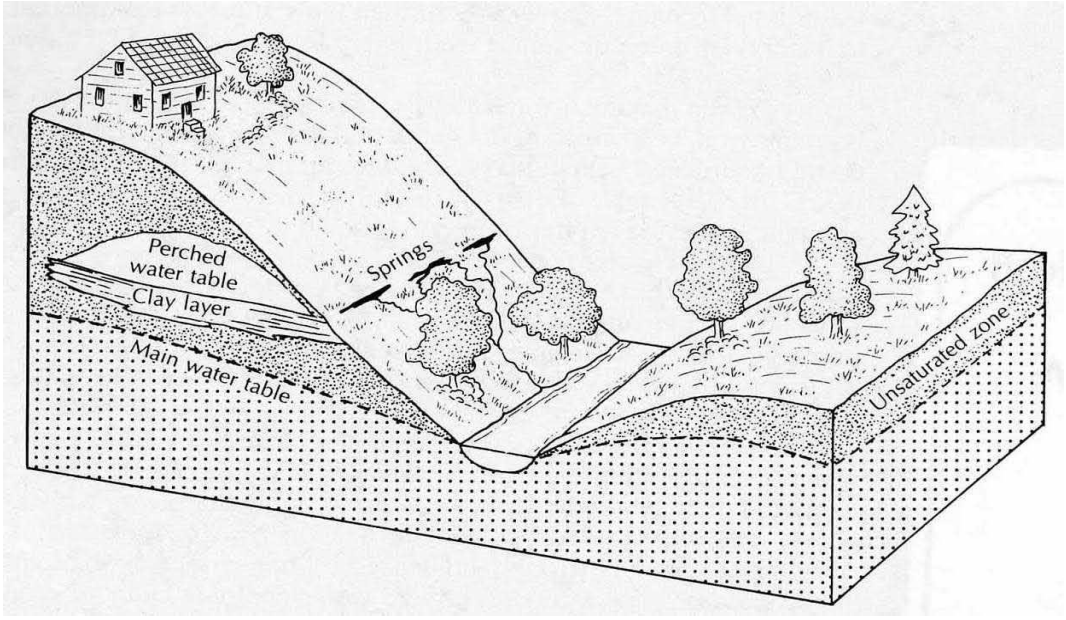

Figure 2.11: Diagram showing a perched aquifer system formed on a lens of clay layer (From Fetter, 1994).

Mbiimbe et al. (2008) carried a study on the groundwater potentials in an Upper Benue River Basin, but on deep borehole logs. Their results show three groundwater systems. The upper was unconfined and corresponded to the Quaternary river course alluvium, the middle was semi confined and corresponded to the Yolde Formation and the lower was confined and corresponded to the Bima Formation. Similarly, a study by Nur et al. (2001) explored groundwater in the Yola region mostly in towns (see Figure 1.1). They compared vertical electric sounding (VES) results with boreholes logs and water table was found to lie between 48 to 51 m below surface. No mention of perched aquifers was made in these two studies.

Robinson et al. (2005) identified 33 perched aquifers along the semi-arid region of Pajarito Plateau in New Mexico, United States, by using electrical geophysics and direct water-level

measurements. Perched aquifers were found in shallow dolomite underlain by sandstone in semi-arid area of south-western Wisconsin, USA (Carter et al., 2011). Perched aquifers occur in the Judea aquifer semi-arid region, Israel (Peleg and Gvirtzman, 2010). Perched aquifers were found in alluvial formations associated with rivers and lakes (Rosenberry, 2000; Niswonger and Fogg, 2008). As was discussed above, perched aquifers are common along alluvial floodplain such as the River Benue floodplain the study site. Understanding the causes of perched aquifers on the alluvial floodplain is useful in relation to the shallow floodplain groundwater especially for abstraction using hand-drilling techniques.

2.2.10 Impact of climate change on groundwater

Many studies in arid and semi-arid environments have highlighted negative impacts of climate change, especially desertification, on groundwater (Taylor et al., 2009; Neukum and Azzam, 2012). Global climate change has a strong impact on water resources crop yield, especially the groundwater in many region of the world (Bates et al., 2008; Knox et al., 2012). The shallow alluvial aquifers in the northern Nigeria are affected by climate change (Maduabuchi, 2002). Climate change in Sahelian northern Nigeria contributed to lack of understanding of the recharge pattern across the floodplain.

To understand the potential groundwater changes of the region due to climate change, a sound knowledge of the floodplain aquifer characteristics is required (MacDonald et al., 2011). Study by Aizebeohai (2011) on the impact of climate change in Nigeria show that it leads to changes to the groundwater, discharge and aquifer storage.

As discussed in Chapter One limited knowledge of African groundwater exists on how they respond to climate change (MacDonald et al., 2005). The recent IPCC 2013 report predicts minor increase in precipitation between 2016 to 2036 in this part of Africa including the study site. This is the main focus of this research and this brief literature review has

highlighted the state of knowledge specifically for the Yola region. It is clear that there is a need for obtaining geology and hydrology data in order to support irrigation development.

2.3 General impact of dams

Dams are constructed for many purposes, for example, for domestic water supply, for irrigation purposes, and for generating electricity. The construction of large dams in the developed countries such as Europe, United States, Australia, Canada and Japan in the 1960s was necessary for the development of these countries (Tchotsoua et al., 2004 and Biswas, 2012). In the 1970s, countries in Asia and Africa also considered dam construction as a means for development, for example, construction of the Hirakud Dam in India, Volta Dam in Ghana, High Aswan Dam in Egypt, dams on Euphrates and Tigris Rivers in Mesopotamia Iraq (El-Shinnawy et al., 2000; Biswas, 2012).

Construction of dams in the environment has both positive and negative impacts downstream (Uyigue, 2006).

2.3.1 Impact of Aswan High Dam on Nile River

The floodplain of River Nile downstream of Aswan High Dam is similar to the present study, irrigation activities take place during the dry season period. The Aswan High Dam is a hydroelectric power plant that produces half of Egypt's electrical power supplies (Arsenault et al., 2007). The Aswan High Dam was started to work in the year 1970. The design details for the dam include: length is 3,600 m, the base width is 980 m, top width is 40 m, and height is 111 m (Arsenault et al., 2007). The Nile River has an average flow of about 50 m^3/day during the dry season period, while in the rainy season the average value is approximately 700 m^3/day. The positive and negative impacts of Aswan High Dam on the downstream include:

Positive impact of the Aswan High Dam

The construction of the Aswan High Dam increases agricultural production in both rainy and dry season farming along the River Nile floodplain by storing excess water and managing release at times of need. The Aswan High Dam construction controls the floods of the Nile River. This enables more irrigation activities by the farmers along the alluvial floodplain of River Nile (Arsenault et al., 2007).

A consequence of the construction of Aswan High Dam is the maintenance of increasing water seepage from the Nile River to the floodplain shallow alluvial aquifers during the dry season period. This has increased agricultural production on the alluvial floodplain (Tahmiscioğlu et al., 2004).

Negative impact of the Aswan High Dam

The construction of the Aswan High Dam has resulted in low water flow in the River Nile during the dry season period, thereby restricting navigation on the Nile River Basin.

The post-dam Nile has created a problem in terms of coastal erosion (Biswas and Tortajada, 2012). Before the dam was constructed, the River Nile carried a high sediment load during flood period. However, after the Aswan High Dam construction, the sediment load increased along the Nile River due to its low flow. The dam has had a serious impact on these sediment loads even far downstream, and has caused significant erosion especially along the Mediterranean coast (Biswas and Tortajada, 2012).

2.3.2 Lagdo Dam in Cameroon

The Lagdo Dam is constructed across the River Benue in Garoua, Cameroon. It links to the Nigerian border at a distance of 100 km (see Figure 2.4) and about 250 km from Yola (see Figure 1.1). Situated at latitude 8° 53’ and longitude 13° 58’, the surface area of the reservoir

is about 700 km^2 while its depth is 45 m (Ali et al., 2010). The dam was built for generating electricity and irrigation activities downstream but still within Cameroon. Table 2.1 shows the design details of the dam.

Table 2.1: Basic design details of Lagdo Dam in Cameroon (Toro, 1997)

Maximum flood level (m)	210
Minimum operating level (m)	206
Reservoir capacity (billion m^3)	8
Height (m)	45
Average inflow (m^3/s)	260
Area of reservoir (km^2)	800
Release from 4 turbines (m^3/s)	230
Irrigation Area (ha)	1,000
Total land area for irrigation (ha)	40,000

2.3.2.1 Impact of Lagdo Dam

The construction of Lagdo Dam in Cameroon has had both positive and negative impact on its immediate downstream users. Since the construction of the dam, Upper Benue River Basin Development Authority (UBRBDA) has been monitoring the hydrological and flow regime within the River Benue valley in Nigeria (Toro, 1997).

2.3.2.2 Positive effects of Lagdo Dam downstream

The construction of the Lagdo Dam on River Benue valley in Cameroon resulted in an increased water flow in River Benue during the dry season period, which keeps the groundwater of alluvial aquifers at an artificially high level downstream. This facilitates abstraction using the low-cost hand-drilling techniques. Therefore, this has a similar positive impact to that of the Aswan High Dam.

Some of the immediate benefits of Lagdo Dam in Cameroon to the downstream users in Nigeria especially Yola region, include the following:

i. Increased in dry-season flow.

ii. Flood control and reclamation.

iii. Regulatory structures to be constructed across the River Benue valley.

Before the Lagdo Dam construction, minimum flow in River Benue at Yola gauge station (November to June) during the dry season period used to be 10 to 20 m^3/s (Toro, 1997). However, after the dam construction and the start of its operation in 1984, the minimum water flows rose to about 60 m^3/s, tripling the water level in the River Benue after the dam's construction. This is very important for irrigation activities along the River Benue valley downstream (Toro, 1997). Increased flows during the dry season will result in more recharge to the aquifers along the floodplain bank, which could be exploited easily for the irrigation activities using hand-drilling techniques.

After the Lagdo Dam construction across the River Benue upstream in Cameroon, high water levels in the River Benue, which used to occur in July to November each year, have been substantially reduced. Reduction of the flood peaks is of benefit to adjacent farm lands for irrigation activities along the floodplain of the River Benue valley and to the settlements such as people living close to the River Benue bank (Toro, 1997). The dam resulted in reducing the floods peaks and water volume downstream especially the study site. This will reduce the cost of any structure to be built across the River Benue (Toro, 1997).

It is important to know that a mutual agreement between the Cameroonian and Nigerian Governments is necessary, in order to allow a constant release of water from Lagdo Dam to maintain flow in River Benue in the dry season period.

2.3.2.3 Negative effects of Lagdo Dam downstream

Some of the negative impacts of Lagdo Dam downstream include i. riverbed siltation, ii. loss of floodplains, and iii. Navigation constrains along the river (Toro, 1997).

The dam resulted to the substantial reduction in the high flow required to clear the sediment load from River Faro and other tributaries. These led to the siltation along the River Benue, which affects the pumping stations along the River Benue floodplain (Toro, 1997). Similarly, siltation of the riverbed has affected gauging and discharge stations measurements.

The Lagdo Dam construction upstream has resulted high peak of water levels in River Benue during the rainy season, which has reduced the navigation period. The navigation period along River Benue used to be four months (July to October) each year. However, after the dam construction the navigation periods were reduced to one and half month (Toro, 1997). In addition, to the year to year natural variability of the flow, one has to now to incorporate changes in the dam management, often made without taking in consideration the fields and the people downstream both in Cameroon and Nigeria.

2.4 Criteria for suitability of hand drilling techniques

This section presents the criteria for assessing the suitability and sustainability of hand drilling techniques for abstracting the shallow floodplain alluvial aquifers. The following parameters would be used to define criteria for assessing the suitability of hand drilling techniques in the present alluvial sediment and of similar alluvial floodplains.

Estimating the suitability for hand drilling methods can be based on the following criteria:

- The geological suitability
- The suitability based on sediment permeability

- The suitability according to the water depth
- The geomorphological suitability
- The suitability according to the shear strength forces

2.4.1 The geological suitability

Geological suitability is related to the hardness of the layers of rock formations (Kane et al., 2013). Hand drilling techniques are only suitable for unconsolidated sediments, but do not allow drilling in hard formations. Sediment formations, which are suitable for application using hand drilling, are soft sand, silt and clay (Weight et al., 2013). However, there is currently no available information on geological suitability in the present study despite hand drilling being commonly used. Characterising of the alluvial floodplain sediment in the present research will be used to assess and understand the geological suitability of hand drilling methods. According to the review above, the geological suitability for hand drilling method is based on the soft unconsolidated alluvial floodplain formations.

2.4.2 The suitability based on sediment permeability

The permeability characteristic suitable for hand-drilled wells is about the possibility to manually drill a small shallow borehole in permeable ground that can yield a significant flow rate (Kane et al., 2013). It is important to understand whether the types of sediment formation been drilled are permeable or impermeable. Permeability is an ability of sediment formations to transmit water through it (RWSN, 2010). Different types of sediment formation encountered during drilling include sand and silt, mixed formations and clay. Table 2.2 shows classification of the particle sizes in an alluvial sediment samples.

- Sand and silt formation: It allows easily flows of water through the open space between the sediment particle sizes and thus, very permeable. When drilled through

this type of formation, water fills the borehole easily, which can be abstracted using hand drilling method for irrigation activities.

- Mixed formations: consists of a mixture of sand, silt and clay. Water flows slowly through the mixed formations and they are described as semi permeable. When drilled through this type of formation, it allows a slow flow of water into the well.

- Clay: clay particles are very sticky and water does not easily flow through its formation and thus, are impermeable. When drilled through this type of formation, it does not allow flow of water into the well and the well will be empty.

Table 2.2: Classification of the particle sizes in a sediment sample (RWSN, 2010)

S/No	Particle name	Particle size (mm)
1	Clay	<0.004
2	silt	0.004 to 0.06
3	Sand	0.06 to 2

Among the criteria discussed above, sand and silt, and mixed formations are suitable for application for hand drilling techniques, because the formations allow the flow of water to recharge a well, which can be easily abstracted for irrigation. Sandy silt formations are very permeable, they allow the flow of the groundwater easily through the open space and are therefore suitable layers for hand drilling methods.

2.4.3 The suitability according to the water depth

Suitability according to water depth is related to the depth where exploitable water level can be found and reached by hand drilling. Study by Kane et al. (2013) reported that the groundwater depth suitability consists of identifying areas where exploitable flowing groundwater at a depth compatible with hand drilling techniques could be found. Generally, hand drilling is suitable when exploiting water not deeper than 40 m (RWSN, 2010; Fussi,

2011; Kane et al. 2013); although in specific areas, it can be applied up to 100 m or more (Forsyth et al., 2010). Therefore, the depth range between 20 and 40 m in the alluvial floodplain groundwater are suitable for abstraction using hand-drilling techniques. Our literature review has shown that the shallow aquifer on the alluvial floodplain formation at Yola does not exceed 40 m (Obiefuna and Orazulike, 2010).

2.4.4 The geomorphological suitability

Geomorphological suitability refers to the existence of a surface morphology that facilitates the accumulation of unconsolidated materials, the presence of thick weathered layers and the limited depth of water. These zones correspond with bottom of the valley and sometimes with flat area with limited slope (Fussi, 2011; Kane et al., 2013).

In general, hand drilling is considered feasible in unconsolidated alluvial formations (sand, silt and clay) with interspersed layers of soft sedimentary rock or laterite (PRACTICA, 2010). General mapping of hand drilling may be based on analysis of existing data such as local hydrogeological information, interviews and discussion with the population. Detailed data regarding existing water points both from existing information as well as direct field observation, topographical maps, well logs, field surveys, geological maps, satellite images and shuttle radar topography information can provide an indication of the potential for hand drilling in a region (PRACTICA, 2010; Carter et al., 2010).

2.4.5 Suitability according to the shear strength forces

This refers to the forces applied on the alluvial floodplain sediment during drilling process (Eijkelkamp, 2009; Chung et al., 2012). Hand drilling methods are undertaken using human muscle power; therefore, it is useful to estimate the forces applied to the alluvial floodplain sediment. Field Shear Vane Tester gives an idea on the shear strength forces on the floodplain

sediment. Understanding shear strength forces on the floodplain sediment is one of the criteria for assessing hand-drilling techniques.

There are no clear correlations between shear strength forces in relation to hand drilling in literature. However, some studies reported values of shear forces in relation to sediment formations. Recent study by Hubbell (2003) reported shear strength forces ranging between 12 and 95.8 kPa obtained using Field Shear Vane, for very soft to stiff sediment formations and between 102 to 179 kPa for very stiff to hard sediment formations. In earlier study, Schjønning (1986) reported shear strength forces ranging between 38 and 102 kPa on coarse sand formations, and shear forces ranging between 96 and 172 kPa on fine loam sediment formations. Schjønning (1986) used a Field Shear Vane together with power drilling to obtain shear strength. However, no mention of shear forces was made only comparing shear forces was reported. Similarly, Eijkelkamp (2009) measured borehole shear forces between 32 to 95 kPa using a Shear Vane. Therefore, based on the above information it can be assumed that the shear strength forces in the range between 12 and 95 kPa are suitable for drilling with human power, and forces greater than 100 kPa are above hand drilling with human power.

In brief, although hand drilling is commonly used in the area of study, we do not know if it is the optimal method, or if it is used near the limit of the (capacity) applicability.

2.5 Reviewing existing hand-drilling techniques

Hand-drillings are being performed by human power. The methods include hand augering, hand percussion, hand sludging, hand jetting, rota sludge, pounder rig drilling, Baptist drilling, EMAS drilling, Water For all International (WFAI) hand drilling etc. (RWSN, 2008). Hand drilling can be undertaken by small enterprises.

Below are reviews of existing hand-drilling techniques for drilling of boreholes in unconsolidated formations especially alluvium formations along riverside area.

2.5.1 Hand augering drilling

Hand augering drilling (Figure 2.12) is performed by rotating and pushing the drilling tool into the ground to the desired depth. The drilling tools consists of heavy tripod, extendable steel rods, drill rods and drill bits (Von, 1988; Naugle, 1991; Bob, 1994; Naugle, 1996; Carter, 2005; Ochoe et al., 2008; Danert, 2009; Van der Wal et al., 2010; Vuik et al., 2010).

Figure 2.12: Auger hand-drilling technique (RWSN, 2009).

The capacity of hand augering is suitable for soft formations to slightly consolidated rock formations, non-collapsing sands and silts (Bob, 1994, 2008; Carter, 2005; Danert, 2009; Vuik et al., 2010). Hand augering drilling can be carried out by two people to drill a well. In practice, about 20 m is the limit depending on geology and formations of the sediment (Carter, 2005; Danert, 2009).

2.5.2 Hand percussion drilling

Hand percussion drilling (Figure 2.13) consists of rising and lowering a hammering drilling bit attached to a rope to the pulley into a hole to lose a formation. The loose material is then extracted using a bailer (Bob, 1994; Carter, 2005; Ochoe et al., 2008; Danert, 2009; Van der Wal et al., 2010; Vuik et al., 2010; Bill, 2011). This kind of drilling technique is suitable on soft formations to slightly consolidated formations, for example, clay and stiff silt (Vuik et al., 2010). Depths of 20 to 30 m can be achieved with this kind of technique (Danert, 2009; Van der Wal et al., 2010; Vuik et al., 2010).

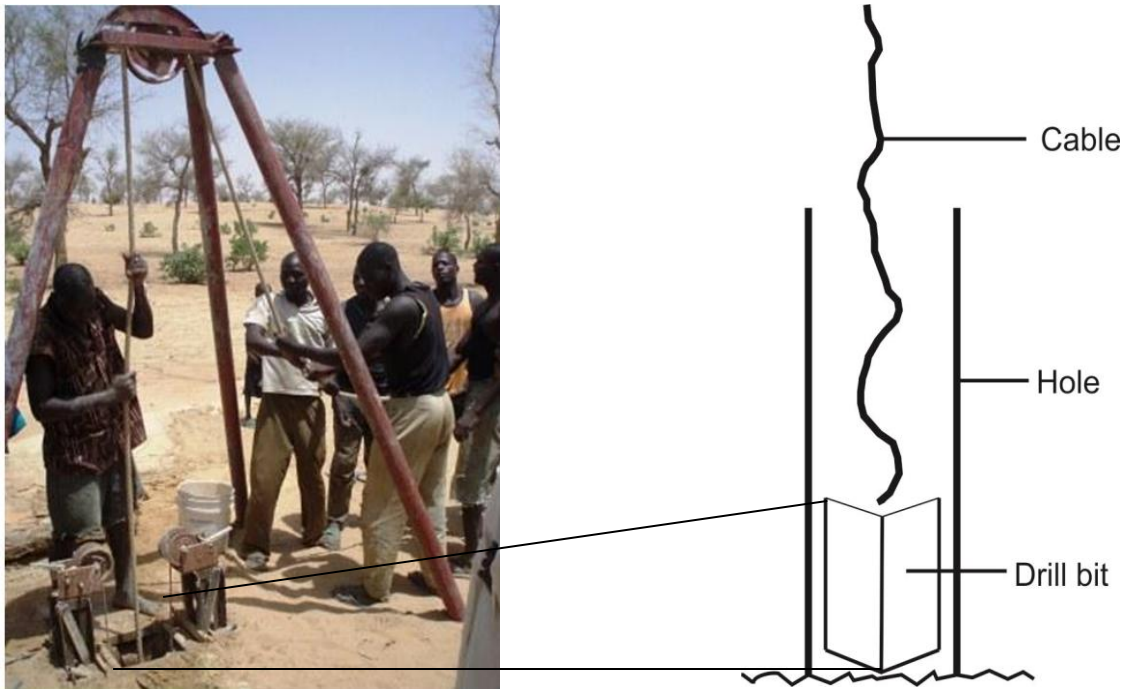

Figure 2.13: Hand percussion drilling (Labas et al., 2010). Sketch of percussion drilling technique.

2.5.3 Sludging hand-drilling

Sludging hand-drilling (Figure 2.14) is a low-cost hand-drilling technique. The operational principle consists of reciprocating a drilling pipe down a hole full of water. One operative who operates the lever accomplishes drilling. On the top stroke and other operative uses his hand to seal the pipe that serve as valve and on the down stroke his hand is released to allow

drilling cuttings out of the hole (Carter, 2005; Danert, 2009). Sludging hand drilling is suitable in sand and silt formation (Carter, 2005; Danert, 2009; Van der Wal et al., 2010; Vuik et al., 2010). Depths of up to 15 m are most common with this type of technique (Danert, 2009).

Figure 2.14: Hand sludging drilling technique (Labas et al., 2010).

2.5.4 Rota sludge hand-drilling

The Rota sludge hand-drilling technique (Figure 2.15) is similar to the hand sludging hand-drilling techniques. Drilling is achieved by placing a hand on the top of the drilling pipe, which acts as a valve. When the pipe is at lower stroke, the hand is released, allowing drilling bits to circulate enable drilling downward (Van Herwijnen, 2005; Danert, 2009). The technique is suitable in unconsolidated formations. Depths of up to 15 m can be reached with this method.

Figure 2.15: Rota sludge hand-drilling (Weight et al., 2012).

2.5.5 Jetting hand-drilling

Jetting hand-drilling (Figure 2.16) consists of pumping water using a machine through a hollow drilling pipe. The impact of the pumped water loses sediment in the hole allowing downward penetration of the drilling pipe to the desired depth (Bob, 1994; Carter, 2005; Segalen et al., 2005; Danert, 2009; Van der Wal et al., 2010; Vuik et al., 2010). Drilling with this type of technique is suitable in unconsolidated material, for example sands and silts formations and soft clay formation. Depths of up to 20 m or more can be achieved (Carter, 2005; Danert, 2009; Vuik et al., 2010; Danert, 2013).

Figure 2.16: Jetting hand-drilling technique (RWSN, 2013).

2.5.6 Baptist hand-drilling

Baptist drilling (Figure 2.17) consists of an operational principle between percussion and sludging hand drilling technique. The difference is that Baptist hand-drilling uses a valve incorporated to the drilling bit at the bottom of the drilling pipe, while percussion and sludging hand-drilling techniques uses a hand as a valve (Paul, 2007a; Danert, 2009; Danert, 2013). This method is suitable in unconsolidated formations and depths of up to 30 m deep or more can reach with this technique (Paul, 2007a).

Figure 2.17: Baptist hand-drilling technique (Paul, 2007 a).

2.5.7 EMAS hand-drilling

The EMAS hand-drilling (Figure 2.18) is a hybrid between percussion and jetting hand-drilling techniques. The operational principle consists of pumping water through a hollow drilling pipe using a hand-pumping machine. Lifting and dropping the drilling pipe mounted on a drilling lever allows downward penetration of the drilling pipe to the desired depth (Paul, 2007b; Danert, 2009; MacCarthy et al., 2013; Danert 2013). This method can reach depths of up to 30 m or more in unconsolidated loose formations, and can be constructed in any available local welding workshop (Paul, 2007b).

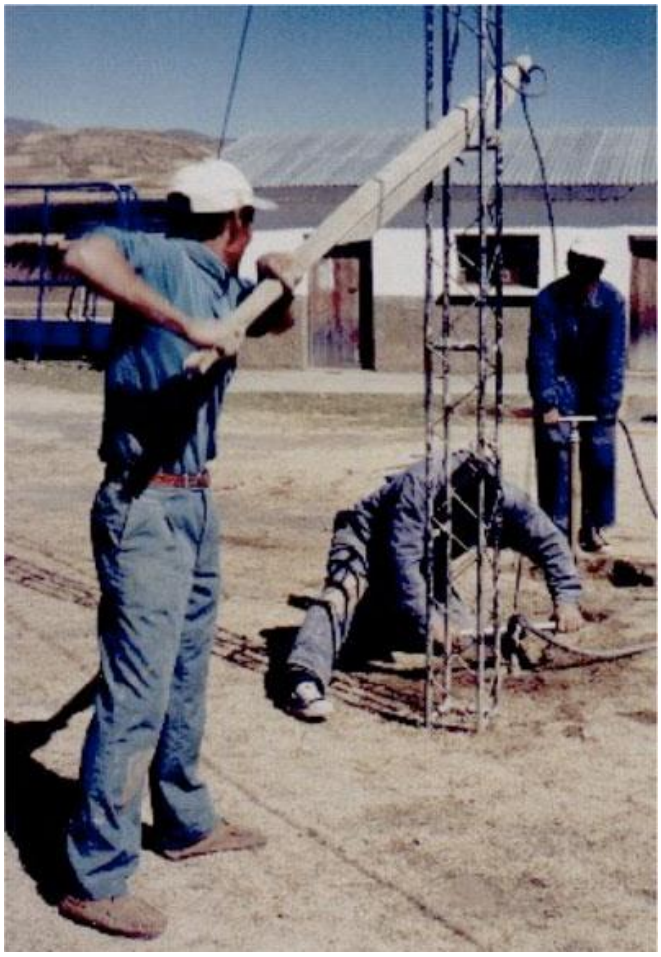

Figure 2.18: EMAS hand-drilling (Paul, 2007b).

2.5.8 Banka hand-drilling

The Banka hand-drilling (Figure 2.19) is intended for use in boring alluvial beds of any kind, to a depth of around 15 m and more. The world record is believed to be 47 m but, at this depth, lowering the sand pump and withdrawal of the same took half to three quarter of an hour and as many as ten men were needed to lift the pump (Akkeringa, 2006). The Banka hand drilling is not suitable where boulders exist. Preliminary boring with a large auger (or a torque drill) starts borehole, which must be kept vertical. At least four men are needed for the operation; two for keeping the bore rod in a vertical position, and the other two men for turning the drill, then the casing (Akkeringa, 2006).

Figure 2.19: Banka hand-drilling (Swiecki, 2011).

2.5.9 Pounder rig hand-drilling

Pounder rig hand-drilling (Figure 2.20) is a derivative of low-cost hand drilling tested on the basement rocks formations in Africa (Carter, 2005). The pounder rig is a human-powered rig, which can drill clay, silt, sand, gravel, laterite and limited amount of hard rock (Carter, 2005). The Pounder rig uses a carbon steel drill pipe, a pipe coupling, a steel frame and pivot and the skill of the operators to rapidly drill through soft alluvial material (Danert, 2003; Carter, 2005; Danert, 2013). The drilling method involves reciprocating a water filled pipe in a water filled hole; the drill bit, at the base of the drill pipe loosens the formation which is carried up inside the pipe due to the operation of a flap valve at the top (Danert, 2003). This valve holds the water and drill cuttings in suction on the upstroke and releases them on the down stroke. The water and cuttings emitted from the top of the pipe are directed on to a plate by a bucket (Danert, 2003). The drill pipe is attached to the lever via a chain and reciprocated by rising and lowering the lever via ropes at both ends. Drill pipe is added as the hole is progressed

(Danert, 2003). A counter balance can be fitted to the lever to aid in lifting the drill pipe as it becomes heavy (Danert, 2003).

Figure 2.20: Pounder rig hand-drilling (Ball and Danert, 1999).

2.5.10 Water For All International drilling

The Water For All International (WFAI) drilling method (Figure 2.21) relies on a hybrid of sludge and percussion drilling technology to drill boreholes up to 105 m deep in soft alluvial formations (Forsyth et al., 2010). With a specialised drill bit and a tripod or derrick system, the WFAI drilling method combines the advantages of percussion drilling, such as being able to drill through soft rocks (Forsyth et al., 2010). The drilling method consists of a tripod stand to prevent the drill pipe from popping out when the poles bend underweight. A pulley is hung from the center pole to ensure maximum stability, and a rope is then run through the pulley and tied to the drilling stem. The drill bit is attached to the bottom of the drilling pipe via a coupling. This bit acts as a one-way valve, while the drilling pipe is suspended via the

opening. Cuttings and mud are forced into the drilling pipe and expelled at the top of the pipe during the peak of the stroke (Forsyth et al., 2010).

Figure 2.21: Water for All International hand-drilling (Forsyth et al., 2010).

2.5.11 Advantages and disadvantages for the various hand-drilling techniques

Table 2.3 summarises the advantages and disadvantages for the hand-drilling techniques discussed above. The most common advantages for the techniques include easy penetration in soft sediment formations and the equipment can be locally constructed in any available arc-welding workshop. The most common disadvantages for the techniques include hard formations, which cannot be penetrated easily, and the methods require human power for the operation so producing a well is time consuming.

Water For All International (WFAI) drilling techniques attain greater depths (>100 m) than the other drilling methods (Table 2.3). This is because WFAI consist of a specialised drill bit and a tripod. The WFAI drilling pipes were made of galvanised steel and this reduces the weight of the pipe and allows for drilling to reach a greater depths.

Table 2.3: Advantages and disadvantages for the various hand-drilling techniques (Source: Bob and Rod, 1994; Sonou, 2010; Van der Wal et al., 2008; Ochoe et al., 2008, Akkeringa, 2006; Segalen et al., 2005; Burrows, 2006; Paul, 2007a). Methods 1 to 9: maximum depth 40 m; method 10: depth down to 100 m

SN	Method	Advantages	Disadvantages
1	Hand augering drilling	- Easy to use above the groundwater table - Penetrates soft materials effectively specially clay	-Slow, compared with other methods -Equipment can be heavy -Water is needed for dry holes -Uncoupling extensions slows work at greater depths
2	Hand percussion drilling	- Suitable for a wide variety of rocks - Operation is possible above and below the water table - It is possible to drill to considerable depths	-Equipment can be heavy -Water is needed for dry holes to help remove cuttings -Difficulty in bringing large gravel or stones to the surface -The equipment is relatively expensive
3	Sludging drilling	- The method does not use much water - Cuttings are removed continually while drilling - Drilling is possible on clay and semi-consolidated formations	-Water is required for pumping -The water table is not known during drilling
4	Rota sludge drilling	- The technique can drill through semi consolidated sandy formations and most clay - Casing is not required during drilling	-The borehole stays open by water pressure, this causes borehole collapsing -Coarse gravel and other highly permeable materials retard drilling process
5	Jetting drilling	- The equipment is simple to use - Possible above and below water table - Drilling is very fast in loose sand formations	-Water is required for pumping -Difficulty in bringing large gravel or stone to the surface
6	Baptist drilling	- Clay mud does not restrict drilling process - Length of extension drilling pipe does not restrict drilling process	-Requires high quality drilling pipes -More manpower is required to pull drilling pipe below depth of 20 m deep
7	EMAS hand-drilling	- It can drill in all kinds of loss soils - Less endangerment of the workers than when digging an open well	-Generally limited to sandy soils and soft clay -Water is required for the drilling
8	Banka hand-drilling	- In sandy or loose soil, boring and sinking the casing are carried out simultaneously - It can be used where a series of borings are to be made at short distances apart	-It requires more men for the drilling process
9	Pounder rig hand-drilling	- Can drill through limited amounts of hard rock	-Slow progress in hard formation -Limited experience available
10	WFAI hand-drilling	- In loose formations it can drill more than 100 m - Can drill cohesive formations	-The diameter of the borehole is less than 10 cm, this limits water production per pump

Table 2.4 shows the comparison between hand drilling and power drilling and it shows the advantages of hand-drilling techniques over machine drilling in terms of drilling to abstract shallow floodplain groundwater. In the environment like Yola region most of its people practice dry season farming along the alluvial floodplain of River Benue. Farmers cannot afford to use power drilling; they need something, which is simple and portable to abstract the shallow alluvial aquifer for their irrigation farming activities. Using hand drilled wells have improved the farming potential among the small-scale farmers around the globe. Small scale farming without access to water is limited to only rainy season farming system. However, access to the shallow alluvial aquifers will improve the small-scale farming activities especially as the case in the present study. The focus of the present study is to assess the suitability of the hand-drilling techniques to abstract the shallow floodplain aquifers for the small-scale farming activities in Yola region. Table 2.4 was produced based on the personal communication with Peter Reading, Technical Director EQUIPEGROUP, UK on the 22nd November 2013.

Table 2.4: Comparison between hand drilling and machine drilling methods

SN	Hand drilling method	Machine drilling method
1	Portable to transport to the site	Require a vehicle for transportation
2	Simple technology	Technology is more sophisticated
3	Cheaper	More expensive
4	Requires little maintenance	The parts requires regular specialist maintenance
5	Level of competency required is low	It requires high level of competency
6	It can assess remote areas	Difficult to assess remote areas
7	The depth of penetration is limited by operators strength	The depth of penetration is more
8	Unable to penetrate hard formation	Hard formations are easily penetrated
9	Spare parts are locally available cheaper to buy	Spare parts are difficult to buy
10	It does not require training operator	It requires training operator

2.5.12 Application of the hand drilling techniques across the River Benue floodplain

The application of the hand-drilling techniques mentioned above along the River Benue valley depends on how they would perform in the floodplain. At the moment, the available hand-drilling techniques in the region used for irrigation purposes for abstracting groundwater are hand augering and jetting hand-drilling techniques, with most farmers using hand augering for irrigation purposes (Figure 2.22). The augering hand-drilling kit in the state can drill up to 20 m deep or even more depending on the alluvial formations. The study carryout by Adekile and Olabode (2009) to assess hand drilling in Nigeria for irrigation along the floodplain, also reported similar practices of hand-drilling techniques.

Figure 2.22: Pulling pipe out of borehole drilled with locally hand drilling augering method in the study area (The photograph taken by Mohammed Abana Girei on 15th April 2011).

2.6 Fieldwork and laboratory descriptions

2.6.1 Surface elevation

Surface elevation will help in understanding the groundwater characteristics underlying the shallow alluvial floodplain, for example, the recharge process and direction of groundwater

flow. Hence, the elevation of the floodplain surface is a key element in a groundwater modelling study and the accuracy to which this elevation is determined is a critical factor in the accuracy of the final modelling results.

Elsewhere, elevation heights have been used to delineate alluvial deposits within the active floodplain. As reported by Sander (2001), elevation height on the floodplain surface plays significant role to the groundwater. For example, the top of the water table across the floodplains depends on the surface elevation because groundwater is always lower than the surface elevation. Similarly, surface elevation affects the rate of precipitation seepage on a catchment area, for example, on a slope surface less water seeps into the ground, while on the flat surface more water infiltrates into the ground to raise groundwater level. Identifying the lower and higher elevation along the floodplain is useful for comparing to the groundwater level and to understand the direction of the water flow. Knowing the groundwater levels and directions across the floodplain is essential in the groundwater modelling.

2.6.2 Sedimentology

This section reviews the process usually followed for understanding and characterising the sediment on the floodplain. A range of sedimentological method was used as a first step to characterise the floodplain, as no studies are available. This is a useful first step before embarking on more specifically hydrological techniques, which are also reviewed here.

2.6.2.1 Particle size distribution

Particle size distribution (PSD) is required to understand the hydrological and structural properties of the sediment samples, which is used to understand the rate of flow through the formation layers. PSD provides a good way of characterising sediments and soils for purposes of assessment and interpretation (Wanogho et al., 1985; Junger, 1996; Sugita and Marumo,

2001; Pye and Blott, 2004; Blott et al., 2004; Blott and Pye, 2006; Cheelham et al., 2008; Di Stefano et al., 2010). PSD is useful in the drilling process as coarser sediment size allows easy drilling while finer grain size reduced drilling rate. Grain-size parameters of bulk sample have been commonly used as environmental indicators in sedimentary samples investigations (Makaske et al., 2002; Watson et al., 2013). The PSD forms one of the key parameters of understanding nature of alluvial sediments as the case for the River Benue floodplain.

Although, no universal model exists to distinguish past depositional environments based on particle size data (McLaren, 1981; McManus, 1988), the PSD of sediment can provide indications of the energy conditions transport mechanisms and sorting processes affecting a depositional location (Asselman and Middlekoop, 1995; Long et al., 1996).

Floodplains are complex and varied in sedimentary environments, where sedimentation is conditioned by a variety of factors, including river flow and topography (Dyer, 1979). Floodplain sedimentary sequences may contain a wide range of particle size, from cohesive clays and silts associated with sands and gravels of channel fills. PSD are therefore a valuable tool in the study of past depositional environments within alluvial floodplain settings, assisting in the identification of both long-term changes related to the evolution of the alluvial floodplain and in the identification of specific sub-environments (Dark and Allen, 2005).

Wide ranges of granulometric techniques are available to the sedimentologist (McManus, 1988). In the study of sediment samples from floodplain and coastal sequences, instruments using X-ray nephelometry or the scattering of laser or polarised light have largely replaced the older methods based on the pipette, hydrometer or coulter counter (Allen and Thornley, 2004). Laser diffraction requires little time for analysis for a wide size range of samples and requires small size samples (Magilligan, 1992; Storti and Balsamo, 2010). The diffraction

pattern is used to determine the size of the particle from light scattering method developed by Mie theory (Allen, 1997).

2.6.2.2 Loss on ignition

Loss on ignition (LOI) is frequently used as a measure of the organic and carbonates content of floodplain sediments. The moisture content, organic matter and carbonate content of the sediment samples can be estimated by weight loss measurement by subjecting the sediment samples to various and successive heating levels (Abbott, 2005). In sediment deposition, organic matter and carbonate content are important in order to understand the sediment through which the water flows. Estimate of LOI in sediment samples consists of all kinds of living and non-living materials, and faecal materials (Rowell, 1994).

Depending on transportation and depositional process mechanisms, sites may receive organic matter or carbonate content from various sources. Determining LOI consists of three stages (Heiri et al., 2001). In the first stage, moisture content of the sediment is determined by heating the sample at 105 $^{\circ}$C overnight, in the second stage organic matter and other stuff are destroyed by heating the samples at 550 $^{\circ}$C for 2 hours, while in the third stage carbonate content is destroyed by heating the samples at 950 $^{\circ}$C for 4 hours (Heiri et al., 2001; Shuman, 2003; Santisteban et al., 2004; Beasy and Ellison, 2013).

2.6.2.3 Magnetic susceptibility

Magnetic susceptibility (MS) estimates the amount of magnetic minerals in sediments and is defined as the ratio of magnetisation induced to intensity of magnetising field. (Thompson et al., 1975; Lees et al., 1998). According to Dearing (1999), measurement using MS may enable us to:

- Classify different kinds of materials.

- Identify the processes and origin of their formation or transport.
- Create environmental fingerprints' for matching materials.

In this study, we are especially interested in sediment origin and diversity. The study of the magnetic properties of environmental materials, or environmental magnetism, has a wide range of applications (Thompson and Oldfield, 1986; Dearing et al., 2001). MS analyses provide information relating to the physiochemical status of iron minerals within sediments and can provide a powerful diagnostic tool in various depositional environments for the study of sediment source areas (Thompson et al., 1975; Oldfield et al., 1985; Nawrocksi et al., 2009). In the floodplain environment, magnetic properties of sediment may be related to sediment sources, hydrodynamic regime and post-depositional diagenesis (Rey et al., 2000; Emiroglu et al., 2004). As reported by Butler (2003) MS of sediment material can have an average of 5×10^{-4} (SI), while for sediments from sedimentary materials it can reach up to 1.5×10^{-3} (SI).

In this study, a basic characterisation of the MS of the sediment samples is undertaken. MS measures magnetism between sediment materials such as ferromagnetic minerals magnetite (Fe_3O_4) and maghemite (γFe_2O_3) (Schwertmann, 1985; Laven et al., 1989). The floodplain alluvial sediments could show magnetic properties from the Fe oxides in different ways, for example, Ferromagnetic minerals, Paramagnetic, anti-ferromagnetic (Hendrick et al., 2005; Fialova et al., 2006; Jonas, 2008).

The magnetic behaviour of all materials can be classified into five major groups which include diamagnetism cations which have not net magnetic moments (e.g. quartz, calcite, water), paramagnetism (e.g. biotite, pyrite, siderite), ferromagnetism (e.g. cobalt, iron, nicket), ferrimagnetisms (e.g. magnetite) and antiferromagnetism (e.g. hematite) (Sandgren and

Snowball, 2002). Sediment deposits generally contain a range of minerals of magnetic properties that belongs to the above groups.

The MS of a site typically has a unimodal distribution with a narrow peak (Bulter, 2003; Pestrovsky et al., 2000). Sediments formed from sedimentary materials typically have a lower MS than igneous source material (Dearing, 1999). MS patterns could originate from different sedimentation processes such as chemical or detrital deposition, variable mixing effects and different accumulation rates (Thompson and Oldfield, 1986; Rowell, 1994). The results may also be used to detect changes in time, in the vertical and in horizontal dimensions.

2.6.2.4 Field Shear Vane Tester

The Field Shear Vane Tester (FSVT) (Figure 2.24) is an instrument used to measure the *in-situ* undrained strength in the field and can determine the maximum shearing force exerted on sediment or cohesive soils. FSVT consists of handle, spiral-spring, upper part, lower part, graduated scale, vane shaft and vane (Figure 2.24). The sizes of the vanes range from 16 x 32 mm (extra) multiplying readings by a factor of 2, 20 x 40 mm (standard) multiplying readings by factor of 1 and 25.4 x 50.8 mm (extra) multiplying readings by factor of 0.5. This makes it possible to measure shear strength of 0 to 260, 0 to 130 and 0 to 65 kPa respectively (ELE International, 2006; Eijkelkamp, 2009). The instrument can determine shear strength on sediment up to 3 m deep.

Table 2.5 is derived from one of the area studies attempting to link shear strength forces to direct drilling (machine drilling). It shows the values for shear strength (kPa) determined for undisturbed soils as compared to values obtained from direct drilling devices such as machine drilling.

The FSVT is considered the reliable and preferred method for estimating the undrained shear strength due to the relatively poor quality data obtained in laboratory tests (Chung et al., 2012). Figure 2.23 shows the failure surface of vane, at the failure surface the shear strength forces on the sediments have reached.

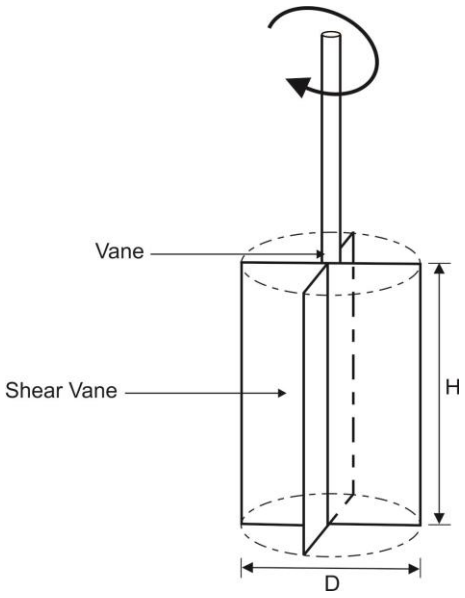

Figure 2.23: Assumed failure surface of the Field Shear Vane Tester on vane surface. H – vane height, D – vane diameter (Modified after Foguet et al., 1998).

Figure 2.24: A Geonor H-60 Field Shear Vane Tester, 3 Vanes and pointer and determining shear strength on sediments (Geonor, 2005; Eijkelkamp, 2009).

The FSVT is an easy way of estimating shear strength forces on sediment along the floodplain, which is useful to compare to drilling strength (Bassoulet and Le Hir, 2007).

Table 2.5: Shear strength determined in undisturbed sediment (Schjϕnning, 1986)

Soil type	Field Shear Vane Tester (kPa)	Direct machine drilling (kPa)
Coarse sand	30	38
	90	72
	150	102
Fine loam	30	96
	90	145
	150	172

Elsewhere FSVT has been used as a means of estimating shear strength on the floodplain alluvial sediments. A study by Adejumo (2012) used Field Shear Vane to estimate shear strength on the clayey floodplain alluvial sediment in Ikoyi district of Lagos, Nigeria. His result showed that shear strength increases with increase in depth because of the presence of clay. A study by Servadio and Bergonzoli (2013) estimated shear strength on agricultural sediment on the sandy alluvial floodplain in Italy and found significant penetration resistance with increase in shear strength because the formation is sandy soils with depth. This study is intended to estimate shear strength on the floodplain alluvial sediment in relation to hand drilling techniques.

2.6.3 Groundwater

This section reviews the processes to be followed for characterising the groundwater on the alluvial floodplain.

2.6.3.1 Resistivity soundings

The apparent resistivity is used to explore the floodplain groundwater and to understand the groundwater levels along the floodplains. Underground water may be characterised using parameters obtained by methods such as electrical resistivity, seismic, magnetic and gravity

methods. Resistivity survey in particular has the potential for tracing the groundwater levels in an area. For the purposes of this research work, electrical resistivity survey method using vertical electrical sounding was applied. Vertical electrical sounding is a geoelectrical method commonly used to measure vertical alterations of electrical resistivity. This method has been recognised to be more suitable for hydrogeological survey of sedimentary basins than the other resistivity methods (Kelly and Stanislav, 1993; Coker, 2012; Chambers et al., 2013; Orlando, 2013; De Carlo et al., 2013). Among the types of geophysical methods available, the Schlumberger electrical method is commonly used in the region (Ariyo and Adeyemi, 2009). Application of the vertical electrical sounding method with a Schlumberger array is popular because of its ease of operation, low-cost and its capability to distinguish between saturated and unsaturated layers (Nejad, 2009; Okolie et al., 2010; Asfahani, 2013).

Earth resistivity is related to important geoelectric parameters which include type of rocks, soil or sediment, porosity and degree of saturation (Ndlovu et al., 2010; Mogren et al., 2011; De Carlo et al., 2013). This method is regularly used to assess a wide variety of groundwater problems, for example, estimation of groundwater level in an unconfined aquifers formations (Song et al., 2012), estimation of aquifer porosity and hydraulic conductivity (Loke, 2010; Niwas and Celik, 2012), assessment of contaminants from unsaturated and saturated zones (Sainato et al., 2012), characterising the origin of the water losses through dams (Al-Fares, 2011; Moore et al., 2011), assessment of aquifer vulnerability (Gemail, 2011; Osazuwa and Chii, 2010), determination of depth, thickness and boundary of aquifer (Bello and Makinde, 2007), groundwater potentials (Coker, 2012), determination of aquifer characteristics (Perttu et al., 2011; Igboekwe et al., 2012), assessment of near-surface alluvial deposits (Orlando and Pelliccioni, 2010), determination of boundary between saline and fresh water zones (Khalil, 2006), determination of aquifer depth for indicating water-bearing strata (Burazer et al.,

2010), determination of groundwater quality (Arshad et al., 2007), estimation of aquifer transmissivity (Tizro et al., 2010) and estimation of aquifer specific yield (Onu, 2003).

Factors affecting the value of resistivity

Resistivity is one of the variable physical properties. It is therefore affected by some factors, which include the presence of water, quality, salinity, temperature and geological factors, etc.

1. Water Saturation: - The basic mechanism affecting resistivity in moist sediments and water bearing rocks occurs as a result of the movement of ions and the ability to transmit ions is governed by the conductivity which is a basic property of all materials (Abu-Hassanein et al., 1996). The presence of water in a formation results in increased conductance of electric current. In general the more water presents in a formation the lower the apparent resistivity (ρ_a).

2. Salinity of the water: - the more saline of the water, the lower its resistivity and the higher the conductivity.

3. Temperature: - Electrical conductivity of electrolytes increases with increase in temperature. For temperature up to 150 to 200 ˚C the resistivity of pore fluid decreases with increasing temperature. The dominant factor is increasing mobility of ions caused by lower viscosity of the water. Dakhnov (1962) described the relation as:

$$\rho = \frac{\rho_{wo}}{1 + \alpha T} \qquad 2.1$$

where ρ is the resistivity value; ρ_{wo} is resistivity of the fluid at temperature T; α is temperature coefficient of resistivity; α is 0.023 for T=23 ˚C and 0.025 for T=0 ˚C.

4. Water quality: - When the ionic contents of dissolve minerals increases the apparent resistivity reading increases.

5. Geological factors: - they include the amount and arrangement of pore spaces, the matrix conductivity, the porosity, sorting, shape and size of the particles, etc. (Abu-Hassanein et al., 1996). Generally, there is an increase in resistivity with decrease in porosity. That is why the basement rocks are characterised by high resistivity because of low intergranular porosity.

Table 2.6 show variation in resistivity range for different types of alluvial sediments along the floodplain.

Table 2.6: Variation in resistivity with some common materials **(**Source: Jackson, 1975 cited in Fikri and Azahar, 2011)

Material	Ranges (Ωm)
Clay and marl	1 to 100
Loam	5 to 50
Top soil	50 to 100
Clayey soils	100 to 500
Sandy soils	500 to 5000
Typical mine water	1 to 100
Typical surface water	5 to 50
Shale	10 to 80
Limestones	80 to 1000
Sandstones	50 to 8000
Coal	500 to 5000

Electronic configuration array

The principle of electrical resistivity prospecting and the technique of electrical prospecting are of different types, namely the vertical electrical sounding (VES) and horizontal resistance profiling (HRP). The various electrodes used in VES are Schlumberger array, Wenner array and dipole-dipole array (Wightman et al., 2003). In fieldwork, the various types of the surface electrode configurations are used for the current and potential electrodes in resistivity. While a large number of electrode types have been used in a resistivity survey, two have gained recognition: Schlumberger array and Wenner array.

For the purpose of this research project, Schlumberger array was used, because the Schlumberger method is easier to use in the field than the Wenner method (Wightman et al., 2003). Another justification for selecting Schlumberger electrode array is because the positions of the potential electrodes are changed only after changes in the current electrodes are noticed (Sirieix et al., 2013). This will reduce the working hours and keeps the operator errors small, because only current electrodes are moved at a time.

Schlumberger array configuration

For the Schlumberger array configuration (Figure 2.25), the current electrodes (AB) are placed much further apart than the potential electrodes (MN). Separation is continuously increased as the survey progresses while the potential difference is kept fixed until such a time when the resistance becomes too low to measure. The operational principle involves introducing current into the ground through pair of current electrode and with the aid of pair of potential electrode resistivity measurements is obtained. The pair of current electrodes is moved while a pair of potential electrodes is kept fixed. The potential electrodes are moved only when measurement become too low to measure (Wightman et al., 2003; Eke and Igboekwe, 2011; Sirieix et al., 2013). The relationship between the potential difference electrode spacing and the current electrode of AB > 6MN has to be achieved.

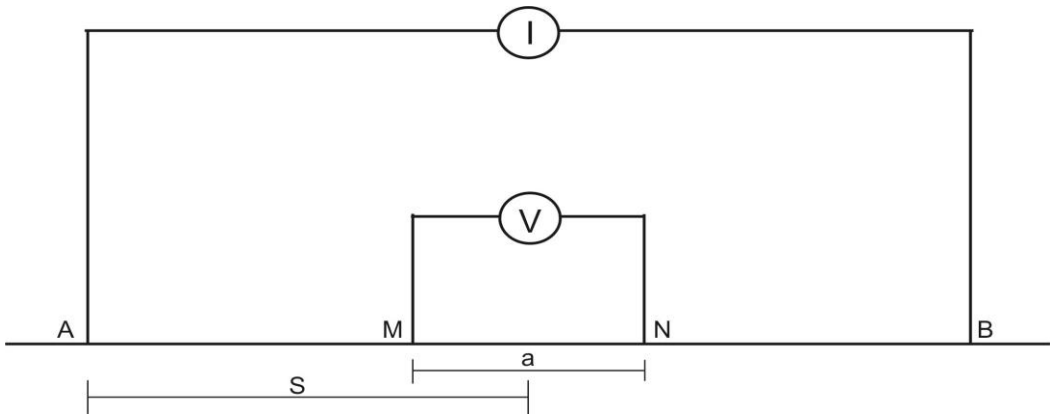

Figure 2.25: Schlumberger configuration array arrangement. AB – current electrode separation, MN – potential electrode separation, a – distance between the potential electrodes, S – midpoint-distance between current electrodes and station.

Wenner array Configuration

In the Wenner array Configuration (Figure 2.26), four electrodes arrays are used at the surface, one pair of electrode introducing current into earth, the other pair of the electrode for the measurement of the potential electrode with the current. In field operation with Wenner array all the four electrodes area moved between the successive observations (Wightman et al., 2003). Each potential electrode is separated from the adjacent current electrode by distance, "a" which is one-third the separation for the current electrode.

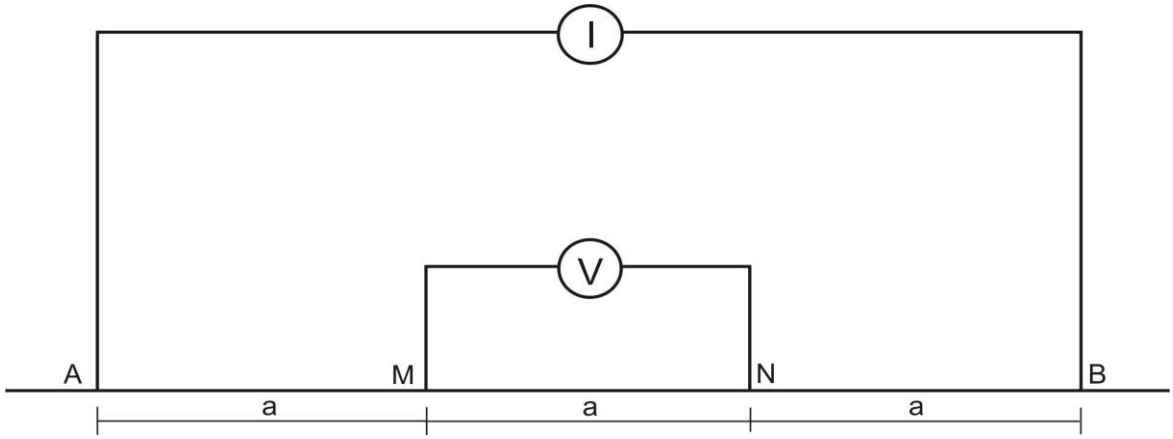

Figure 2.26: Wenner Configuration array arrangement. AB – current electrode separation, MN – potential electrode separation, a – distance between the electrodes.

2.6.3.2 Hydraulic conductivity

This section reviews the processes to be followed in order to estimate hydraulic conductivity in the floodplain alluvial sediment from both laboratory and pumping test analysis.

2.6.3.2.1 Laboratory hydraulic conductivity

Permeability is the ability of a material, for example sediment or soil, to allow the passage of a fluid such as flow of water through it, also known as hydraulic conductivity (BS 1377 – 1, 1990; BS EN ISO 22282-4, 2012). Hydraulic conductivity is an important parameter in relation to the flow of groundwater through an aquifer system; it is defined as the capacity of

a permeable medium to transmit water (Driscoll, 1986). Table 2.7 shows different ranges for the hydraulic conductivities for sediments and soils, it will serve as a guide to interpret my results.

Table 2.7: Different ranges for the hydraulic conductivities for sediments and soils

	Minimum value (m/s)	Maximum value (m/s)	Mean value (m/s)	Method
1	9.03×10^{-3}	3.3×10^{-1}	7.53×10^{-2}	Hazen (1893)
2	1.60×10^{-3}	2.16×10^{-1}	4.63×10^{-2}	Harleman et al. (1963)
3	3.77×10^{-5}	2.13×10^{-4}	1.20×10^{-4}	Masch and Denny (1966)
4	9.50×10^{-5}	1.28×10^{-2}	2.86×10^{-3}	Uma et al. (1989)
5	6.80×10^{-7}	1.13×10^{-5}	3.46×10^{-6}	Uma and Leohnert (1994)

Hydraulic conductivity is an important factor in relation to the flow of groundwater through an aquifer system. Hydraulic conductivity depends on sediment porosity and connectivity of pores, which are functions of the type of sediment (size distribution and percentage of fine material) (Freeze and Cherry, 1979). The typical hydraulic conductivity ranges for clay, silt, sand and gravel are shown in Table 2.8.

Table 2.8: Typical hydraulic conductivity ranges for clay, silt, sand and gravel (Freeze and Cherry, 1979; Driscoll, 1986)

Lithology	Hydraulic conductivity range (m/day)
Clay	10^{-7} to 10^{-4}
Silt	10^{-4} to 1
Sand	10^{-2} to 10^{3}
Gravel	10^{2} to 10^{5}

2.6.3.2.2 Pumping test

The pumping test is used to estimate *in-situ* aquifer properties across the floodplain sediment. Hydraulic parameters in an unconfined aquifer include hydraulic conductivity, transmissivity and specific yield, etc. (Robbins et al., 2008). The principle of a pumping test involves extracting groundwater from a well using a pumping machine and the drawdown is monitored with a function of time.

The importance of carrying out pumping test includes the following:

1. To quantify how much groundwater are abstracted from a well in relation to long-term yield and efficiency
2. To determine the aquifers hydraulic parameters in the floodplain
3. To assess the effects of pumping on the floodplain groundwater
4. To determine the suitable of pump on the floodplain aquifers

Measurement required for pumping test include the static water level before commencement of the test, starting time, pumping rate, pumping levels and time the pumping stopped.

2.6.3.3 Groundwater monitoring

Measurements of the depth below the ground surface of the water table, or its height above mean sea level, are necessary for understanding the groundwater condition of an area, e.g. for the recharge an aquifer in the floodplain. The data from groundwater level measurement can be used to understand the flow direction of groundwater and to measure the impacts of abstraction. The measurement of water level fluctuations in piezometers and observation wells is an important parameter for many groundwater studies. The variation of groundwater levels across the floodplain can result from different hydrologic activities (Freeze and Cherry,

1979). Measurements of water levels in wells provide useful means for assessing the quantity and quality of groundwater and its relation with the shallow alluvial aquifers along the floodplain (Taylor and Alley, 2001).

2.7 Development of groundwater modelling

This section describes the groundwater modelling process for assessing the shallow alluvial floodplain and its future changes. The floodplain of the present study site is a typical example of shallow alluvial aquifers. The purpose of the review is to understand the groundwater model processes. The information will be useful on how to estimate the hydraulic heads across the floodplain for abstraction using hand-drilling techniques and its future.

Globally groundwater modelling has been used by many researchers to investigate groundwater flow along the floodplains, for example, Brouyère et al. (2004); Holman (2006); Alemayehu et al. (2007); Zume and Tarhule (2011); Neukum and Azzam (2012), etc. Zume and Tarhule (2011) demonstrated that over-pumping in the Southern Great Plains, United States, had lowered groundwater levels in the shallow alluvial aquifers extending along the floodplain. Modelling has also enabled an assessment of the impact of climate change on the floodplain groundwater. For example, Jyrkama and Sykes (2007) investigated the impact of climate change along alluvial floodplain in the semi-arid areas of Grand River in Canada, and found increasing groundwater recharge. However, Hsu et al. (2007), working on the Pingtung Plain in semi-arid floodplain Taiwan, found a decrease in floodplain groundwater levels, which is contrary to what was observed by Jyrkama and Sykes (2007). Climate change across the world has many different impacts. For example, overall, there is global warming, but there are places on the earth, which are cooling. The same is true for precipitations.

The application of groundwater models is useful in hydrogeology in understanding the relationship between groundwater and surface water. Model applications depend on how the

mathematical solution represents the real situation in the field (Wake, 2008; Alvarez et al., 2012). Models can be applied in three ways, (i) predictive: used to predict the future conditions, (ii) interpretive: used for studying system dynamic or organising field data, (iii) generic: used to analyse flow in hypothetical hydrogeologic systems (Anderson and Woessner, 1992).

The present study considered the application of interpretive: used for studying system dynamic and predictive: used to predict the future conditions. The interpretive application was considered in the model to understand floodplain hydraulic heads. The application of the model in a predictive manner helped assess the future sustainability of the floodplain groundwater for application using hand-drilling techniques.

2.7.1 Choice for the groundwater modelling software

Various types of groundwater modelling software exist for simulating groundwater flow across the alluvial floodplain. The most common groundwater modelling software include MODFLOW, Visual MODFLOW, MODPATH, PLASM, AQUIFEM-1, PHREEQE, GEOPACK, GSFLOW, PEST, AQTESTSS, PHAST (Anderson and Woessner, 1992; Kumar, 2012).

Many examples of successful applications of MODFLOW, similar to those used in the present study, are reported. For example, a study by Bradley (2002) uses MODFLOW to simulate water table variation along the floodplain wetland of Narborough Bog, UK. The study reveals the importance of water storage function of the wetland and its relationship to the lowland river. Zume and Tarhule (2011) applied MODFLOW to simulate the impacts of pumping and recharge variability on an alluvial aquifer in semi-arid northwestern Oklahoma, USA. The simulation showed that groundwater withdrawal leads to declining streamflow of ~ 40%. Barron et al. (2013) used MODFLOW to simulate the effect of urbanization on the

alluvial floodplain groundwater in Western Australia. The simulation showed that the urban density and the rate of local groundwater abstraction for irrigation mostly influence the magnitude of urbanization on the catchment fluxes. Kumar et al. (2011b) also used MODFLOW to inform groundwater management along the alluvial floodplain in Nadia District, West Bengal India. The simulation showed that the floodplain groundwater pattern feeds the adjacent river throughout the year.

It can be observed from the above that MODFLOW solves various alluvial floodplain groundwater flows, as is the case of the present study. Among the various groundwaters modelling software, MODFLOW was selected for assessing groundwater flow along the shallow alluvial aquifers of the floodplain due to the following reasons. i. MODFLOW is widely accepted and has been validated software developed by U.S. Geological Survey (McDonald and Harbaugh, 1988) and is also free software available in the public domain; ii. the software is accessible, can be readily used and features fast data generation for understanding the floodplain groundwater responses and behaviuors; iii. it is well documented, each part of the software that represents a relevant physical process to the groundwater flow has its own document about the main considerations taken in the simulation; iv. MODFLOW is highly adaptable to answering a variety of groundwater problem; v. MODFLOW is modular and continuously updated; vi. MODFLOW uses the block-centered Finite-Difference Method and can simulate flow from external stresses, such as flow to wells, aerial recharge, evapotranspiration, flow to drains and flow through riverbeds; vii. MODFLOW represents well the physical processes related to groundwater flow. Evapotranspiration, which can account for significant groundwater losses, is well configured in MODFLOW and runs without major computational requirement (Gidahatari, 2013).

2.7.2 Low-flow in river during dry season period

Assessing the water available in a river or stream during low-flow in the dry season period is necessary to quantify its impact on the floodplain, especially when using low-cost hand-drilling techniques to extract the groundwater for irrigation activities. Information from low-flow in stream or rivers especially during dry season period may give the threshold values of the floodplain groundwater levels and this is useful in water resource management (Tallaksen, 1995; Goswami et al., 2010).

In arid and semi-arid environments, shallow alluvial aquifers tend to discharge during the dry season and recharge in the rainy season (Townley, 1998; Love et al., 2006). Thus where alluvial deposits are found, they can play a significant role in the river basin water balance (Love et al., 2006). It has been established in Namibia desert that recharge can consume a significant portion of flood flows (Lange, 2005; Mansell and Hussey, 2005).

2.7.3 Interaction between surface water and groundwater

The interactions between surface water and groundwater flow systems take a wide variety of forms, depending on both the nature of the water body and the aquifer system (Winter, 1999; Bradley and Petts, 1995; Rodriquez et al., 2005; Bansal and Das, 2011). The interaction between streams and groundwater can be classified into four basic model categories (Figure 2.27). These models are based on the relationship between stream stage (water levels in river or stream) and groundwater head (groundwater level in the alluvial aquifer).

The methods for assessing the interaction between river and groundwater of the floodplain can be based on modelling and field estimation (Ekrail and Long-Cang, 2009). Factors that control the hydrological exchange between groundwater and rivers include the following: i) the hydraulic conductivity, ii) different between river water stage and groundwater levels

along the floodplain, iii) geomorphology of river and the floodplain (Sophocleous, 2002 and Scott et al., 2008).

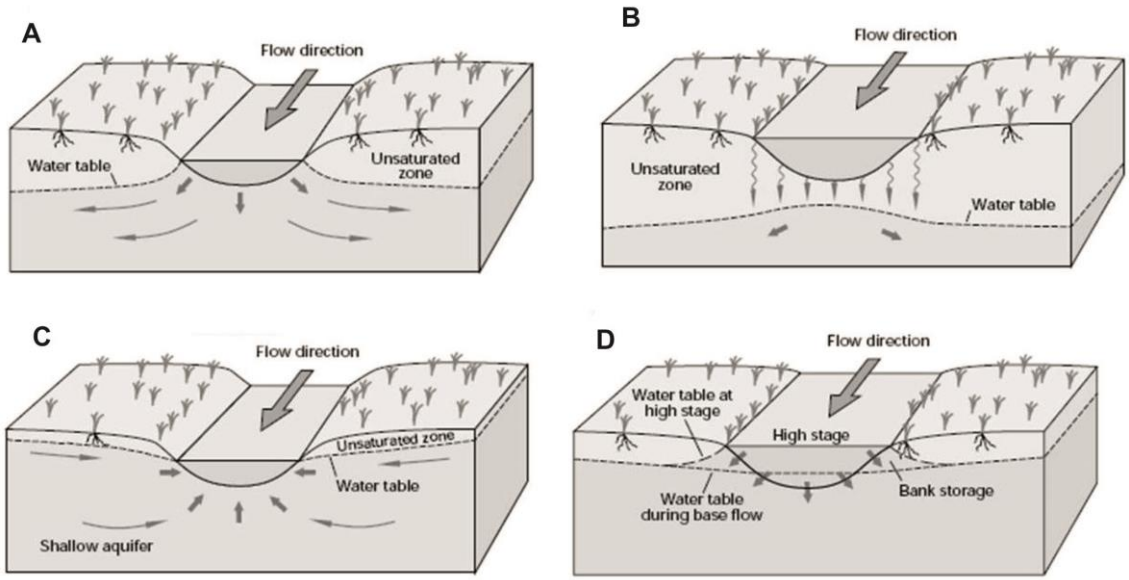

Figure 2.27: Four basic conceptual models indicating direction of flow between a stream and floodplain aquifer. A – stream water body losing water to groundwater by outflow (influent), B – stream water body disconnected from the groundwater system loosing stream, C – stream water body gaining water from inflow of groundwater (effluent) and, D – stream water body with excess storage, loosing stream. (Adapted from Winter et al., 1998; Woessner, 2000 and Guggenmos, 2010).

The variability and distribution of the hydraulic conductivities (heterogeneity) of streambed deposits and aquifer materials act as the key factors for determining the volume of large-scale and small-scale exchange processes, as well as the residence time of water within the riverine aquifer (Brunke and Gonser, 1997). The direction of the exchange processes varies with hydraulic head, which is subject to the influence of precipitation events and seasonal patterns; whereas water flow depends on the contrast in hydraulic conductivity at different parts of the system, as well as the connectivity of the preferential flow network (Faybishenko, 2000).

Sjodin et al. (2001) and Chen and Chen (2003) have identified a type of interaction between streams and groundwater caused by bank storage. This process occurs from storm

precipitation or from the upstream releases, whereby the loss of water from river to the floodplain groundwater and its return back to the river in a matter of days, weeks or months reduces high stream level (Winter et al., 1998; Idowu, 2007; Wake, 2008). If water stage in a river or stream overflows the floodplain, it will allow recharging of the shallow alluvial aquifers across the floodplain for rising water levels in wells (Winter, 1999). These will enable easy extraction with the hand drilling method.

2.7.4 Groundwater modelling equation

Groundwater flow modelling is a useful way for assessing groundwater conditions along the floodplain. Groundwater models can be used for estimating changes of the floodplain aquifers, for understanding floodplain dynamic, for knowing groundwater flow direction (Kresic, 1997; Grapes et al., 2006, Owais et al., 2007; Kumar et al., 2011a). Typically, groundwater models use the following three – dimensional flow equation (equation 2.2):

$$\frac{\partial}{\partial x}\left(K_{xx}\frac{\partial h}{\partial x}\right)+\frac{\partial}{\partial y}\left(K_{yy}\frac{\partial h}{\partial y}\right)+\frac{\partial}{\partial z}\left(K_{zz}\frac{\partial h}{\partial z}\right)-W=S_s\frac{\partial h}{\partial t} \qquad 2.2$$

where K_{xx}, K_{yy} and K_{zz} are hydraulic conductivities along the x, y and z direction (md^{-1}), respectively; h is head (m); W is a volumetric flux per unit volume (m^3d^{-1}), Ss is the specific storage (d^{-1}) and t is time (d) (Kumar et al., 2011a). Figure 2.28 shows discretised aquifer cell for modelling groundwater heads across the alluvial floodplain.

MODFLOW has been designed to manage groundwater resources, and enable a range of future water use, land use and climate scenarios to be considered. The groundwater – surface water interactions element of MODFLOW conceptualises a groundwater body that underlies the river, through a saturated or an unsaturated connection. The processes of the exchange fluxes between the surface water and groundwater influence the connections. The exchange fluxes comprises the following components: 1) low flow flux, 2) flux due to river bank

fluctuations, 3) flux due to changes in aquifer recharge, 4) flux due to groundwater extraction and flux due to changes in evapotranspiration (Xu et al., 2009; Xu et al., 2011; Rassam, 2011).

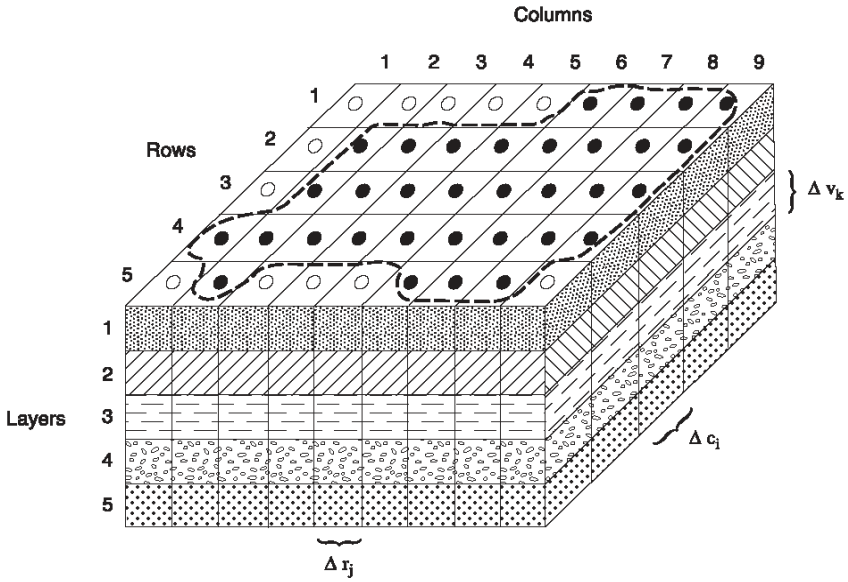

Figure 2.28: General discretised aquifer (From Harbaugh, 2005).

2.7.5 Conceptualisation

The development of a groundwater model of the alluvial aquifer relies upon the specification of an appropriate conceptual model to assess: i. rates of groundwater flow; ii. flow through the floodplain; and iii. the impacts of changes in the flow of the River Benue. Model conceptualisation is the process by which data obtained during the characterisation of a site are examined to determine relevant groundwater flow processes, and all available geological and hydrogeological data are summarised in a simplified block diagram or cross-section (Anderson and Woessner, 1992). The first step in building the conceptual model is to define the geological framework including the thickness, continuity, lithology and structure of aquifers and confining units. Establishment of the geological framework allows the hydrological framework to be defined involving four important steps: identifying the boundaries of the hydrological system, defining hydrostratigraphic units, preparing the water

budget and defining the flow system. Preparation of a water budget involves the identification and quantification of all water flows into the system as well as flow direction and water flows out of the system. Water inflows into the system include recharge from precipitation and rivers or streams. Water outflows include base flow to streams, model evapotranspiration and groundwater abstraction from wells. The steps in a modelling process are summarised in Figure 2.29.

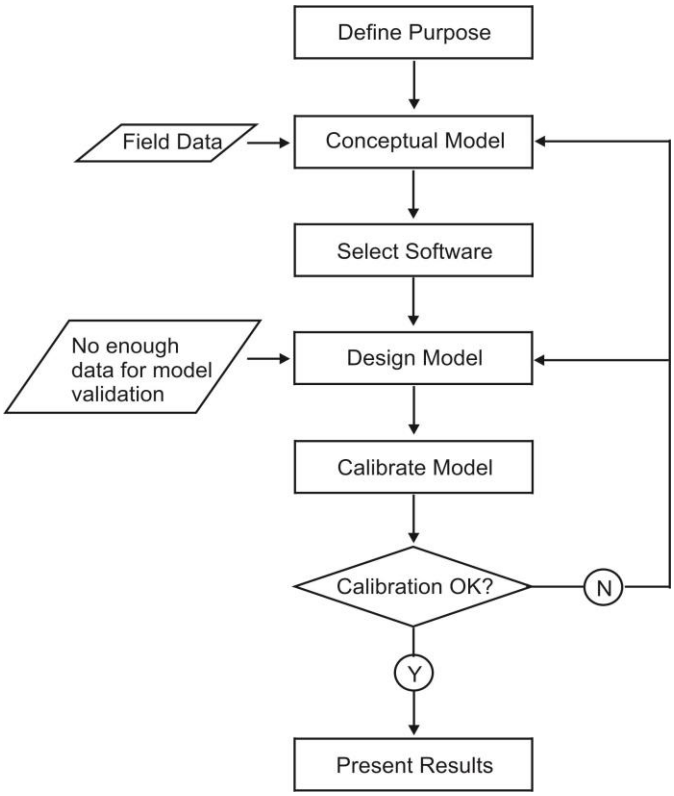

Figure 2.29: Flow chart showing the processes of model application (From Anderson and Woessner, 1992).

2.7.6 Numerical modelling

Modelling water exchange between aquifers and rivers requires the simultaneous solution of two separate equations, which describe river flow and groundwater flow through alluvial sediments, moreover, quantifying groundwater storage requires a number of simplifying assumptions to represent a particular hydrogeological situation, some of which may not be

justified (Anderson and Woessner, 1992). Most models assume a homogeneous aquifer, whilst variations in floodplain sedimentology, reflecting, for example, the location of palaeochannels, may lead to local variations in groundwater flow (Sophocleous et al., 1988).

2.7.7 Types of boundary conditions

The boundary conditions can be natural hydrogeological boundaries, which include the surface of the water table, groundwater divides and impermeable contacts between different geological units. The selection of boundary conditions requires considerations of actual floodplain hydrogeologic conditions. Boundary conditions consist of the following types:

1. Constant-head boundary: - A constant-head boundary occurs where a part of the boundary surface of an aquifer coincides with a surface of a constant-head. An example is an aquifer that is linked to the bottom of a lake in which the surface water stage is nearly uniform with the floodplain water level and does not vary appreciably with time. In the present study, Lake Geriyo is an example of constant-head boundary, which is located west of the floodplain, and it has water throughout the year.
2. Specified-head boundary: - Specified-head boundary is a type of boundary where head can be specified as a function of position and time over the boundary surface of a groundwater system. An example of the specified-head boundary condition can be hydraulic heads along the floodplain. In the present study water level in wells across the floodplain can be used as specified-head boundary conditions.
3. Streamline (no flow) boundary:- A streamline is a curve that is tangent to the flow-velocity along its length, thus no flow components exists normal to streamline and no flow crosses a streamline (Franke et al., 1987). An example of a streamline (no flow) boundary is an impermeable boundary such as unconsolidated material. Impermeable

formation such clayey silt, which is available in the floodplain, can serve as no flow boundary condition.

2.7.8 Input packages for the groundwater modelling

The various parts of the code that deal with defining the groundwater flow equation are divided into hydrologic packages. The hydrological packages used to simulate the groundwater flow includes: Basic (BAS), Recharge (RCH), Evapotranspiration (ET), General-Head Boundary (GHB), River (RIV), Block-Centered Flow (BCF) and Output Control (OC) (McDonald and Harbaugh, 2005) (Figure 2.30).

i. Basic (BAS) Package: The BAS Package performs most of the model tasks, for example computation of the water budget for the system.

ii. Block-Centered Flow (BCF) Package: The Blocked-Centered Flow Package handles the rate of flow into and out of the model cells.

iii. Recharge (RCH) Package: The Recharge (RCH) Package computes the recharge rate across the groundwater of the floodplain. Recharge applied to the model is defined as:

$$QR_{i,j} = I_{i,j} DELR_j DELC_i \quad 2.3$$

where $QR_{i,j}$ is the recharge flow rate to the model, $I_{i,j}$ is the recharge flux to the map area, $DELR_j DELC_i$ (DELR – is the grid width along a row, L; DERC – is the grid width along a column, L) of the cell.

iv. Evapotranspiration (ET) Package: The Evapotranspiration (ET) Package computes water loss from the system through model evapotranspiration. Evapotranspiration applied to the model is defined as:

$$Q_{ETi,j} = R_{ETi,j} * DELR_j * DELC_i \quad 2.4$$

$$R_{ETi,j} = R_{ETMi,j}\left\{\frac{h_{i,j,k} - \left(h_{si,j} - d_{i,j}\right)}{d_{i,j}}\right\} \quad 2.5$$

where $Q_{ETi,j}$ is the Evapotranspiration; $R_{ETi,j}$ is the rate of loss per unit surface area of water table due to evapotranspiration; $DELR_jDELC_i$ is loss from horizontal surface area; $R_{ETMi,j}$ is the maximum possible value of $R_{ETi,j}$; $h_{i,j,k}$ is the head; $h_{si,j}$ is the ET surface elevation; $d_{i,j}$ is the cutoff or extinction depth.

v. River (RIV) Package: The River Package assesses the interaction between river and the floodplain groundwater. The River Package equation is

$$QRIV = KLW/M\left(HRIV - h_{i,j,k}\right) = CRIV\left(HRIV - h_{i,j,k}\right) \quad 2.6$$

where QRIV is the flow between the stream and the aquifer; HRIV is the head in the stream; CRIV is the hydraulic conductance of the stream-aquifer interconnection (KLW/M); $h_{i,j,k}$ is the aquifer head; L is the length of a river reach; K is the streambed saturated hydraulic conductivity; W is the width of the river; M is the thickness of riverbed (McDonald and Harbaugh, 1996; Harbaugh et al., 2000; Mehl and Hill, 2005; Mehl et al., 2006).

vi. Well (WEL) Package: The Well Package is used to compute rate of water flow into and out of the wells across the floodplain.

vii. General-Head Boundary (GHB) Package: The General-Head Boundary (GHB) Package computes water flow into and out of the system from external source. The relation between flow into the cell and head in the cell is:

$$QB_n = CB_n\left(HB_n - h_{i,j,k}\right) \quad 2.7$$

where n is a boundary number, QB_n is the flow into cell from the boundary, CB_n is the boundary conductance, HB_n is external source head and $h_{i,j,k}$ is the head in cell.

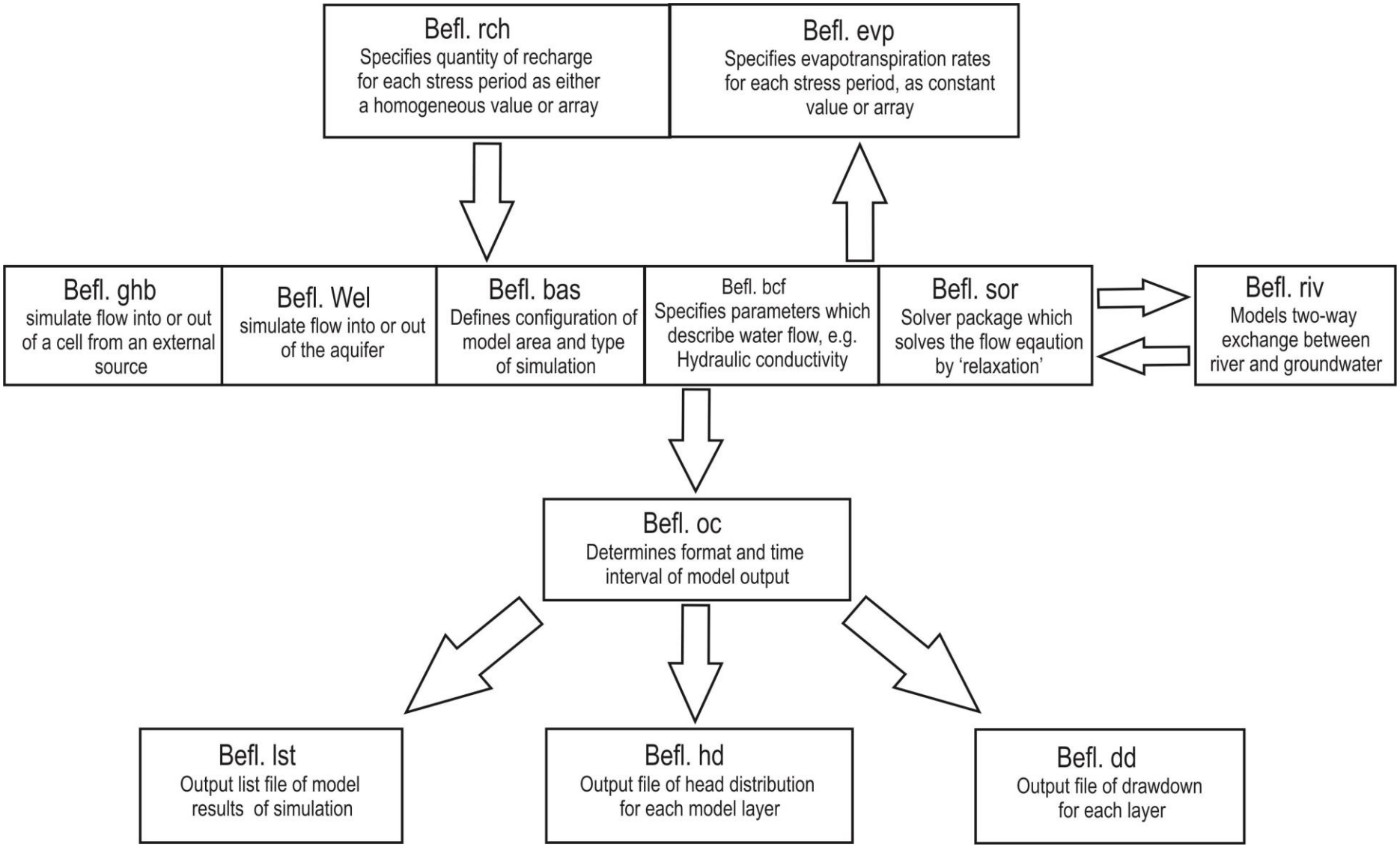

Figure 2.30: Schematic flow chart showing input packages for simulating groundwater modelling (Modified from Bradley, 1994). Befl – Benue floodplain.

viii. Solver (SOR) Package: Solver Packages focuses on how to produce an acceptable solution to the flow equations with a minimum of computation time. The criterion for solver package selection include; ability to solve the equations for the simulation, minimising the time to solve the equations and minimising the amount of memory to be used for the model.

ix. Output Control (OC) Package: The Output Control Package determines format and time interval of model output.

2.7.9 Groundwater recharge

Groundwater recharge estimation is a fundamental part of groundwater resources investigation. In arid and semi-arid environments, groundwater recharge is usually focused topographically, such as river flows and channels along the floodplain (Scanlon et al., 2002; Sanford, 2002). Groundwater recharges are from infiltration of river water, precipitation, runoff from terraces, irrigation return flow, infiltration from tributary streams and overland flow (Sharp, 1988; Idowu, 2007 and Brodie et al., 2007). Recharge to the alluvial aquifers occurs during time of rising river stages, which enters bank storage. In wider floodplain, precipitation becomes most important, for an example on the lower Mississippi River floodplain, recharge (by precipitation) dominates the terrace deposits and piezometer heads are observed to rise significantly because of rapid influx of precipitation (Sharp, 1988). Groundwater recharge is the most important factor for sustainability in arid and semi-arid environments (Taylor et al., 2013b). Recharge and discharge areas can be delineated based on topography, piezometric patterns, and hydrogeochemical trends, the use of environmental isotopes and soil and land surface features (Kelbe and Germishuyse, 2000; Brassington, 2006).

Groundwater recharge modelling faces challenges in arid and semi-arid areas as potential evapotranspiration generally exceeds rainfall and groundwater recharge depends mainly on high rainfall intensity events and streams, therefore, direct recharge is likely to be less

important than indirect recharge (Wang et al., 2010). Groundwater recharge studies in Africa have usually been done at a small-scale, focusing on small areas to define aspects of groundwater recharge, such as its source, timing, magnitude and distribution. Adanu (1991) study the source of groundwater recharge in northeast Nigeria and found that the primary source of recharge is from direct infiltration of rainfall at the soil surface. Carter and Alkali (1996) estimated groundwater recharge at 0.9 mm/a in the northeast arid zone of Nigeria, using a one-dimensional flow equation. Similarly, Edmunds and Gaye (1994) estimated annual recharge, which ranges between 0.1 – 1.3 mm/a in Sahel arid region. Scanlon et al. (2006) made a global analysis from about 140 alluvial floodplains recharge studies in arid and semi-arid environments (including Africa) which provides useful findings on the shallow alluvial aquifers recharge rates and their processes. According to Scanlon et al. (2006), average recharge rates in most of the arid and semi-arid environments range between 0.2 to 35 mm/a, representing 0.1 – 5% of average annual precipitation.

2.7.10 Model calibration

Calibration is generally carried out by identifying key flow parameters, such as boundary conditions, flow into and out of the model that represent real situation on the floodplain (Anderson and Woessner, 1992). Calibration of an inverse problem involves modifying the boundary conditions, hydraulic properties and stresses of the model until the simulated heads match the observed heads (Anderson and Woessner, 1992). In an inverse problem such as this study, it is usual to match the head outputs of the model to the observed heads as head measurements are likely to be the most accurate and most readily available from monitored wells.

Transient calibration yields modelled water levels that represent the aquifer's response to stresses such as recharge over a given time period. It is essential to determine the magnitude of this flux for the duration of the modelling period to achieve accurate model calibration.

The model can be calibrated with parameters that are consistent with field-measured parameters (Watts, 1989), for example, aquifer properties determined from pumping tests, groundwater levels in wells. Owing to lack of large seasonal water level or steady-state data sets, model can be calibrated with transient conditions using water level in wells along the floodplain (Luckey et al., 1986; Anderson and Woessner, 2002). Calibration can be achieved by manual trial-and-error and automatic methods (McDonald and Harbaugh, 2005). Tens to hundreds of model runs are typically needed to achieve calibration. Maclay and Land (1988) reported 300 simulations to achieve calibration.

2.7.11 Application of the model for sustainable groundwater use and management

The groundwater model in this study was intended to examine whether groundwater use is likely to exceed a sustainable use in the floodplain for the application using the low-cost hand drilling technique. Groundwater quality was not considered in the assessment of sustainability due to lack of data and it could easily become the topic of another PhD dissertation in itself.

The criteria implemented for the sustainable groundwater development in this study focused on the changes of the river stages and of water levels over a time horizon across the floodplain. To understand the sustainability of the groundwater for irrigation farmers along the alluvial floodplain of River Benue, low-cost hand-drilling technique is used for groundwater abstraction. As the regional government of Yola wishes to expand the area under irrigation, it is necessary to assess whether groundwater will remain accessible with the low-cost techniques. Several threats may change the depth of groundwater.

Factors such as land use and climate changes have an impact on groundwater sustainability. The model will be designed to reflect the dynamics of the floodplain water-table level by considering the variations in stresses that will influence the system, such as 1. global change, 2. river flow stages and wells pumping rates and 3. the impact of a dam built upstream in

Cameroon. The conceptualisation of the River Benue floodplain aquifer will be built by assembling all the available subsurface information from borehole logs, water level monitoring and groundwater abstraction. This information will be used to construct the nature of the subsurface geology and hydrodynamics for numerical representation of the floodplain.

2.8 Concluding remarks

1. The existing topographic map is insufficient for the purpose of the present research.
2. Little is known on the sedimentology and hydrogeology of the study area.
3. It is observed from the review that management of Lagdo Dam upstream in Cameroon has a positive impact to the study site during the dry season period. However, its future is uncertain.
4. It is also observed that the criteria for assessing the suitability of hand drilling techniques consist of geological, permeability, geomorphology, groundwater depth and shear strength suitability. These criteria will be used to assess the suitability of the floodplain alluvial sediment for the application of hand drilling techniques.
5. Processes for developing groundwater model were reviewed in order to assess the sustainability of the floodplain groundwater for abstraction with the hand-drilling techniques.
6. The review has provided valuable insight into the techniques used to assess the suitability of the floodplain sedimentology and sustainability of the floodplain groundwater for application with the hand drilling techniques.

In conclusion, the state of the current knowledge detailed above in this review has identified both research questions and approaches needed to assess and quantify the future sustainability of the floodplain groundwater for improving irrigation activities along River Benue floodplain.

CHAPTER THREE – MATERIAL AND METHODS

3.1 Introduction

This chapter describes the material and methods used for obtaining reliable data to address the research questions. i. the meteorology and hydrology collection of secondary data collection (section 3.2). ii. the correct estimation of the floodplain surface elevation (section 3.3). iii. the floodplain sediment analysis that needs to be studied as a preliminary to the study of groundwater (section 3.4). iv. new groundwater analysis (section 3.5). v. and the process to model the groundwater of the alluvial floodplain (section 3.6).

3.2 Collection of secondary hydro-meteorological data

Meteorological and hydrological data were obtained from the Department of Hydrological Unit of Upper Benue River Basin Development Authority (UBRBDA), Yola, for analysis. The meteorological data are the rainfall (1960 – 2012), temperature (1960 – 2012) and evaporation (1982 – 2012). The meteorological gauge station is located at UBRBDA, Yola head office southeast, approximately 5 km from the study site, at a latitude of 9˚ 11' N and a longitude of 12˚ 30' N, and an altitude of 177.69 m (amsl). Evaporation was measured by evaporative pan method. The hydrological data are the water stage and discharge of River Benue (1960 – 2012). The discharge gauge station is located on River Benue near Yola Bridge approximately 500 m from the study site at a latitude of 9˚ 15' 20" N and a longitude of 12˚ 28' 04" N, and an altitude of 151.17 m (amsl). The meteorological and hydrogeological data are analysed and discussed in detail in Chapter 4.

The UBRBDA monitors and collects these data on daily bases. Interpolations were made to obtain all the missing data (~45). The interpolation was done by considering data value

before and after the missing value and reasonable values were obtained for all the missing data.

3.3 Determining elevation height

A ProMark3 GPS Dual Frequency instrument (Figure 3.1) was used to determine elevation height across the floodplain as the available map (see Figure 2.2) is not sufficient. The ProMark3 is a complete GPS system providing precision surveying in post-processing. The instrument gives readings in vertical accuracy between 0.01 m. A typical ProMark3 system used in post-processing surveys includes two ProMark3 GPS receivers, two GPS antennas, and a GPS tripod for fixing the survey instrument at a base station. The ProMark3 GPS collects data from the GPS satellite for further processing (Magellan, 2007).

Figure 3.1: A ProMark3 Global Positioning System instrument for determining the height elevation across the floodplain at borehole location 1 transects 1 (see Figure 2.8) (the photograph taken by Mohammed Abana Girei on 13th April 2012).

The procedure followed includes positioning one ProMark3 GPS receiver at a base station and the other ProMark3 GPS known as Rover is moved around to collect readings at each of the survey points. The ProMark3 GPS instrument was set at 10 seconds as a logging time. The data were corrected for positional errors using the National Geodetic Survey Online Positioning User Service (OPUS). The data obtained at each of the survey stations was used to construct a contour map for the study site.

3.4 Sedimentology

This section presents the methods and material for a preliminary assessment of the alluvial floodplain sedimentology. No records in the region provide information of the floodplain sediment; therefore, it is useful to make this preliminary investigation to understand the floodplain alluvial sediments. Field description, particle size analysis, loss on ignition and magnetic susceptibility were presented here in order to understand the process of formation of the floodplain alluvial sediment.

3.4.1 Field description

This section describes the characterisation of sedimentology in the field along River Benue outcrops and in the sediment cores in the floodplain, in order to assess the sediments of the research area for application with the hand drilling method. Alluvial sedimentology is useful for 1) assessing the suitability of the hand drilling method to abstract the shallow floodplain groundwater, 2) understanding the origin of the sediment and its 3-D distribution and 3) quantifying groundwater flow.

3.4.1.1 Sediments sampling along River Benue Valley outcrops

A total of 5,500 g of sediment from 191 sediment samples were collected along the outcrops of River Benue valley bank, for the purpose of laboratory analysis. Sampling technique was

followed in accordance with the British Standard guideline (BS EN ISO 22475 – 1, 2006). A hand-held Global positioning System (GPS) system was used for fixing the position of sediments collected at each sampling location in the field. The primary purpose of collecting sediment samples here is for characterisation of the subsurface lithology and stratigraphy of the area (Bob, 2008). At each sampling point, samples were collected at every change of sediment/soil type from the top to the bottom of River Benue outcrops bank (Figure 3.2). The sedimentological description of outcrops using the lithological table/chart was used to describe the samples during sampling. Photographic record with label, scale and colour chart was used for the purpose of description. A small plastic coated (to avoid rust) hand trowel was used for sediment sampling. Samples were put into sealed sampling bags for laboratory analysis.

Figure 3.2: Sampling sediment using a plastic trowel along River Benue Valley Bank, Yola outcrops at sampling location G along transect 3 (see Figure 2.28) (The photograph taken by Mohammed Abana Girei on 19th April 2011).

Samples were also taken in Cameroon in Benue and Faro Rivers. Figure 1.1 shows the sampling locations. It was hypothesised that the volcanic fields (see Figure 2.4) found in

Benue and Faro Rivers may have left an impact on the sediment of Benue and Faro Rivers, which contributes sediment to the Nigerian portion of the Benue River. It is hypothesised that magnetic susceptibility measurement would be able to show a volcanic component in the sediment (Dearing, 1999).

Preliminary identification for the sediment/soil grain size in the field was made by feeling the texture of sediment between fingers. For each sediment collected, a small amount was rubbed between fingers in order to determine the difference between sand, silt and clay. Sand feels gritty, silt feels smooth and clays feel sticky.

3.4.1.2 Field sediments sampling using hand augering method

Fieldwork was carried out in April to May 2011, in order to determine the maximum depth of groundwater levels to be available for farmers to irrigate farm land at the peak period of the dry season. The technique used for the sampling and understanding of the groundwater levels at each drill hole followed the British Standard guideline (BS EN ISO 22475 – 1, 2006). The survey campaign was completed in April and May 2011, which is the peak dry period of the region. The hand augering technique (Figure 3.3) was locally constructed to test in the floodplain. The maximum depth obtained was 18 m deep during this fieldwork period.

During the fieldwork survey, I had an informal interview with farmers on the usage of the hand drilling techniques. The farmers' prefer using augering drilling method than other methods of hand drilling especially jetting, because augering is affordable and easy to use.

During the fieldwork survey, it was also observed that some boreholes fail in the floodplain according to my interaction with the farmers. Therefore, it is useful to understand the causes for the boreholes failure across the floodplain in order to improve the sustainability of the floodplain groundwater for irrigation activities.

Figure 3.3: Borehole drilling using hand augering method for sediment sampling in the floodplain at borehole location 4 transect 2 (see Figure 2.8) (The photograph taken by Mohammed Abana Girei on 4th May 2011).

The visual description of the colour of the fresh sediment samples was described according to the Munsell soil colour chart during sampling. Colour patterns of sediment or soil are extremely important for lithological analysis. It is essential to identify the colour of sediment during sampling because some sediments change their colour very quickly in air. An example of this is fine sediment containing iron oxide compounds which, in the fresh-water saturated condition, often has an olive green colour but which rapidly oxidizes to red on exposure to air (BS EN ISO 14688 – 1, 2002). Such kinds of the sediments are the predominant in the floodplain. Colour changes such as those due to oxidation or desiccation should be recorded.

Figure 3.4: Sampling sediment samples from the drill boreholes using augering hand-drilling method at borehole location 6 along transect 3 (see Figure 2.8) (The photograph taken by Mohammed Abana Girei on 4th May 2011).

Sediment samples were obtained at the different drill points in the floodplain for laboratory analysis and to estimate the maximum depth with hand drilling until water is reached during the dry season period. Twelve boreholes were drilled using locally made augering methods at twelve points at approximately 500, 1500 and 2500 m intervals along five transects (Figure 3.4) perpendicular to the River Benue and approximately 500 m between the transects. This seems a reasonable spacing to cover the area of the Upper Benue Irrigation Project. A total of 4,800 g of sediment samples in a total number of sixty-five sediment samples were collected from twelve cores for detailed analysis of particle size, magnetic susceptibility, loss on ignition and permeability.

Sampling bags (Figure 3.5) are used to store and to avoid moisture loss of samples for the laboratory analysis. Clear marks were labelled on each sample.

Figure 3.5: Sediment samples in sampling bags to prevent moisture loss from the sediments (The photograph taken by Mohammed Abana Girei on 29th May 2011).

3.4.2 Particle size analysis

For the present study, a CILAS laser diffraction instrument was used (Figure 3.6). The instrument proved to be a good method for analysing the range of grain size found in the Yola floodplain. The CILAS 1180 can characterise particle size distributions between 0.04 and 2,500 µm (Dietmar, 2006). The fine particles are measured by the diffraction pattern by using Fraunhofer or Mie theory (CILAS, 2004). Two hundred and fifty six air-dried sediment samples were analysed. The results obtained from the CILAS were analysed using Gradistat version 8.0, a statistical package develop by Blott (2011).

The sediment samples were weighed to 0.05 g, soaked in 10 ml 10% tetra sodium pyrophosphate, and left over night to deflocculates, before starting measurement. The samples were then added into the CILAS 1180 instrument and analysed using the program Size Expert (Figure 3.6). Care was taken in introducing the amount of sample into the CILAS mixing chamber to avoid high obscuration of sample in the mixing chamber. Optimal obscuration

occurs when a sufficient number of suspended particles are present in the mixing chamber, which significantly diffract the laser beam, without blocking it. The obscurations for the samples were maintained between 15 to 25% for coarse-grained sediment (following Sperazza et al., 2004). Background measurements and rinsing were performed in between each sample measurement in order to keep the results consistent and reliable. Twenty seconds of ultrasound, twenty seconds of pumping and ten seconds of fast pumping were used for each sample before taken readings. Each sample was run three times for the data consistency and reliability.

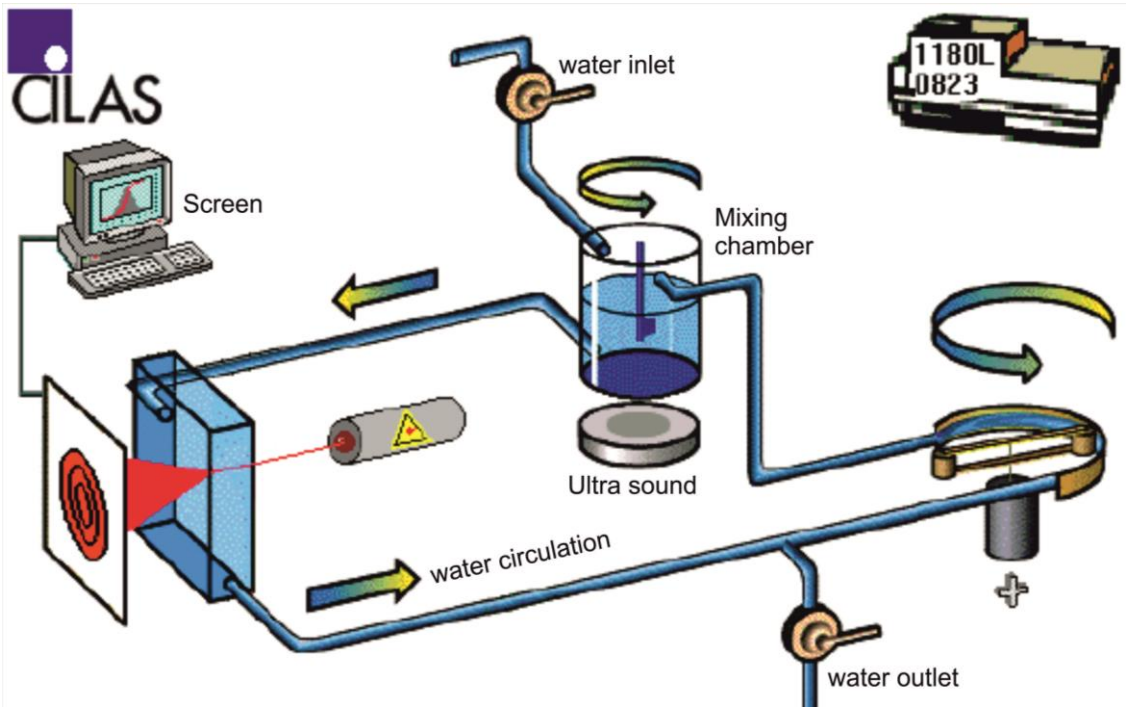

Figure 3.6: Schematic diagram showing particle size analyser setup for wet mode's mimic screen (Modified after CILAS, 2004).

The statistical analysis for the alluvial sediment samples was carried out using the Gradistat software produced by Blott (2011). As suggested by Pye and Blott (2004) statistics can be calculated using the method of moments either arithmetically (based on normal distribution) or geometrically (based on a log normal distribution) that gives a good approximation for well-sorted soils and sediments in the present study. The approach used here was the

arithmetic method as this gives a normal distribution of the floodplain alluvial sediments. The statistical descriptive method (mean, D10, D50, D60, D90, D90/D10, D90-D10, D75/D25, D75-D25, Cu, Skewness and Kurtosis), for sediment samples were used to describe the particle size distribution of the sedimentary deposits, as these parameters describe key components of a given distribution for use in the interpretation for the grain size deposition. The particle size distributions were also presented on the surface plot. Surface plots allow a quick overview of the sediment particle size distribution, so providing useful information on the sediment conditions (Beierle et al., 2002).

3.4.3 Loss on ignition

Loss on ignition (LOI) for the sediment samples was determined in the laboratory following the method by Bengtsson and Enell (1986) as shown in Appendix B. The method is fast, inexpensive; it gives good estimates of the sediment LOI and thus is useful for analysis of a large number of sediment samples. The method by Bengtsson and Enell (1986) is widely used by many researchers to estimate LOI of the alluvial sediment, for example Heiri et al. (2001), Veres (2002), Santisteban et al. (2004), Beasy and Ellison (2013), and Ledger et al. (2013).

There was a time gap of 3 months between the determination of the LOI and the sampling of the sediment in the field. The sediment samples were collected in April and May 2011. The LOI for the sediments were determined in August 2012. Even though the samples were stored in a sealed bag, there nevertheless a risk of moisture loss.

Three stages are involved in determining the LOI of the sediment samples and the samples losses were determined by mass with a scale at a precision of two decimals. In the first stage, moisture content of the sediment was determined by heating the sample at 105 $^{\circ}$C (Figure 3.7). At first the samples were heated at 105 $^{\circ}$C for about 12 hours period and were further heated at 105 $^{\circ}$C for more 12 hours period and lastly the samples were further heated at 105 $^{\circ}$C

for 12 hours period making in total of 36 hours period until constant weight at room temperature was reached. In the second stage, LOI at 550 °C was determined by heating the samples at 550 °C for 2 hours period in order to destroy the organic matter and other stuffs in the sediment. In the third stage, the samples and ash were heated at 950 °C for 4 hours period to destroy carbonate content in the sediment samples. The LOI by mass were calculated for each sample by taking the average of five readings for the sediment sample in order to obtained representative values. When the LOI is very low, it may be loss of moisture bond within a clayey silt of the sediments.

Figure 3.7: Crucibles with samples heated in a muffle furnace for the determination of loss on ignition for the sediment samples (The photograph taken by the author on 2nd September 2011).

3.4.4 Magnetic susceptibility

Sub-samples of air-dried sediments were packed into standard plastic vials. The magnetic susceptibility (MS) measurements were taken on a Bartington MS2 instrument, which was housed within the sedimentology laboratory of the Institute for the Environment, Brunel

University London, UK. A total of two hundred and fifty six different sediment samples were analysed in order to determine the sources for the sediment and the process of their formation in the floodplain.

Figure 3.8 shows the set up for MS instrument. MS was measured five times on each sample and an average value was taken for each measurement. All MS measurements were determined as soon as possible after the sediment was placed into the vial to avoid magnetic diagenesis when exposed to air.

Figure 3.8: Taking reading for magnetic susceptibility in the laboratory with the Bartington MS2 instrument (The photograph taken by Nik Nik on 10th August 2011).

3.4.5 Field Shear Vane Tester

In order to assess the suitability of the hand drilling method, shear strength forces on the alluvial floodplain sediment is one of the key parameter. Field Shear Vane Tester (FSVT) is

used in this study to understand shear strength forces on the floodplain alluvial sediments for the suitability of the hand drilling method.

The FSVT was applied at twelve different drilling locations on the floodplain during my fieldwork survey in April and May 2011 in order to determine the shear strength forces on the sediment. The maximum depth of the FSVT is 3 m that is the limitation for the instrument. The FSVT was carried out according to the British Standard guideline (BS EN 1997 – 2, 2007).

Figure 3.9: Taking readings with the Field Shear Vane Tester on the floodplain at borehole location 2 transect 1, for location (see Figure 2.28) (The photograph taken by Mohammed Abana Girei on 9th May 2011).

The operation principle involves pushing the FSVT into the ground to the required depth, then gradually turning the handle in a clock-wise direction until the sediment/soil fails. Then readings for the shear strength forces on sediments were obtained on a graduated scale (Figure 3.9). After taking the reading, the graduated scale is turned back to zero position for the next

reading. This process was repeated for the rest of the locations. At each location, shear strength forces were determined for 15, 30, 50, 75, 100, 130, 170, 210, 250 and 300 cm depth. The maximum depth that could be reached by the available FSVT was 3 metres.

The distributions of stresses around the shear vane failure were computed from the following equations:

$$T_v = \frac{1}{2}\pi D^2 H Su \qquad 3.1$$

where T_v is torque employed in creating a vertical failure surface; D is Vane diameter; H is Vane height and Su is Undrained Shear Strength.

$$T_h = \frac{1}{6}\pi D^3 Su \qquad 3.2$$

where T_h = torque on two horizontal failure surfaces at the top and the bottom of the material. From equations 3.1 and 3.2 above, the shear strength (Su) at the shear vane failure surface can be computed as follows:

$$T = \frac{1}{2}\pi D^2 H Su + \frac{1}{6}\pi D^3 Su \qquad 3.3$$

$$Su = \frac{T}{\pi\left[\frac{D^2 H}{2} + \frac{D^3}{6}\right]} \qquad 3.4$$

where T is the total torque applied on the shear vane (Griffiths and Lane, 1990; Foguet et al., 1998; International Organization for Standardization, 2009).

The shear strength was corrected to account for the effect of time and strength anisotropy as proposed by Chung et al. (2007). The corrected vane strength is defined as:

$$S_{u(corr)} = \mu . S_u \qquad 3.5$$

where μ is the correction factor varied from 0.225 to 0.245 with the lower value used for sand sediment an high value for silt and clay sediment, S_u is shear strength.

The most common errors that occurred from the FSVT include incorrect computation of the spring factor and if the sediment contains organic materials (e.g. decayed wood). Care was taken for the spring factor during computation for the shear forces. The error, which may occur as plasticity in clayey silt of the floodplain, were corrected using empirical correction factors as proposed by Aas et al. (1989).

3.4.6 Principal Component Analysis

Principal Component Analysis (PCA) is a statistical analysis used for correlating different variables in a simplified form by means of vector transformation. It provides a clear way for understanding how variables are correlated to each order (Shlens, 2009). The PCA analysis helps to show sediment variables that are more complex to a simply way of understand the system. The statistical correlation analysis shows that some of the variables are positively correlated while some are negatively correlated.

The statistical correlations of the six major variables which include moisture content, depth, magnetic susceptibility, LOI at 550 $^{\circ}$C, LOI at 950 $^{\circ}$C and particle size distribution for the sediment samples were analysed using the JMP software (Parsad and Khandelwal, 2010).

3.5 Groundwater

This section presents the method followed to understand the groundwater level across the alluvial floodplain for abstraction with the hand-drilling techniques.

3.5.1 Resistivity soundings

Resistivity soundings were carried out on the Lake Geriyo Irrigation Project southeast of River Benue, NE Nigeria (see Figure 2.8) in order to explore the floodplain groundwater. This is useful to understand the floodplain groundwater levels for abstraction with the hand drilling techniques. The selection of the geophysical survey sites is based on factors such as geological structures, hydrogeological information and accessibility for an efficient and effective survey. As shown in Figure 2.8, the specific location of the survey site is bounded by River Benue from the north-east. The survey transects were extended from the northeast boundary of River Benue of the site toward the south-west parts across the floodplain. The soundings were made along ten transects away from River Benue and at a spacing of 1,000, 1,500 and 2,500 m which cover the research area.

Resistivity survey was carried out using Schlumberger method in the field with the aid of a sensitive ABEM (SAS) Signal Averaging System, 1000 Terrameter by introducing current into the ground through a pair of current electrodes (Figure 3.10) and with the aid of a pair of potential electrodes. Resistivity data were obtained for each measurement, apparent resistivity values are computed using equation (3.1). Figure 3.8 shows resistivity sounding readings in the field with the ABEM Terrameter Equipment in the floodplain.

The groundwater levels along the floodplain of River Benue are shallow in the range between 5 to 20 m depth shown from the drilling logs. However, in order to attend a depth of 30 m with the resistivity sounding, an electrode spacing of 100 m is required. The depth of the resistivity sounding is typically 1/3 of the electrode spacing (Park et al., 2007).

Apparent resistivity (ρ_a) values were estimated using the following:

$$\rho_a = K\frac{V}{I} \qquad 3.6$$

where K is the geometric factor, and $\frac{V}{I}$ is the reading taking from resistivity meter.

$$K = \frac{\pi(S^2 - a^2)}{2a} \qquad 3.7$$

where "a" is spacing between potential electrodes and S is spacing between current electrodes (Robein et al., 1996; Raimi et al., 2011).

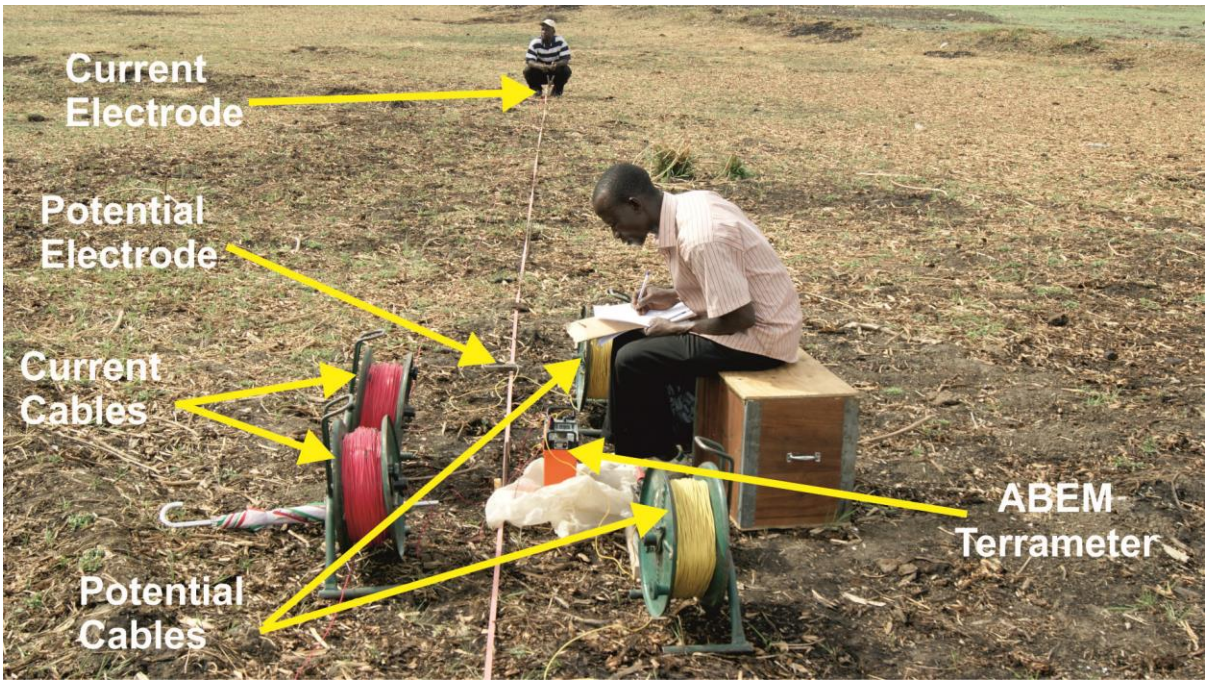

Figure 3.10: Taking resistivity sounding readings in the field with the ABEM Terrameter equipment at borehole location 8 transects 4 (see Figure 2.8) (The photograph taken by Mohammed Girei on 10th April 2011).

Correction of temperature

Resistivity is a function of temperature as described in section 2.6.1. There is no need to correct for temperature. The temperature at the time of the survey was between 30 and 40 °C, although high, was still within acceptable levels.

3.5.2 Hydraulic conductivity

This section describes the method followed to determine the hydraulic conductivity of the floodplain alluvial sediment from both laboratory and field pumping tests analysis. This will enable to understand the rate of water flow through the floodplain alluvial sediment formation for abstraction with the hand drilling techniques.

3.5.2.1 Laboratory hydraulic conductivity

Permeability tests were conducted at the Federal Polytechnic Mubi Adamawa State, northeastern Nigeria, for the sediment samples using a falling head permeameter (Figure 3.11). Eighty-seven samples were taken from the field site. Three different types of sediment samples (sand, sandy silt and clayey silt) were taken at each sampling location. The samples were taken from both the borehole cores in the field and outcrop along River Benue valley with an emphasis being placed on the clay silt, sandy silt and sand fractions. In order to obtain good results, the samples were properly sealed in plastic bags to avoid moisture loss and were carefully transported from the field site to the laboratory.

The sediment collected were samples disturbed in the field. The weight of samples plus mould, weight of mould and weight of sample, volume of cylinder were determined. The densities of samples were determined by dividing mould by volume of cylinder (M/V). The samples were compacted in the mould by applying 25 blows to each of the samples. However, if the sediments were not properly compacted in mould will not give proper estimate for the hydraulic conductivity.

Figure 3.11: Taking reading for laboratory permeability test using falling head permeameter (The photograph taken by Garba on 20th May 2011).

The falling head specimen contained the permeameter device connected to a burette that provides a means of measuring both the quantity of water passing through the sample and the applied head on the sample (Figure 3.11). Measurements were taken at different time intervals for each of the sediment. The coefficient of permeability was computed according to equation 3.8. Three tests on the same sample specimen were performed and averaged.

$$K = \frac{aL}{At} \ln\left(\frac{h_o}{h_1}\right) \qquad 3.8$$

where K is the saturated coefficient of permeability of the sample; 'a' is cross-sectional area of stand pipe; 'A' is cross-sectional area of the sample; h_o is initial height of water; h_1 is final height of water (h_o - Δh); L is length of sample column and t is time required to get head drop from h_0 to h_1 (Davis and Christenson, 1981; Binod, 2008).

3.5.2.2 Pumping test for estimating aquifer parameters

Laboratory hydraulic conductivity was determined in my first fieldwork survey in May 2011. However, due to consultation with the experts in the field of groundwater modelling studies, I was advised that field hydraulic conductivity values are more appropriate for the groundwater modelling than the laboratory hydraulic conductivity. That is the reason for doing the field-pumping test in my second fieldwork in April 2012 in order to get a reliable value for the hydraulic conductivity for the groundwater modelling.

In planning for the pumping test, the following were considered ahead of the fieldwork according to the British Standards Code (BS EN ISO 22282-4: 2012):

- Site reconnaissance survey was carried out to identify wells status and geologic features in the field.
- Pumping tests were carried out within the range of the designed rate.
- Pumping nearby wells shortly before the test was avoided.
- Pumping tests was carried out with open-end discharge pipe.
- The water discharged during the test was ensured that it does not interfere with shallow aquifer tests.
- The groundwater levels in both the pumping test wells and observation wells were measured before of start pumping.
- The reference points of water levels in wells were determined.

Prior to the start of pumping the following assumptions for unconfined aquifers were made:

- The aquifer is unconfined.
- The aquifer has infinite aerial extent.
- The aquifer has uniform water flow.

- The water table is horizontal prior to pumping.
- The well penetrates the full aquifer thickness.

Twelve different pumping tests (Figure 3.12) were carried out during the second fieldwork survey in April and May 2012, in order to estimate the aquifer parameters, such as hydraulic conductivity in the floodplain sediments. The pumping tests procedure was carried out according to the British Standards Code (BS EN ISO 22282-4: 2012).

Figure 3.12: Pumping test carried out in the field at borehole location 10 transects 5 (see Figure 2.28) (The photograph taken by Aishatu Abubakar on 23rd April 2012).

Instruments used for the pumping test include car for transportation, water pump machine, inlet pipe host, outlet pipe host, graduated measuring cylinder for measuring the discharge, data logger, stop watch, Vernier caliper for measuring the well diameter and recording sheet for recording data. At each pump station before the commencement of the pumping test, the

following parameters were measured: the static water levels for the twelve pumping wells and twelve observation wells, well depth, well diameter, the distance between the twelve pumping wells and the twelve observation wells, starting time and the stopping time. At each station, the well was pumped at constant rate for six-hour durations at 0.004 m^3/s, and an interval time of one hour was observed for drawdown for both the pumping and observation wells. The data obtained was recorded on the data sheet for the determination of hydraulic conductivity for the sediments.

The data obtained was used to estimate the aquifer parameters of the floodplain sediment.

Hydraulic conductivity, K, is the ease with which water can move through an aquifer. Hydraulic conductivity for an unconfined aquifer as defined by Nielsen (1991) was used to estimate the hydraulic conductivity through the floodplain sediment. It is represented mathematically as:

$$K_h = \frac{Q}{2\pi(H^2 - h_w^2)} \ln\left(\frac{R}{r_w}\right) \quad 3.9$$

where k_h is the horizontal hydraulic conductivity, H is the aquifer thickness, h is the water level after pumping, $H - h_w$ is the drawdown during pumping test, Q is discharge rate, r_w is the radius of the well screen and R is the radius of influence for the pumping well.

Transmissivity, T, is defined as the ability of the aquifer to transmit groundwater throughout its entire saturated thickness. It is the product of aquifer thickness and hydraulic conductivity. It is represented mathematically as:

$$T = Kh \quad 3.10$$

where h is the aquifer thickness of the unconfined aquifer or the height of the water table in meter (Freeze and Cherry, 1979).

The specific yield is defined as the volume of water pumped during the pumping test divided by the volume of the aquifer. The specific yield gives the quantity of water produced from the well per unit depth of drawdown. It is represented mathematically as:

$$S_y = \frac{Qt}{7.48V} \qquad 3.11$$

where S_y is the specific yield; Q is the discharge rate of the pumped well; t is the time since pumping began; V is the volume of the aquifer determined from equation 3.12.

$$V = \frac{Qr^2 e^{4\pi Twd/Q}}{4T} \qquad 3.12$$

where r is the distance from the axis of the pumped well to a point on the cone of depression; T is the aquifer transmissivity, wd is the aquifer drawdown (Ramsahoye and Lang, 1993).

3.5.3 Groundwater monitoring

This section describes the method used for monitoring the shallow alluvial groundwater of the floodplain. Monitoring hydrological processes at the River Benue floodplain was carried out for one-year period to investigate the variability in water storage and water flow through the alluvial floodplain. This helps to develop a hydrological model of the alluvial floodplain. Understanding hydrological processes in alluvial floodplain is important to identify the main controls on rates and directions of water movement (Bradley, 1997).

Twelve different borehole wells were monitored manually to observe the groundwater levels of the floodplain. For the period of two months during my fieldwork survey in April and May 2012, measurements were taken on daily bases. The manual measurements were taken by using deep stick in the wells. Deep stick was inserted into the well down to the bottom of the well. Depth of wells and static water levels wells were measured and recorded.

Two automatic piezometer MAlog itmsoil instrument (Figure 3.13) were installed 500 and 1,000 m away from River to continue monitoring the water levels in wells for the period of twelve months in order to estimate the changes for the groundwater levels. The time I was away from the site between May 2012 and April 2013, Mohammed Abana Girei helped with monitoring of the weekly water levels in wells on my behalf.

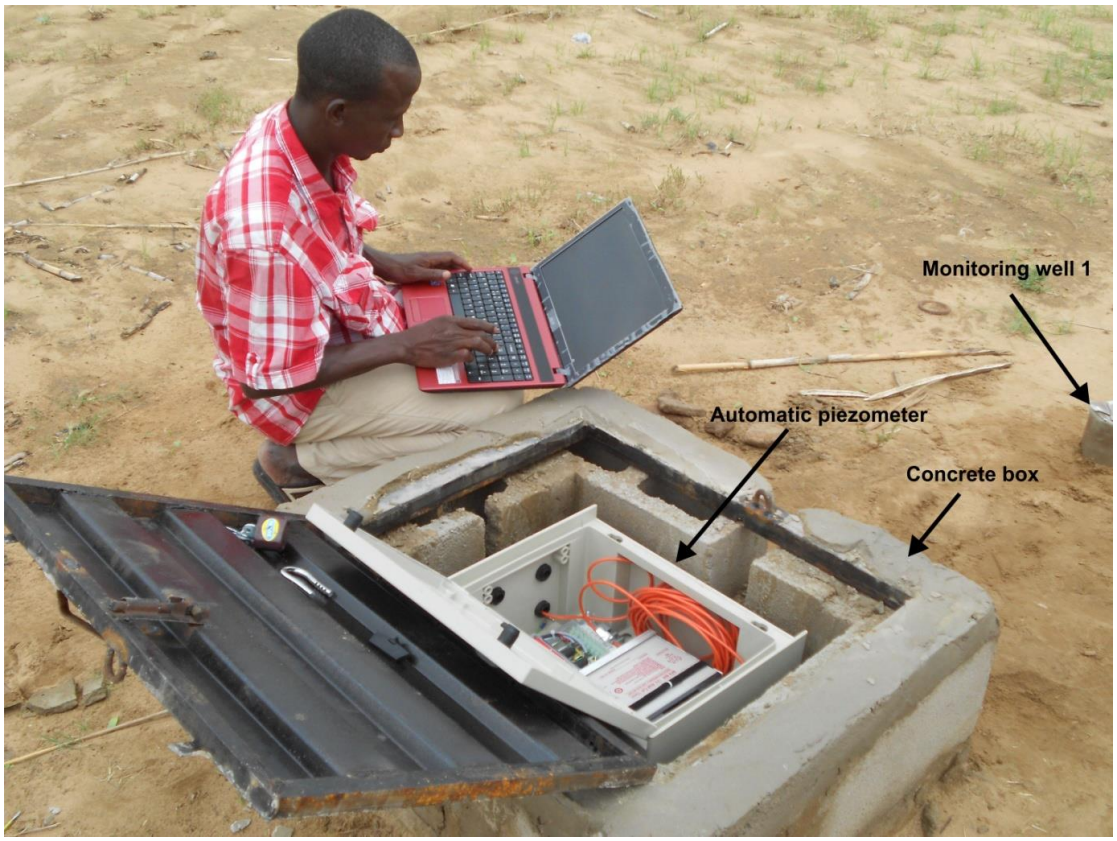

Figure 3.13: Configuring MAlog automatic piezometer in the field for monitoring groundwater level at borehole location 1 transects 1 (see Figure 2.28) (The photograph taken by Mohammed Abana Girei on 10th April 2012).

The piezometers were used to examine the variation in hydraulic head with distance from the River Benue to determine the hydrological significance of the river and to investigate the relationship of water table of the floodplain to precipitation. Weekly groundwater level measurements were measured with MAlog automatic piezometer to the vertical accuracy of ± 0.0002 cm. The elevations of the piezometers were determined with respect to a standard datum with an approximate accuracy of ± 0.01 m (see section 3.3). The automatic

piezometer, MAlog (mili-Amp logger), is designed as a low power, easily installed, web-enabled data acquisition system which can read 4-20 mA sensors (Itmsoil, 2012). Effort was made in order to obtain static water levels across the floodplain. Error may have occurred because measurements were obtained during intensive irrigation activities in the project area, which is unavoidable. It was observed that some farmers are over-exploiting the shallow groundwater of the floodplain, in excess of what their crops need.

A concrete box of 600 x 900 mm of 6" cement blocks was constructed to protect the piezometers at the site (Figure 3.13). The box was covered with a metal fabricated roofed lid, to provide rain proof shelter. A padlock key was used to securely lock the box.

The two automatic piezometers stopped working (Figure 3.14) in mid-August 2012 as result of the severe flood that occurred in 2012 which submerged the floodplain.

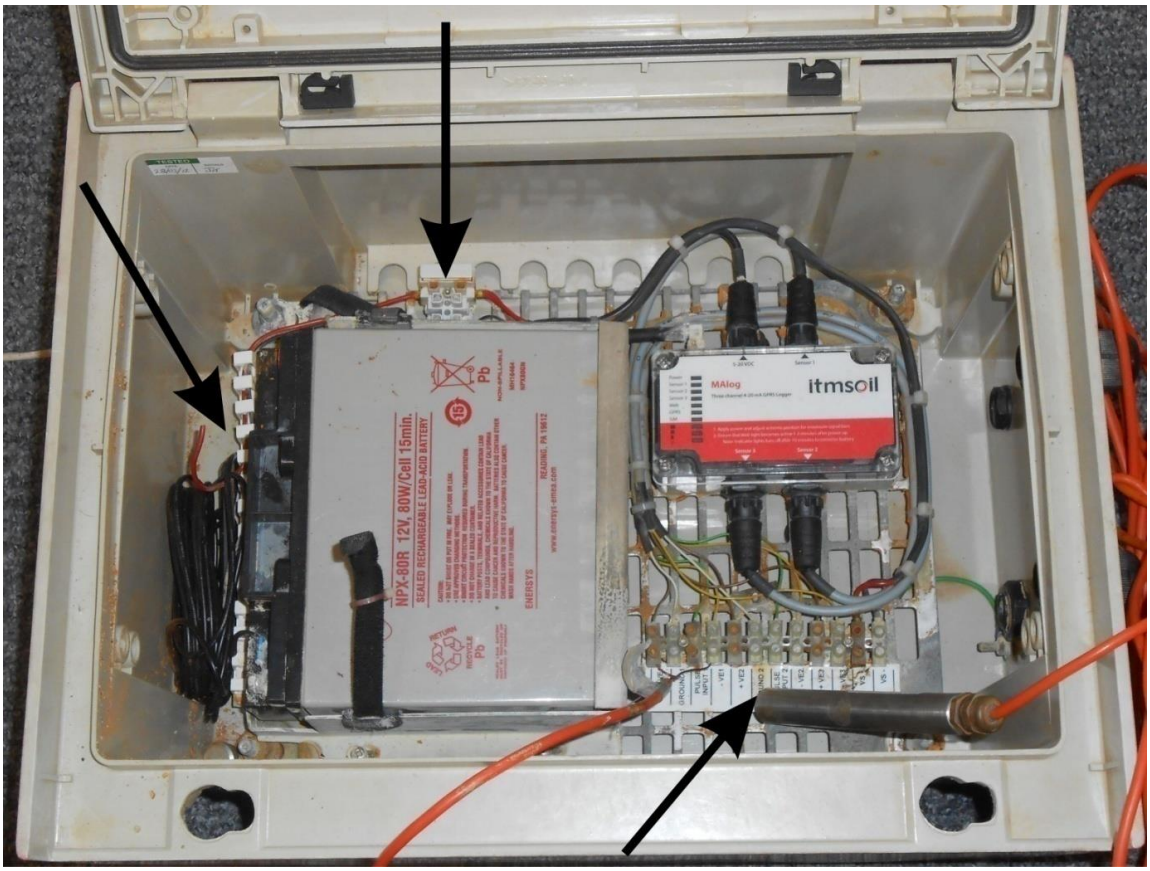

Figure 3.14: The damaged automatic piezometer due to the severe 2012 flood that submerged the floodplain. Arrows showing the damaged locations on the automatic piezometers (The photograph taken by the author on 20th May 2013).

3.6 Groundwater modelling

The purpose of the groundwater modelling in the present study was: (i) to develop a basic groundwater flow model for the Lake Geriyo Irrigation Project alluvial floodplain of River Benue; (ii) to understand the sustainability of current rates of abstraction of alluvial groundwaters using hand-drilling techniques; and (iii) to estimate the effects of groundwater extraction for irrigation during the dry season period. These parameters are essential to understand what the potential yields of irrigation wells are for the farmers especially during the dry season period, and understand how suitable they are.

The process of model development drew upon preparatory work that included i. determining changes in floodplain water levels using local piezometer measurements, ii. estimating the aquifer geometry from geophysics of the floodplain and permeability measurement through pumping tests, iii. obtaining the lithology of the boreholes, and iv. compiling rainfall, evaporation and river stage data for River Benue valley.

3.6.1 Conceptual model

Conceptual model is the process by which data obtained during characterisation of a site are examined to determine a relevant groundwater flow processes, and all available geological and hydrogeological data may be summarised in a simplified block diagram or cross-section (Anderson and Woessner, 1992). A conceptual model diagram showing both the floodplain and model water inflows and outflow is presented in Figure 3.15.

The floodplain system works in the order: In the dry season, water inflows comprise recharge from the river (due to the maintenance constant river water levels by the Lagdo Dam upstream), recharge from rainfall to the alluvial aquifer and recharge from the perennial Lake Geriyo. Water loses from the alluvial aquifer consist of water abstractions from wells for

irrigation and actual evapotranspiration (AET). The soil water balance is a function of vegetation cover, crop water requirement, rooting depth, bare soil evaporation (Figure 3.15) was not considered in the present study.

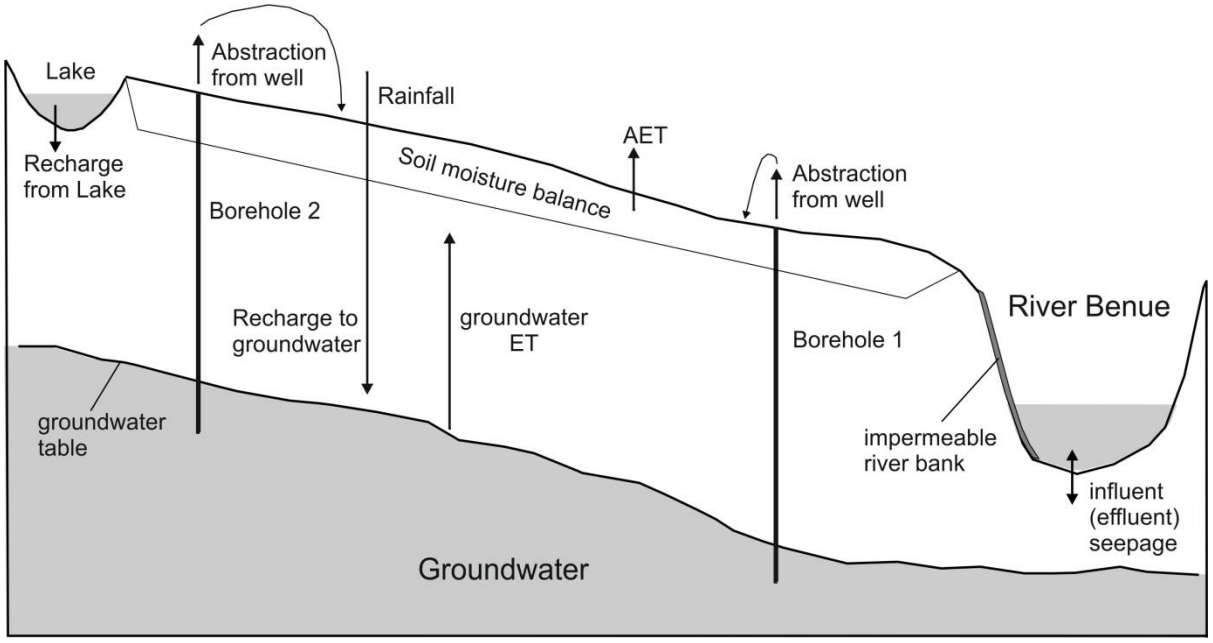

Figure 3.15: Conceptual model diagram. AET – actual evapotranspiration; Model ET – evapotranspiration from the model groundwater.

The model system works in the order: During the dry season, model inflows consist of rainfall recharge, seepage through the riverbed (described by a conductance term) and recharge from the Lake Geriyo to the model floodplain. Model outflows consist of water abstracted from wells, model evapotranspiration (model ET) which is the drawdown of the groundwater table induced directly by evapotranspiration from the alluvial aquifer (by deeply rooted vegetation) which is described as a function of the water table. The model only calculates water abstracted from the groundwater level in the floodplain (Payne et al., 2013). Similarly, the model only considers waters in the groundwater body, 20 m below the ground surface. This assumption is based on the results of the drilling and resistivity soundings that were undertaken in the field, which found the maximum depth of the floodplain water table to vary between 5 and 20 m. However, assumptions was made for the soil water balance (i.e.

vegetation cover, crop water requirement, rooting depth, bare soil evaporation) to be negligible.

3.6.2 Hydrostratigraphy of the alluvial floodplain

The hydrostratigraphy for the alluvial floodplain was obtained from borehole drilling logs, hydrogeology across the floodplain, geological maps, etc. (Maxey, 1964; Seaber, 1988). This drew upon data from 12 borehole-drilling logs, 12 pumping tests across the shallow floodplain aquifers, 24 resistivity soundings, and a geological survey of the site.

3.6.3 Model parameterisation

Model parameterisation utilised the following data, in seeking to develop a groundwater model of the floodplain using MODFLOW.

The model input data include the hydraulic properties, the boundary conditions, groundwater recharge from precipitation and discharge from River Benue during the dry season period, and evapotranspiration.

3.6.3.1 The hydraulic properties

Hydraulic properties are used to define and characterise individual aquifers and include hydraulic conductivity (or transmissivity), and specific yield (or storage). The most reliable aquifer properties are those obtained from controlled aquifer tests with known pumping rates, pumping duration, accurate well locations and accurate water level measurements.

Groundwater flow across the floodplain depends on the distribution of alluvial sediments, including particle size (Singh, 2005; Dor et al., 2011; Sikandar and Christen, 2012). Hydraulic conductivity, specific yield, and transmissivity were estimated from individual pumping tests, while the riverbed conductance was estimated from the literature (Freeze and Cherry, 1979; Fitts, 2002). Aquifer properties such as hydraulic conductivity, specific yield,

riverbed conductance are important parameters used by the model to assess groundwater flow (Baalousha, 2012). The River Benue is located to the right of the cross-section and exchanges of water between the floodplain and River Benue are assumed to occur through the riverbed and the shallow floodplain aquifers especially during the dry season period. The aquifer parameters obtained were used for the model to assess the exchange between River Benue and the shallow alluvial aquifers and to understand hydraulic heads across the floodplain.

3.6.3.2 Boundary conditions and their justification

No-flow boundary conditions were prescribed to the East and South of the model area and no water fluxes were permitted across these boundaries because the model was considered as a closed basin preventing flow into or from the model domain. Thus, the only means of groundwater flow is through the surface water outflow at the northwestern boundary of the area by River Benue and Lake Geriyo. It is necessary to simplify reality in order to model it with MODFLOW.

The northeastern boundary was described using a specified-head boundary condition, as this represents the point of contact between the River Benue and the floodplain. Water flow in River Benue is maintained by the Lagdo Dam upstream in Cameroon during the dry season period.

Specified-head boundary conditions were specified at top and bottom of the river, estimated from the river water stages in River Benue for the stress periods January to June (1960 to 2012).

Specified-head boundary conditions were specified at the top and bottom of the aquifer (from water levels observed in the well network across the floodplain). Water level elevations across the floodplain were estimated from 24 resistivity sounding points and water level measurements.

The base of the aquifer layer was assumed to be provided by an impermeable clayey silt layer. This was represented as a no flow boundary with a mean hydraulic conductivity of 4.37 x 10^{-8} m/s (obtained from laboratory analysis). The justification for the clayey silt formation underlying the aquifer across the floodplain lies in the floodplain sedimentology observed in the 12 borehole logs and resistivity survey across the floodplain.

A constant-head boundary condition was specified to the west of the model. This is the contact between Lake Geriyo and the floodplain. Lake Geriyo has water throughout the year and it represents a source of water to the floodplain during the dry season period.

The arrangement of the top and bottom boundary conditions enables recharge cells in the model to have different flux values for each time period in the transient simulations. The model was developed for the period January to June 2012 (26 weeks or 26 stress periods). This enables the aquifer response to changes in river level and abstraction to be determined during the dry season period. The period also coincides with a time when floodplain water levels were measured. The initial, starting, heads for the model were taken as the observed heads measured at the beginning of the model period (1st January 2012).

3.6.3.3 Groundwater recharge

For the present study, groundwater recharge was assumed to be derived mainly from rainfall, the average annual rainfall in the region is 914 mm. Rainfall recharge was computed using weekly data, and recharge was assigned to the top surface of the model.

3.6.3.4 Evapotranspiration

The evapotranspiration (ET) package of the model computes the impact of plant transpiration and direct evaporation in removing water from the floodplain groundwater storage. One of the principal mechanisms of groundwater discharge in vegetated and shallow groundwater

systems of semi-arid regions is evapotranspiration (Ajami et al., 2011). The weekly evaporation data obtained from the hydraulic unit of UBRBDA, Yola, was used to integrate evapotranspiration into the model. In estimating model evapotranspiration, negligible water losses were assumed for vegetation cover, crop coefficient, rooting depth, and bare soil evaporation. This is because the model considers water loss from the groundwater at 7 m depth. As mentioned in the literature, the irrigated crops include cereals like maize, rice, wheat, and vegetables like amarantus (alefo), okra, spinach, onions, lettuce, tomatoes (see section 2.2.7). The rooting depth for these crops is insufficient to reach the groundwater at 20 m depth.

3.6.4 Numerical modelling

In this study, measured floodplain water levels were used to describe the potentiometric-surface, while pumping tests were completed to estimate the hydraulic conductivity and specific yield. The laboratory hydraulic conductivity result shows some variations, while the field tests give fairly uniform hydraulic conductivity values and these were used as input to the model. Drilling logs from wells were used to define aquifer lithology and aquifer saturated thickness.

The floodplain was assumed homogenous and isotropic, i.e. groundwater flows are uniform through the system. Figure 3.16 shows the simplified cross-section used to represent hydraulic properties along a floodplain section perpendicular to the River Benue. The floodplain was envisaged as constituting an alluvial hydrogeological layer, with a high hydraulic conductivity of 0.021 m/s (Table 3.1).

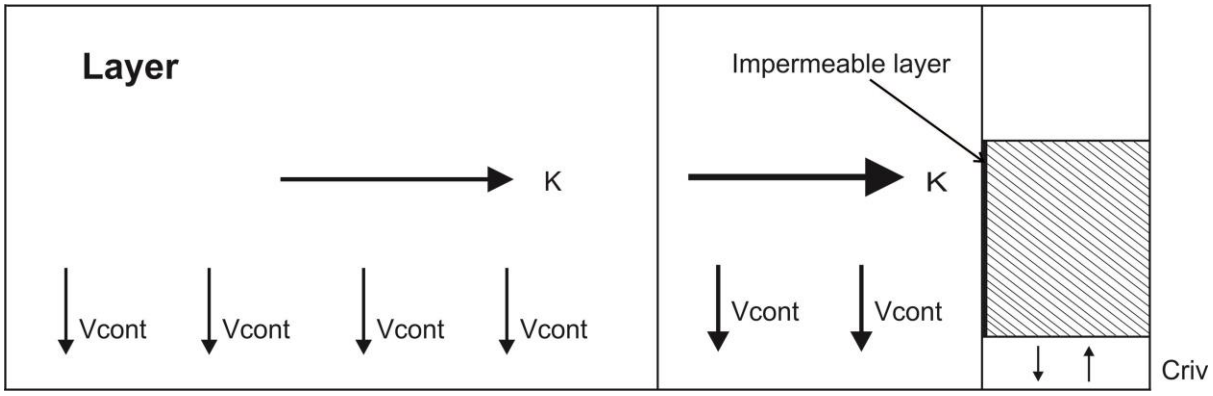

Figure 3.16: Schematic cross-section through floodplain profile illustrating the relationship between vertical and horizontal permeability for the hydrogeological layer (vcont and K) and for the river bed conductance (Criv) (Modified from Bradley, 2002).

The River Benue is situated to the right of the cross-section and exchanges of water between the floodplain and the river were assumed to occur through the riverbed and the alluvial floodplain aquifer. Quantification of the direction and magnitude of riverbed seepage is necessary to improve the accuracy of numerical models. This assumption seems to be justified because of the accumulation of sand and sandy silt sediments adjacent to the river. This is represented in Figure 3.16 as cells in the layer with horizontal and vertical arrows.

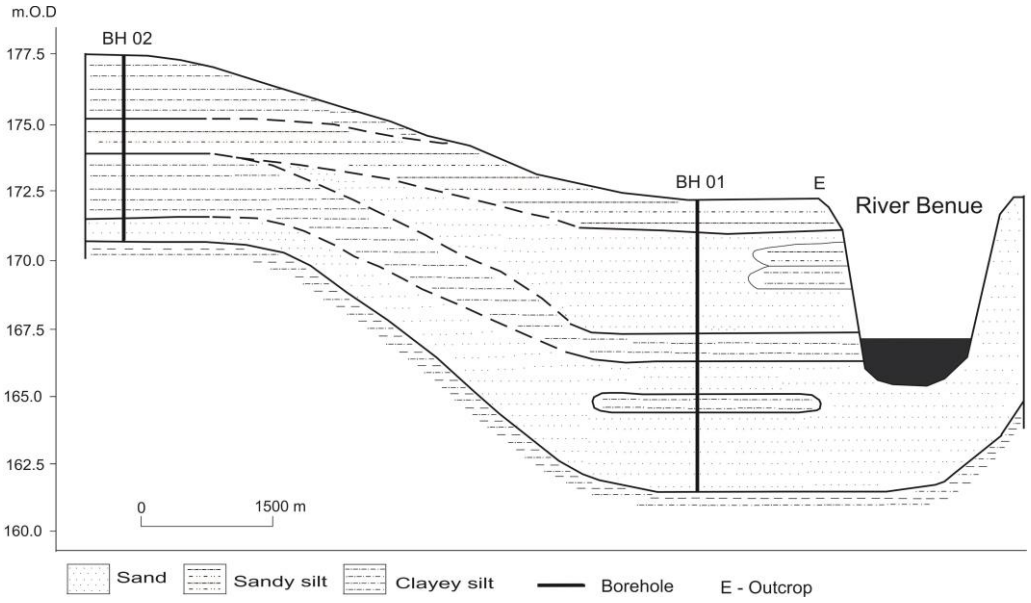

Figure 3.17: Hydrostratigraphy of the alluvial floodplain obtained by hand augering drilling and outcrop along transect 1 at 1,500 m transect from River Benue. BH – borehole; E – outcrop sampling.

The cross-section in Figure 3.17 provided the basis for model development, which was constructed by overlaying a rectangular model grid extending ~1,500 m to the north and 2,000 m to the west, orientated to coincide with the monitoring wells centered upon one borehole transect extending from the River Benue transect 1. The floodplain sedimentology in Figure 3.17 was represented by a single layer (as described in borehole drilling logs along the floodplain transect). A clayey silt formation was assumed to underlain the entire model area, and to form the lower no-flow boundary of the model. The layer comprised sand, sandy silt and clayey silt deposits, which formed an unconfined layer, extending 1,500 m across the floodplain of the River Benue. Individual cells had dimensions of 100 x 100 m to form 1 row and 100 columns grid.

Model simulations were undertaken using a time unit specified in days, and length specified in metres, and with hydraulic conductivity, recharge and evaporation specified into the model package accordingly. The data used for the model included >50 years of rainfall and river stage data (see section 3.2) and thirty years of evaporation data (see section 3.2), supplemented by groundwater data collected over a 3 year period of fieldwork to enable modelling over the period January to June 2012. The simulation period was divided into 26 stress periods and each stress period was divided into 10 time steps. Hydraulic conductivity and specific yield were obtained from pumping test data, while riverbed conductance was assumed (2,000 m^2/day) according to text book as recommended by Freeze and Cherry (1979) and Fitts (2002). In selecting the value of hydraulic conductivity, least value was used because of interest in the worse situation. Boundary conditions were assigned to the model, in reference to top boundary condition, bottom boundary condition and side's boundary conditions. The water level along the floodplain formed the top boundary condition, no-flow boundary was assigned to the bottom of the aquifer and no-flow boundary was assigned to the sides, a general head boundary was used to assess the exchange between Lake Geriyo and

floodplain groundwater. Top and bottom elevations for each individual layers were represented with information obtained from 24 resistivity sounding points and water level measurements. More detailed explanations for boundary conditions are provided in methodology section 3.6.3.2 above.

Model evapotranspiration was estimated in MODFLOW by assuming water loss across the floodplain as a function of the water table depth and a specific 'cut-off' depth. Daily evaporation, recorded by the UBRBDA at Yola weather station (see section 3.2), was used to estimate evapotranspiration to the model. The soil water balance was assumed negligible as the model only considered loss of water from the groundwater depth of 7 m. The approach taken to simulate evapotranspiration (ET) in MODFLOW is based on the following assumptions, which are based on relevant cited studies (Payne et al., 2013): i. when the water table is at or above ground level then ET losses occur at the potential rate (ET); ii. when the water table depth is below ground level exceeds a certain interval (termed the ET extinction depth); a value of 7 m was assumed here, ET losses cease; and between these limits, ET varies linearly with water table elevation, see Figure 3.15.

Modelling is the best way to accurately assess the groundwater budget across the floodplain (Panagopoulos, 2012). Water budget data indicate the relative magnitude of groundwater flow components. If any errors in the iterative solution exist, then this is likely to be apparent in the water budget. The available data for the study site were used to assess the water budget across the alluvial aquifer. A summary of the model data required and an indication of how the values were obtained is provided in Table 3.1.

Table 3.1: Hydrologic parameters used to describe the model cross-section

S/NO	Parameter	Value	Remarks
1	Hydraulic conductivity (K) (m/s)	0.021	Obtained from pumping test data
2	Specific yield (S_y)	0.05	Obtained from pumping test data
3	River bed conductance (m/d)	2,000	Assumed
4	Depth to water table	Piezometer data for the period January to June 2012	Monitoring wells in the fieldwork

3.6.5 Model calibration

Groundwater flow models are commonly calibrated using observed groundwater levels and river stage (Allen et al., 2004; Brouyère et al., 2004). Figure 3.18 shows the calibration process for the model. Model parameters, which can be adjusted during the calibration process, include hydraulic conductivity, specific yield, streambed conductance. In this case, model calibration was performed by varying hydraulic conductivity and specific yield with the aim of understanding the variation of hydraulic head throughout the model. Varying the hydraulic conductivity and specific yield in the model until the simulated hydraulic heads matched with measure hydraulic heads as shown in Figure 3.18.

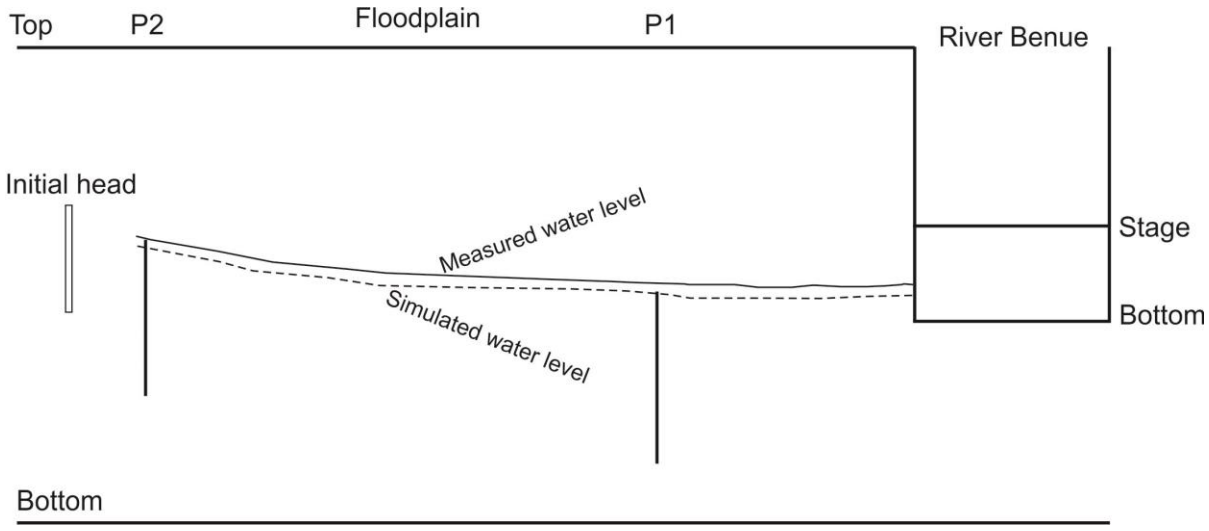

Figure 3.18: Model calibration using monitored water levels at piezometers 1 and 2 situated 500 and 1,000 m from River Benue.

3.6.6 Sensitivity analysis

The model was calibrated by a manual trial-and-error process. Manual calibration may not accurately assess the model reliability result. Therefore, calibration was further carried out by detailed sensitivity analysis. Sensitivity analysis is a very important step in all modelling applications (McDonald and Harbaugh, 2005). The aim of the model sensitivity analysis is to verify that the model accurately simulates the floodplain groundwater flow (Lachaal et al., 2012). Aquifer parameter values that were considered in the sensitivity analysis include hydraulic conductivity, specific yield and riverbed conductance. The model was run, having varied values for each of these aquifer parameters to assess model reliability.

3.6.7 Model limitations

A groundwater model is a simplified approximation of actual conditions. The accuracy of the groundwater results depends on the accuracy of the input data, and the validity of the conceptual model. The groundwater flow model for this study was constructed with available historical, site-specific hydrologic data and assumptions to determine groundwater flow direction, river seepage (influent flow) to the wells in the River Benue alluvial aquifer in the floodplain. To correctly interpret model results the following limitations of the model should be considered.

1. Model parameters such as hydraulic conductivity, recharge from precipitation and discharge by evaporation are applied uniformly to a model cell. The assumption of homogeneity can cause inaccuracies because geologic material and climatic conditions are typically heterogeneous and isotropic.
2. The groundwater flow model was discretised using a grid with cells measuring 100 m x 100 m. Model results were evaluated on a relatively large scale and cannot be used for

detailed analyses such as simulating water-level drawdown near a single well. A grid with smaller cells would be needed for such detailed analyses.

3. Although the model was calibrated with transient conditions, analyses of groundwater flow, river seepage (influent flow) and discharge from evaporation were based on simulated transient conditions. In alluvial aquifers like the River Benue alluvial aquifer, transient conditions only rarely, if ever, occur because of constantly changing river stage, rainfall and well pumping. Analyses based on transient conditions alone without steady-state conditions should be considered approximations of actual or historical conditions.

4. Well pumping rates used in the groundwater flow model were based on: the estimated pumping rates (172.8 m^3/day) were at the rate farmers use to irrigate their crops on a weekly basis (i.e. 6 hours a week) computed from pumping test and assumption was made based on considering a total of 40 active wells along transect 1. Inaccuracies in estimated pumping rates may introduce some errors in the model results.

3.6.8 Predictive scenarios

In a predictive simulation, the hydraulic head values obtained during calibration process were used to predict the response of the groundwater body to future events. The model prediction depends mostly on the result of the calibration and sensitivity analysis (Anderson and Woessner, 1992). Predictions can be used to test various scenarios of how a calibrated model will respond to different system stresses such as recharge and extraction. Here, the calibrated model was used to predict the groundwater resources in the floodplain. Having successfully simulated observed conditions, the model was used to consider three different combinations of predictive model runs to assess the response of the alluvial aquifer to different stress scenarios including:

i. Low, average and high river water stages for the period January to June 1960 – 2012. The lowest river stage may occur if the Lagdo Dam authorities were to reduce the limited amount of water released under a scenario of climate change.

ii. Low, average and high wells pumping rates for irrigation across the floodplain, according to the plans of Lake Geriyo Irrigation Project, and the demand of an increasing population.

iii. Global climate change: i. low precipitation and high evaporation for the period January to June, 1966, this is a period when a severe drought occurred in the region; lower river water stages, and high pumping rate; ii. Average precipitation and evaporation for the period January to June 1960 to 2012; average river water stages and normal pumping rate, iii. High precipitation and low evaporation for the period January to June, 2012; high river water stages and low pumping rates.

CHAPTER FOUR - CLIMATE VARIABILITY AND RIVER BENUE DISCHARGE IN THE UPPER BENUE BASIN

Yola is located in the semi-arid savanna zone, just south of arid Sahel. The analysis detailed in this chapter (including precipitation, evaporation, River Benue discharge and water stages) was needed for the groundwater modeling analysis.

4.1 Introduction

This chapter presents analyses of hydrological and meteorological data. The first section (4.2) describes the River Benue in Yola and Garoua. The second section (4.3) analyses climate variability in the Sahel region, and in Yola and Garoua regions. The third section (4.4) analyses hydrological data of River Benue. Finally, the fourth section (4.5) uses the Standardised Precipitation Index (SPI) for estimating flood and drought events in the region.

4.2 River Benue

4.2.1 River Benue in Yola

River Benue (see Figure 1.1) is a major tributary of the River Niger in Nigeria. It starts in the mountains of central Cameroon and flows south-west for 1,400 km. From its source, it flows west and crosses the Lagdo reservoir in Cameroon through the town of Garoua and then flows into Nigeria south of the Mandara mountains and through Yola (Sarch et al., 2001). During flood periods, River Benue water is linked via the Mayo-Kebbi tributary with Lake Chad, which increases approximately 100 fold its drainage area. The valley contains seasonally inundated floodplain, which provides important irrigation activities along the valley after the flood has receded during the dry season period.

4.2.2 River Benue Basin in Cameroon

The Upper Benue River watershed has a total surface area of about 95,000 km^2, which is unequally distributed among three countries, Chad (18,000 km^2), Cameroon (75,000 km^2) and Nigeria (2000 km^2) (Tamfuh et al., 2011). The main tributaries contributing to the River Benue area in Cameroon are the River Faro and Mayo Kebbi. Both empty into River Benue in Nigeria east of Yola (Figure 4.1).

The Lagdo Dam (Figure 4.1) that was constructed on River Benue in Cameroon resulted in an increased water flow during the dry season. The Lagdo Dam discharge keeps the groundwater of alluvial aquifers at a high level downstream during the dry season, especially for the Yola region, which is the study site.

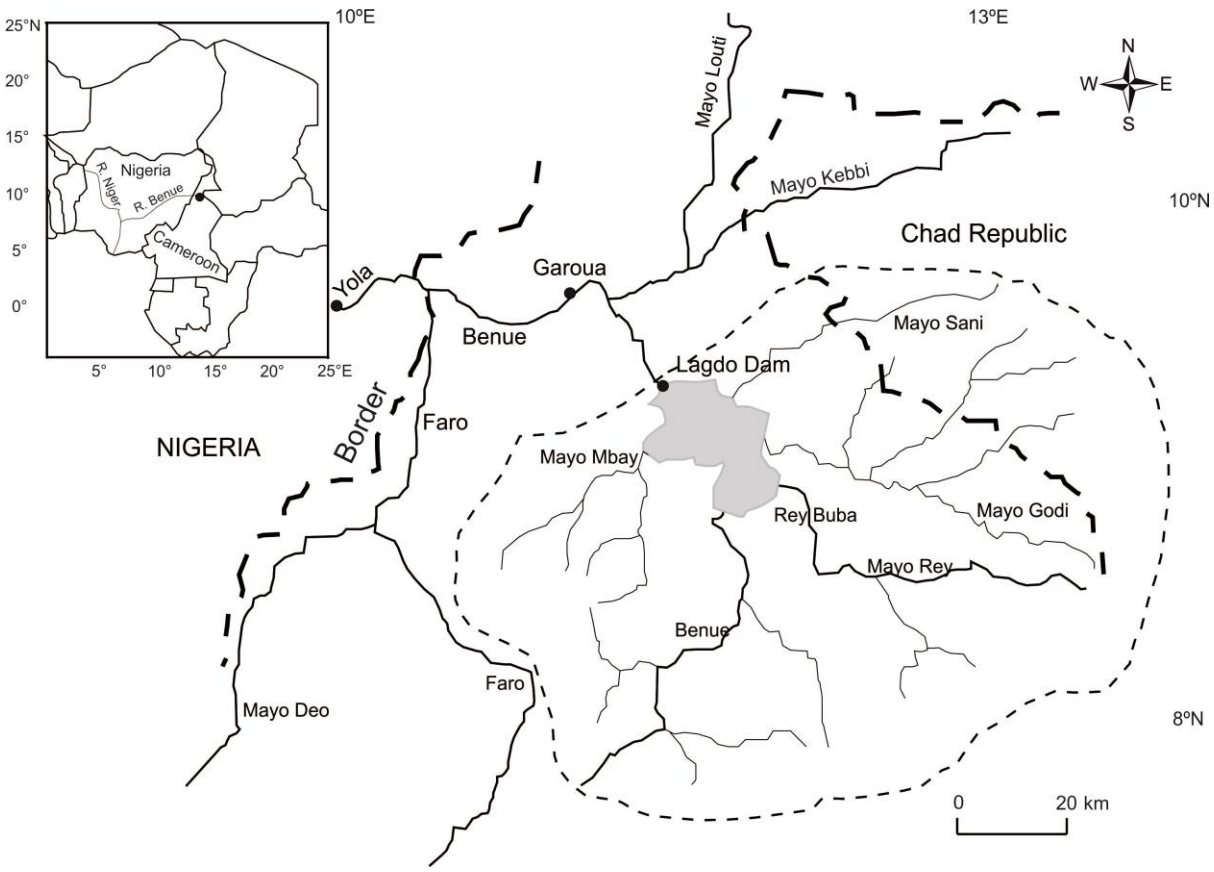

Figure 4.1: Map of River Benue Basin in Cameroon showing the location of Lagdo Dam. Dotted line: Lagdo Dam Drainage Basin (Modified after Kamga, 2001).

The River Benue has a maximum monthly mean discharge rate of 1,268 m^3/s at Garoua station during the rainy season (Kamga, 2001). This causes floods downstream. The floodplain of Benue valley is formed of alluvial deposits and is flat with an altitude of 242 m in Garoua.

4.3 Climate variability in Sahel Region

As Yola and Garoua's climate have some characteristics common to the Sahel, despite their 1,000 mm of annual precipitation, it is appropriate to include a section on the Sahel. The Sahel region and its climate have been studied in more details than the Yola region, because of the famous Sahel droughts (Nicholson, 1979; Lamb, 1978; Lamb, 1983; Lamb and Peppler, 1992).

Globally, in arid and semi-arid environments, droughts are the main cause that contributes to low agricultural production that leads to famine periods (Sivakumar et al., 2005). Rainfall in semi-arid Africa has been noted for its inter-annual fluctuations, with greater impacts on the general hydrological cycle, floodplain groundwater and food security. Many researchers have discussed the causes of droughts in the Sahel during the 1970s and 1980s. According to Nicholson (1979) and Lamb (1978), several drought periods followed by wet events occurred. The devastating droughts of the early 1970s prompted researchers such as Lamb (1983), Lamb and Peppler (1992) and others to look into possible mechanism behind such temporal and spatial variability. Some of the major droughts in West Africa in the last century occurred in 1913 – 1914, 1966 – 1968, 1972 – 1973, 1982 – 1983 and 1997 – 1998 (Molua and Lambi, 2006).

Le Barbe et al. (2002) carried out a study on rainfall variability in West Africa between 1950 and 1990 and noted a systematic decrease in the number of rainfall events, which appeared comparable to the decrease of mean inter-annual rainfall. Nicholson and Palao (1993) made

an overview of Sahel rainfall fluctuations and found this region to have experienced rainfall variability since the 1960s, depicting decreasing trends. As reported by Calow et al. (2011) the decrease in the precipitation in the West African region occurs in spring, this is because recently more and more delayed in the summer rainfall. In contrast, Dai et al. (2004) showed rainfall to have positive trends since late 1990s. A similar study by Niang et al. (2008) showed a significant increase of yearly rainfall from the early 1990s in a semi-arid region of southwestern Mauritania. Ekpoh and Nsa (2011) analysed long-term data from various gauge stations in the Sahel parts of northern Nigeria, and they obtained an increased severity of droughts in the region.

Forcing by sea-surface temperature in the Atlantic Ocean has caused dry summers in Sahel (Druyan, 1991; Giannini et al., 2003). Studies have shown that warm sea-surface temperature anomalies in the Atlantic Ocean may cause reductions of precipitation over the African continent by lowering atmospheric pressures (Druyan, 1991).

Precipitation variability initiates variability in river flow. Coupled spatio-temporal interconnections exist between precipitation, local topography, geology, sediment types and groundwater recharge and river flow (Calow et al., 1997; Vincent et al., 2007). A critical analysis of precipitation patterns over a given drainage basin would serve a great deal of insight into the connection between groundwater recharge and long-term river discharge variability. The influence of climate variables on river flow regimes is complex with intricate interactions between evaporation losses, soil moisture conditions, catchment geology, land use and artificial changes to streams (Biggs, 2009).

Several studies have stressed the necessity of management of water resources in Nigeria (Deve, 2000; Ojo et al., 2003). However, as pointed by MacDonald et al. (2005), limited knowledge of how African groundwater responds to climate change is available. This part of

the present study analyses the climatic variability and River Benue discharge in Yola, northeast Nigeria and Garoua in northern Cameroon.

4.3.1 Climate variability in Yola region

The region is characterised by a tropical dry climate, with strongly contrasted dry and rainy seasons. The dry season is from late November to May and is characterised by the Harmattan wind blowing from the Sahara Desert (Adebayo, 1999). Figure 4.2 reveals that the maximum monthly mean temperatures range from 30 to 40 °C and minimum temperatures range from 15 to 23 °C. Highest temperatures are recorded in April; this is the peak period of the dry season in the region. The lowest mean monthly temperatures are recorded in the months of December and January; this is winter period in the region. The increase in temperature raises the evaporation (Conway, 2011). This will have an impact on the shallow alluvial aquifers of the floodplain.

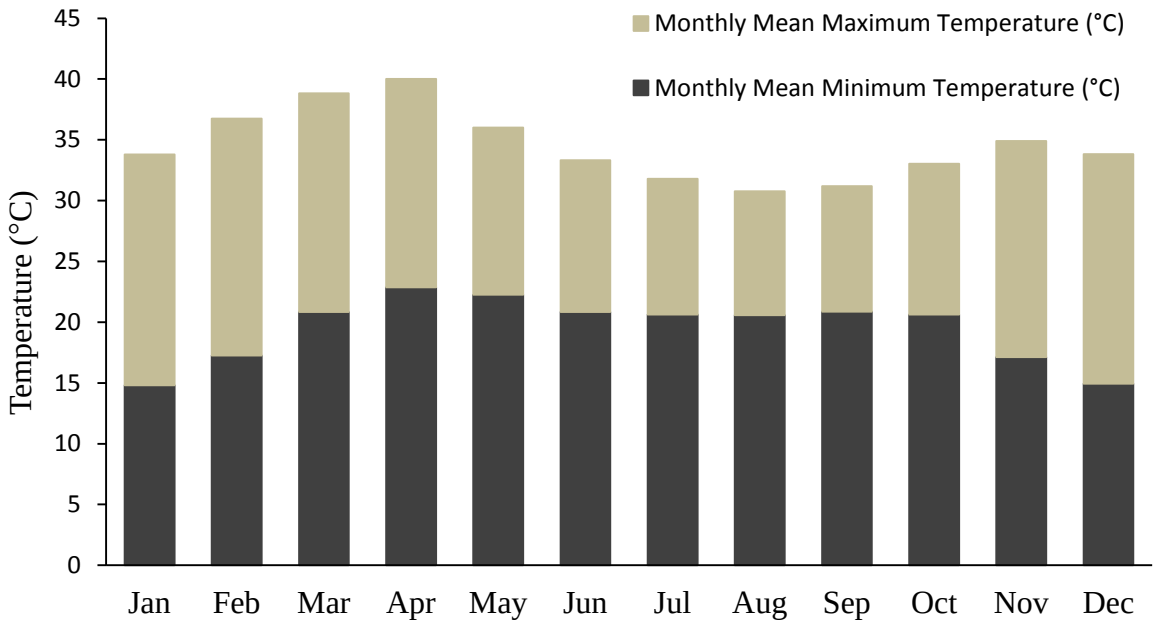

Figure 4.2: Monthly mean temperature for Yola region for the period 1980 to 2012 (Produced from data obtained from Upper Benue River Basin Development Authority (UBRBDA) Yola hydrological year book 1960 to 2012).

The temperatures in the region are generally high and this has an impact on the groundwater, especially during the dry season period. As reported by IPCC (2013), between 2016 and 2035 global average temperature is predicted to increase by 1 to 1.5 °C (Kirtman et al., 2013). In the northeastern Nigeria over the period 1961 to 1991, the observed average temperature increased by about 1.5 °C (Hess, 1998). The floodplain alluvial sediment of the Yola region consists mainly of sand and sandy silt, therefore any increase in temperature will rapidly increase the rate of water lost from the alluvial floodplain, which will lead to lowering of the groundwater level.

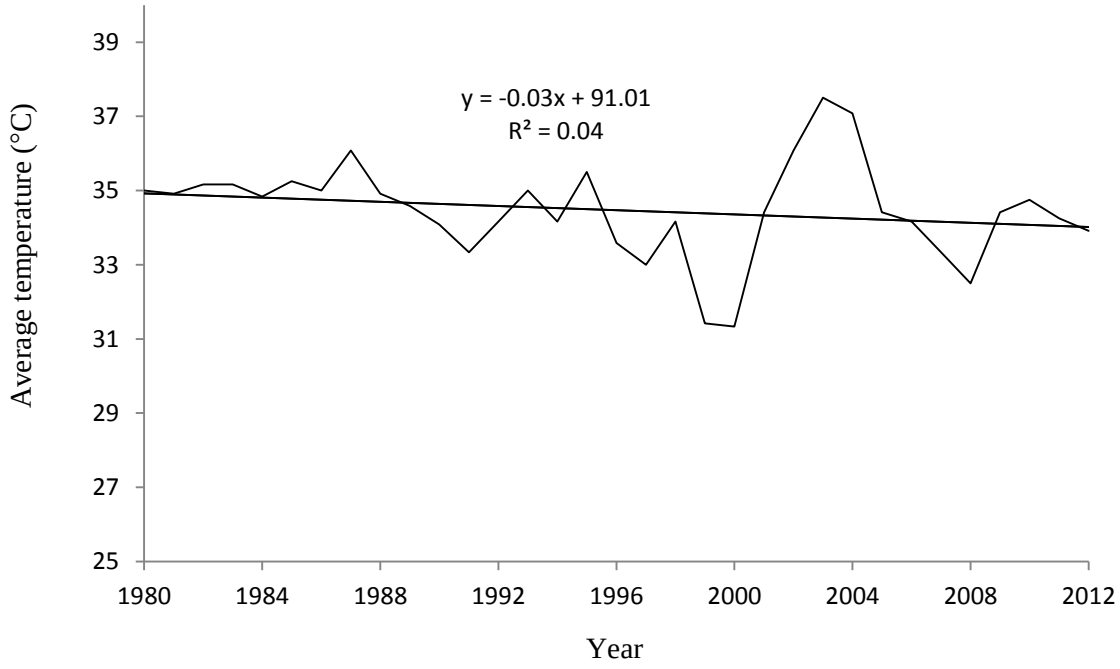

Figure 4.3: Annually mean temperature for Yola region for the period 1980 to 2012 (For source of data see Figure 4.2).

Figure 4.3 shows the average annual temperature for the Yola region for the period 1980 to 2012. It can be seen that fairly consistent patterns is observed between 1980 and 1986. Decrease in temperature by 4.5 °C is however observed between 1995 and 2000. A very weak negative trend is highlighted.

Rainfall distribution in the northeastern Nigeria is unimodal (Hess et al., 1995). The rainfall regime is characterised by a single peak, the rainy season starting in May/June as the Inter-Tropical Convergence Zone (ITCZ) passes northwards, with a maximum in August and finishing quite rapidly in October (Hess et al., 1995; Adebayo, 1999). The total annual precipitation of the area is on average 914 mm (taken over the period 1960 to 2012). The higher rainfall rate is observed between June and October each year; while the rest of the months are virtually dry (November to May). This will result in lowering the floodplain groundwater in winter and spring, which will influence irrigation in the region.

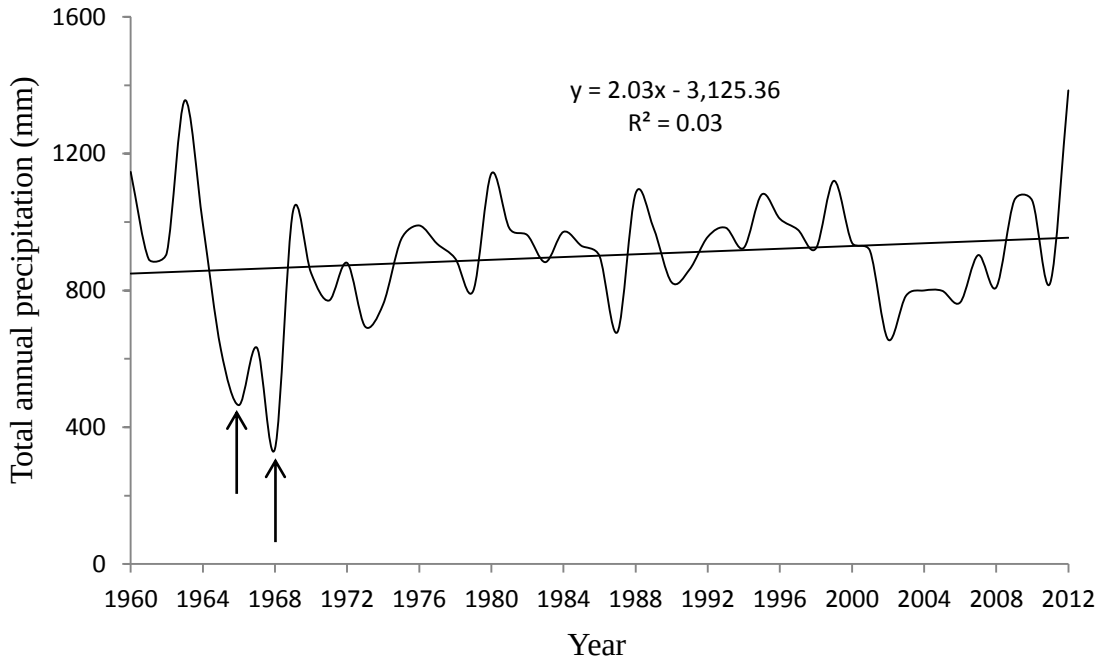

Figure 4.4: Yola total precipitation per year for the period 1960 to 2012 showing the rainfall associated with the 2012 flood. Arrows showing the droughts of 1966 and 1968 (For source of data see Figure 4.2).

High rainfall usually experienced in August and September each year, with changing flood frequency, varies from year to year. For example when the 2012 flood occurred, it submerged the State, caused destruction of life and properties and displaced over 3,000 families (BBC web site 2012). Figure 4.4 shows the variation of the annual rainfall from 1960 to 2012. It can be seen that, after the dip in 1964 to 1968, and then a further dip with a starting point at the

beginning of the 1970s, the area had nearly constant precipitation between 1980 to 2000 as recently pointed out by Dai et al. (2004). The earlier study by Hess et al. (1995) on the rainfall variability of the northeastern Nigeria for the period 1961 to 1990 shows a decrease in the annual rainfall. The present analysis does not show any trend.

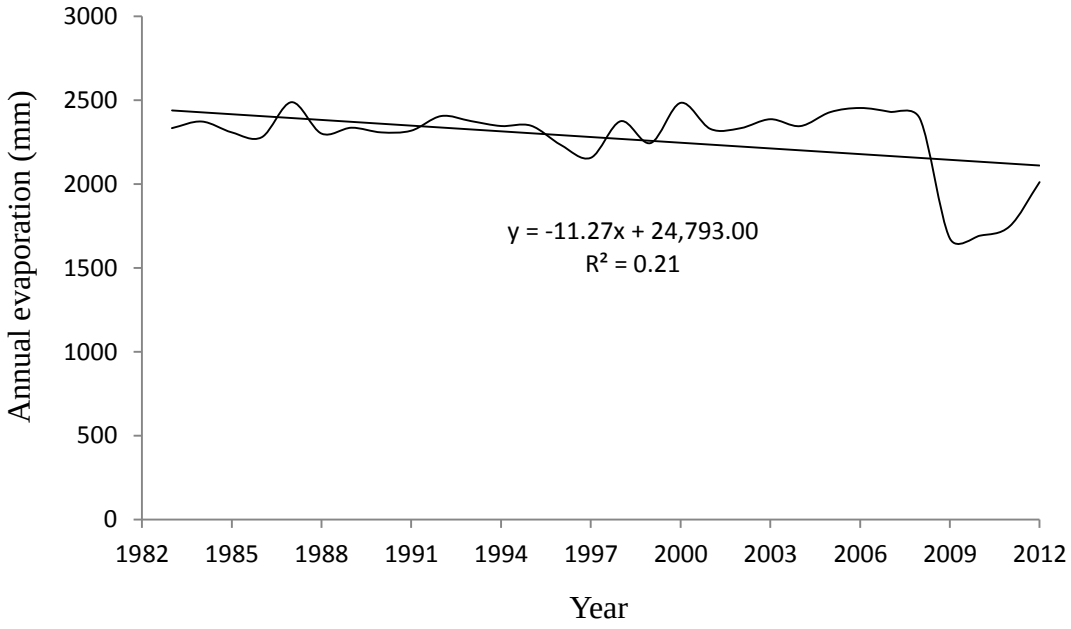

Figure 4.5: Variation of annual evaporation in Yola for the period (1983 – 2012) (For source of data see Figure 4.2).

Evaporation considerably exceeds precipitation with total annual values between 1,676 to 2,788 mm. This phenomenon explains the farmers' strong dependence on groundwater for water supply and irrigation in the region. Evaporation is generally high due to high insolation and high relative humidity in the region, which is low between January and March and increases from April to reach the peak in August and September. Figure 4.5 shows the variation of the annual evaporation for the period from 1983 until 2012. It can be seen that, after the increase shown towards 2004, the area start experiencing a generally lower rates from 2009 onwards. The sharp changes observed in 2008 and following years could be due to the error in the data measurement, this is hardly a real value. These suggested that the

evaporation patterns in the region decreases with a weak negative trend (see Figure 4.5). It can be seen that the evaporation trend in the region is higher as compared to rainfall trend.

4.3.2 Climate variability in Garoua, Northern Cameroon

Garoua is located at latitude of 9° 18' N and a longitude of 13° 24' E in Northern Cameroon and at an altitude of 242 m (see Figure 4.1). It is characterised by a tropical dry climate having a dry season from October to April and rainy season from May to September (Moussa et al., 2011), similar to Yola which is 250 km from there. Garoua local government area covers an area of about 4,700 km^2 and is drained by the River Benue, which is the most important river of the area (Cheo et al., 2013).

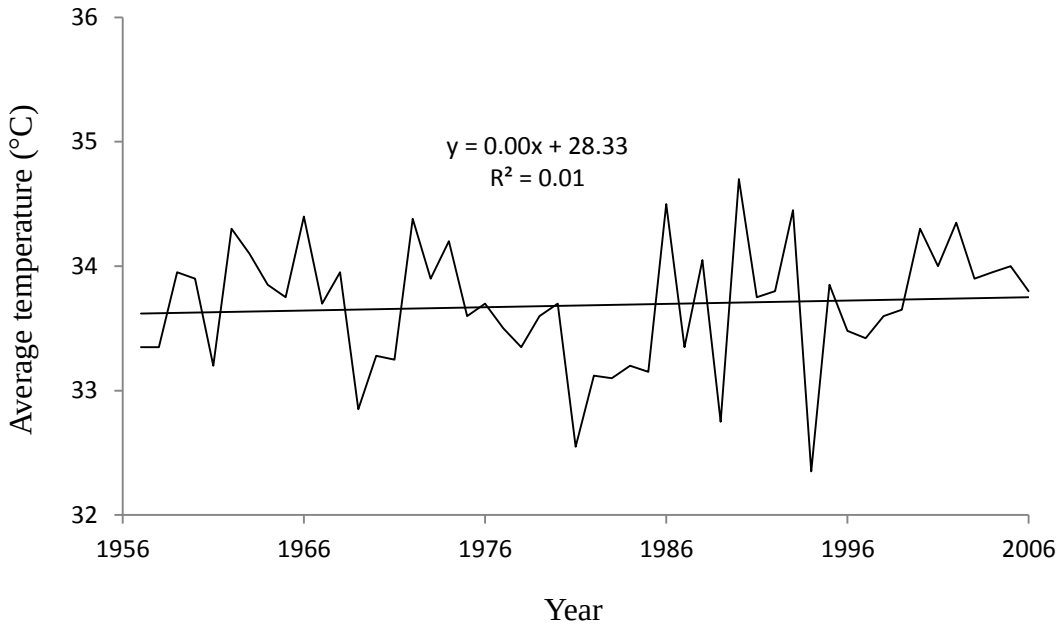

Figure 4.6: Garoua annual average temperature (Produced from data obtained from Cheo et al., 2013).

Figure 4.6 shows the average annual temperature in Garoua over the period 1956 to 2006. The mean annual temperature is about 33.68 °C. The maximum and minimum temperatures of the region generally follow the seasonal change, being higher during the dry season (October to May). Maximum value reach up to about 42 °C in March and lower during the

rainy season (June to September), with minimum value around 18 °C in January. Mean annual temperatures increased from 1957 to 1966 by 1.2 °C. However, from 1967 to 1969 a short decrease in annual mean temperature was observed. This was followed later by a marked decrease in mean annual temperature between 1972 to 1981 by 1.8 °C. Nevertheless, as reported by Ayonghe (2001) and as shown on Figure 4.6, overall there is hardly any change in the temperature in Northern Cameroon (Cheo et al., 2013).

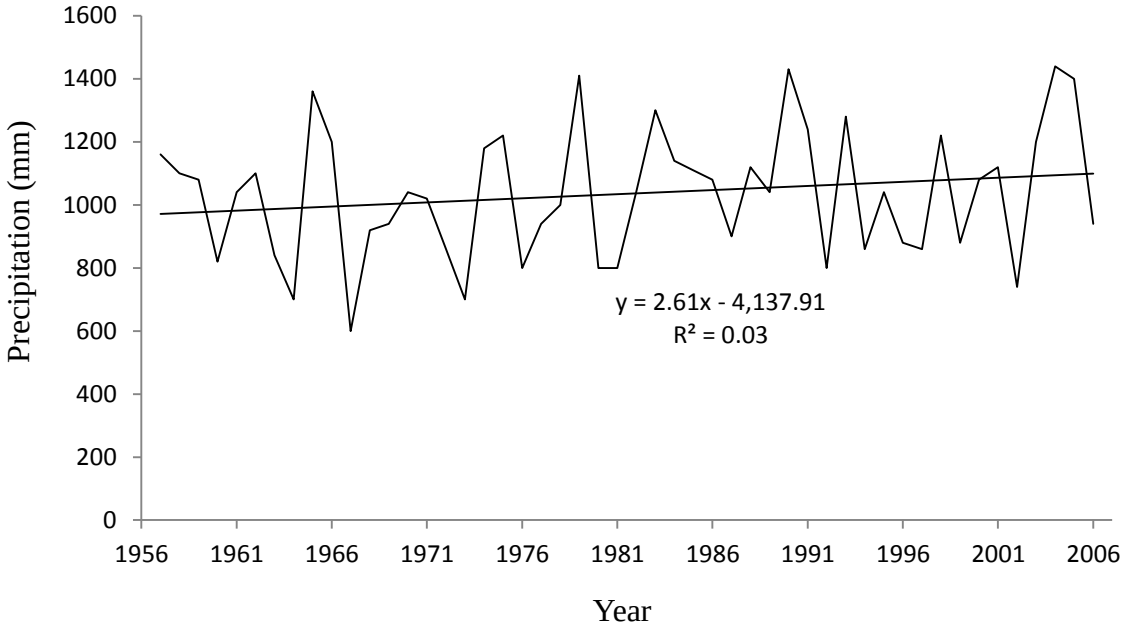

Figure 4.7: Garoua total precipitation per year (Produced from data obtained from Cheo et al., 2013).

Figure 4.7 shows the total rainfall distribution over Garoua region. The wet period occurs from May to September with over 1,000 mm rainfall. The peak is usually recorded during the July to September period (Mohr and Thorncroft, 2006). The dry period occurs from November to April.

The mean annual rainfall amounts to 1,018 mm (from 1957 to 2006), hence slightly higher than at Yola. Precipitations occur either as low altitude monsoon rains or as occasional high altitude squally showers (Njitchoua et al., 1995). Despite the high value of the annual rainfall, only a small fraction of precipitation contributes to the groundwater recharge because of the

high annual evaporation (about 1,800 mm) which is nearly double of the mean annual rainfall (Njitchoua et al., 1995).

The precipitation pattern shows noises over the years, with a nearly absence of trend. Droughts and floods events have occurred in the region with an increasing frequency over time (Molua and Lambi, 2006).

4.3.3 Comparison between Yola and Garoua climate variability

Figure 4.8 shows the comparison for the observed annual average temperature in Yola (1983 – 2012) and Garoua (1957 – 2006). Consistency between these 2 stations was only observed from the period 1990 to 1999. However, for the rest of the years, much difference occurred. An inconsistency was especially observed between 2000 to 2009. This inconsistency could be due to error in the data measurement. No statistical correlation is observed between Yola and Garoua region (Table 4.1), indicating that these two regions behave differently.

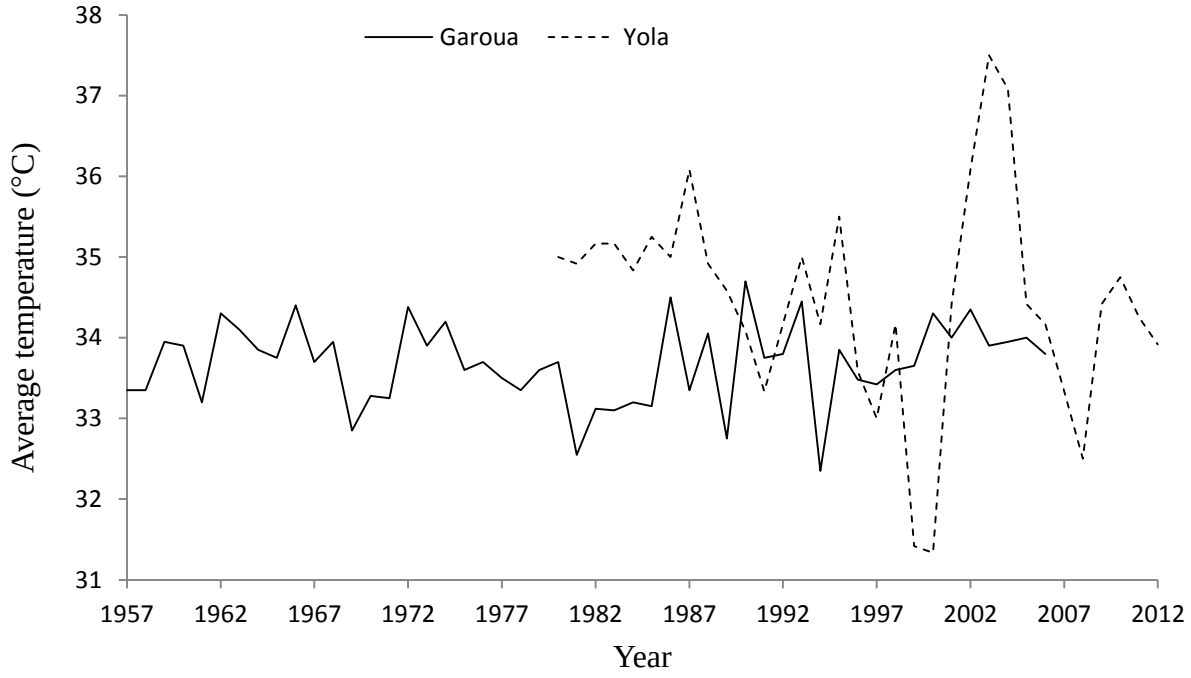

Figure 4.8: Annual average temperature in Yola and Garoua (For source of data see Figures 4.2 and 4.6).

Table 4.1: Statistical correlation values and significance range between Yola and Garoua annual average temperature (Significant p-value range 0 to 0.05, not significant p-value range 0.06 to 1)

Parameters		Yola	Garoua
Yola	Correlation	1	
	P-value	0	
Garoua	Correlation	-0.012	1
	P-value	0.952	0

Figure 4.9 shows a comparison of the total annual precipitation in Yola and Garoua regions. It can be seen that Garoua region shows slightly higher precipitation values: 100 mm more of mean average rainfall. This is possibly because Garoua (242 m) is 90 m higher than that of Yola (151 m). Garoua is located on the Mandara Mountains (the Adamawa highlands), while Yola is located on the lowland of Adamawa Mountains. The higher catchment area receives more moist air than the lower catchment areas (Dettinger et al., 2004). However, both regions showed noises of total annual precipitation over the years. No correlation is observed between Yola and Garoua regions (Table 4.2). This suggests that Yola and Garoua regions have different climate patterns.

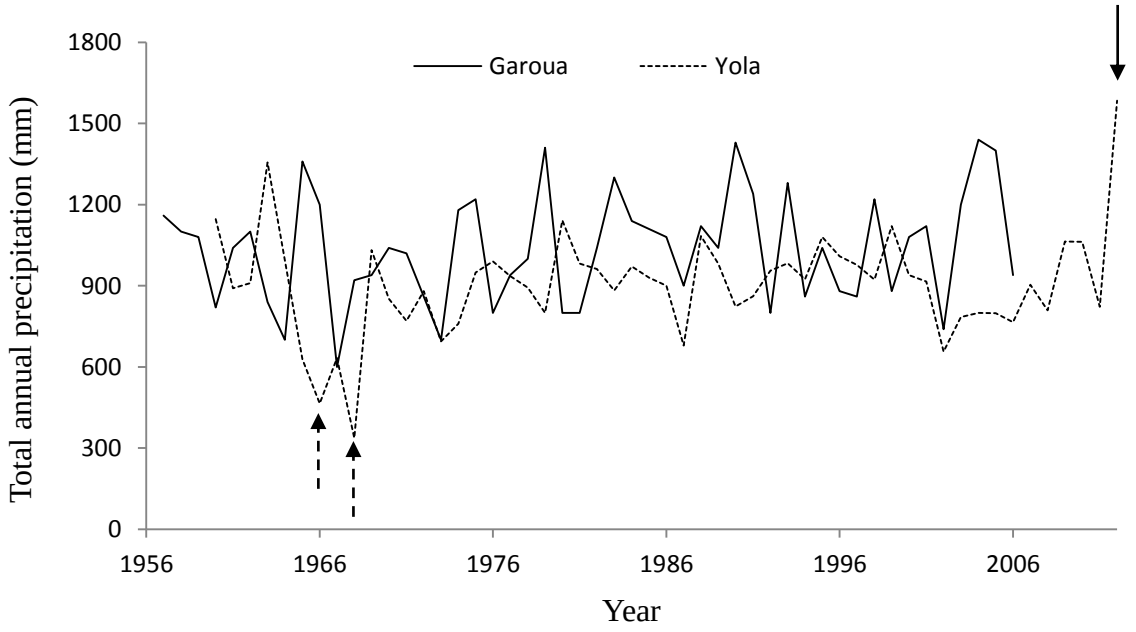

Figure 4.9: Total precipitation per year in Yola and Garoua. Dotted arrows show drought years in Yola, black line arrow show flood in Yola of 2012 (For source of data see Figures 4.2 and 4.6).

Table 4.2: Statistical correlation values and significance range between Yola and Garoua total precipitation (Significant p-value range 0 to 0.05, not significant p-value range 0.06 to 1)

Parameters		Yola	Garoua
Yola	Correlation	1	
	P-value	0	
Garoua	Correlation	-0.172	1
	P-value	0.248	0

4.4 River Benue discharge and water stage

Numerous tributaries in Cameroon (see Figure 4.1) join river Benue. Gauge stations are installed along River Benue at Garoua and Yola, i.e. 250 km apart, for monitoring the flow patterns of the river. Mayo Kebbi and River Faro are the main tributaries of River Benue in Cameroon and the flows empty into Nigeria east of Yola (see Figure 1.1). The average discharge of River Benue at Garoua gauge station is about 375 m^3/s (Shahin, 2002 cited in Molua and Lambi, 2006). As a result of the increased flows from Mayo Kebbi and River Faro downstream of Lagdo Dam, the monthly discharge of River Benue increases to over 3,500 m^3/s (discharges measured at Yola gauge station) (see Figure 4.10).

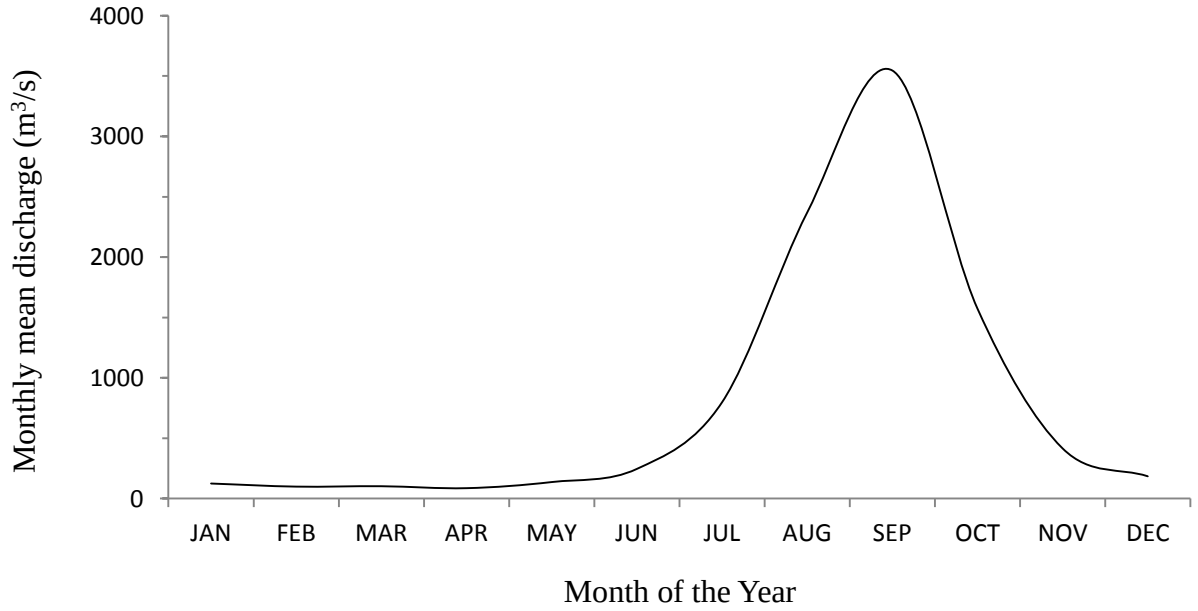

Figure 4.10: Monthly average discharge for the period 1960 to 2012 for River Benue at Yola gauge station (For source of data see Figure 4.2).

Figure 4.11 shows the low season discharge during the driest months for River Benue for the period 1960 to 2012 in Yola station. It gives the lowest low river water stages in River Benue during the dry season period and it is important to recharge alluvial aquifers. The lowest low discharge is observed between 1960 to 1982, i.e. the period before Lagdo Dam construction. Due to the dam construction, the discharge has become distributed slightly more evenly throughout the year. However, a jump occurs in 1984 for the low season discharge that shows the positive impact of the dam downstream. A gradual increase in the lowest low discharge is observed between 1985 and 2011. It is due to the positive impact of Lagdo Dam upstream. It was also observed that 2012 recorded a high minimum discharge, because of flooding.

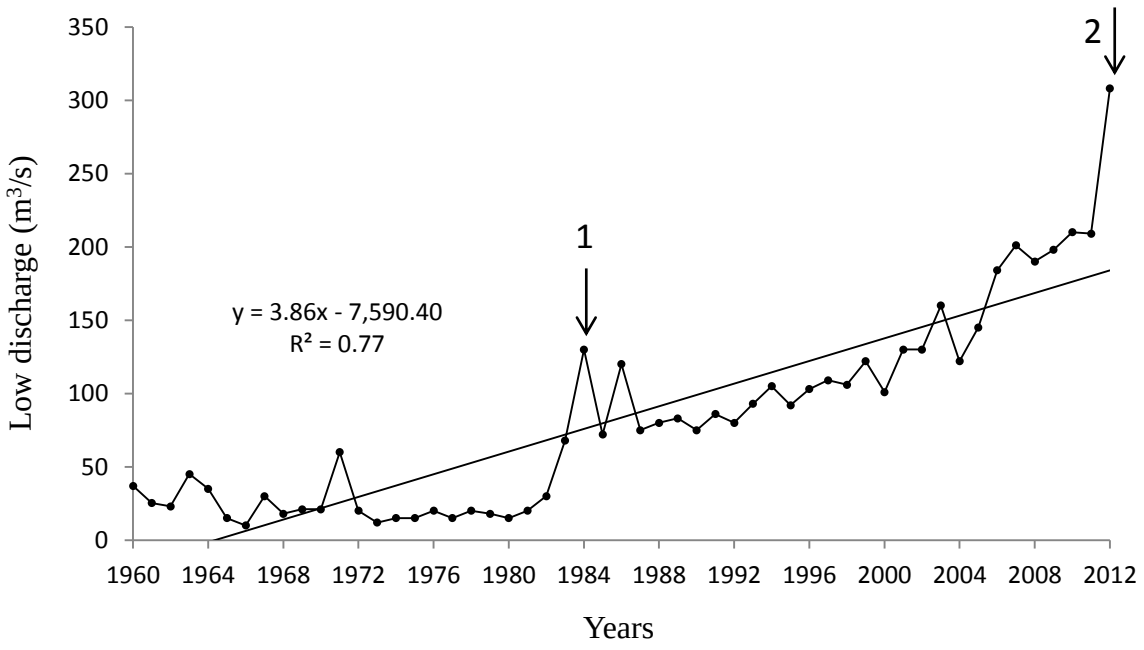

Figure 4.11: Lower annual discharge period (1960 to 2012) for River Benue Valley in Yola station. Arrow number 1 shows the sharp change in river discharge that took place after the building of the Lagdo Dam in Cameroon. Arrow number 2 shows the flood that occurred in 2012 (For source of data see Figure 4.2).

The Benue River water level is at its highest peak in August and October each year (Figure 4.12). As rainfall ceases towards the end of October, the River Benue's water level begins to

fall. It can be observed that low mean river stages were recorded in the period January to June. The lowest water level of River Benue at Yola gauge station is observed between April and May each year.

Figure 4.12 shows the mean river stage hydrograph for River Benue at Yola gauge station, for 1960 to 2012. Figure 4.12 also shows the impact of Lagdo Dam upstream before and after its construction, i.e. 1984. It can observed that in the dry season period before the dam construction the floodplain water table is lower. This suggests that Lagdo Dam has positive impact downstream, especially in the study site during the dry season period. This is the time farmers' exploit the shallow alluvial groundwater for irrigation with low-cost hand-drilling techniques.

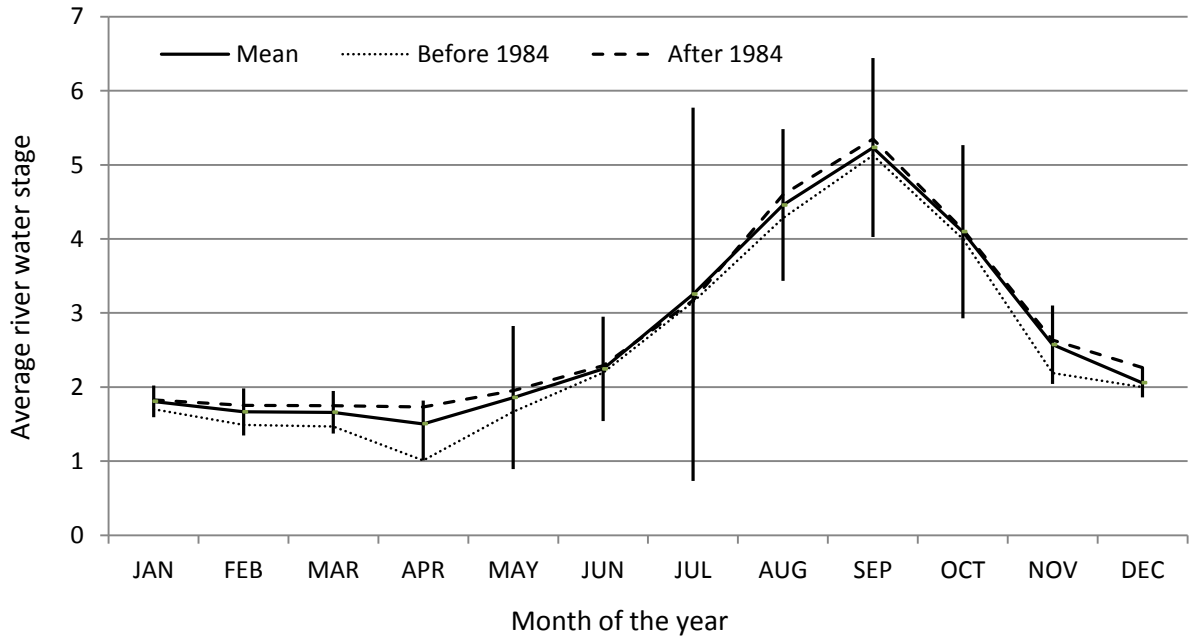

Figure 4.12: Stage hydrograph of the mean monthly water level for the period 1960 to 2012 for River Benue at Yola. The vertical lines show the confidence limits for the mean annual monthly water stages of River Benue at Yola gauge station (For source of data see Figure 4.2).

The confidence limits show significance ranges for the water stages accept May and July that show slightly insignificant confidence limits range. This suggests that mean monthly water stages in River Benue gives significant value range and that the stages are more erratic at the beginning of the wet season. These values for the mean water stages will be used in the groundwater modelling section.

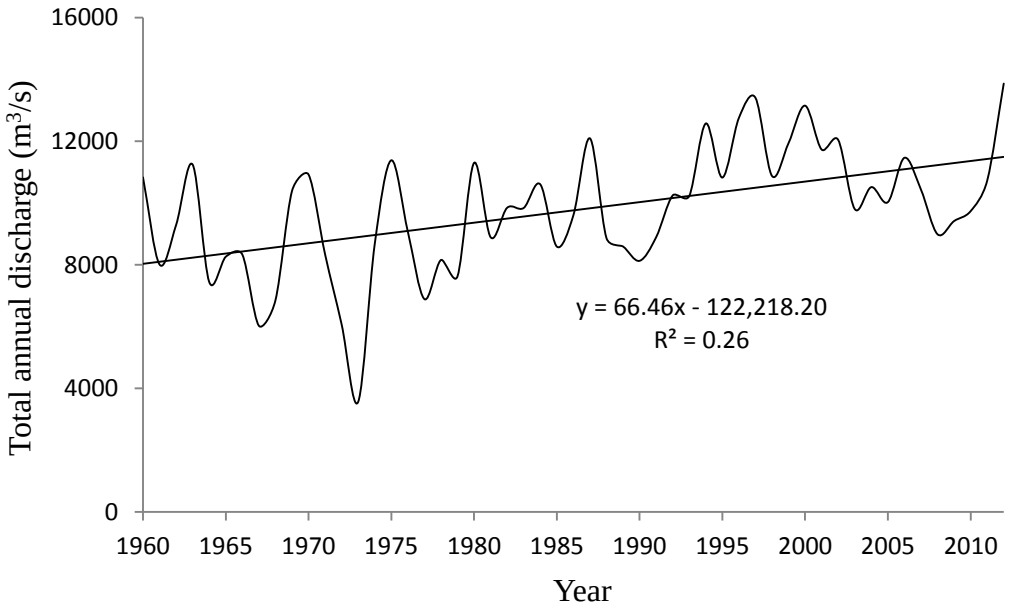

Figure 4.13: Total annual discharge of River Benue in Yola for the period 1960 to 2012 (For source of data see Figure 4.2).

Figure 4.13 shows the annual peak River Benue discharge observed at the Yola gauge station for the period 1960 to 2012. Figure 4.13 suggests an increase in peak discharge. The slope (66.5 m^3 s^{-1} y^{-1}) statistically significant and may be attributed due to contribution from tributaries into River Benue upstream of Yola and Garoua. The lowest discharge is observed in 1973. This may be linked to the drought that occurred in the early 1970s. The droughts that occurred in 1966 and 1968 in Yola and West Africa (Figure 4.4) are not well reflected in the discharge plot. The highest discharge is observed in 2012. This reflects the severe flood that occurred that year. It can be seen, despite noises over the years, an increase trend occurs with R^2 of 0.26.

In comparison between discharge and precipitation patterns, it is observed that discharge shows significant increase in trend (R^2=0.26) while precipitation shows no trend. The increase in the discharge trend could be attributed to the tributaries upstream of Yola. We already know that there is a difference between Yola and Garoua. Therefore, it is likely that there is more divergence upstream with some areas in the highlands receiving more precipitation.

4.4.1 River Benue flow rate

Knowing the flow rate of River Benue and the time it takes for the water to reach Yola from Lagdo Dam in Cameroon is important in order to warn the downstream users if the dam spill way is over-topped.

It could have been useful to find a mean speed of the flow further upstream and signal of increased water flow from opening the dam and later the speed of the river flow. At the time of making this estimation, this information was not available. However, the estimation presented here is a first guess and this serve as basis to understanding the speed of the flow between Lagdo Dam and Yola.

Considering River Benue as a trapezoidal channel (Figure 4.14), the trapezoidal equation was used to estimate the velocity and duration of water flow in River Benue.

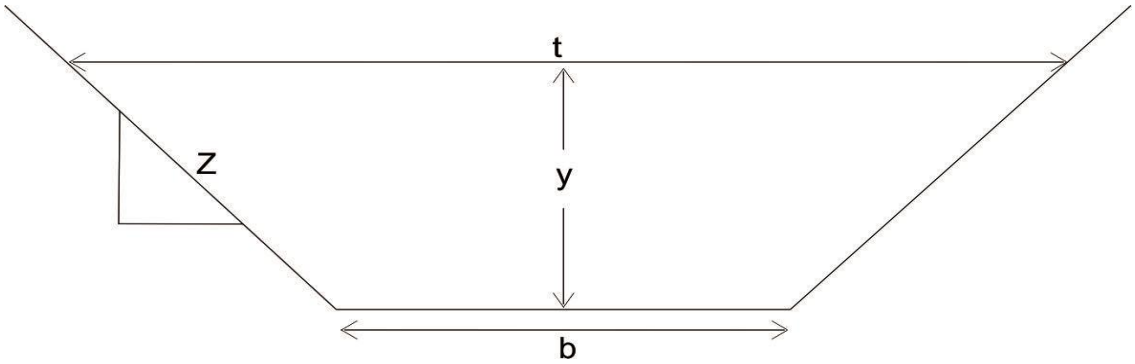

Figure 4.14: Trapezoidal open channel. t – river top with, b – river bottom width, y – water depth in the river, z – river side slope.

The bottom and top widths of the river are assumed 500 and 700 m respectively, and the river water stage of 6 m (Figure 4.12). The cross-sectional area for the River Benue was estimated from equation 4.1, for an open trapezoidal channel:

$$A = \frac{y}{2}(b + T) \quad 4.1$$

$A = 3{,}600\ m^2$

Given the discharge of River Benue to be ~ 3,500 m^3/s (Figure 4.10), the water taken from the maximum discharge (see Figure 4.10), flow velocity in the River Benue was estimated from equation 4.2:

$$Q = VA \quad 4.2$$

$V = 0.972\ m/s$

Given the distance between Yola and Lagdo Dam as 250 km, the velocity of flow is given as:

$$\text{Velocity} = \frac{\text{Distance}}{\text{Time}} \quad 4.3$$

Time = 257,201s = 2.977 days = ~3 days

The flow duration of River Benue from Lagdo Dam to Yola is approximately three days. This shows that any discharge released from Lagdo Dam will take a bit of delay to reach Yola. For example, in the past flood events, for any announcement for the excessive rainfall storm being observed in Cameroon that led to over-topping Lagdo Dam spill way, the impact should have been noticed at Yola, in two or three days. This would give enough time for warnings for the downstream inhabitants along the river, if this information were given immediately.

4.4.2 History of droughts and floods events in the region

Drought is caused by deficiency in precipitation for a long period that causes crop failure, water shortages, death of livestock, famine, etc. (Abaje et al., 2013). The West Africa

Sahelian region has been going through a long-term drought since 1960s (FRN, 2003; Amogu et al., 2010). This trend has been particularly noted in the northeastern parts of Nigeria.

The recorded droughts and floods events in the region are summarised in Table 4.3, which presents, from the historical information, the number of each type of events recorded from 1960 to 2012 (Ankidawa, 2011; UBRBDA, 2012). An increase in the number of flood events occurred compared to drought events. Regarding the causes of floods in the region, Tukur and Ray (1994) and Ankidawa (2011) found out that observation of flood events over the years suggests that the release of water from Lagdo Dam in Cameroon upstream or prolonged rainfalls due to climate change are largely responsible.

Table 4.3: Number of drought and flood events from historic records in the region (Ankidawa, 2011; UBRBDA, Yola, 2012)

Period	Drought events	Flood events
1966	1	
1968	1	
1977		1
1981		1
1989		1
1993		1
2004		1
2012		1

Although flood events are consistently being observed in the past, only few drought events however occurred in Yola such as in 1966 and 1968, which led to drying of River Benue and its floodplain. Such event will likely re-occur in the region. This will potentially lead to lowering of groundwater level of the floodplain.

It should be noted that the occurrence of droughts in Yola region is not the same with the occurrence of droughts in the Sahel. Increase in drought events in the Sahel and decrease in

the drought events in the Yola region have been shown. This may be due to the differences in the climate been observed between Sahel and Yola region. Sometime Yola climate behaves as Sahel climate for example droughts that occurred in 1966 and 1968 were both observed in the Sahel and Yola region. However, the Sahelian droughts in 1972 to 1973, 1982 to 1983 and 1997 to 1998, which were observed in the Sahel, were not observed in the Yola region.

The aggregate impacts of droughts on the Nigerian economy are in the order of 4 – 6%, which can be neglected (Benson and Clay, 1998). As pointed out by Izinyon and Ajumuka (2013), general concern exists about increasing risk from hydrological extremes, from recent changes in frequency and severity of floods as well as droughts leading to increase in hydrological variability.

During the 1966 and 1968 droughts, as many as 250,000 people, along with 12 million animals, are estimated to have died from starvation (Tarhule and Lamb, 2003). Many families and some of their members became engaged in waged employment that involved migration to the urban areas. Nomads living in the traditional grazing lands in the northern parts of the northeast region have had to move southward of Nigeria (Afolayan and Adelekan, 1998). Agricultural yields fell to about 40% of normal yields. It was also reported by Ati et al. (2007), that the droughts of the 1960s were responsible for the social backwardness, left farmers impoverished with poor quality of life, especially among the less privileged ones in the northern Nigeria.

Some of the measures taken after the 1960s drought are the following: farmers had to change from mono cropping to multi-cropping and herders had to keep goats and drought-tolerant animals in place of cows (Swinton, 1988). As reported by Afolayan and Adelekan (1998) droughts lead to migration of families due to famines in northern Nigeria.

4.5 Standardised Precipitation Index (SPI)

National Climatic Data Center (2013) defined Standardised Precipitation Index (SPI) as an index based on the probability of recording a given amount of precipitation, and the probabilities are standardized. Therefore, an index of zero indicates the median precipitation amount (half of the historical precipitation amounts are below the median, and half are above the median). Among the several proposed indices for analysing climate variability are methods such as Standardised Precipitation Index (SPI) and Palmer Drought Severity Index (PDSI), etc. SPI is widely used by different researchers for assessing climate variability (Guttman, 1998; Hayes et al., 1999; Rossi and Cancelliere, 2002; Cancelliere et al., 2007). For the purpose of this study, SPI was used to assess the climate variability of the region for correlating with River Benue discharge in Yola.

Table 4.4: Standardised Precipitation Index classification of wet and drought ranges (McKee et al., 1993)

SPI values	Remarks
2.00 and above	Extremely wet
1.50 to 1.99	Very wet
1.00 to 1.49	Moderately wet
-0.99 to 0.99	Near normal
-1.00 to -1.49	Moderately drought
-1.50 to -1.99	Severe drought
-2.00 and less	Extreme drought

Standardised Precipitation Index (SPI) is used to determine the effects of precipitation shortages to groundwater level, river discharges and soil water content (Ceglar et al., 2008). SPI is designed to assess the precipitation deficit in different time scale such as 3, 6, 9, 12, 24 months. The SPI defines negative values as drought and positive values as wet conditions. Table 4.4 shows classification for various droughts and wet conditions. As suggested by

McKee et al. (1993), to obtain a reliable result, SPI requires a continuous monthly precipitation data of at least 30 years or more. For the case of Yola: fifty two year data were used to estimate the rainfall variability for the region.

Figure 4.15 shows the comparison between Garoua and Yola SPI. Between 1970 to 2003, the trend shows some similarity for the two regions. However, major inconsistencies are observed between 1960 to 1969. A sharp decrease is shown for the Yola average SPI value between 1966 to 1970 indicating drought that occurred in 1966 and 1968, but is not seen in Garoua. Showing a clear difference in the precipitation pattern, however, 1966 and 1968 droughts is seen in Sahel. Table 4.5 shows the statistical correlation of Standardised Precipitation Index between Yola Garoua regions. No correlation is observed between Yola and Garoua region. This suggests that Yola and Garoua region behaves different in climate. It is also observed that Garoua region did not show any sign of drought events, whilst Yola region showed drought events between 1966 and 1974. This suggests that Yola region is experiencing shortages of water than Garoua region. The 1960s droughts of Yola were part of a wide Sahelian pattern that did not reach Garoua.

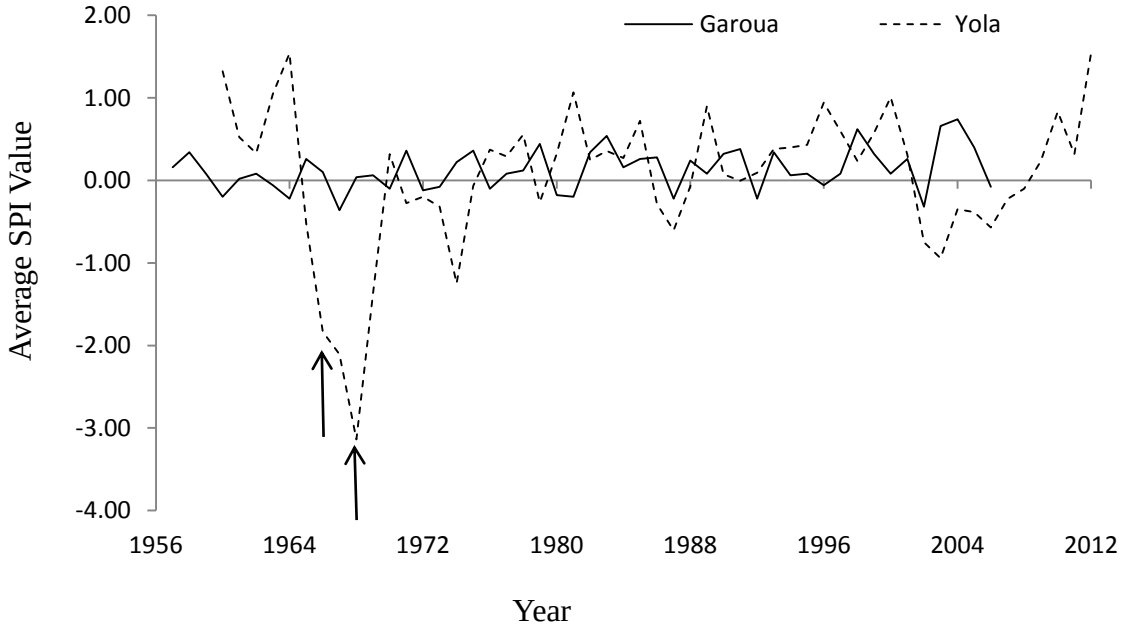

Figure 4.15: Average Standardised Precipitation Index value for the different years in Yola and Garoua. Arrows showing the drought of 1966 and 1968 in Yola region.

Table 4.5: Statistical correlation values and significance range between Yola and Garoua Standardised Precipitation Index (Significant p-value range 0 to 0.05, not significant p-value range 0.06 to 1)

Parameters		Yola	Garoua
Yola	Correlation	1	
	P-value	0	
Garoua	Correlation	-0.052	1
	P-value	0.73	0

4.6 Concluding remarks

It has been shown that over the period of the last 50 years that: 1. the temperature shows hardly any trend (see Figures 4.3 and 4.6), 2. the precipitation shows hardly any trend (see Figures 4.4 and 4.7), 3. the evaporation shows an unrealistic drop in 2008 to 2010 (see Figure 4.5), 4. the River Benue discharge is on the increase (see Figures 4.13). However, it has also been shown that the variability is large. It was also observed that the climate of Garoua, only 250 km upstream of Yola, is different in terms both of temperature and of precipitation.

The outcome of our critical analysis shows that the Yola region climate sometime behaves as a Sahelian country. For example, the droughts that occurred in 1966 and 1968 were observed in both Yola region and in the Sahel region. Sometime the Yola region climate does not behave as Sahel country. For example, the major droughts in West Africa in the last century that occurred in 1913 – 1914, 1972 – 1973, 1982 – 1983 and 1997 – 1998 did not occur in the Yola region. The weak increase of temperature and precipitation trends observed in this study is in line with what was reported by IPCC (2013). Therefore, it was necessary to understand the variation in the Yola region climate; this will enable understanding the groundwater levels in the region for abstraction with hand-drilling techniques.

Finally, it is critical to understand water abstraction sustainability in the context of the climate of Yola.

CHAPTER FIVE - RESULTS AND INTERPRETATION

5.1 Introduction

This chapter presents results obtained from surface elevation, sedimentology, groundwater investigations and groundwater modelling and proposes an interpretation for our new data. The surface elevation was estimated across the alluvial floodplain for understanding groundwater levels on the floodplain. The sediments and groundwater were characterised along the River Benue and Faro in Cameroon outcrops and River Benue outcrops along Nigeria side and from the cores in the floodplain. Groundwater modelling was used to quantify the interaction between River Benue and floodplain during the dry season period and its sustainability for application of hand drilling techniques in the future.

5.2 Elevation height

The topographical map (see Figure 2.2) available before our study was not sufficiently detailed for the research purpose. So a fieldwork survey was necessary (see Figure 3.1). This provided a suitable elevation control across the floodplain (Figure 5.1) for the groundwater modelling.

The survey shows that the elevations across the floodplain range between 172 and 178 m, i.e. a range of 6 m (Figure 5.1). The lower elevations are located in the southwest part (point B on Figure 5.1) while higher elevations are located northeastern part of the floodplain near the river (point B^1 on Figure 5.1). Elevation height decreases along southeast to northwest $A^1$and northeast to southwest B^1directions (Figure 5.1) reflecting the direction of the river flow.

As it will be shown, the water table depth across the floodplain ranges between 5 and 18 m (12 m of range). The floodplain elevation variations are therefore relevant in precisely

estimating groundwater level, which will be useful for the modelling section. The water level in River Benue during the dry season is at a lower elevation than Lake Geriyo.

The surface elevations obtained in the present survey shows a clear difference with the previous topographic map (see Figure 2.2). Twenty metres more is observed in the lower elevation while five metres less is observed in the higher elevations.

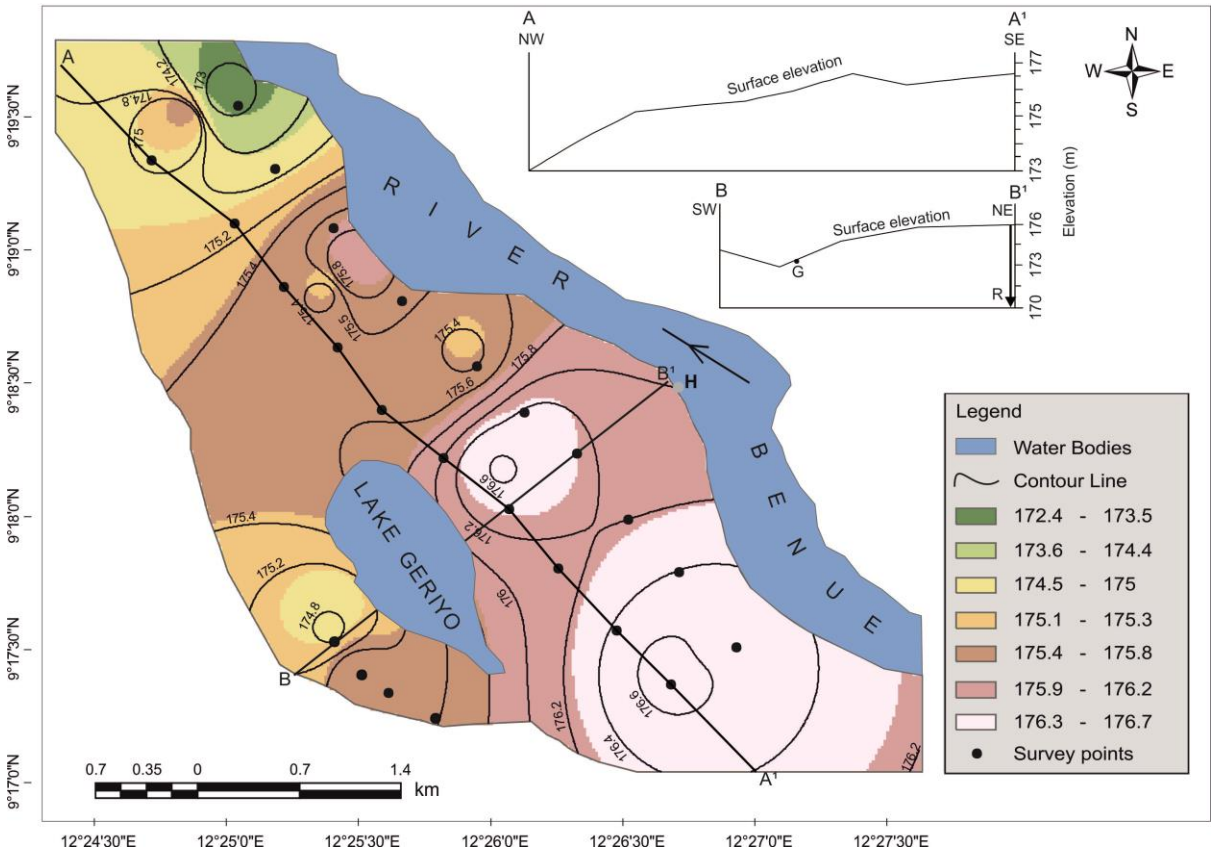

Figure 5.1: Topographic map showing elevation heights of the research area. The values 172.4 to 176.7 are surface elevations in metres (masl) across the floodplain. In inset: transects A and B and R is showing water level in River Benue. G – Lake Geriyo.

5.3 Sedimentology

This section assesses the sedimentology of the floodplain for its suitability with the hand drilling techniques. The floodplain alluvial formation is one of the criteria in assessing the suitability of hand drilling techniques. This alluvial sediment has never been studied before.

Statistical analysis is applied on the data in two steps: First method by method with depth and secondly to highlight the links between methods.

5.3.1 The floodplain alluvial sediment

The sedimentology of the alluvial floodplains, obtained by hand augering along several 2,500 m long transects on the left bank of River Benue valley is shown in Figure 5.2. The studied alluvial sediment deposits range between 6 to 18 m in depth at twelve different boreholes before reaching groundwater. The coring always remains in the alluviums overlying sandstone bedrock of the Yola formation but never reaching it. The visual logs are presented with measured particle size distribution data (overlying curve) showing distribution of the sediment sizes along the cores at various depths. Visual descriptions of the sediment in field were based on the finger feeling method.

The visual sedimentology results show clayey silt, sandy silt and sand alluvial deposits with sandy silt sediments dominating the alluvial of the floodplain. Clayey silt beds intermixed with sandy silt sediments at different locations and depths (see Figure 5.2) may serve as local aquitards. The clayey silt on the floodplain would have a significant influence in the aquifer recharge.

The aquifer in the alluvial floodplain is made up of fine to medium-grained sand with occasional sandy silt. It can be observed that borehole location 1 (see Figure 5.2) closer to the river consists of sand formation and this could be influenced by the river flow. Borehole location 11 at a distance 2,500 m away from the river contains thick deposition of sand and interfingering with clayey silt and sandy silt deposits. The deposition of sand formation at that location may be likely influenced by the presence of Lake Geriyo.

The location of the finest sediment was along River Benue in Cameroon. This outcrop is somewhat an outlier on comparison to all other studied locations.

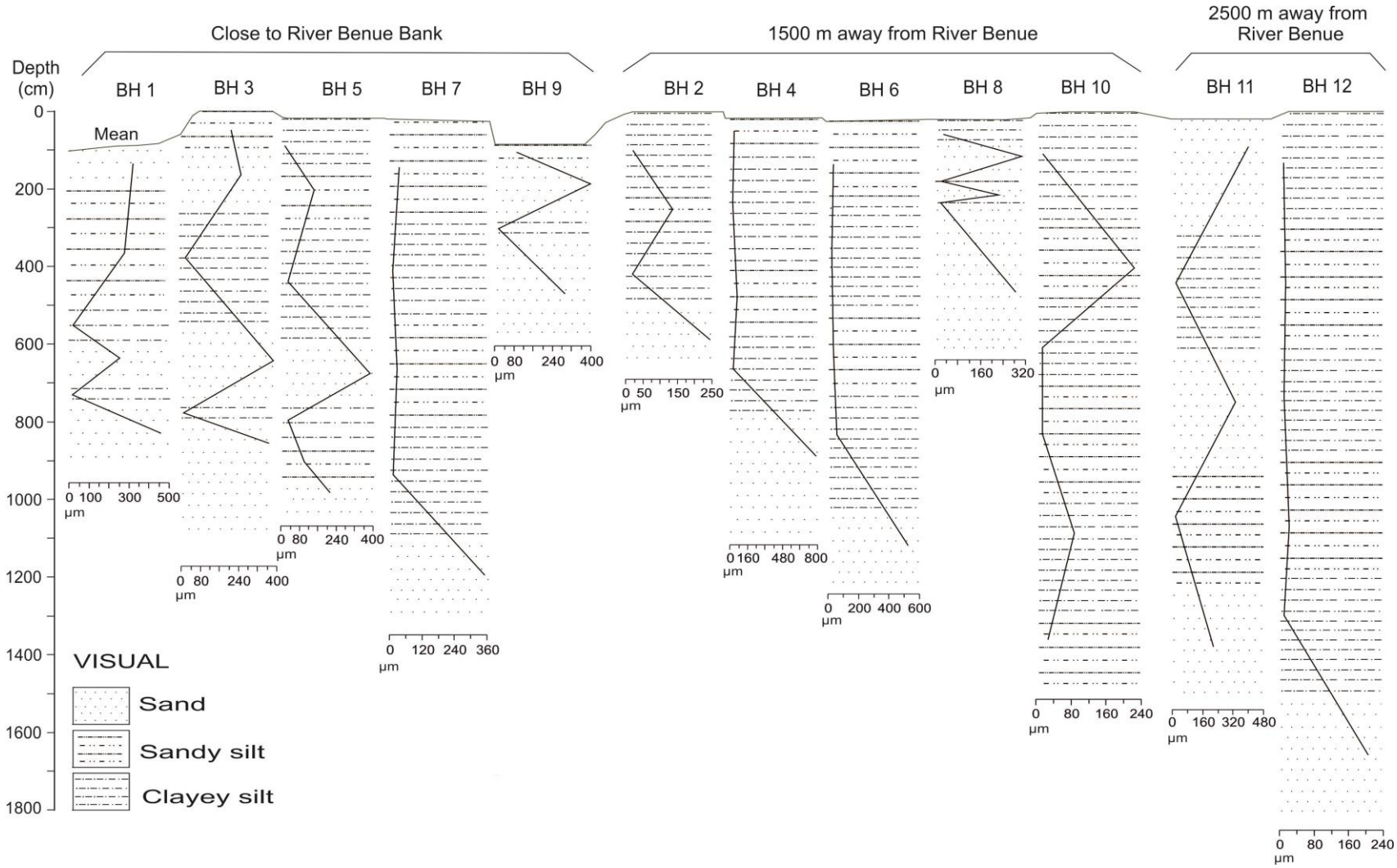

Figure 5.2: Visual sedimentology of the alluvial floodplain with measured mean particle size data (overlying curve), obtained on twelve different hand augering drilling boreholes 1 to 12 along a 2,500 m transects from River Benue. For position of borehole (see Figure 2.8) water level 2011.

The floodplain alluvial sediment colour are mostly light reddish brown with a range between pale red, red, weak red, pale brown, light yellowish brown, gray, and pinkish gray. Only few samples shows olive, olive gray, dark greenish gray, olive yellow, dusty red and pinkish white (see Table B in Appendix B) at various location and depth across the floodplain.

5.3.2 Particle size distribution

The details of the particle size distribution (PSD) analysis results for the two hundred and fifty six sediment samples are presented in surface plots Figures 5.3 to 5.6 and in Figures A1 to A8, Appendix A.

The floodplain grain size is confirmed to be sand, sandy silt and clayey silt by quantitative analysis. Sand and sandy silt samples are dominant across the floodplain having 46% and 52% respectively, and clayey silt samples showing a much lower value of only 2%.

The PSD of the alluvial sediments also demonstrates that sand and sandy silt sediments are interfingered with lenses of clayey silt along the river outcrops and across the floodplain (see Figures 5.3, 5.4, 5.5 and 5.6).

The PSD for borehole cores along the floodplain different deposition layer sequences is observed (see Figure 5.3). The interfingering of sandy silt and clayey silt sediments with sand is observed at the depth between 450 to 750 cm and 1050 to 1350 cm respectively in borehole location 11. It is observed that alluvial sediment depositions along River Benue Nigerian portion and the boreholes cores correspond to the sediment deposition for Faro River in Cameroon.

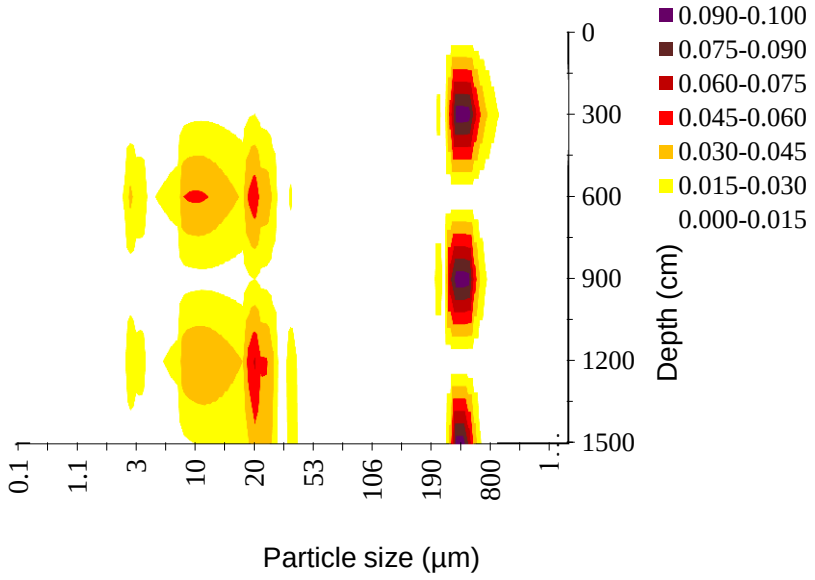

Figure 5.3: Particle size distribution surface plot for sediment sample at location borehole 11. For location of sample point (see Figure 2.8). The values 0.000 – 0.100 are percentage concentration of the sediment.

Along the Nigerian portion of River Benue (Figure 5.4), the interfingering of sand with sandy silt and clayey silt alluvial sediments is observed down the cores. For example, at depths of 225, 345 and 360 cm the interfingering of sand deposits with sandy silt and clayey silt sediments are observed in outcrop location N.

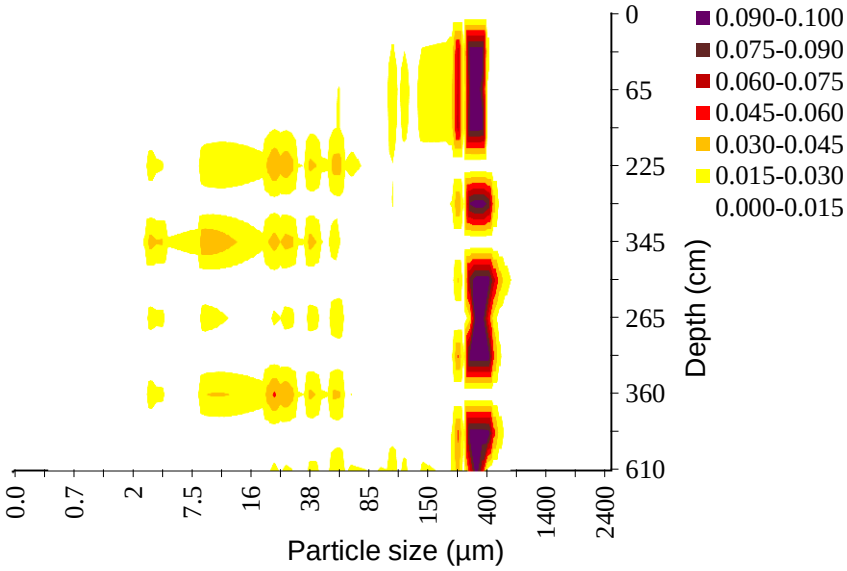

Figure 5.4: Particle size distribution surface plot for the outcrop sediment sample at location N along River Benue in Nigeria. For location of sample point see outcrop sampling along transect 9 (see Figure 2.8). The values 0.000 – 0.100 are percentage concentration of the sediment. Depth scale not linear.

The PSD for River Faro in Cameroon (Figure 5.5) is dominated by sandy silt at the top between 0 to 30 cm depth. Below this depth, higher concentration is observed at the grain size range between 115 and 345 µm, showing layers of sand interfingering with the lenses of sandy silt. Therefore, it is observed that River Benue in Cameroon consists of finer clayey silt sediments than Faro River. Sediments from these two rivers are source of sediment to the study site.

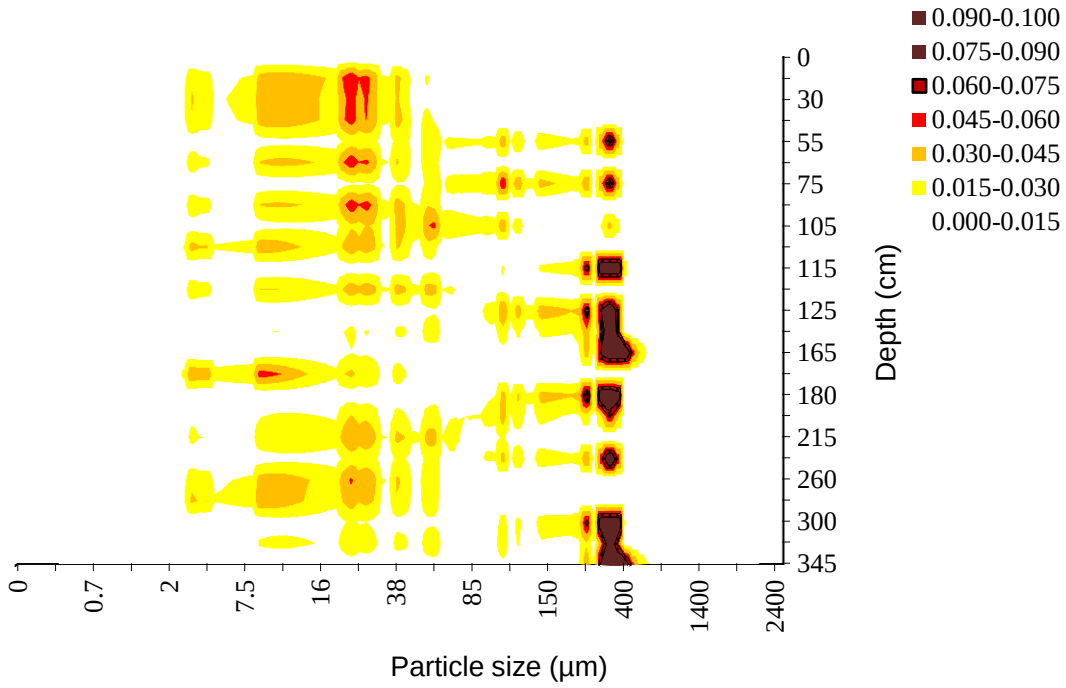

Figure 5.5: Particle size distribution surface plot for outcrop sediment samples on Faro River in Cameroon. For location of sample point (see Figure 1.1). The values 0.000 – 0.100 are percentage concentration of the sediment. Depth scale not linear.

The PSD for River Benue in Cameroon (Figure 5.6) shows by far the lowest values of all locations studied. The grain size decreases with an increase in depth. The concentration of clayey silt deposition is observed at the depth range between 165 and 415 cm as the grain size diameter in this range is 2.6 and 9 µm. This sequence represents the only exception to the otherwise nearly coarse sequences analysed in this investigation.

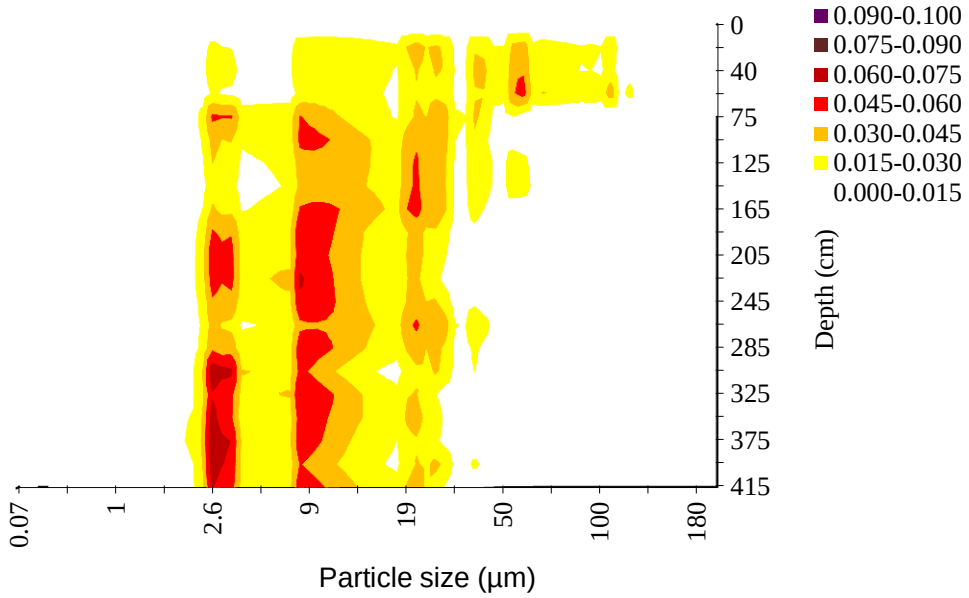

Figure 5.6: Particle size distribution surface plot for outcrop sediment sample on River Benue in Cameroon. For location of sample point (see Figure 1.1). The values 0.000 – 0.100 are percentage concentration of the sediment. Depth scale not linear.

Assessing the suitability of the floodplain alluvial sediment for application with hand drilling techniques is one of the objectives of the present study. As shown above the floodplain alluvial particle size distribution are mainly sand and sandy silt formations (see Figures 5.3 to 5.6). These types of alluvial sediment are suitable for application with the hand drilling techniques. Sand and sandy silt formations as the case in this study allow an easy flow of water to recharge the shallow floodplain aquifers that can be extracted with hand drilling techniques.

Figure 5.7 shows the relationship between percentages of sand with distance away from the river. It can be seen that distance between 0 to 1,000 m away from the river consists of higher percentage of sand than at a distance 2,500 m away from the river. Soil/sediment near to the channel is more likely to be sandy. For example, borehole locations 1, 3 and 9 closer to the river consist of more sandy sediments (see Figure 5.2). A weak negative correlation was

observed between the percentage sand and distance from the river with the correlation value of -0.268 (p-value of 0.031) (Table 5.1). This shows that sand sediments decrease away from the river; it could be due to different deposition processes because of the high-energy environment closer to the river.

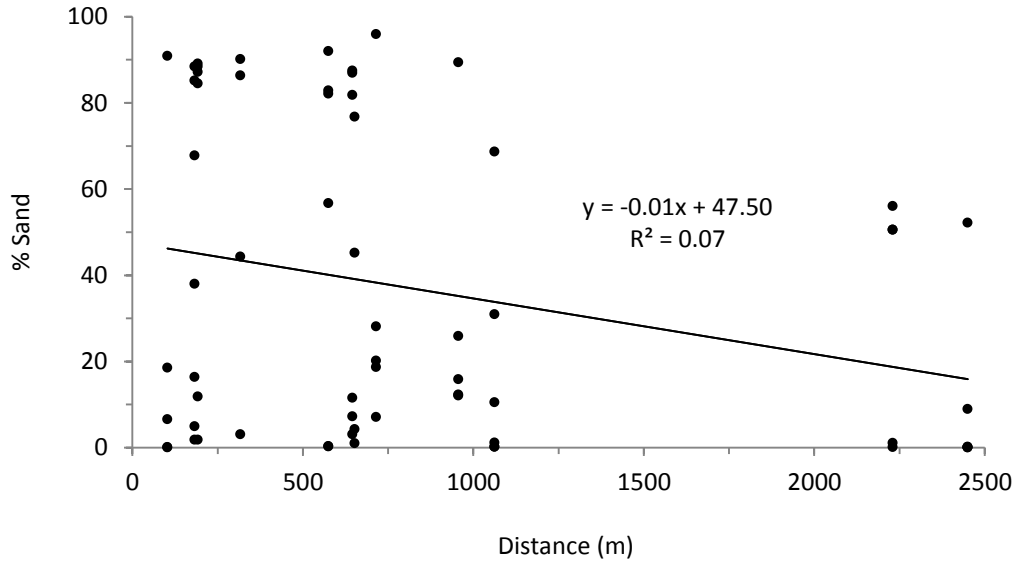

Figure 5.7: Relationship of sand percentage with distance away from the river.

Table 5.1: Statistical correlation values and significance range between sand percentages with distance (Significance p-value range 0 to 0.05, not significant p-value range 0.06 to 1)

Parameters		% Sand	Distance (m)
% Sand	Correlation	1	
	P-value	0	
Distance (m)	Correlation	**-0.268***	1
	P-value	**0.031**	0

5.3.3 Loss on ignition for the sediment samples

Loss on ignition (LOI) values for 256 subsamples is shown in Figures 5.9 to 5.11 and Table B, Appendix B.

5.3.3.1 Loss on ignition at 105 °C

Despite the limitations highlighted in the method section (time spent in plastic bags before analysis), it can be seen from Figure 5.8 that the samples at greatest depths have the highest moisture content. The statistical analysis show a very significant positive correlation of 0.684 (p-value=0) (Table 5.2). This means that during drilling process the alluvial sediment at the top surface will be harder to penetrate and that as the drilling proceeds downward the alluvial sediment becomes softer.

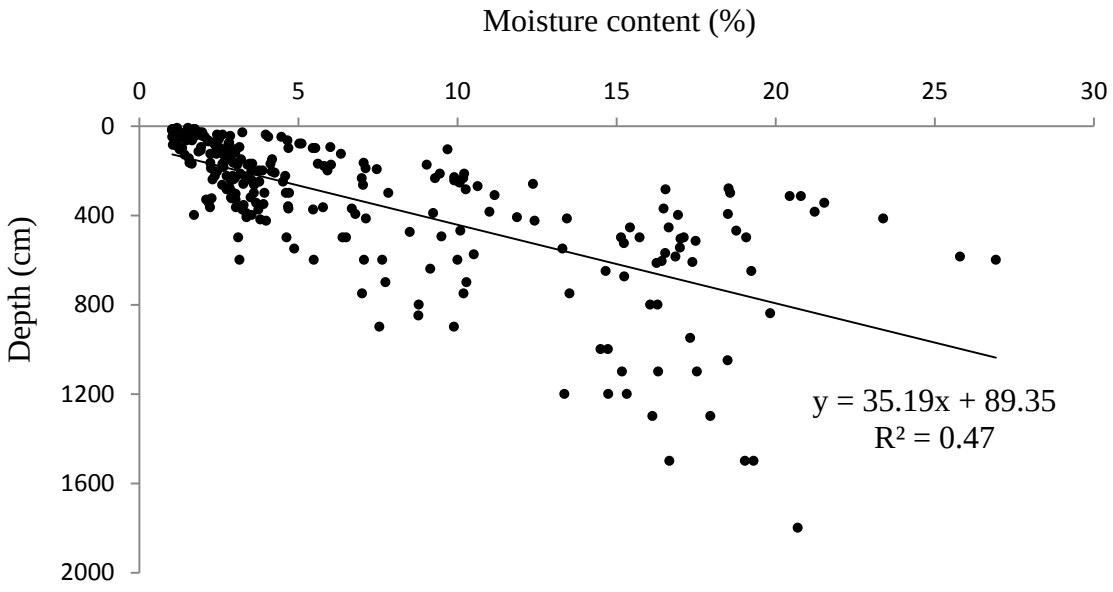

Figure 5.8: Relationship of moisture content with depth across the floodplain.

Table 5.2: Statistical correlation values and significance range between moisture content and depth (Significant p-value range 0 to 0.05, not significant p-value range 0.06 to 1)

Parameters		Moisture content (%)	Depth (cm)
Moisture content (%)	Correlation	1	
	P-value	0	
Depth (cm)	Correlation	**0.684****	1
	P-value	**0**	0

5.3.3.2 Loss on ignition at 550 °C

The percent values of LOI at 550 °C along the Nigeria floodplain for the twelve-drill boreholes range from a maximum of 8.79% to a minimum of 0.32% with a mean percent of 3.33% (Figure 5.10). Similarly, the percent values of LOI at 550 °C along the River Benue Nigeria outcrops sediments range from a maximum of 7.11% to a minimum of 0.17% with a mean percent of 2.87% (Figures 5.11 and 5.12). The total LOI at 550 °C is high in the clayey silt and sandy silt sediments and lower in the sand sediments.

The percent values of LOI at 550 °C for the Faro River in Cameroon range from a minimum of 0.38% to a maximum of 6.90% with a mean percent of 2.87% (Figure 5.11). The outcrops of Benue in Cameroon show special lithology sequence. Finer sediments are dominating the outcrop. The LOI at 550 °C on River Faro sediment decreases with increasing in depth. This could be because the sediment is coarser at the base.

The percent values of LOI at 550 °C for the River Benue in Cameroon range from a minimum of 2.64% to a maximum of 8.28% with a mean percent of 6% i.e. higher than for all the other outcrops and boreholes (Figure 5.11). The LOI at 550 °C is higher at the base and low at the top. It is observed that LOI at 550 °C in sediment of River Benue in Cameroon increases with depth.

Indeed darker samples have higher LOI at 550 °C. The four higher values in the present study show that two are darker while the other two are weak red. Hence, this general principle cannot be used here.

Looking at the LOI at 550 °C, values in the sediment they are generally low (<8%) this shows that there is no significant amount of the LOI at 550 °C in the samples. The very low value of LOI may be due to loss of moisture bond within clayey silt in the sediment. It can be seen

from Figure 5.9 that the samples at top surface (between 4 m depth) have the high amount of LOI at 550 ˚C. The statistical analysis show no correlation between LOI at 550 ˚C with depth, correlation of 0.063 (p-value=0.313) (Table 5.3).

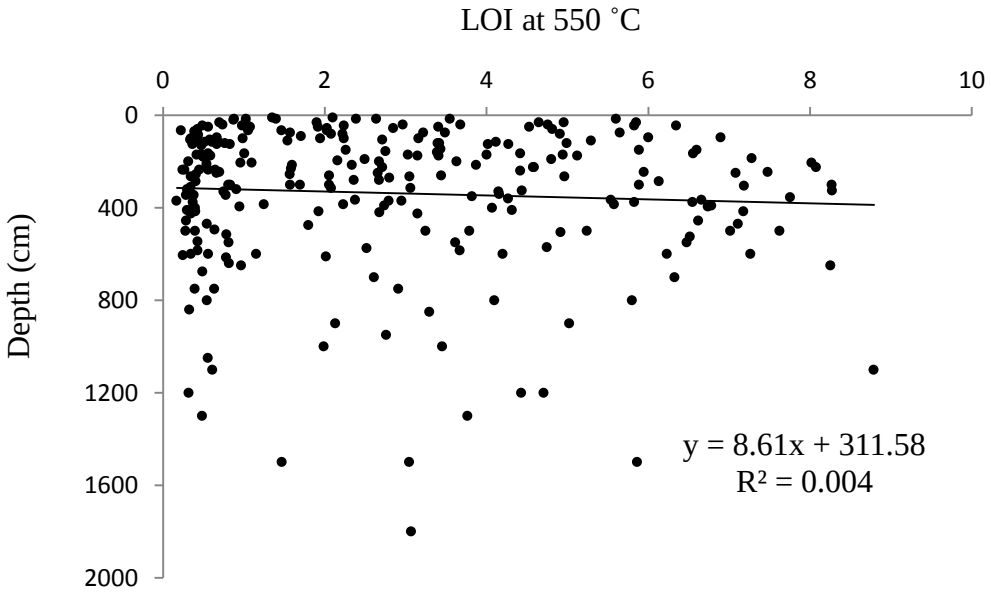

Figure 5.9: Relationship of LOI at 550 ˚C with depth across the alluvial floodplain.

Table 5.3: Statistical correlation values and significance range between LOI at 550 ˚C and depth (Significant p-value range 0 to 0.05, not significant p-value range 0.06 to 1)

Parameters		Depth (cm)	LOI at 550 ˚C
Depth (cm)	Correlation	1	
	P-value	0	
LOI at 550 ˚C	Correlation	0.063	1
	P-value	0.313	0

5.3.3.3 Loss on ignition at 950 ˚C

LOI at 950 ˚C is lower than 2.3% (see Figures 5.9, 5.10 and 5.11), and therefore so low that it hard to separate the signal from the noise. Therefore, no attempt was made to explain the changes.

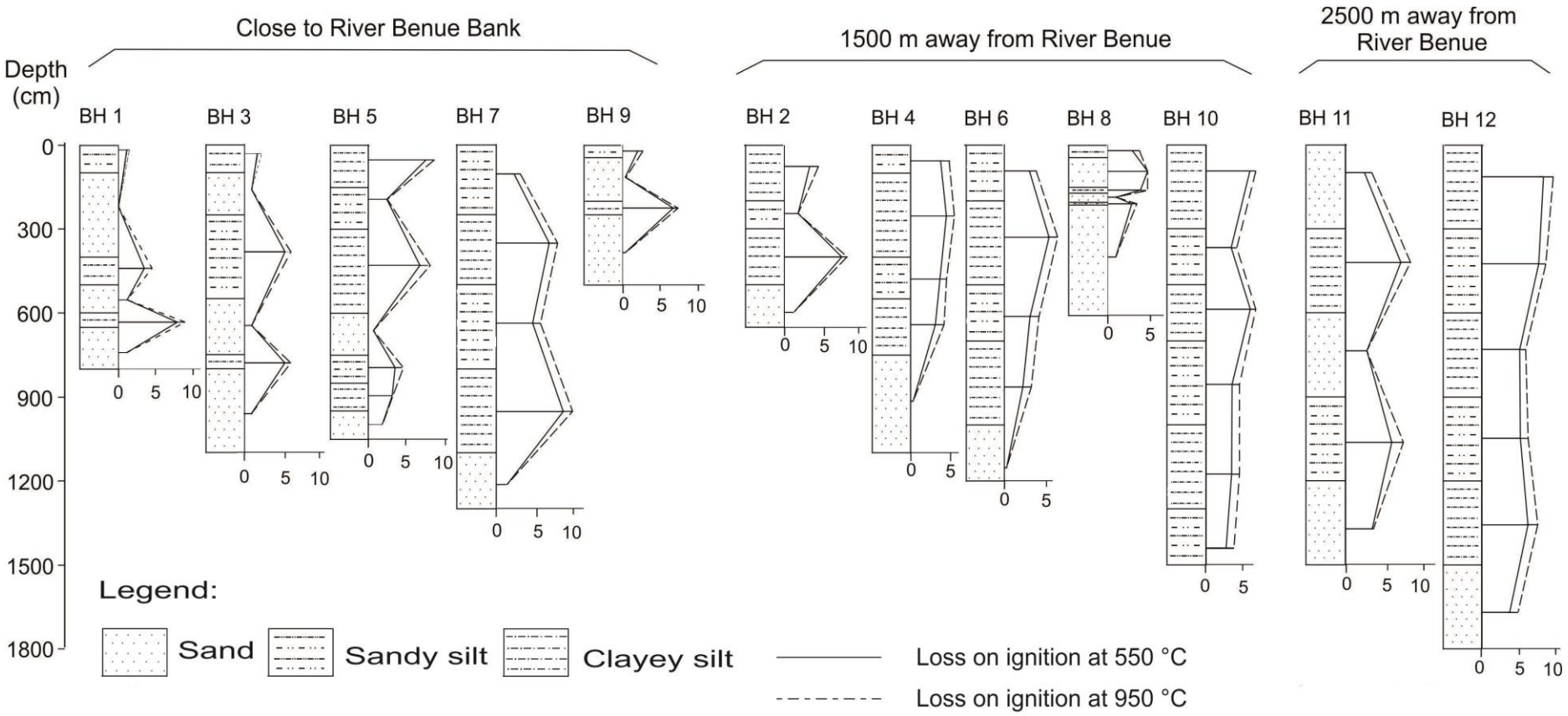

Figure 5.10: Cumulative curves of loss on ignition at 550 °C and 950 °C for the twelve boreholes sediments.

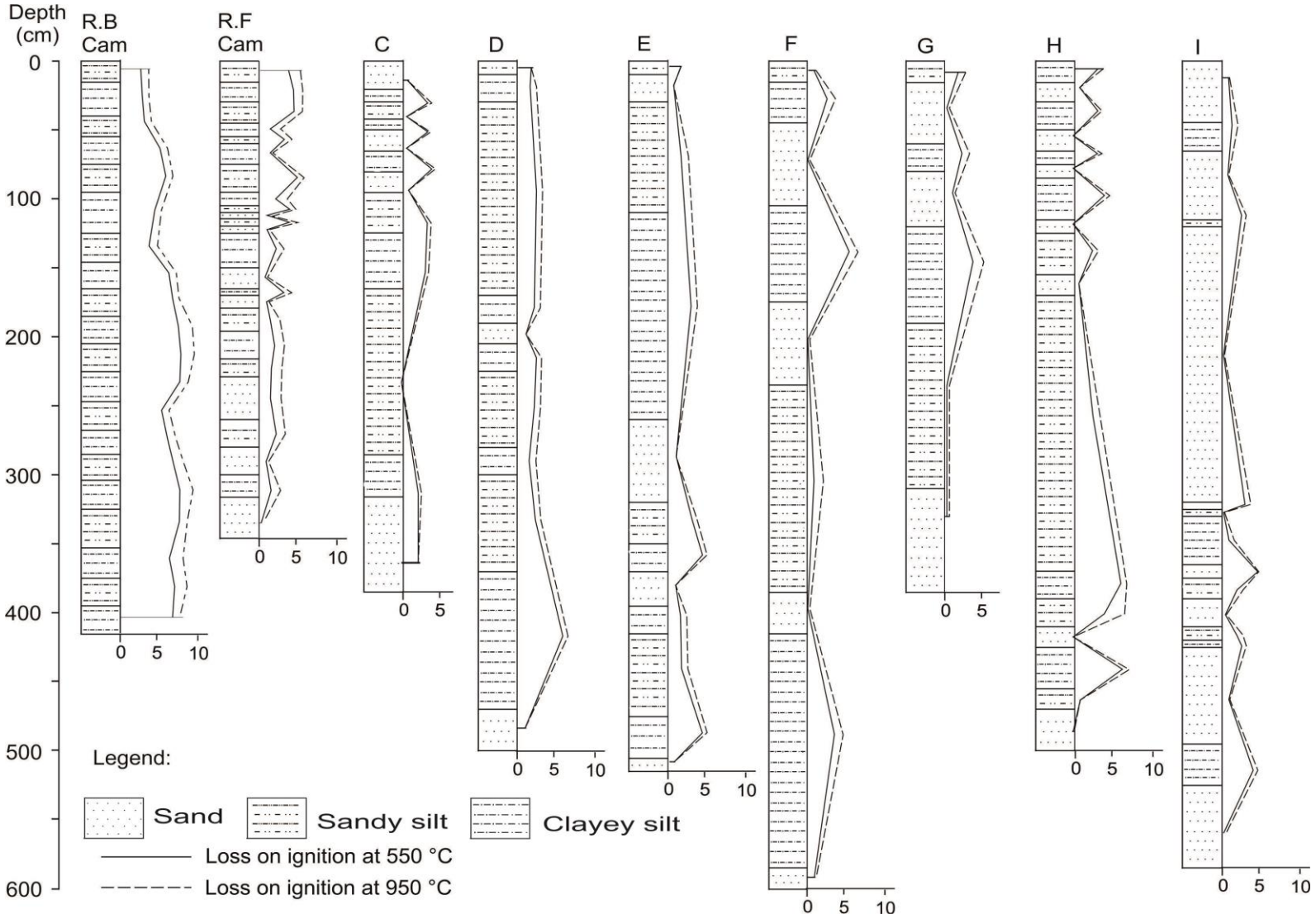

Figure 5.11: Cumulative curves of loss on ignition at 550 °C and 950 °C for sediment samples outcrops (C and I) along the Nigerian portion of River Benue Yola region and the 2 main rivers in Cameroon. R.B Cam is River Benue in Cameroon; R.F. Cam is River Faro in Cameroon.

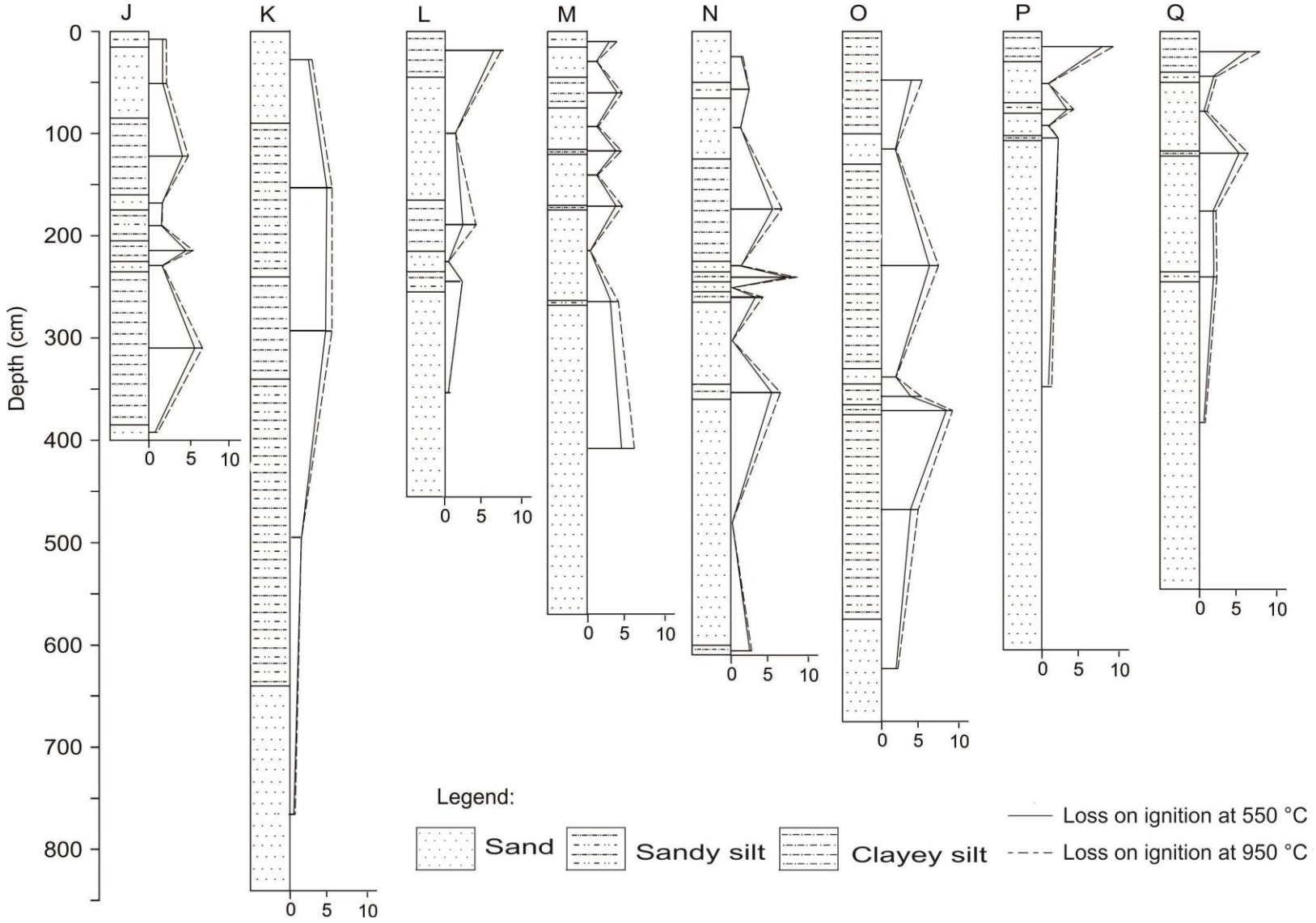

Figure 5.12: Cumulative curves of loss on ignition at 550 °C and 950 °C for sediment samples outcrops (J to Q) along the Nigerian position of River Benue Yola region.

5.3.4 Magnetic susceptibility

Magnetic susceptibility (MS) results are presented in Table 5.4 and Figures 5.13, 5.14 and 5.15. The detailed data for the MS analyses results for the two hundred and fifty six sediment samples collected are presented in Table C, Appendix C. Overall very minor changes have been detected suggesting a rather homogenous origin of the magnetisable elements and hence of the sediment.

Magnetic susceptibility is slightly higher in the Faro River sediments than in the Benue River sediments (Table 5.4). These two rivers are the main sources of sediment to the Yola floodplain. This difference is probably due to sediments derived from a difference in the distribution of igneous rocks in the two alluvial floodplains as shown in Figure 2.4. According to Dearing (1999), sediments formed from sedimentary materials typically have lower MS values than those from igneous material (see Figure 2.4 section 2.2.3).

The MS for River Benue outcrops in Yola is higher than the sediments in boreholes cores (Table 5.4). The high magnetic value may be likely influenced by the river flow or grain size.

Table 5.4: Magnetic susceptibility (MS) values for the River Benue outcrops and cores samples

Location	Minimum MS (10^{-6} m^3 kg)	Maximum MS (10^{-6} m^3 kg)	Mean MS (10^{-6} m^3 kg)
River Benue in Cameroon	0.25	0.39	0.30
River Faro in Cameroon	0.40	1.74	0.80
River Benue in Nigeria	0.21	4.16	1.07
Borehole cores	0.13	2.19	0.70

The MS values obtained along River Benue in Nigeria and borehole cores show some slight variations in high values than the values obtained from Benue and Faro River in Cameroon. Generally, MS values are low except at some discrete depths. For example at location C, at 95 cm depth (see Figure 5.13), MS value is high, 4.03 10^{-6} m^3 kg. Similarly at location J, at 400 cm depth (see Figure 5.14), MS value is high, 4.16 10^{-6} m^3 kg. This could likely be because of environmental factors resulting in heavy minerals from sedimentary rocks or fire.

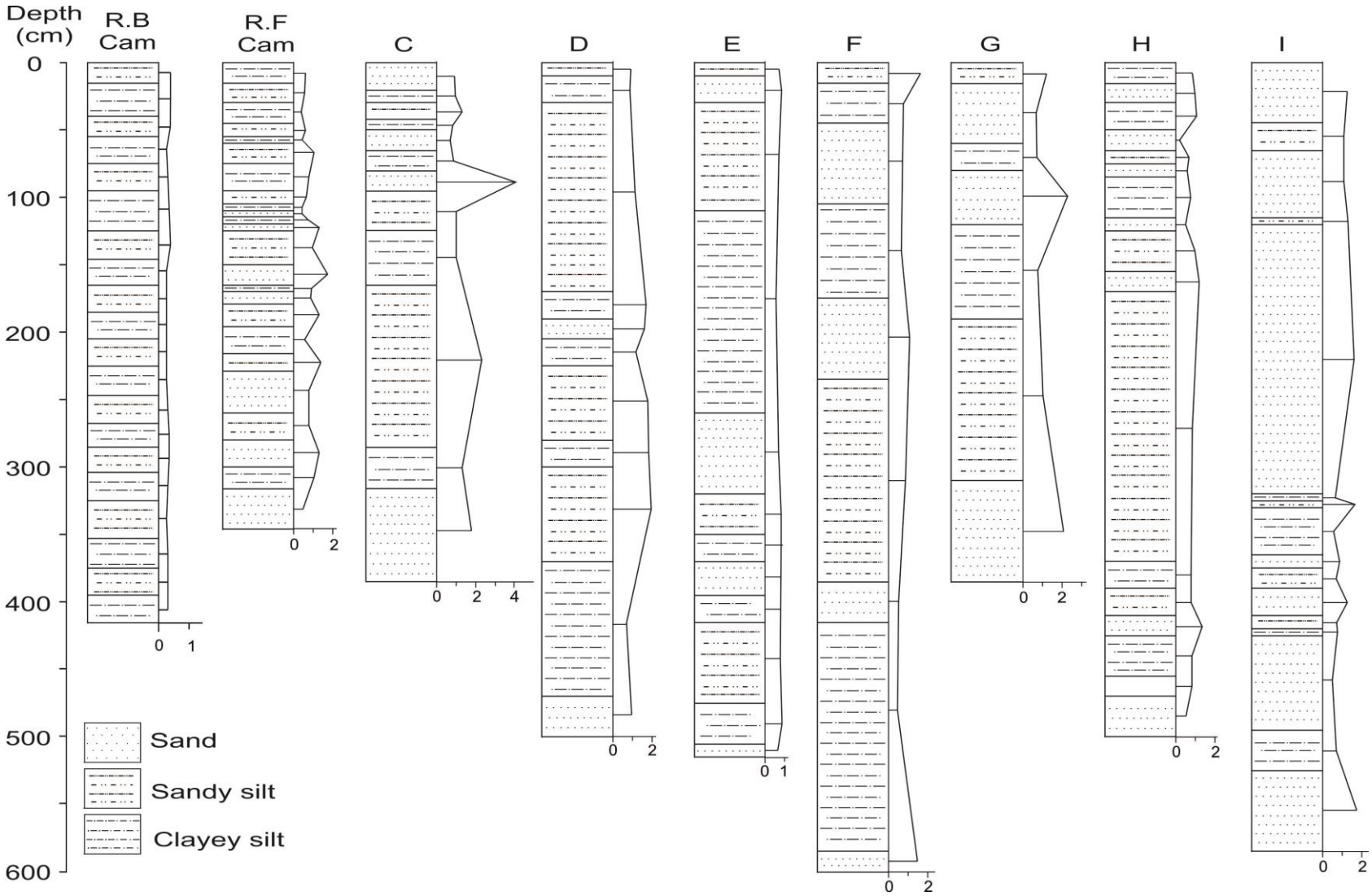

Figure 5.13 Magnetic susceptibility values in 10^{-6} m^3 kg for sediment samples outcrops (C to I) along the Nigerian position on the River Benue, Yola Region and the 2 main rivers in Cameroon. R.B Cam – River Benue Cameroon; F.R Cam – River Faro Cameroon.

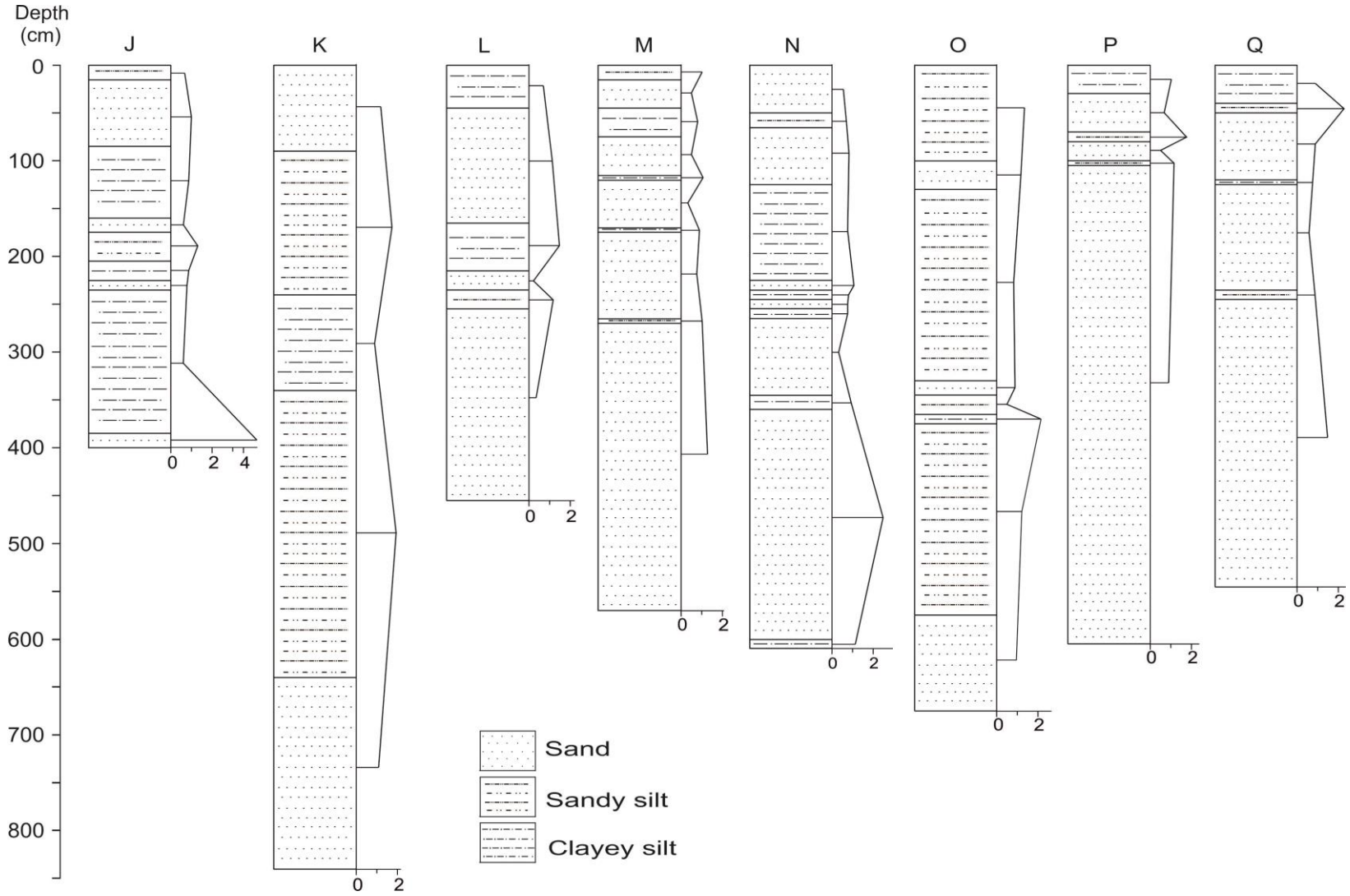

Figure 5.14: Magnetic susceptibility values in 10^{-6} m^3 kg for sediment samples outcrops (J to Q) along the Nigerian position on the River Benue, Yola Region.

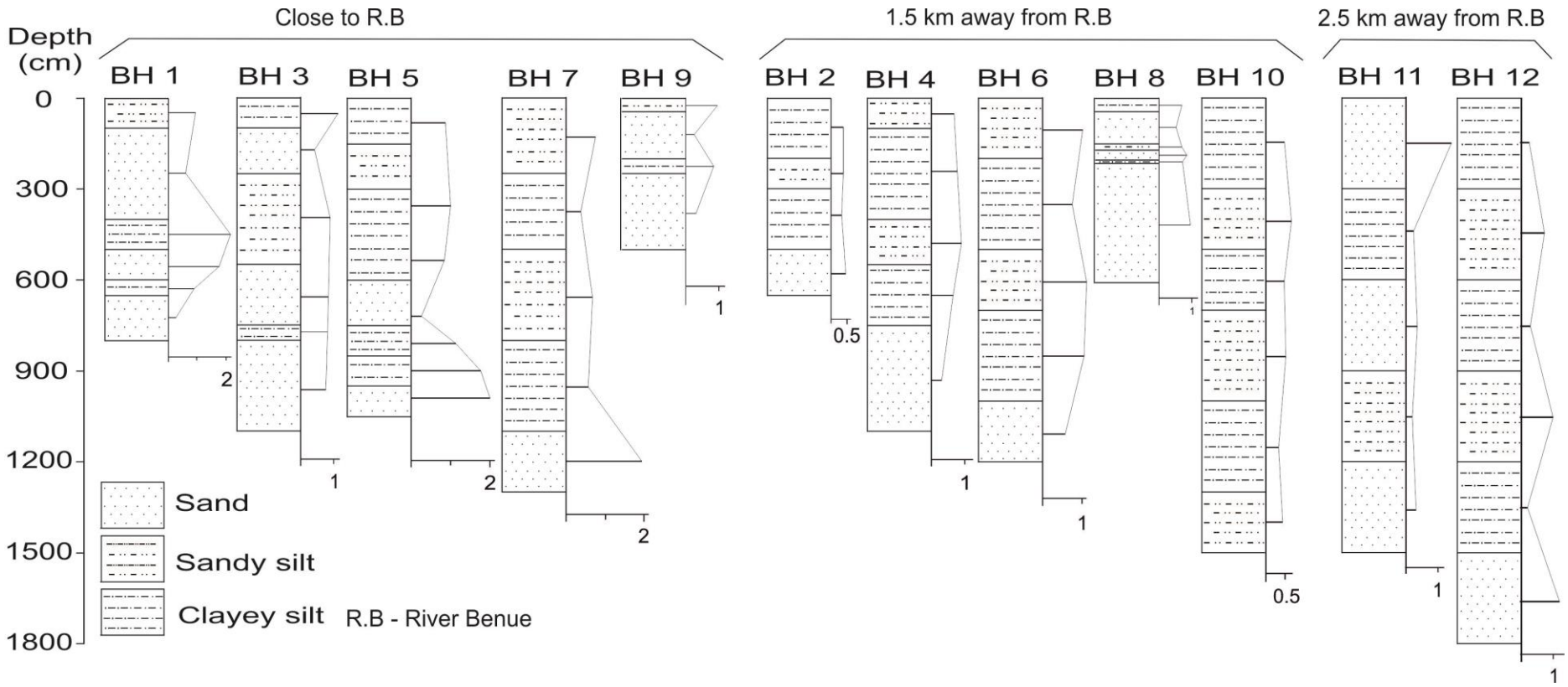

Figure 5.15: Sedimentological logs of the twelve drill boreholes 1 to 12 showing magnetic susceptibility values in 10^{-6} m^3 kg in the Yola Region. For location of boreholes (see Figure 2.8).

5.3.5 Field Shear Strength on floodplain sediment

This section presents and interprets the shear strength forces on the alluvial floodplain sediment. Understanding the shear strength forces on the alluvial floodplain sediment is necessary to assess the suitability of the hand drilling techniques.

The results from the Field Shear Vane Tester (FSVT) are shown in Figure 5.16 and Table D, Appendix D. These show the various shearing forces exerted on alluvial sediments at twelve different drill boreholes points on the floodplain. Borehole locations BH 1, BH 3, BH 7, BH 8 and BH 11 (Figure 5.16) show low shear forces on sediment, with the shear forces values ranging from 15 to 80 kPa. This implies that drilling at these locations requires less energy for the drilling to produce a well. Borehole locations BH 2, BH 4, BH 5, BH 6, BH 9, BH 10 and BH 12 (Figure 5.16) show higher impact of shear forces on sediments, with values ranging from 40 to 160 kPa. Drilling in these locations requires more human energy because of the harder formation to produce a well.

The shear force on sediments varies across the floodplain. For example, borehole locations BH 2, BH 3, BH 4, BH 5 and BH 9 show decrease in shear strength of the sediments with increase in depth. While borehole locations BH 6 and BH 7 shows increase in shear strength of the sediments with depth. Borehole locations BH 1, BH 8, BH 10, BH 11 and BH 12 shows consistent shear forces on sediments with increase in depth. The difference in the variations of the shear forces is due to the type of formations. Soft sediments shows low shear forces while consolidated sediments shows high shear forces.

Positive high correlation between 0.707 and 0.923 (p-value between 0.022 and 0) are observed at borehole points 6, 7 and 12 with depth (Table 5.5). This suggests that shear strength increases with depth. Negative high correlation between -0.689 and -0.929 (p-value between 0.028 and 0) are observed at borehole points 4, 5, 9 and 10 with depth (Table 5.5). This suggests that shear strength deceases with depth.

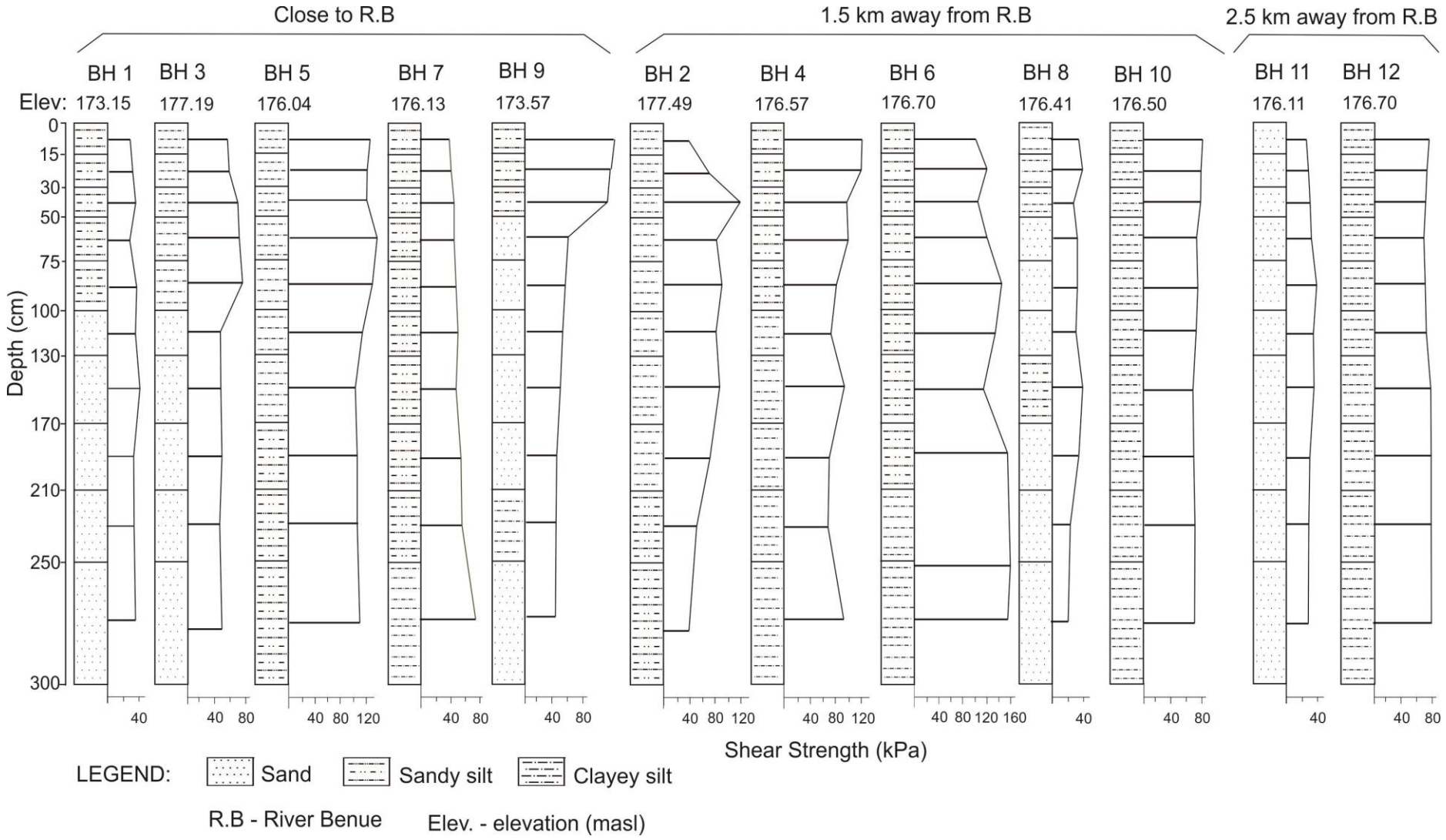

Figure 5.16: Shear strength forces on sediments at twelve borehole locations1 to 12, with their sedimentological descriptions in the floodplain. For position of boreholes (see Figure 2.8).

Table 5.5: Statistical correlation values and significance range between shear strength at twelve boreholes (BH 1 to 12) and depth (Significant p-value range 0 to 0.05, not significant p-value range 0.06 to 1)

Parameters		Depth (cm)	BH 1	BH 2	BH 3	BH 4	BH 5	BH 6	BH 7	BH 8	BH 9	BH10	BH11	BH12
Depth (cm)	Correlation	1												
	P-value	0												
BH 1	Correlation	0.503	1											
	P-value	0.139	0											
BH 2	Correlation	-0.407	0.35	1										
	P-value	0.244	0.321	0										
BH 3	Correlation	-0.609	-0.377	0.538	1									
	P-value	0.062	0.283	0.108	0									
BH 4	Correlation	**-0.689***	-0.56	-0.084	0.347	1								
	P-value	**0.028**	0.092	0.817	0.326	0								
BH 5	Correlation	**-0.708***	-0.629	0.252	**0.882****	0.477	1							
	P-value	**0.022**	0.051	0.482	**0.001**	0.163	0							
BH 6	Correlation	**0.825****	0.234	-0.389	-0.337	**-0.738***	-0.393	1						
	P-value	**0.003**	0.514	0.267	0.342	**0.015**	0.262	0						
BH 7	Correlation	**0.923****	0.399	-0.374	-0.445	-0.524	-0.556	**0.760***	1					
	P-value	**0**	0.253	0.287	0.198	0.12	0.095	**0.011**	0					
BH 8	Correlation	-0.566	-0.087	0.152	0.02	0.503	0.086	-0.568	**-0.674***	1				
	P-value	0.088	0.811	0.674	0.957	0.138	0.813	0.086	**0.032**	0				
BH 9	Correlation	**-0.825****	-0.547	0.134	0.371	**0.808****	0.43	**-0.770****	**-0.685***	0.375	1			
	P-value	**0.003**	0.102	0.711	0.291	**0.005**	0.215	**0.009**	**0.029**	0.286	0			
BH10	Correlation	**-0.929****	-0.577	0.253	0.574	**0.739***	**0.658***	**-0.777****	**-0.770****	0.363	**0.935****	1		
	P-value	**0**	0.081	0.48	0.083	**0.015**	**0.039**	**0.008**	**0.009**	0.302	**0**	0		
BH11	Correlation	-0.023	0.56	0.591	0.348	-0.377	0.194	0.104	-0.052	0.111	-0.423	-0.175	1	
	P-value	0.949	0.092	0.072	0.325	0.282	0.592	0.776	0.887	0.761	0.223	0.629	0	
BH12	Correlation	**0.707***	0.163	**-0.687***	**-0.741***	-0.221	**-0.767****	0.436	0.617	-0.251	-0.283	-0.519	-0.559	1
	P-value	**0.022**	0.652	**0.028**	**0.014**	0.539	**0.01**	0.208	0.057	0.484	0.429	0.124	0.093	0

There is hardly any published information available for the correlation between shear strength forces and hand drilling (Dr Kerstin Danert, Coordination of the hand-drilling topic within the Rural Water Supply Network, SKAT Consulting Ltd, Switzerland, personal communication dated 12th December 2013). The suitability of the shear strength forces for hand drilling techniques is discussed in literature review chapter (see section 2.4.5). In the present study, an attempt was made to compare the shear strength in relation to hand drilling based on the values of the shear forces obtained on the floodplain alluvial sediment (see Figure 5.16). On the floodplain, the lower shear strength forces on sediment are in the range between 15 and 95 kPa, which is assumed to be within the limit for hand drilling with human power (see section 2.4.5). Higher shear forces on alluvial sediment are in the range between 100 and 160 kPa. This range is assumed to be slightly beyond the limit for hand drilling. However, in reality many wells have been drilled by the farmers throughout the floodplain, including areas where values of 160 kPa were measured (Figure 5.17).

Some more suitable zones (see Figure 5.17) were identified across the floodplain for the application of the hand drilling methods, which required lower shear strength (below 95 kPa). The suitable drilling locations include BH 1, BH 3 and BH 13 in the northeast, BH 11 and BH 23 in the south-west, and BH 7, BH 8, BH 9, BH 19 and BH 20 in the north-west (Figure 5.17).

This is the first attempt to compare shear strength forces on alluvial sediments in relation to hand drilling method. This comparison should be viewed as preliminary attempt; however, more studies are required in order to make a good comparison of shear strength forces on sediment in relation to hand drilling method.

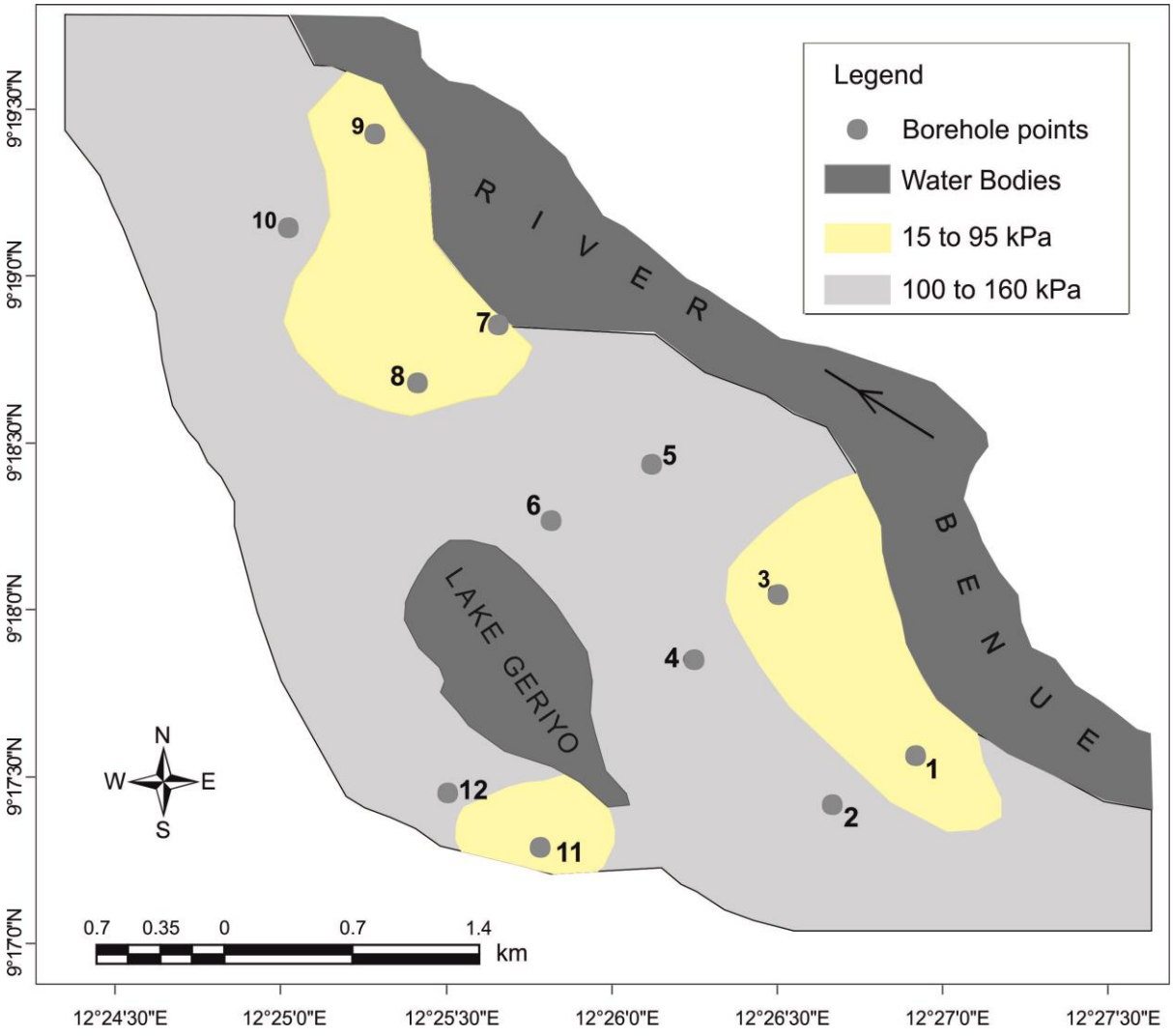

Figure 5.17: Shear strength distribution across the floodplain.

5.3.6 Statistical analysis for the sediment samples variables

This section presents the statistical analysis of the floodplain alluvial sediment variables in order to derive conclusions on the link between the data obtained.

5.3.6.1 Correlation of loss on ignition with grain sizes

Figure 5.18 shows the relationship between LOI at 550 $^{\circ}$C and of percentage sand, clayey silt, sandy silt, and sandy silt plus clayey silt for the floodplain alluvial. They all show highly significance correlations. Correlation values ranging between -0.882 to 0.899 (P-value of 0) (Table 5.6). The percentage clayey silt, sandy silt, and sandy silt plus clayey silt show highly

positive correlation, and the percentage sand shows highly negative correlation (Table 5.6). This indicates that clayey silt and sandy silt sediments have higher amount of LOI at 550 ˚C than sand sediments in the alluvial floodplain.

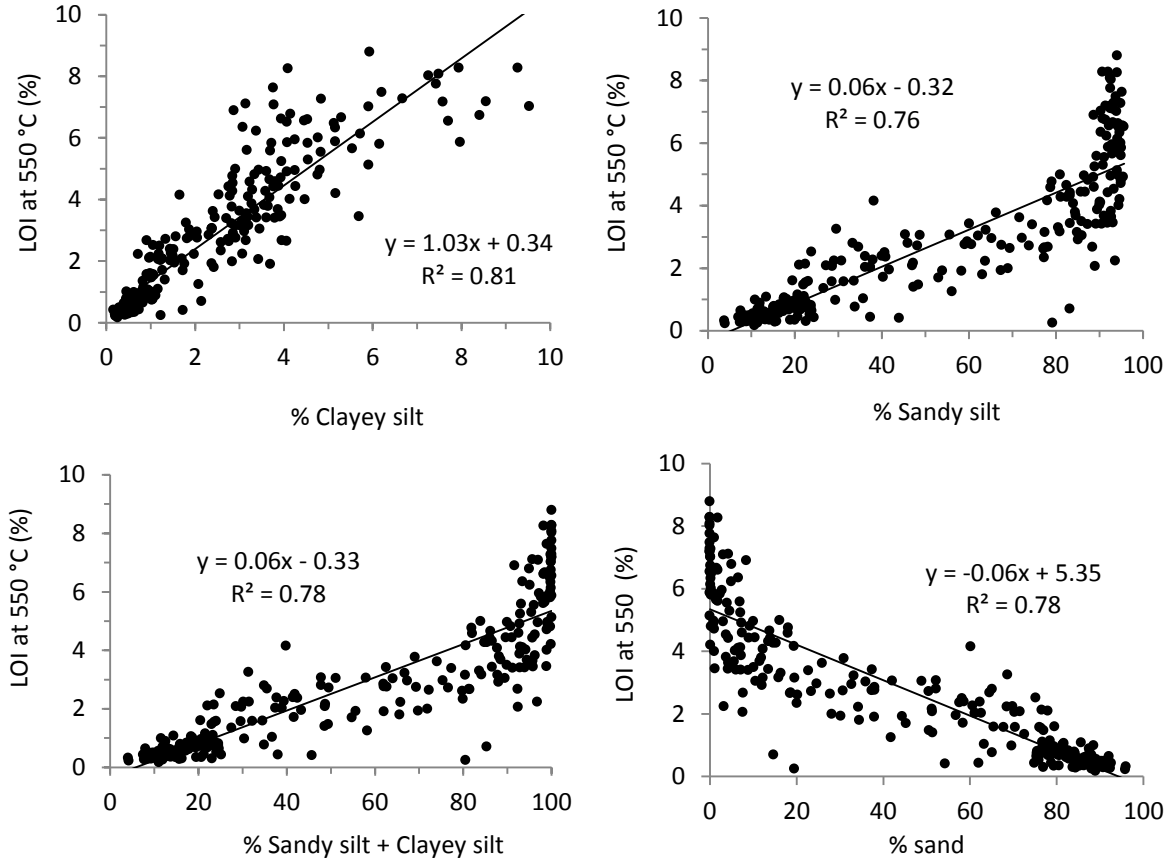

Figure 5.18: Relation between LOI at 550 ˚C and percentage of clayey silt, sandy silt, sandy silt + clayey silt and sand for the floodplain alluvial sediments.

Table 5.6: Statistical correlation values and significance range between LOI at 550 ˚C and percentage of clayey silt, sandy silt, sandy silt + clayey silt and sand (Significant p-value range 0 to 0.05, not significant p-value range 0.06 to 1)

Parameters		LOI at 550 ˚C
LOI at 550 ˚C	Correlation	1
	P-value	0
% Clayey silt	Correlation	**0.899****
	P-value	0
% Sandy silt	Correlation	**0.874****
	P-value	0
% Sand silt + Clayey silt	Correlation	**0.882****
	P-value	0
% Sand	Correlation	**-0.882****
	P-value	0

The LOI at 550 °C are generally higher in finer sandy silt and clayey silt sediments and lower in coarser sand sediments. As reported by Vereş (2002) higher percentage of LOI is commonly associated with finer sediments e.g. clay-silt and silt, this is because of the higher adsorption capacities of finer particle sizes such as clayey silt. Finer particles such as clayey silt contain hydroxyl groups $(OH)^-$ as structure of water. These hydroxyl groups when subjected to heating liberated as water, part of the loss result to chemically bound water loss with high clayey silt and low LOI (Vereş, 2002). Other possible reason is that finer sediment is deposited in perimeter environments more conducive to be a reducing environment where LOI at 550 °C is better preserved.

5.3.6.2 Correlation of shear forces with grain sizes

Shear force (limited to top 3 m) experience in the clayey silt median particle sizes varies between 20 to 160 kPa and on the coarse sand median particle sizes varies between 20 to 70 kPa (see Figure 5.19A). A high negative correlation of -0.541 (p-value of 0) was observed between them (Table 5.7). Similarly the relationship between shear strength with coefficient of uniformity (Figure 5.29B) shows that higher shear force is found on finer sediment in the range between 10 to 160 kPa and lower on coarser sediments in the range between 10 to 50 kPa and a weak negative correlation of -0.188 (p-value of 0.039) was observed (Table 5.7). This indicates that particle size strongly influences the rate of shear force on the floodplain sediments. Shear force on the alluvial sediments closer to the river varies between 10 to 130 kPa and on the sediments 1,000 m away from the river varies between 20 to 160 kPa (see Figure 5.19C). A weak positive significance correlation of 0.186 (p-value of 0.042) (Table 5.7) was observed indicating shear strength increases away from the river as the moisture from the river decreases. However, at distance 2,500 m away from the river it shows low shear force on the sediments in the range between 40 to 100 kPa. This may be due to the moisture from the Lake Geriyo that has water throughout the year. The relationship between

shear strength and moisture content showed strong negative correlation -0.490 (p-value of 0) (Table 5.7) as expected.

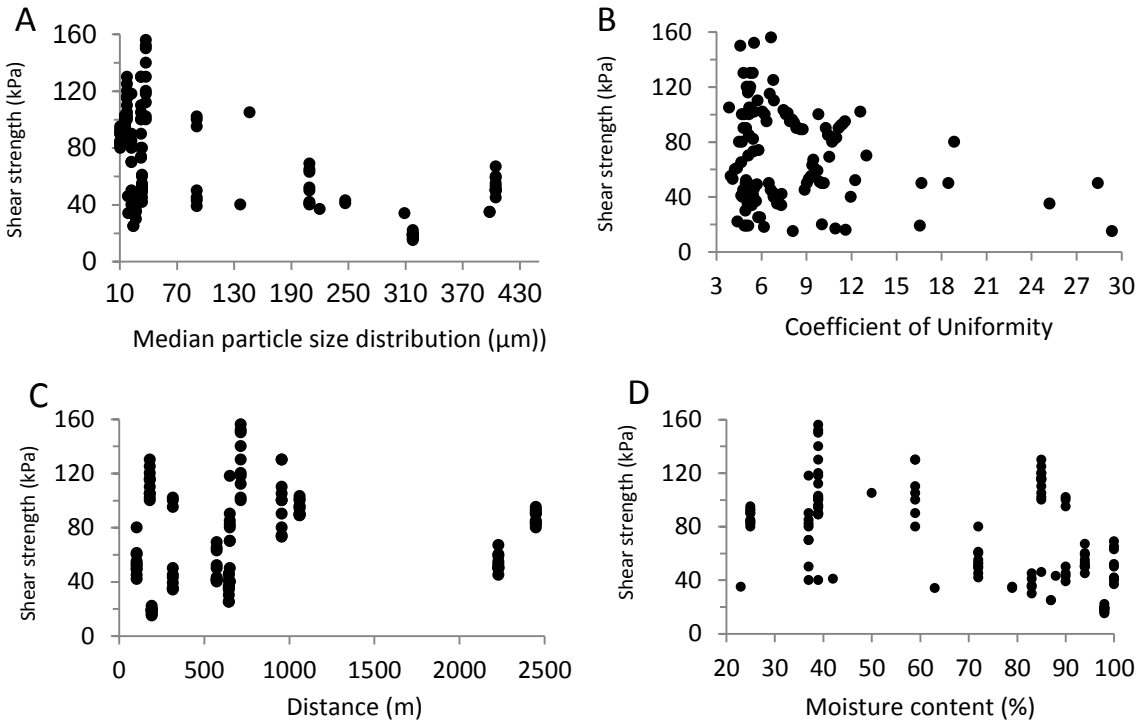

Figure 5.19: Relationship between shear strength with: A – particle size distribution; B – moisture content; C – distance away from River Benue; D –coefficient of uniformity (Cu).

Table 5.7: Statistical correlation values and significance range between shear strength with median particle size distribution, coefficient of uniformity (Cu), distance away from River Benue and moisture content (Significant p-value range 0 to 0.05, not significant p-value range 0.06 to 1)

Parameters		Shear strength	Median PSD	Cu	Distance (m)	Moisture content
Shear strength	Correlation	1				
	P-value	0				
Median PSD	Correlation	**-0.541****	1			
	P-value	**0**	0			
Cu	Correlation	**-0.188***	0.081	1		
	P-value	**0.039**	0.378	0		
Distance (m)	Correlation	**0.186***	0.149	**0.210***	1	
	P-value	**0.042**	0.104	**0.021**	0	
Moisture content	Correlation	**-0.490****	**0.558****	-0.158	**-0.338****	1
	P-value	**0**	**0**	0.085	**0**	0

5.3.6.3 Correlation of magnetic susceptibility with grain size and loss on ignition

Figure 5.20A shows that magnetic susceptibility (MS) values in finer sediments vary between 0 to 2.5 10^{-6} m^3 kg and in coarser sand sediments varies between 0.2 to 4.16 10^{-6} m^3 kg. The high values outliers were not included in the analysis. Weak positive correlation of 0.14 (p-value of 0.025) is observed between MS with median particle size diameter D50 (Table 5.8). This indicates that higher MS value tend to be found in slightly coarser alluvial sediments.

Figure 5.20B shows that MS value in alluvial sediment closer to the river varies between 0.2 to 2.5 10^{-6} m^3 kg and in the alluvial sediments at a distance 2,500 m away from the river varies between 0 to 1.5 10^{-6} m^3 kg. Significant correlation of 0.487 (p-value is 0) is observed (Table 5.8) between MS with distance away from the river, which suggests that distance away from the river is important.

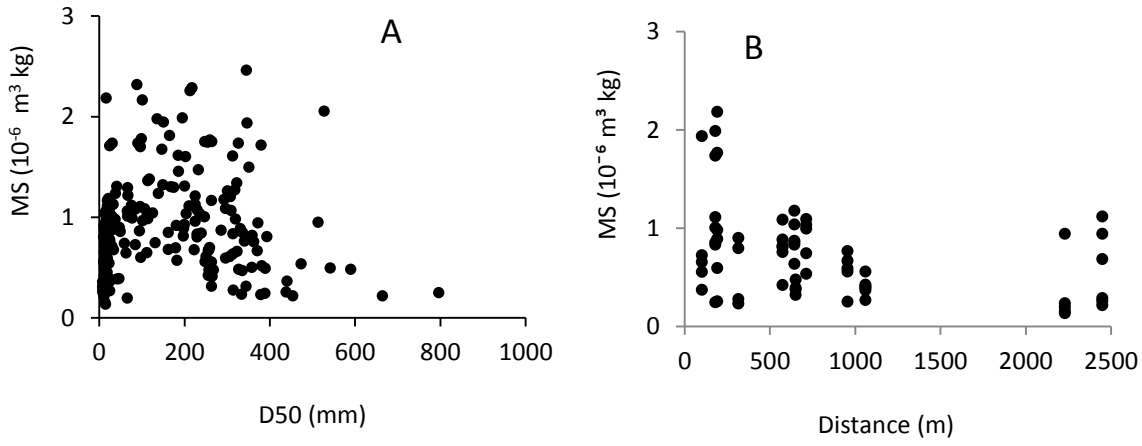

Figure 5.20: Relationship between magnetic susceptibility: with median particle sizes (A) and distance away from the river (B).

Figure 5.21 shows the relationship between MS and LOI at 550 °C. A negative correlation of -0.348 (p-value of 0) is observed (Table 5.8) between MS and LOI at 550 °C. However, the clustering suggests that all the alluvial sediments may possibly originate from a similar source.

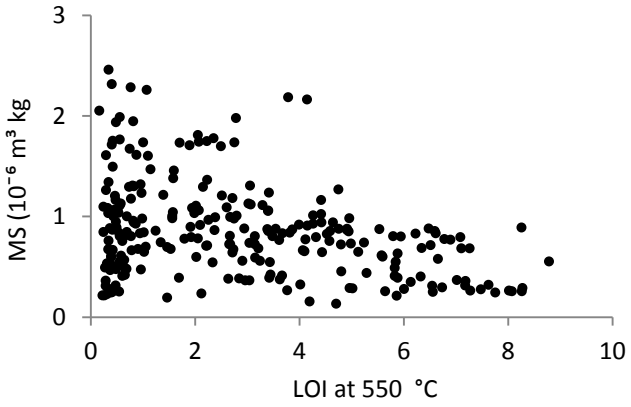

Figure 5.21: Relationship between magnetic susceptibility with loss on ignition.

Table 5.8: Statistical correlation values and significance range between magnetic susceptibility with median particle size, distance away from the river and loss on ignition (Significant p-value range 0 to 0.05, not significant p-value range 0.06 to 1)

Parameters		MS	D50 (µm)	Distance (m)	LOI at 550 ˚C
MS	Correlation	1			
	P-value	0			
D50 (µm)	Correlation	**0.140***	1		
	P-value	**0.025**	0		
Distance (m)	Correlation	**0.487****	0.19	1	
	P-value	**0**	0.129	0	
LOI at 550 ˚C	Correlation	**-0.348****	**-0.729****	-0.195	1
	P-value	**0**	**0**	0.12	0

5.3.6.4 Principal Component Analysis for sediment variables

Figure 5.22 shows the loading plot for the statistical correlation using Principal Component Analysis (PCA) from 256 sediment samples obtained along River Benue outcrops and borehole cores across the floodplain.

Clayey silt, sandy silt and LOI at 550 ˚C are positively correlated, with their correlation values ranging from 0.865 to 0.922 (p-values of 0) (Table 5.9); their values indicate significance correlated variables. However, they are negatively correlated with sand with the correlation value ranging from -0.143 to -0.757 (p-values from 0.021 to 0) (Table 5.9). This shows that the LOI at 550 ˚C is higher in clayey silt and sandy silt sediment samples and lower in sand sediment samples on the contrary.

Moisture content MC) and depth show positive significant correlation value of 0.685 (p-value of 0) (Table 5.9). This shows that MC increases with depth. Although the MC results are taken with caution because of the three months delay between sampling and measurement. However, the result indicates that MC increases with depth (see Figures 5.8 and 22).

Sand and magnetic susceptibility (MS) are positively correlated, with their correlation value of 0.404 (p-value of 0) (Table 5.9). MS with sandy silt and clayey silt are negatively correlated with their correlation values between -0.352 and -0.370 (p-value of 0) (Table 5.9). This shows that MS values tend to be higher in sand sediment samples and lower in the sandy silt and clayey silt sediment samples across the floodplain.

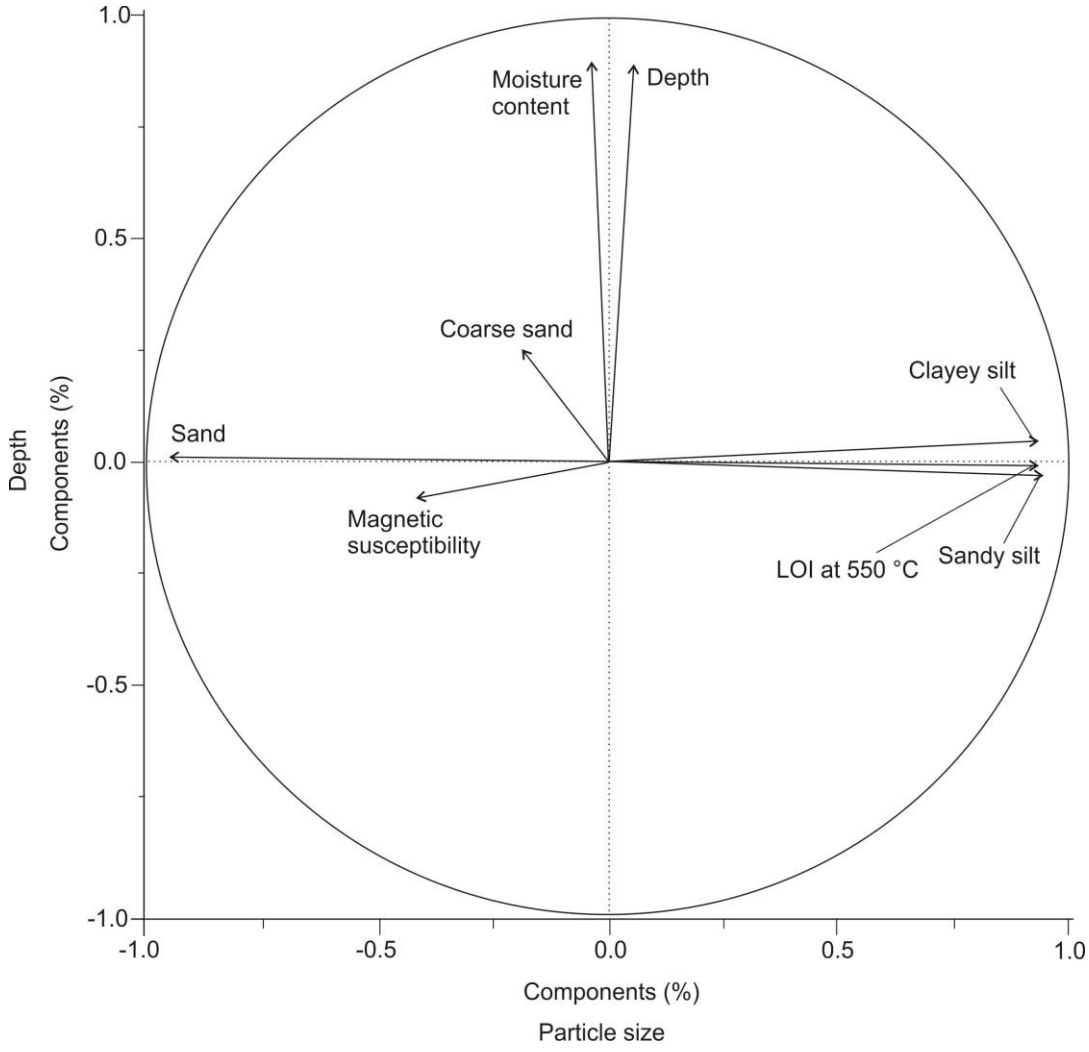

Figure 5.22: Loading plot showing the statistical correlation for the 256 sediment samples variables using Principal Component Analysis.

Table 5.9: Statistical correlation values and significance range of the variables for two hundred and fifty six sediment samples using Principal Component Analysis (Significant p-value range 0 to 0.05, not significant p-value range 0.06 to 1)

Parameters		Depth	Magnetic Susceptibility	Moisture content	LOI at 550 ˚C	Coarse sand	Sand	Sandy silt	Clayey silt
Depth	Correlation	1							
	P-values	0							
Magnetic Susceptibility	Correlation	-0.062	1						
	P-values	0.326	0						
Moisture content	Correlation	**0.685****	0.058	1					
	P-values	**0**	0.357	0					
LOI at 550 ˚C	Correlation	0.042	**-0.341****	-0.049	1				
	P-values	0.506	**0**	0.438	0				
Coarse sand	Correlation	0.058	-0.025	**0.155***	**-0.144***	1			
	P-values	0.358	0.69	**0.013**	**0.021**	0			
Sand	Correlation	**-0.199****	**0.404****	**-0.121**	**-0.645****	-0.072	1		
	P-values	**0.001**	**0**	**0.053**	**0**	0.249	0		
Sandy silt	Correlation	0.067	**-0.352****	-0.023	**0.878****	**-0.143***	**-0.757****	1	
	P-values	0.283	**0**	0.714	**0**	**0.022**	**0**	0	
Clayey silt	Correlation	0.094	**-0.370****	-0.005	**0.865****	**-0.140***	**-0.654****	**0.922****	1
	P-values	0.136	**0**	0.939	**0**	**0.025**	**0**	**0**	0

Figure 5.23 shows the loading plot for the statistical correlation for the alluvial sediment samples variables at 3 m depth using PCA for 120 sediment samples obtained in borehole cores in the floodplain. In order to be able to include shear strength data too.

The results are as in Figure 5.22. However, specifically shear strength, depth and sand are positively correlated with their correlation values ranging from 0.204 to 0.324 (p-value ranging from 0.025 to 0) (Table 5.10). This shows those shear strength on the alluvial floodplain sediment decreases with depth and has lower shear strength on sand alluvial sediment formations in the floodplain.

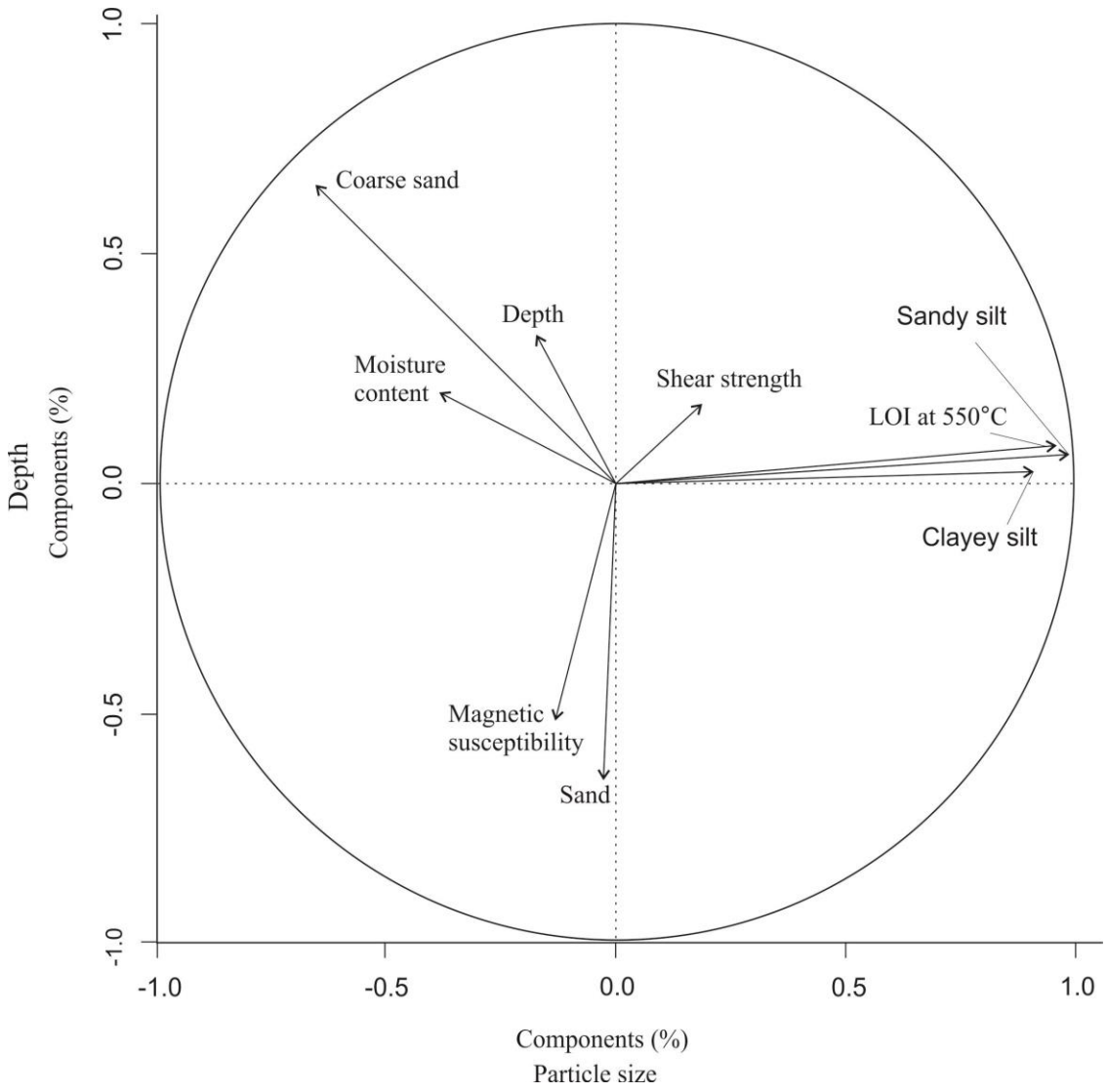

Figure 5.23: Loading plot showing the statistical correlation for the sediment samples variables limited to three metres depth using Principal Component Analysis.

Table 5.10: Statistical correlation values and significance range of the variables for one hundred and twenty sediment samples (three metres depth) using Principal Component Analysis (Significant p-value range 0 to 0.05, not significant p-value range 0.06 to 1)

Parameters		Depth	Magnetic susceptibility	Moisture content	LOI at 550 ˚C	Coarse sand	Sand	Sandy silt	Clayey silt	Shear strength
Depth	Correlation	1								
	P-values	0								
Magnetic susceptibility	Correlation	0.029	1							
	P-values	0.753	0							
Moisture content	Correlation	0.**755****	-0.09	1						
	P-values	**0**	0.33	0						
LOI at 550 ˚C	Correlation	**-0.203***	-0.023	**-0.363****	1					
	P-values	**0.026**	0.807	0	0					
Coarse sand	Correlation	**0.324****	-0.076	**0.281****	**-0.545****	1				
	P-values	**0**	0.408	0.002	0	0				
Sand	Correlation	-0.075	**0.413****	-0.105	-0.138	**-0.350****	1			
	P-values	0.417	**0**	0.254	0.133	0	0			
Sandy silt	Correlation	-0.124	-0.076	**-0.291****	**0.854****	**-0.583****	-0.177	1		
	P-values	0.176	0.411	0.001	0	0	0.053	0		
Clayey silt	Correlation	-0.102	-0.051	**-0.282****	**0.820****	**-0.604****	-0.11	**0.974****	1	
	P-values	0.269	0.58	**0.002**	**0**	**0**	0.231	**0**	0	
Shear strength	Correlation	**0.204***	0.094	-0.007	0.127	0.016	0.179	0.124	0.169	1
	P-values	**0.025**	0.309	0.938	0.167	0.86	0.051	0.178	0.066	0

5.3.7 Summary for sedimentology data

It was observed from the floodplain sedimentology analysis that:

1. The floodplain alluvial sediments are completely dominated by sand and sandy silts.
2. Loss on ignition at 550 $^{\circ}$C is generally low in the floodplain alluvial sediment, this may be due to loss of moisture bond within clayey silt. Moisture (LOI at 105 $^{\circ}$C) increases with depth.
3. The homogeneity of the magnetic susceptibility results suggests that all the floodplain alluvial sediment may originate from a similar source.
4. Some more suitable zones with lower shear strengths have been identified across the floodplain, better suited for application of hand drilling methods.

In conclusion, the sedimentology results have provided a new understanding of the structure and composition of alluvial sediments plus more suitable locations for hand drilling for water abstraction on the floodplain.

5.4 Groundwater

This section presents the results of the floodplain hydrology.

5.4.1 Resistivity soundings

The resistivity (ρ) results (from 24 vertical electrical sounding) reveal five different types of curves (Table 5.11).

Table 5.11: Resistivity curve types and their description. VES – vertical electric sounding

Location	Curve type	Description
VES (2, 13 & 23)	A	$\rho_1 < \rho_2 < \rho_3$
VES (1, 4, 5, 7, 11, 12, 16, 22 &24)	H	$\rho_1 > \rho_2 < \rho_3$
VES (3, 9, 14, 18 &21)	HK	$\rho_1 > \rho_2 < \rho_3 > \rho_4$
VES (6 , 8, 15, 17, 19 & 21)	K	$\rho_1 < \rho_2 > \rho_3$
VES 10	Q	$\rho_1 > \rho_2 > \rho_3$

Three groups of electro-stratigraphic earth models were obtained from the analysis of the resistivity data (Table 5.12): group 5 with 5 layers, group 4 with 4 layers and group 3 with 3 layers.

The first group of electro-stratigraphic model are VES 5, VES 12 and VES 15 with five distinct earth layers (Table 5.12). This electro-stratigraphic group shows a decrease in resistivity values with an increase in the layer thickness. Generally, the layer shows a low resistivity value, indicating better groundwater saturation condition. The high value of resistivity at the top layer may correspond to the unsaturated zone, as observed by Van Overmeeren (1989), since the soundings were carried out during the dry season period.

The second group of electro-stratigraphic model are VES 1, VES 3, VES 4, VES 9, VES 11, VES 13, VES 14, VES 18, VES 19, VES 21, VES 22 and VES 24; four distinct earth layers exists (Table 5.12). Here resistivity value decreases as the layer thickness increases, indicating better groundwater saturation condition.

Table 5.12: Average resistivity and thickness values for the three groups of electro-stratigraphic earth model

Model type		First layer	Second layer	Third layer	Fourth layer	Fifth layer
Five	Resistivity (Ωm)	159.46	1,460.00	49.21	174.47	184.50
	Thickness (m)	0.74	5.44	5.45	16.12	-
Four	Resistivity (Ωm)	246.19	1,402.42	470.07	154.55	-
	Thickness (m)	1.90	4.84	22.36	-	-
Three	Resistivity (Ωm)	327.69	702.03	545.13	-	-
	Thickness (m)	3.29	11.62	-	-	-

The third group of electro-stratigraphic model are VES 2, VES 6, VES 7, VES 8, VES 10, VES 16, VES 17, VES 20 and VES 23; three distinct earth layers exists (Table 5.12). This electro stratigraphic model shows increase in resistivity value with an increase in layer

thickness, it exhibits low resistivity value at the bottom of the layer this shows an indication of the aquifer potential at that point.

The results obtained from the computer modelling are presented in Table E, Appendix E, from the resulting curve and their final model parameters after iterations. The result shows VES using the Schlumberger array and their interpretation. This gives quantitative interpretations of observed curves in the field with the computed curves. The VES fitting error obtained ranges between 0.9 to 3.99%, with an average of 2.73% (Table E, Appendix E), which falls within the acceptable error limits, which is 0 to 15%.

The comparison of drilling logs with geo-electric resistivity soundings are presented in Figures 5.24 to 5.29. The depth of the boreholes varied between the twelve holes drilled, which ranged from 6 to 18 m. From the transects it was observed that the groundwater level of the floodplain fell away from the River Benue's channel. Transects 2, 3, 5, 6, 7, 8 and 9 show decrease in groundwater levels moving away from the River Benue valley.

The values obtained indicate the potentiality of the floodplain groundwater (aquifers) for the area. Similarly, VES results reveal five types of curves in the area (Table 5.12). The curves indicate the amount of resistivity along the floodplain for delineating the shallow groundwater of the floodplain.

It was also observed that no exact clear cut exists in the resistivity ranges corresponding to different layer formations; but if a layer exhibits high resistivity, then the layer could be a dry or soft formation. If in the medium range, it could be suggested that a layer composed of permeable formation or water bearing layer (aquifers), while low values of resistivity could suggest the presence of water bearing layers (aquifers) (Coker, 2012; Chambers et al., 2013; Orlando, 2013). Generally, the bottom layers show low resistivity values indicating water-bearing formations.

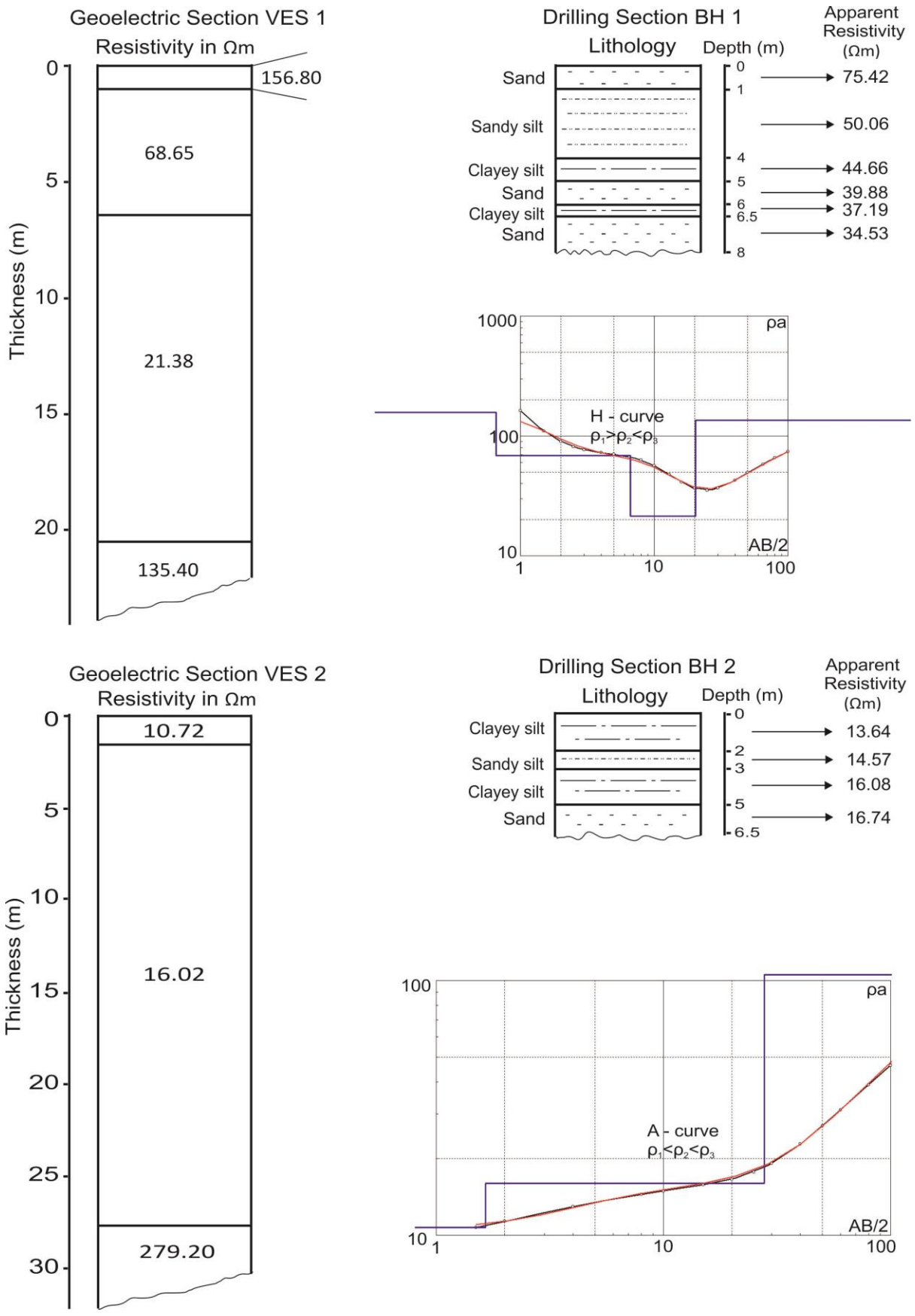

Figure 5.24: Comparison of vertical electrical soundings (VES) 1 and 2 interpretation results with corresponding drilling logs at boreholes (BH) 1 and 2.

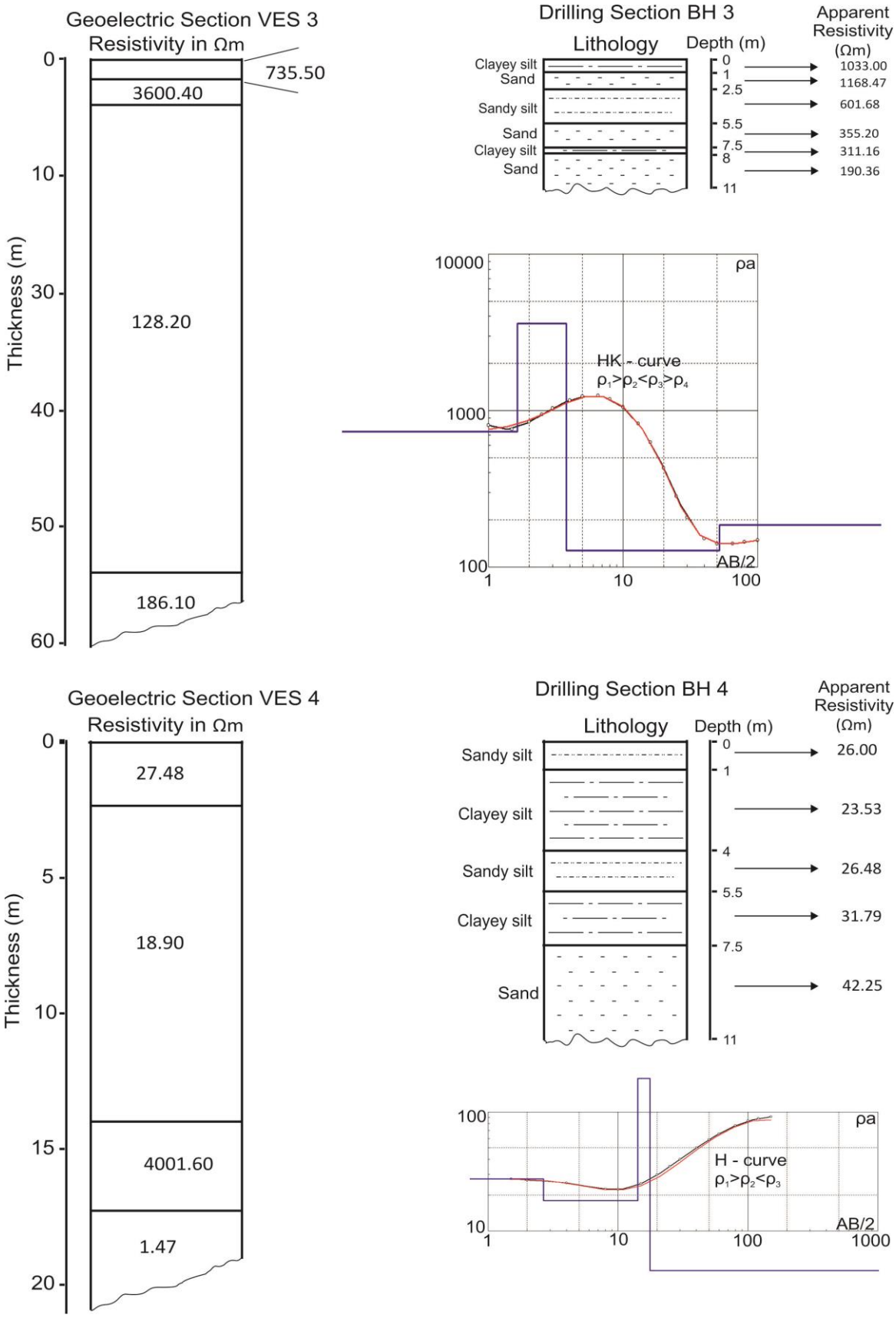

Figure 5.25: Comparison of vertical electrical soundings (VES) 3 and 4 interpretation results with corresponding drilling logs at boreholes (BH) 3 and 4.

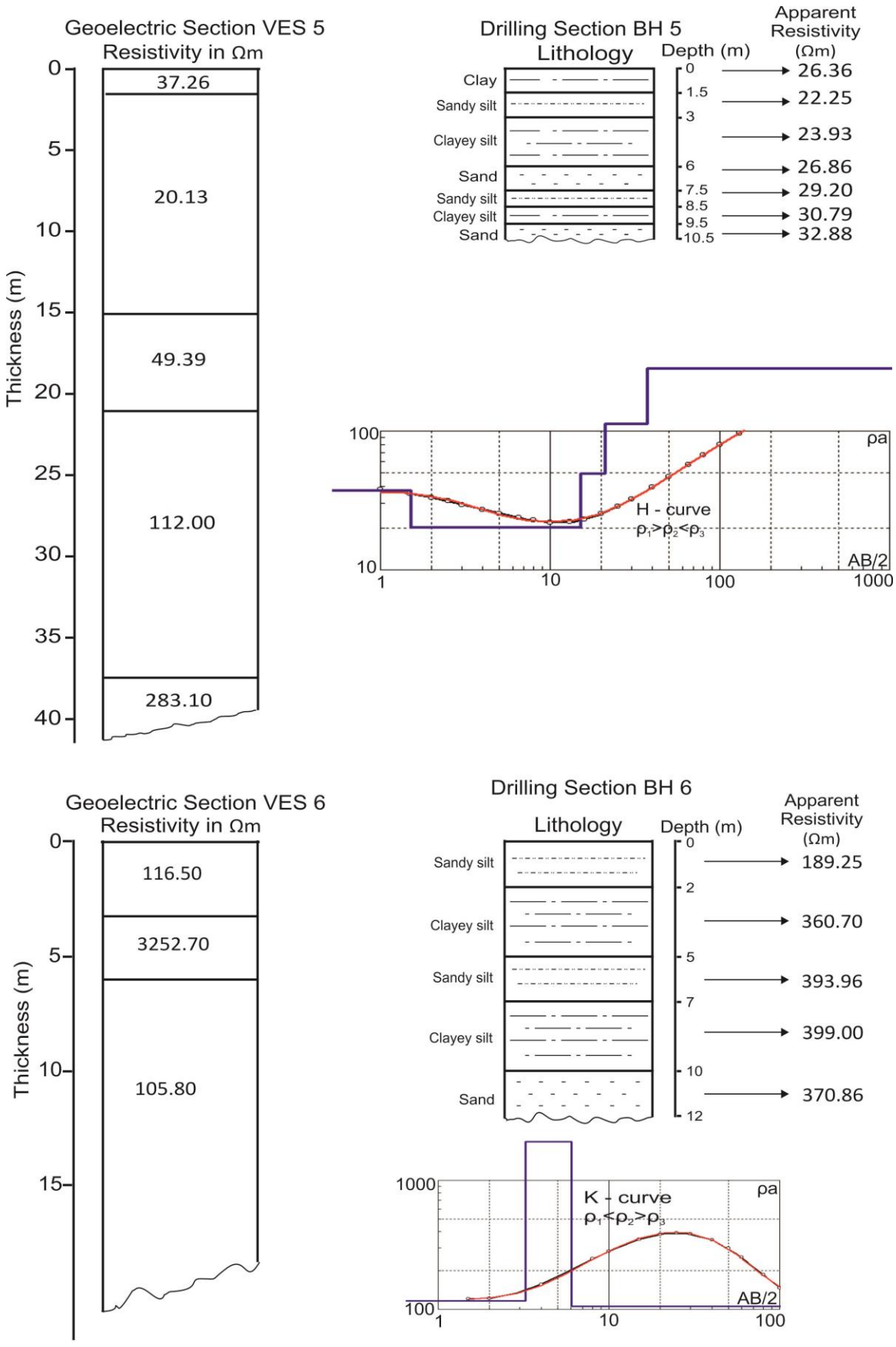

Figure 5.26: Comparison of vertical electrical soundings (VES) 5 and 6 interpretation results with corresponding drilling logs at boreholes (BH) 5 and 6.

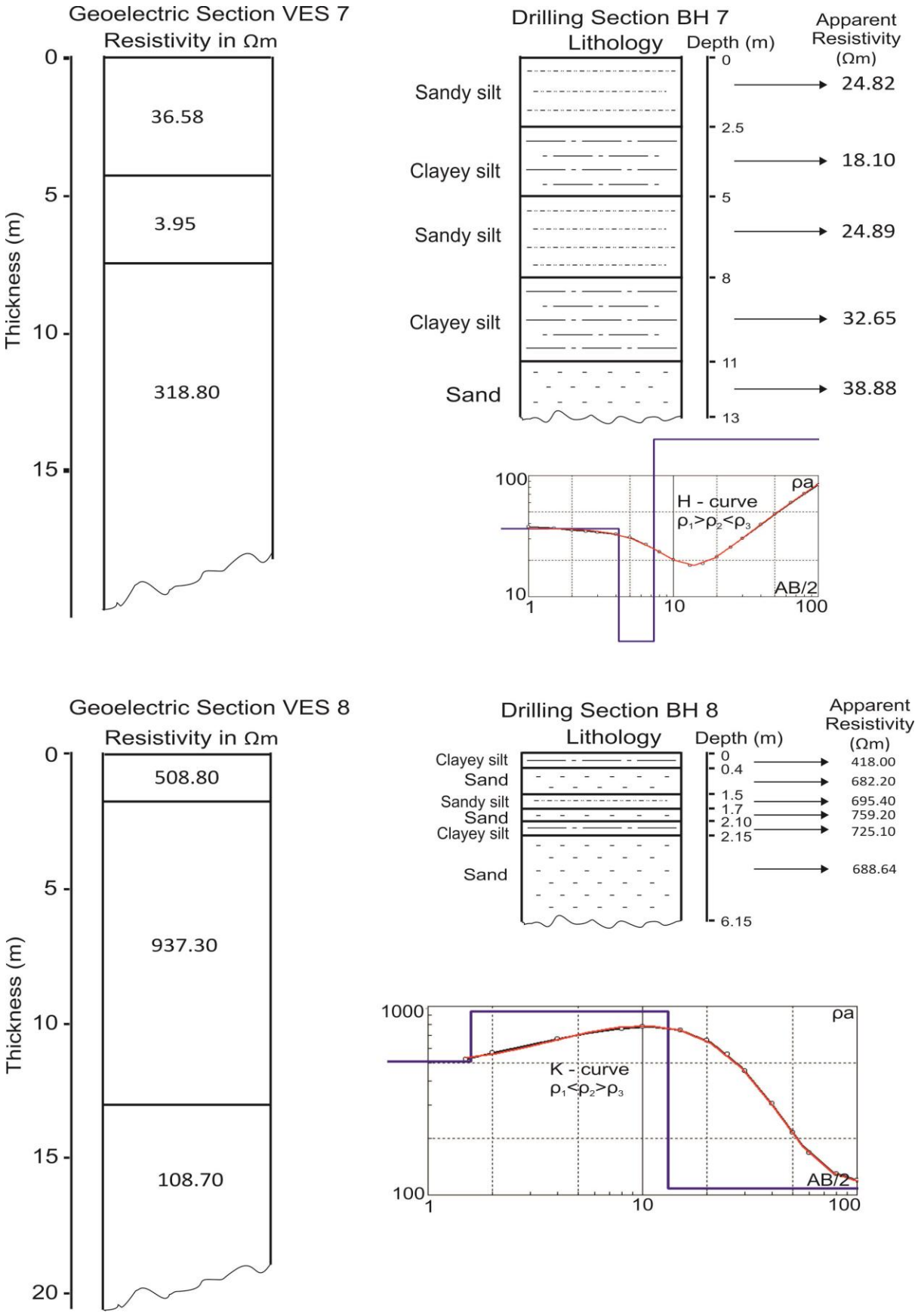

Figure 5.27: Comparison of vertical electrical soundings (VES) 7 and 8 interpretation results with corresponding drilling logs at boreholes (BH) 7 and 8.

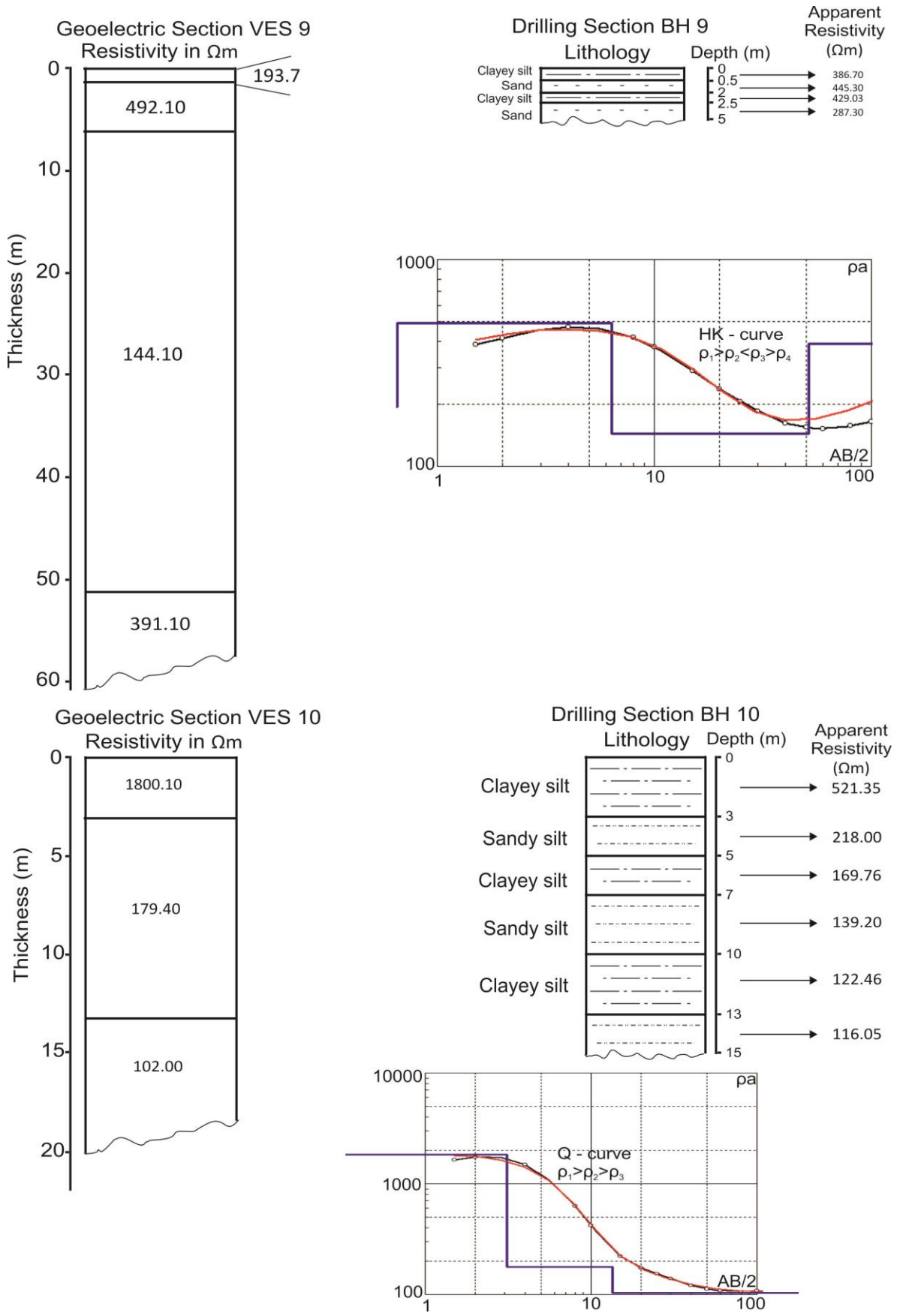

Figure 5.28: Comparison of vertical electrical soundings (VES) 9 and 10 interpretation results with corresponding drilling logs at boreholes (BH) 9 and 10.

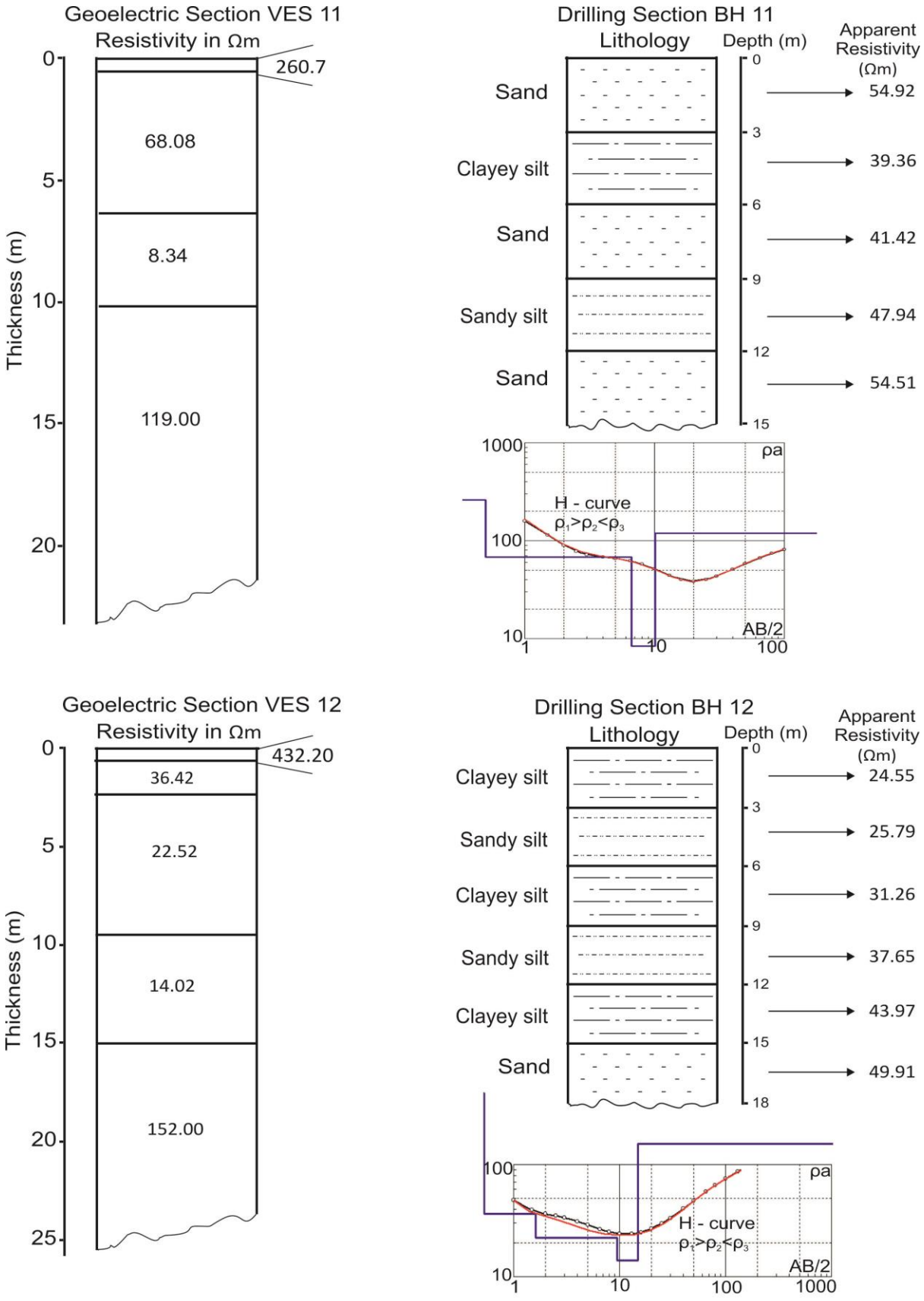

Figure 5.29: Comparison of vertical electrical soundings (VES) 11 and 12 interpretation results with corresponding drilling logs at boreholes (BH) 11 and 12.

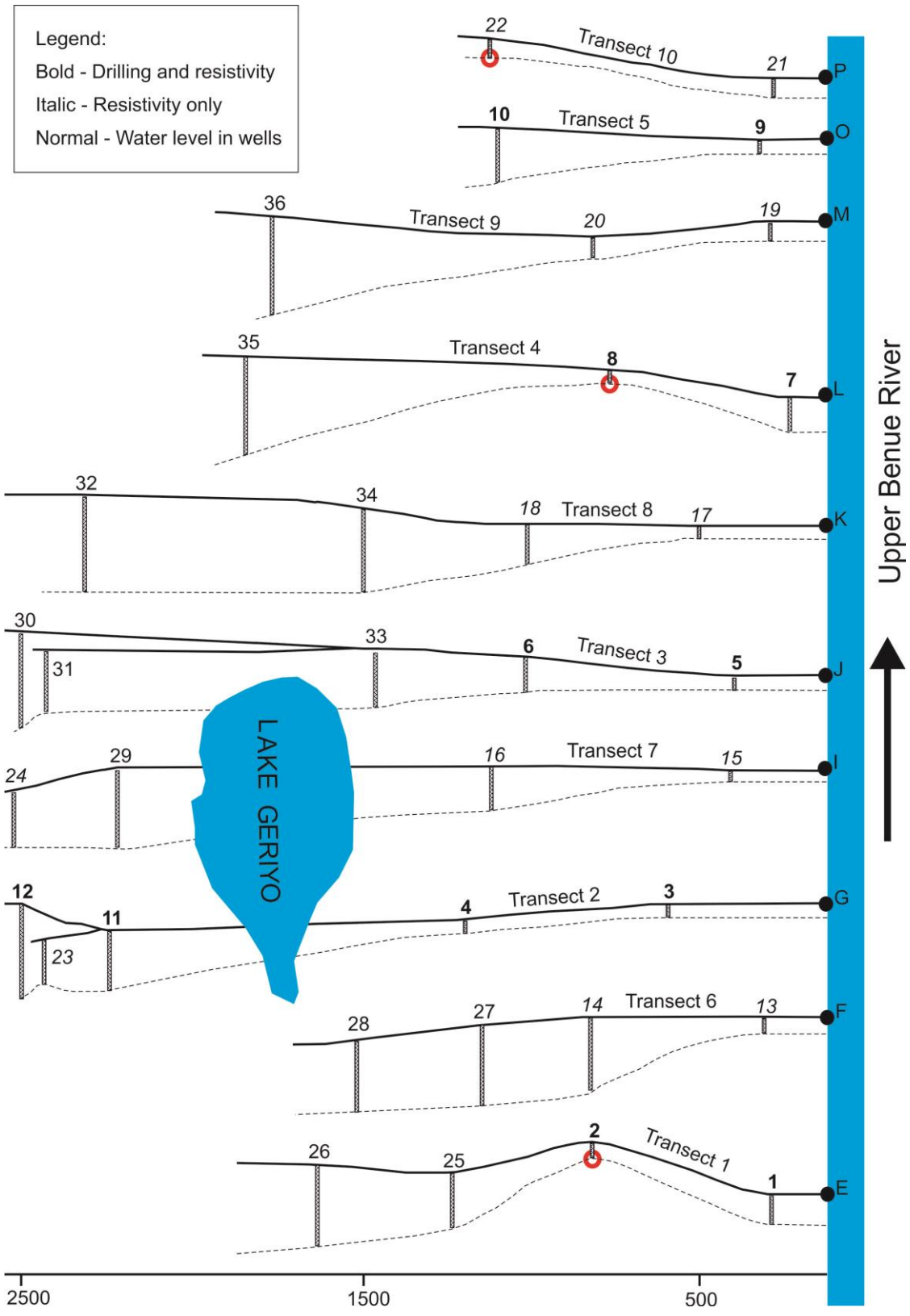

Figure 5.30: Graph showing the groundwater levels at the location of the ten vertical electrical sounding transects. The red circles showing the proposed position of perched aquifers as moving away from River Benue. Locations: (1 to 12) is resistivity and water levels 2011, (13 to 24) is resistivity water level 2012, (25 to 36) is water level 2013, black line is surface elevation, dotted line is groundwater level, black dots point is outcrops sampling. For location of boreholes and outcrops (see Figures 2.8 and 5.17).

The reason for combining the floodplain groundwater levels for the three different years (i.e. the 3 field period) was that river water stages in River Benue during the dry season period for the three different years did not showed much difference. River water stages in 2011 is 174.25 m; 2012 is 174.4 m and 2013 is 174.8 m. This shows that combining the three different years of water is reasonable.

Figure 5.31 shows the locations for the groundwater points studied over the three years along the floodplain and Lake Geriyo.

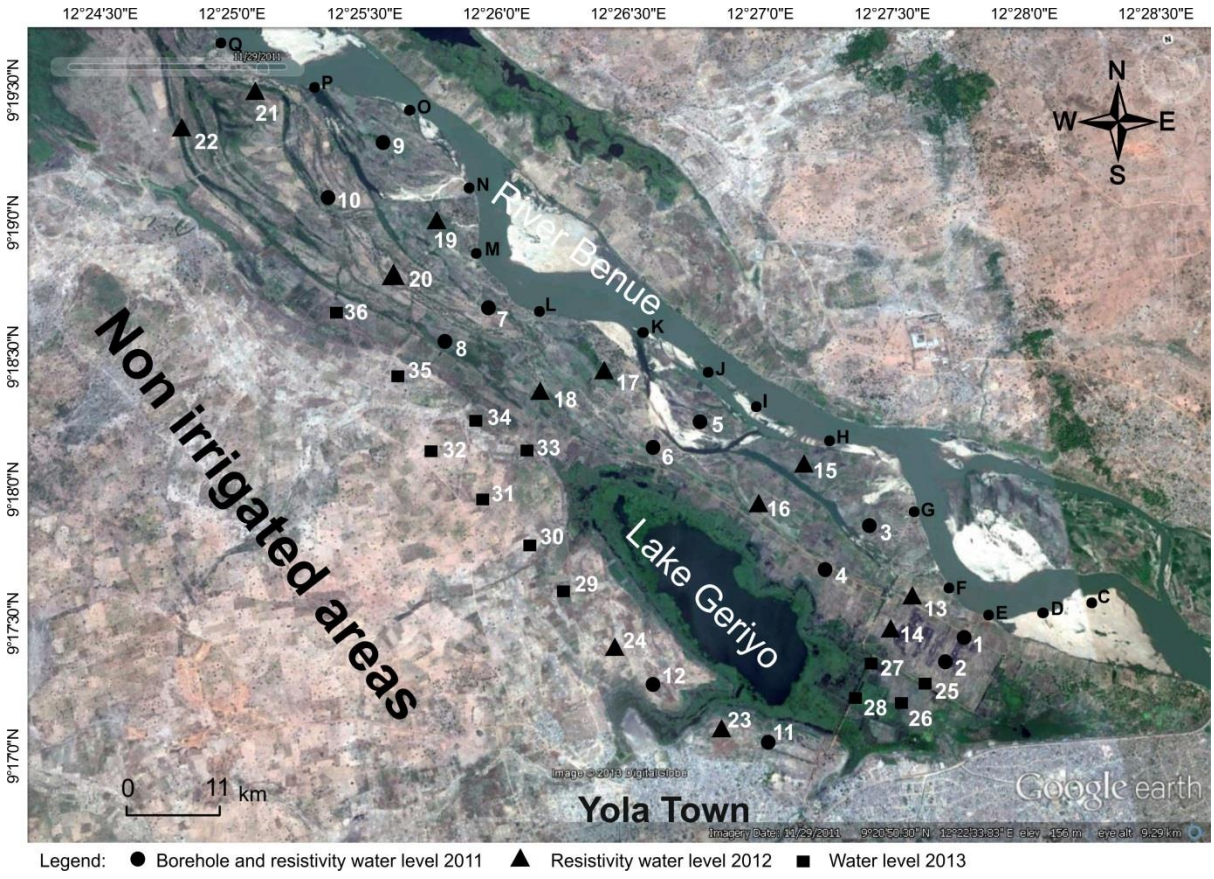

Figure 5.31: Map showing the locations for water level measurements along the floodplain and outcrops sampling (Modified from Google Earth Image, 2011). Black circles are boreholes and resistivity water levels 2011, black triangles is resistivity water levels 2012, black rectangles is boreholes water levels 2013.

5.4.2 Perched aquifer

As mentioned earlier perched aquifers are commonly found along alluvial floodplains. In order to identify possible perched aquifers in this study, information based on resistivity surveys (24 points), augering drilling up to the water levels and beyond (24 locations, but of which only 12 overlap with the VES), may be combined. Ideally, these two methods should show the same results.

The map on Figure 5.32 shows the floodplain groundwater levels obtained from resistivity soundings and borehole 2011, and groundwater measurement 2013. Two most likely perched aquifers were identified at well points 2 and 8.

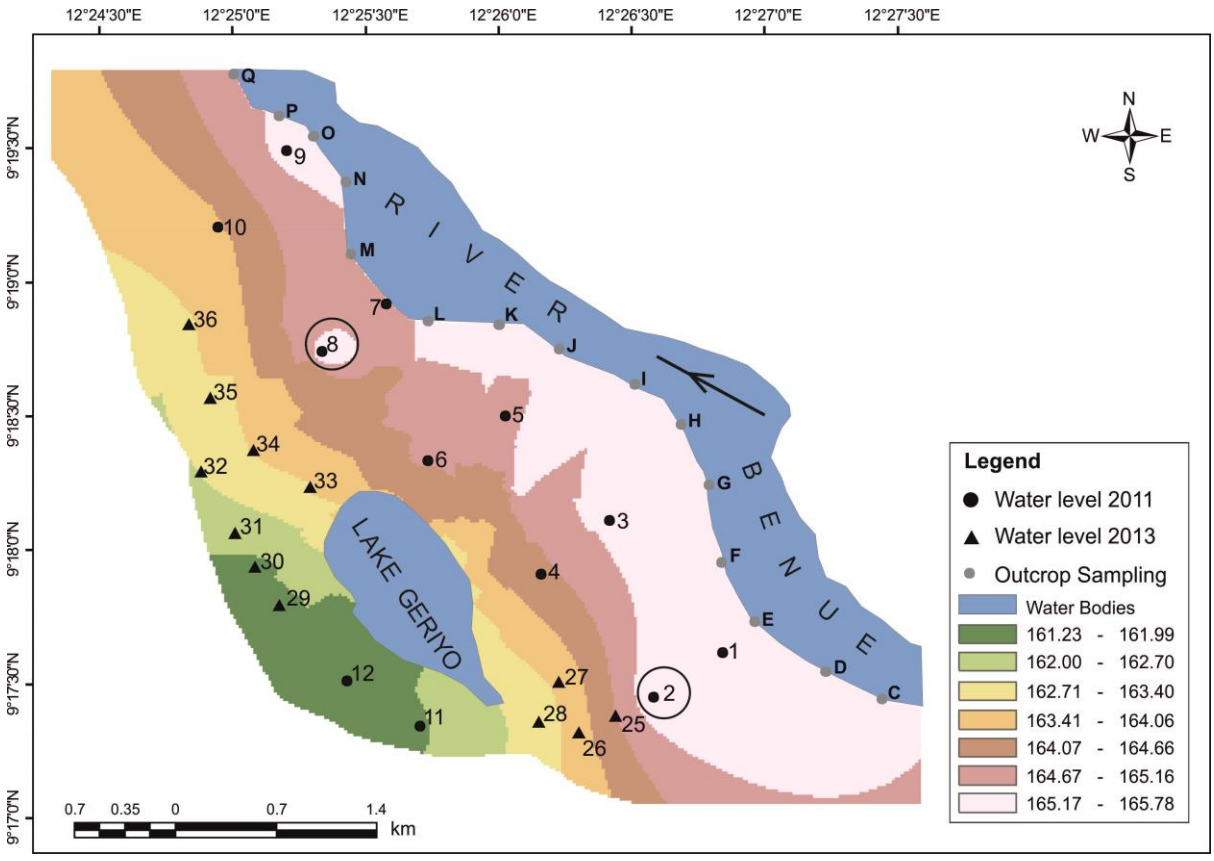

Figure 5.32: Spatial distribution of the floodplain groundwater levels. The white and pink locations shows high water levels in wells. The values 161.23 to 165.78 are elevations in metres of groundwater levels on the floodplain. The black circles show the proposed perched aquifer formations.

Figure 5.33 shows the floodplain groundwater levels obtained from resistivity soundings 2012. One most likely perched aquifer is observed at resistivity point 22.

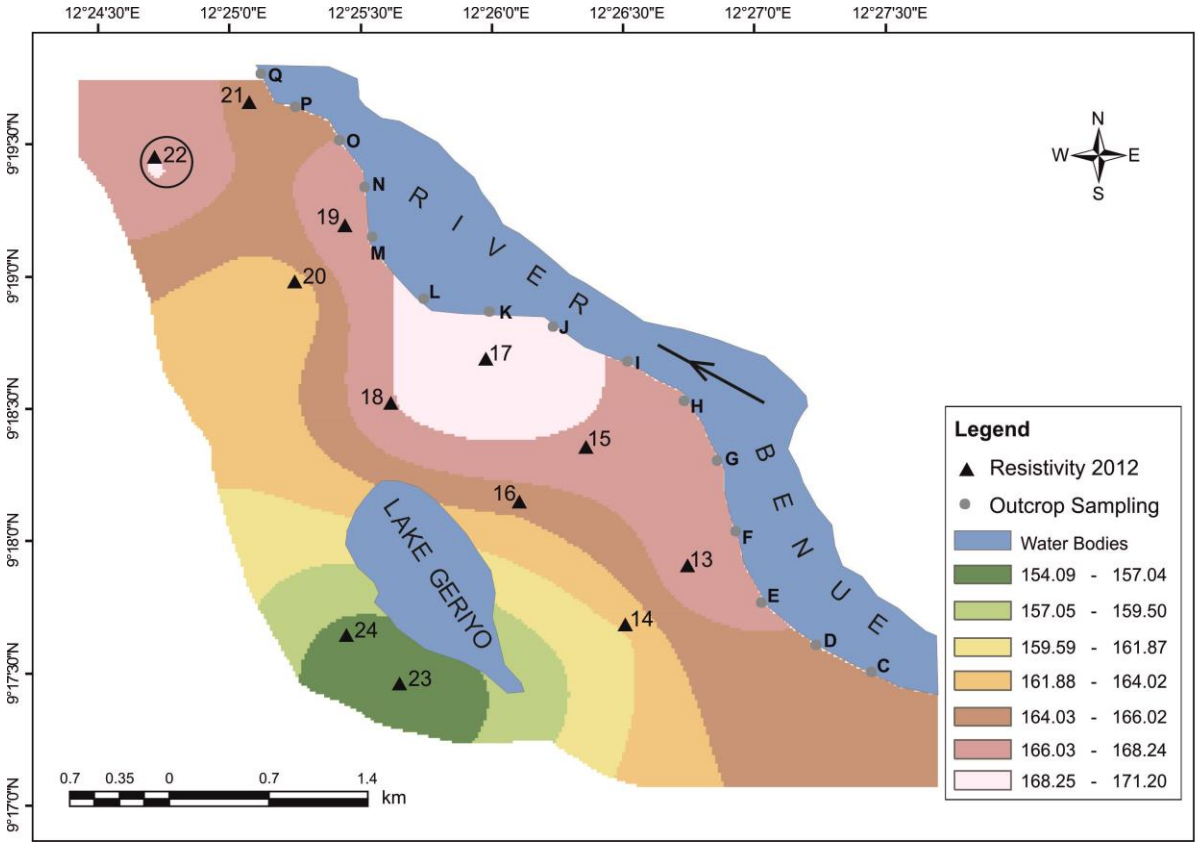

Figure 5.33: Spatial distribution of the floodplain groundwater levels for resistivity 2012. The white and pink locations shows high water levels in wells. The values 154.09 to 171.20 are elevations in metres of groundwater levels on the floodplain. The black circle shows the proposed perched aquifer formation.

Transects 1, 4 and 19 (Figures 5.30, 32 and 5.33) show an unexpected increase in groundwater levels as moving away from River Benue valley in point BH 2, BH 8 and BH 22. Specifically, the data for these three locations are summarised in Table 5.13.

Table 5.13: Data suggesting anomalously high water table

Borehole (BH) name	2	8	22
Depth of water in borehole in m	6.5	6.15	n/a
Vertical electrical sounding (VES) value in Ωm	16	937	24

Table 5.13 shows a complex image, which requires a critical analysis. In BH 2 all the information fits to suggests the presence of perched aquifer; but it is not the case in BH 8 where a high observed water table is not reflected in expected low values for the VES (Table 2.6). In BH 22, only VES data are available. Hence, although the existence of perched aquifers is likely in the Yola floodplain, our data are somehow contradictory and inconclusive.

5.4.3 Hydraulic conductivity

This section presents and interprets the hydraulic conductivity values obtained from both the laboratory and field pumping tests.

5.4.3.1 Laboratory hydraulic conductivity

The permeability values for borehole sediment samples for sand are in the range of 1.08×10^{-2} – 3.02×10^{-2} m/s with a mean value of 2.51×10^{-2} m/s; for sandy silt they are in the range 1.12×10^{-7} – 2.03×10^{-7} m/s with a mean value of 1.51×10^{-7} m/s; and for clayey silt they are in the range 1.71×10^{-8} – 9.24×10^{-8} m/s with a mean value of 4.37×10^{-8} m/s (Table 1G, Appendix G). Similarly, the permeability values for the outcrops sediment samples for sand they were in the range 8.76×10^{-4} – 8.52×10^{-2} m/s with a mean value of 2.41×10^{-2} m/s; for sandy silt they were in the range 1.06×10^{-7} – 8.49×10^{-7} m/s with a mean value of 3.85×10^{-7} m/s; and for clayey silt they were in the range 6.79×10^{-10} – 4.03×10^{-8} m/s with a mean value of 7.83×10^{-9} m/s (Table 2G, Appendix G).

As shown in Table 2.8, different sediments or soils have different hydraulic conductivities. This is reflected in the Benue River samples, where hydraulic conductivity varies from 7.83×10^{-8} to 4.01×10^{-1} m/s. The minimal value is not in the Table 2.8. The maximal value fits with silt and sand in Table 2.8.

This shows that as expected sand alluvial sediment formations have high rate of flows, while sandy silt and clayey silt alluvial sediments have low rate of flows. This suggests that the alluvial floodplain is permeable, i.e. it allows flow of water for the recharging shallow aquifers. This will enable easy abstraction of the shallow groundwater in the floodplain by the farmers with the hand drilling techniques.

5.4.3.2 Hydraulic conductivity by field pumping tests

Pumping tests were carried out in the field on twelve different wells to determine aquifer properties. The pumping wells range from 5 to 10 m in depth (Figure 5.34). Drawdown and discharge data were recorded. The estimated aquifer yield is 172.8 m^3/ day.

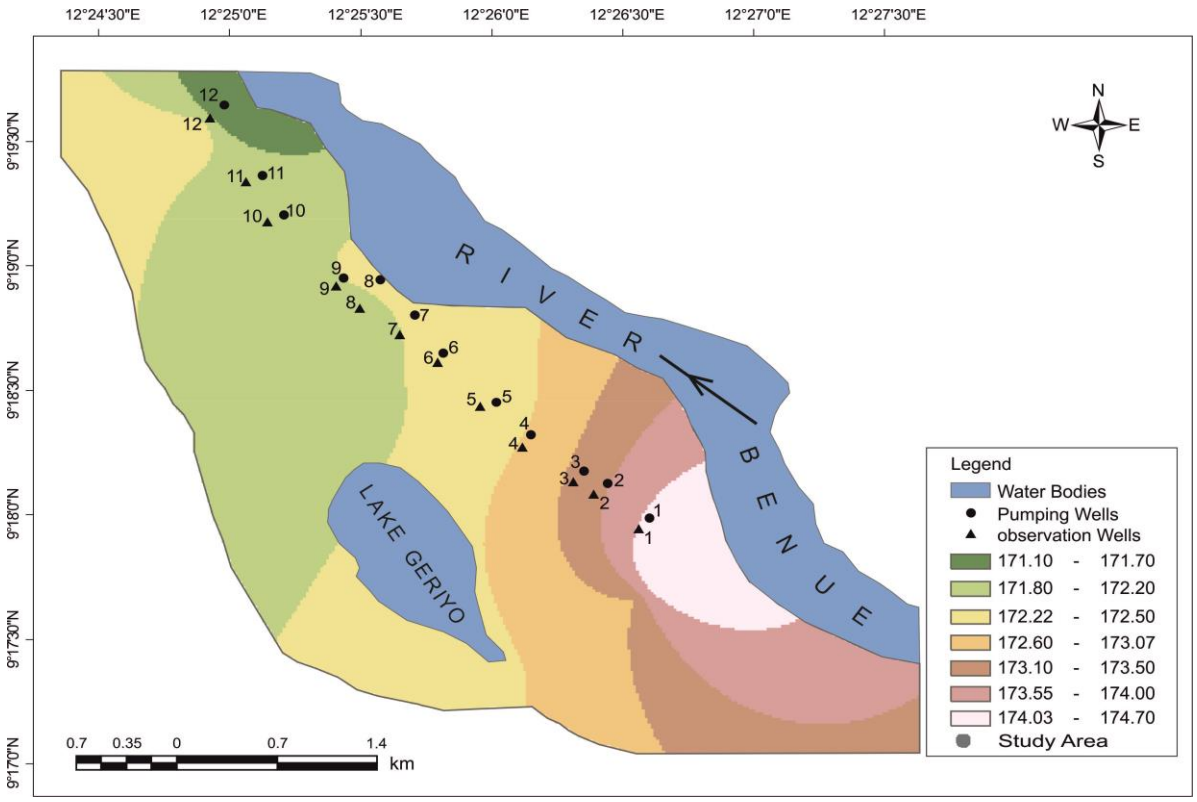

Figure 5.34: Spatial distribution for the water level in the twelve pumping wells and twelve observation wells for the pumping tests. The white colour shows higher water levels in wells and green shows lowest water levels in wells. The range values 171.10 to 174.70 are elevation height of the groundwater in metres.

The hydraulic conductivity values obtained by field pumping tests range from 2.137 x 10^{-3} to 4.011 x 10^{-1} m/s with a mean value of 1.18 x 10^{-1} m/s (Table 5.14). When using Table 2.8, the values fit with typical values for silt and sand. The higher value of 4.011 x 10^{-1} m/s is found in the location of pumping well 6 (Table 5.14). The lower value of 2.137 x 10^{-2} m/s is found in the location of pumping well 2. As reported by Todd (1995) hydraulic conductivity, values in range between 10^{-3} to 10^{-2} m/s shows good aquifer performance.

Table 5.14: Estimated hydraulic conductivity, transmissivity and specific capacity at the twelve pumping wells

Pumping station	Hydraulic conductivity (m/s)	Transmissivity (m^2/s)	Specific yield
Well 1	4.74 x 10^{-2}	1.33 x 10^{-2}	0.01
Well 2	2.14 x 10^{-2}	1.02 x 10^{-2}	0.01
Well 3	1.25 x 10^{-1}	4.65 x 10^{-2}	0.04
Well 4	1.36 x 10^{-1}	6.56 x 10^{-2}	0.07
Well 5	9.40 x 10^{-2}	4.64 x 10^{-2}	0.04
Well 6	4.01 x 10^{-1}	1.34 x 10^{-1}	0.13
Well 7	6.46 x 10^{-2}	2.49 x 10^{-2}	0.02
Well 8	4.80 x 10^{-2}	3.26 x 10^{-2}	0.03
Well 9	1.56 x 10^{-1}	7.92 x 10^{-2}	0.07
Well 10	5.71 x 10^{-2}	2.19 x 10^{-2}	0.02
Well 11	1.64 x 10^{-1}	5.99 x 10^{-2}	0.06
Well 12	1.06 x 10^{-1}	5.36 x 10^{-2}	0.04
Mean	1.18 x 10^{-1}	4.90 x 10^{-2}	0.05

The transmissivity values for the shallow alluvial aquifers of the floodplain ranges from 1.019 x 10^{-2} to 1.340 x 10^{-1} m^2/s, with a mean value of 4.90 x 10^{-2} m^2/s (Table 5.14). The higher value 1.340 x 10^{-1} m^2/s is found in the location of pumping well 6. The lower value 1.019 x 10^{-2} m^2/s is found in the location of pumping well 2. The resistivity range is consistent to what was reported by Kumar and Alamgir (2013) 4.63 x 10^{-6} m/s on the Murray

Darling alluvial floodplain in a semi-arid area of Australia because the floodplain is similar to the study site.

The specific yield values for the shallow alluvial aquifer of the floodplain ranges from 0.01 to 0.13, with mean value of 0.05 (Table 5.14). The higher value 0.13 is found in the location of pumping well 6. The lower value 0.01 is found in the location of pumping well 2, these data will used for modelling.

As noted before, alluvial sand produced the highest values of hydraulic conductivity with mean value of 3.46×10^{-1} m/s. Hydraulic conductivity obtained from pumping tests shows higher values in the range 2.14×10^{-2} to 4.011×10^{-1} m/s. The highest hydraulic conductivity value was recorded at the pumping well 6 of 4.01×10^{-1} m/s reflecting the coarser sediment particles in that location.

The results of laboratory test produced low hydraulic conductivity values whereas the field hydraulic conductivity values obtained by pumping test in the field range produced high hydraulic conductivity values. This indicates that hydraulic conductivity values obtained from laboratory tests typically are several orders of magnitude smaller than values measured by pumping tests.

5.4.4 Groundwater monitoring

Hydrological data were obtained through the monitoring of groundwater level at twelve boreholes across the floodplain for a two-month period by two automatic piezometers and additional two manual piezometers for the period of one year.

The spatial distribution of the static water levels for the twelve monitoring wells is shown in Figure 5.35. Table G1 (Appendix G) shows weekly water levels for the two manually monitored wells for piezometers 1 and 2. Table G2 (Appendix G) shows manual daily water levels measurement for the twelve wells along the floodplain.

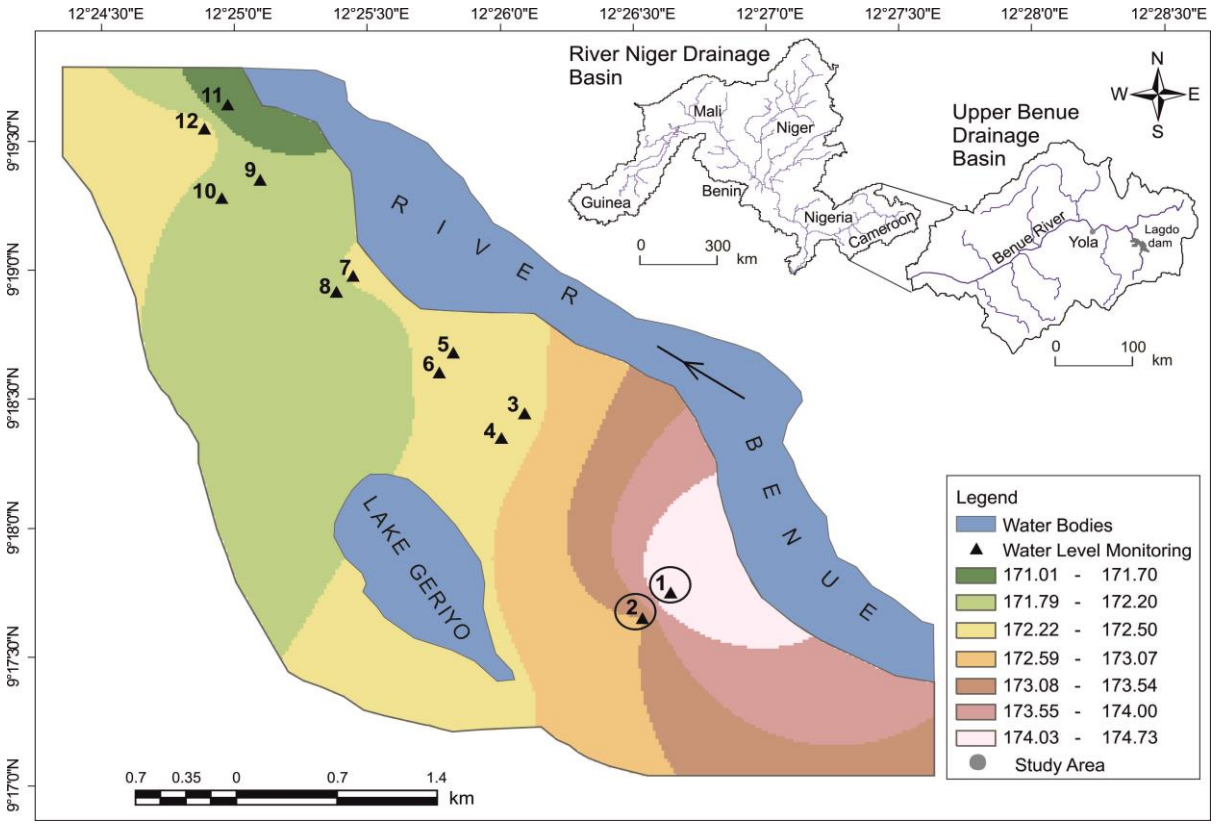

Figure 5.35: Spatial distribution for the water level of the twelve monitoring wells and their locations in the floodplain. The green colour shows the lowest water levels and white shows the highest water levels in wells across the floodplain. The black circles indicate the two automatic monitoring wells. The range values 171.01 to 174.73 are water level height in metres.

Figure 5.36 shows plots of groundwater levels at twelve different water levels on the floodplain. It can be seen that Borehole 1 (further upstream) shows the highest water level whilst Borehole 11, further observation, recorded the lowest water level. Boreholes 1 and 11 (downstream) are both close to the river, but they show high variation of water levels. Similar observation is shown between Boreholes 2 and 8 where possible perched aquifers were observed, with much variation of water levels between these two wells. Consistent water levels were observed in Boreholes 3, 4, 5, 6, 7, 9, 10 and 12.

These differences observed at four Boreholes location could be due to the differences in elevations along the floodplain. Because the boreholes are located at different points in the floodplain and they have different elevations. Table 5.15 shows the statistical analysis for the twelve boreholes on the floodplain. Strong correlation is observed between boreholes 2, 5, 6, 7, 8, 11 and 12, with their correlation values ranging between 0.5 to 0.88 (p-value of 0). This suggests that less variation of the water levels in the wells.

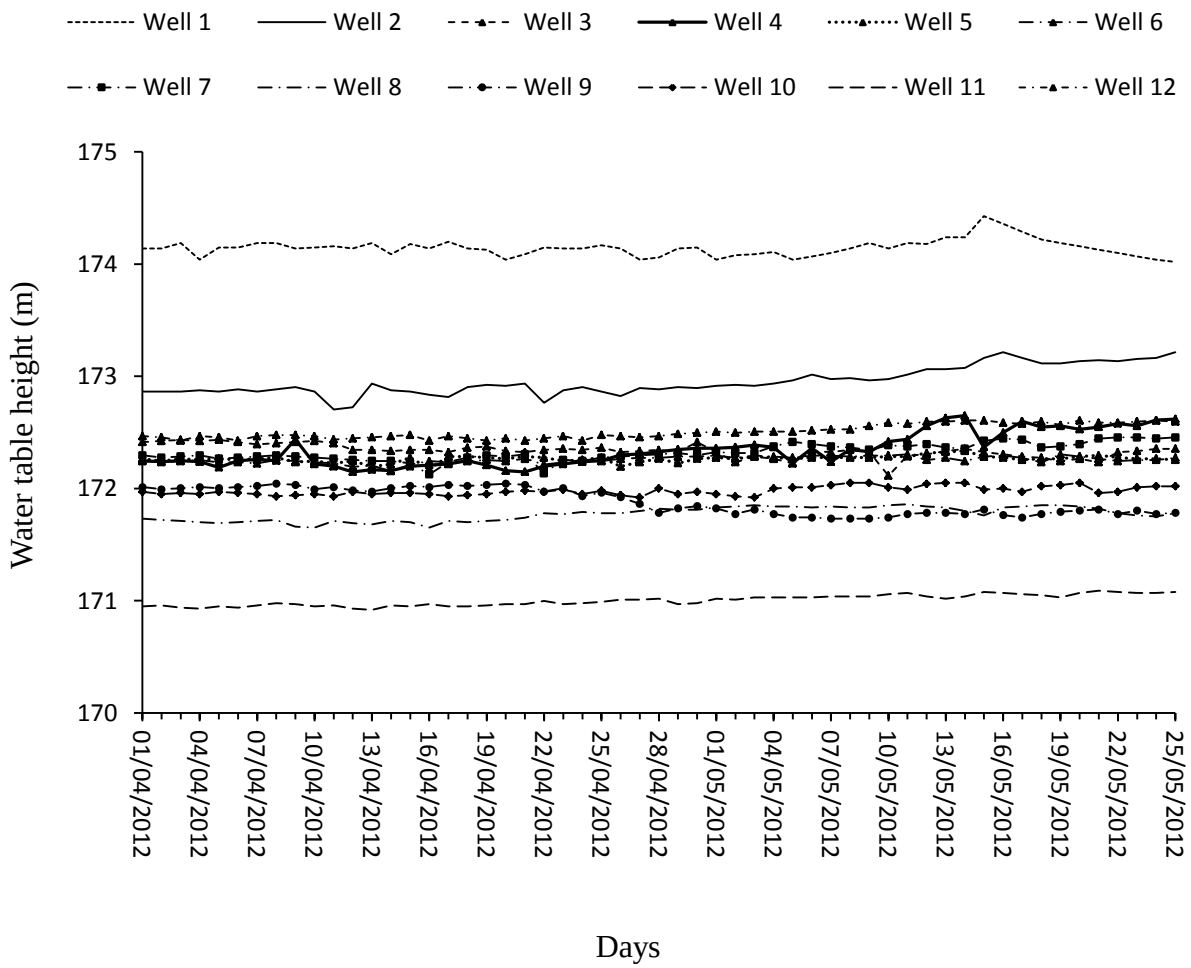

Figure 5.36: Daily water levels at twelve boreholes on the floodplain for the period April to May 2012.

Table 5.15: Statistical correlation values and significance range between twelve monitored wells (Significant p-value range 0 to 0.05, not significant p-value range 0.06 to 1)

Parameter		Well 1	Well 2	Well 3	Well 4	Well 5	Well 6	Well 7	Well 8	Well 9	Well 10	Well 11	Well 12
Well 1	Correlation	1											
	P-value	0											
Well 2	Correlation	0.232	1										
	P-value	0.088	0										
Well 3	Correlation	0.007	-0.452**	1									
	P-value	0.96	0.001	0									
Well 4	Correlation	0.174	0.848**	-0.386**	1								
	P-value	0.203	0	0.004	0								
Well 5	Correlation	0.205	0.384**	-0.231	0.442**	1							
	P-value	0.133	0.004	0.089	0.001	0							
Well 6	Correlation	0.019	0.487**	-0.438**	0.460**	0.356**	1						
	P-value	0.891	0	0.001	0	0.008	0						
Well 7	Correlation	0.095	0.874**	-0.448**	0.768**	0.457**	0.573**	1					
	P-value	0.489	0	0.001	0	0	0	0					
Well 8	Correlation	0.027	0.534**	-0.692**	0.577**	0.461**	0.722**	0.602**	1				
	P-value	0.842	0	0	0	0	0	0	0				
Well 9	Correlation	-0.046	-0.709**	0.632**	-0.723**	-0.379**	-0.693**	-0.773**	-0.870**	1			
	P-value	0.736	0	0	0	0.004	0	0	0	0			
Well 10	Correlation	0.142	0.577**	-0.329*	0.545**	0.490**	0.360**	0.565**	0.536**	-0.650**	1		
	P-value	0.302	0	0.014	0	0	0.007	0	0	0	0		
Well 11	Correlation	0.128	0.842**	-0.618**	0.793**	0.423**	0.619**	0.820**	0.756**	-0.860**	0.588**	1	
	P-value	0.351	0	0	0	0.001	0	0	0	0	0	0	
Well 12	Correlation	0.280*	0.882**	-0.518**	0.889**	0.508**	0.471**	0.840**	0.631**	-0.799**	0.692**	0.876**	1
	P-value	0.038	0	0	0	0	0	0	0	0	0	0	0

Figure 5.37 shows weekly water levels at wells 1 and 2 situated from 500 and 1,000 m from the River Benue. It can be observed that the water level quickly rises as the rainy season approaches and lowers more slowly in the dry season. Water levels were monitored during periods of extensive irrigation, which was not possible to prevent during the study, and this will have slightly affected the measurements such as brief low in 16/06/2012. Two month manual water level measurements at wells 1 and 2 were made. No variations between the automatic and manual water level (Figure 5.37) are observed.

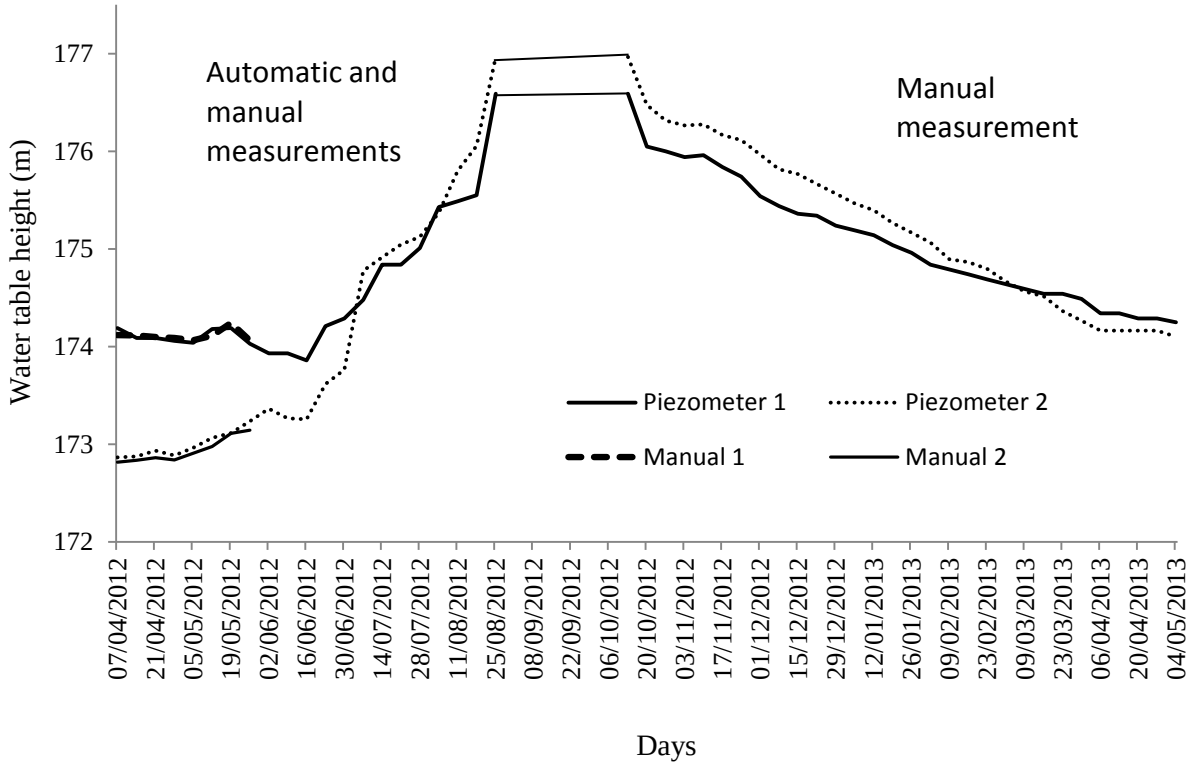

Figure 5.37: Weekly water levels at wells 1 and 2 situated 500 and 1,000 m respectively from River Benue for the period April 2012 to April 2013. The horizontal lines shows the missing data and the time the piezometers stopped working as result of severe flood that occurred that year

The period between 7th April 2012 to 25th August 2012 in Figure 5.37 shows the time until which the automatic piezometers worked. The horizontal line between 25th August 2012 and 13th October 2012 shows the missing data and the time when the piezometers stopped

working because of the severe flood that occurred that year, which submerged the floodplain. However, weekly monitoring of the groundwater levels continued manually afterwards. Figure 5.38 shows a switch in the hydraulic gradient when the rains start: piezometer 1 is higher than piezometer 2, and then a switch occurs on 7/7/2012. This suggests that in the dry season after 7/7/2012, the river is recharging the aquifer, but in the rainy season, the gradient is towards the river. This is because the groundwater levels are lower in the peak dry period, as rainfall approaches the groundwater levels tend to rise. The relationship between the water levels in the two piezometers (Figure 5.38) suggests a linear relationship when P1>174.25 m, shows time of flow to river.

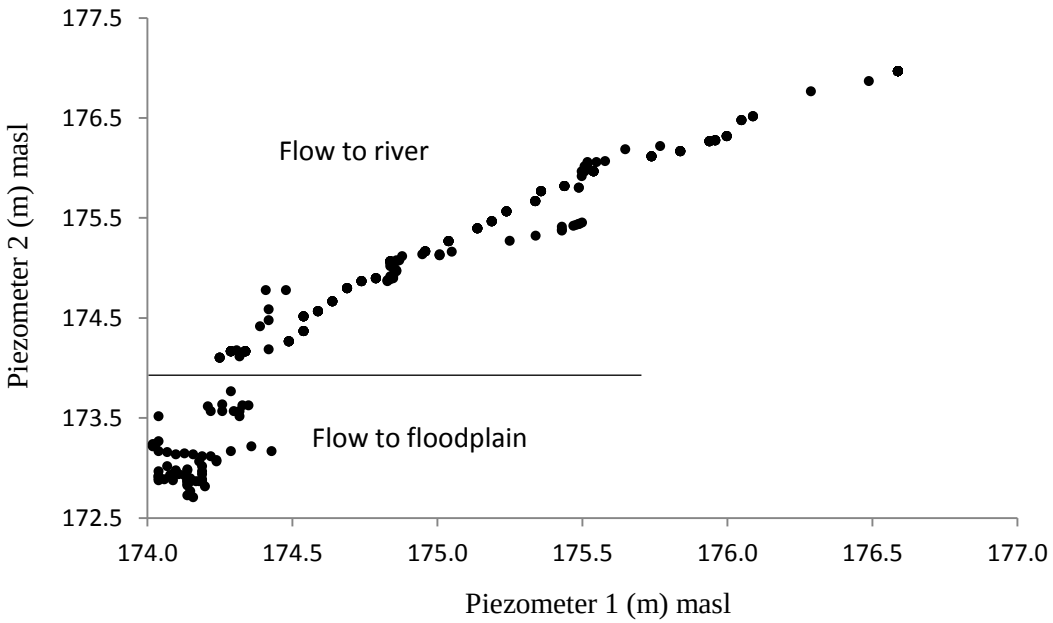

Figure 5.38: Relationship between Piezometers 1 and 2 groundwater levels.

Table 5.16: Statistical correlation values and significance range between piezometers 1 and 2 (Significant p-value range 0 to 0.05, not significant p-value range 0.06 to 1)

Parameter		Piezometer 1	Piezometer 2
Piezometer 1	Correlation	1	
	P-values	0	
Piezometer 2	Correlation	**0.966****	1
	P-values	**0**	0

Highly significant correlation is observed between Piezometer 1 with Piezometer 2 water levels having correlation value of 0.966 (p-value of 0) (Table 5.16), indicating no much variation between groundwater levels at piezometer 1 and piezometer 2.

5.4.5 Groundwater of the floodplain

The results of the water level measurements help to quantify the variable response of hydraulic head and also help to indicate the direction of water movement. This will be used in the model. Weekly usable precipitation is obtained by subtracting the evaporation from total precipitation occurring over 7-day periods from January to June 2012 (Figure 5.39A). The groundwaters of the floodplain are low between stress periods (weekly measurement) 1 and 18, and begin to rise between stress periods 19 and 26 (Figure 5.39A). Figure 5.39B shows detailed time-series plots of water-table positions for the two Piezometers, numbers 1 and 2.

The groundwater levels of the floodplain are responsive to rainfall events, which accounts for the high peaks in the water-table level. The Piezometers show an immediate variation of the water table in response to the rainfall events. For example on 19th May 2012 (stress period 19) (Figure 5.39B), groundwater level rises as the rainy season started. The water table is at the lowest position between April to June (Figure 5.3B) and begins to rise as rainfall increases up to the peak in August and September (Figure 4.4). August and September months are when the water table of the floodplain reaches its highest peak (see Figure 5.37) due to high rainfall storm during this period. In November, the water table starts to decline as the rainfall ceases.

The water levels also fluctuate due to groundwater withdrawal rates. For example it is likely that it is what happened on 10th March 2012 in piezometer 1 (Figure 5. 39B). The floodplain was flooded on 10th March 2012 due to high storm rainfall and sudden release of water from Lagdo Dam in Cameroon upstream.

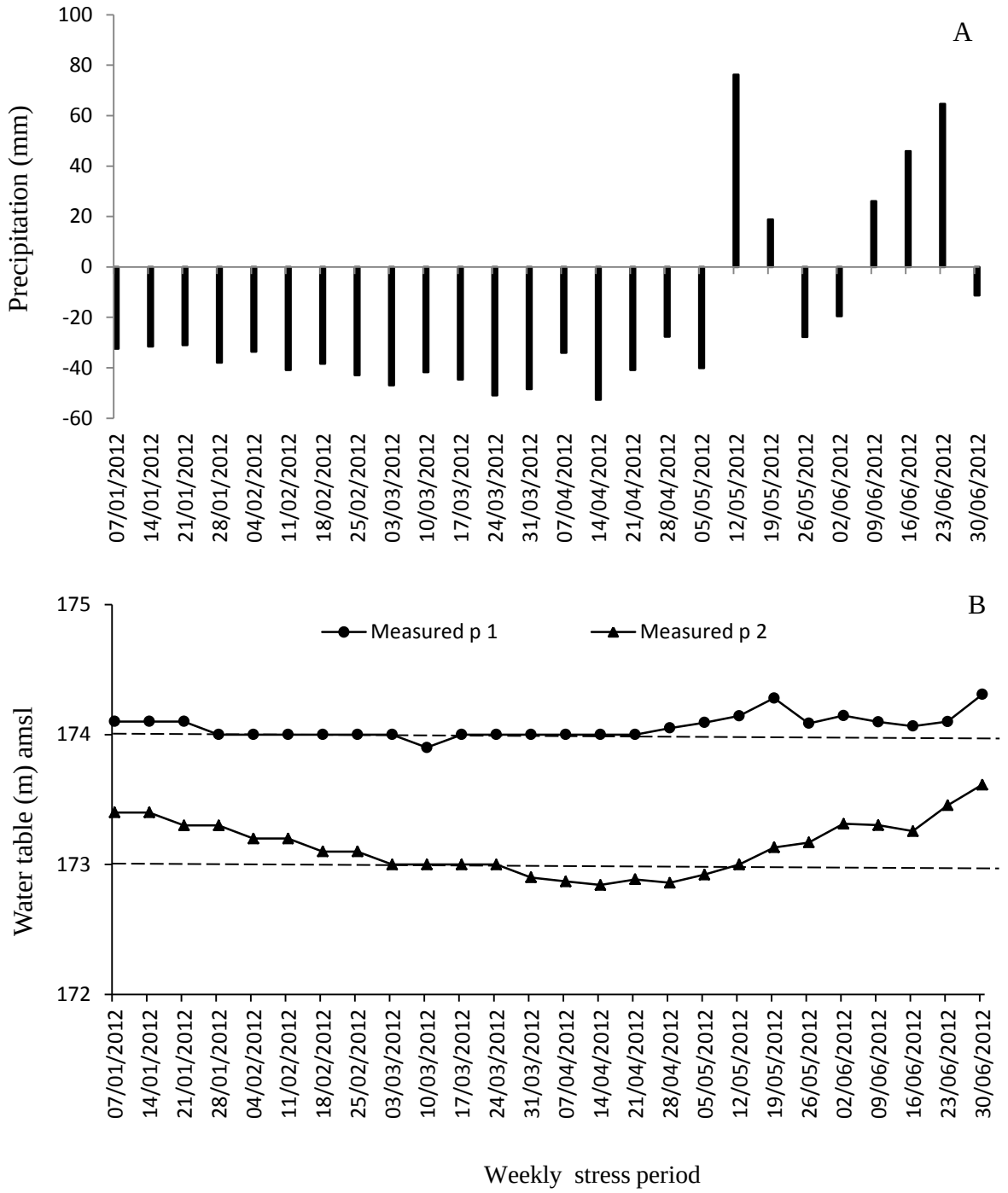

Figure 5.39: Comparison between precipitation and groundwater level for the period January to June 2012. A – shows weekly precipitation (precipitation – potential evaporation) for the period January to June 2012; B – shows weekly time series of water table variation for piezometers 1 and 2 for the period January to June 2012 situated 500 and 1,000 m away from River Benue.

5.4.6 Summary for groundwater data

It was observed from the analysis of the hydrology of the floodplain that:

1. The resistivity result indicates the potentiality of the shallow alluvial aquifers across the floodplain.

2. The existence of perched aquifers is likely on the floodplain. But present data are somewhat contradictory and inconclusive.

3. The hydraulic conductivity has now been quantified. The results show that the floodplain alluvial sediments are permeable and this allows water to easily flow to recharge the floodplain shallow groundwater.

4. The results from the two monitored piezometers shows that, in the dry season, the river is recharging the aquifer, but in the rainy season, the gradient is towards the river.

5.5 Groundwater modelling

This section presents the results of the groundwater modelling of the alluvial floodplain shallow aquifers and considers the sustainability of different scenarios of groundwater abstraction.

5.5.1 Comparison between measured and simulated water levels

The model groundwater levels were compared to observed groundwater levels. The root mean square (RMS) error between actual hydraulic head measurements and model generated hydraulic head was used to estimate model accuracy. The root mean square error and the mean absolute error (MAE) were estimated from the following equations:

$$\mathrm{MAE} = \frac{1}{n}\sum_{i=1}^{n}(h_m - h_s)_i \qquad 5.1$$

$$RMS = \sqrt{\frac{\sum_{i=1}^{n}(h_m - h_s)^2}{n}} \quad 5.2$$

where h_m and h_s are the observed and simulated values of aquifer hydraulic conductivity, n is the total number of the monitoring wells (n = 2) (Panagopoulos, 2012). The relatively low MAE and RMS (0.41 and 0.58 m) (Table 5.17) suggests that the model calibration under transient conditions has reasonable results. The correlation coefficient is 0.87; this value tends to 1 for optimal calibration (Middlemis, 2000). Typically, an error less than 5% is indicative of an acceptable calibration, as recommended by the Murray-Darling Basin Commission Groundwater Flow Modelling Guideline (Middlemis, 2000). The error represents a small part of natural groundwater level variations. Figure 5.40 shows the measured and simulated groundwater levels above mean sea level (amsl). It can be seen in Table 5.17 both MAE and RMSE increase during the measuring season. The values are low in the dry season, but the error increases as the rainy season approaches. This could reflect the difficulty in quantifying the proportion of rainfall that recharges the alluvial aquifer and the errors are proportional to the precipitation values.

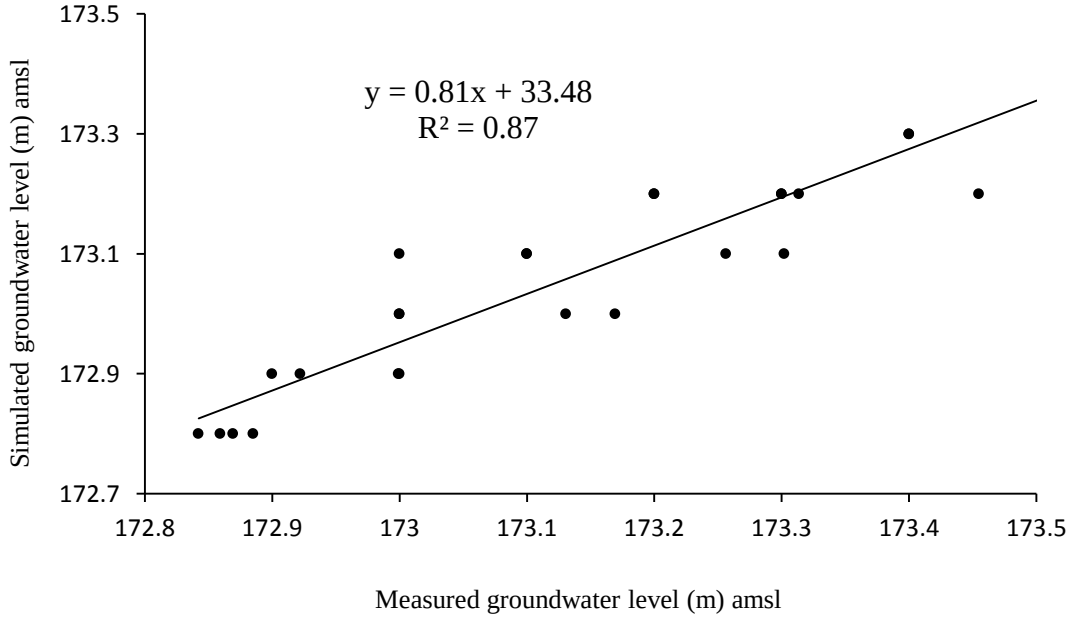

Figure 5.40: Scatter diagram of measured versus simulated groundwater levels using calibrated model parameters.

Table 5.17: Transient state calibration results for each stress period. MAE - Mean Absolute Error, RMS - Root Mean Square

Stress period	MAE (m)	RMS (m)	Stress period	MAE (m)	RMS (m)
07/01/2012	0.05	0.07	07/04/2012	0.13	0.19
14/01/2012	0.05	0.07	14/04/2012	0.12	0.17
21/01/2012	0.00	0.00	21/04/2012	0.19	0.27
28/01/2012	0.05	0.07	28/04/2012	0.20	0.29
04/02/2012	0.05	0.07	05/05/2012	0.26	0.36
11/02/2012	0.05	0.07	12/05/2012	0.22	0.31
18/02/2012	0.05	0.07	19/05/2012	0.36	0.50
25/02/2012	0.00	0.00	26/05/2012	0.28	0.39
03/03/2012	0.05	0.07	02/06/2012	0.38	0.54
10/03/2012	0.00	0.00	09/06/2012	0.30	0.42
17/03/2012	0.05	0.07	16/06/2012	0.21	0.30
24/03/2012	0.10	0.14	23/06/2012	0.23	0.32
31/03/2012	0.05	0.07	30/06/2012	0.41	0.58

5.5.2 Model output

Simulated versus measured groundwater levels are plotted in Figure 5.41 for points corresponding to the two observation piezometers located 500 and 1,000 m away from the River Benue during the period January to June 2012. Well locations are shown in Figure 5.35. Figure 5.41 shows a good match (i.e. values are within 0.1 m through the period modelled) between simulated and measured groundwater levels at these two points. On this basis, it was concluded that the numerical model provides a reasonable representation of the variation in hydraulic heads across the modelled area of floodplain.

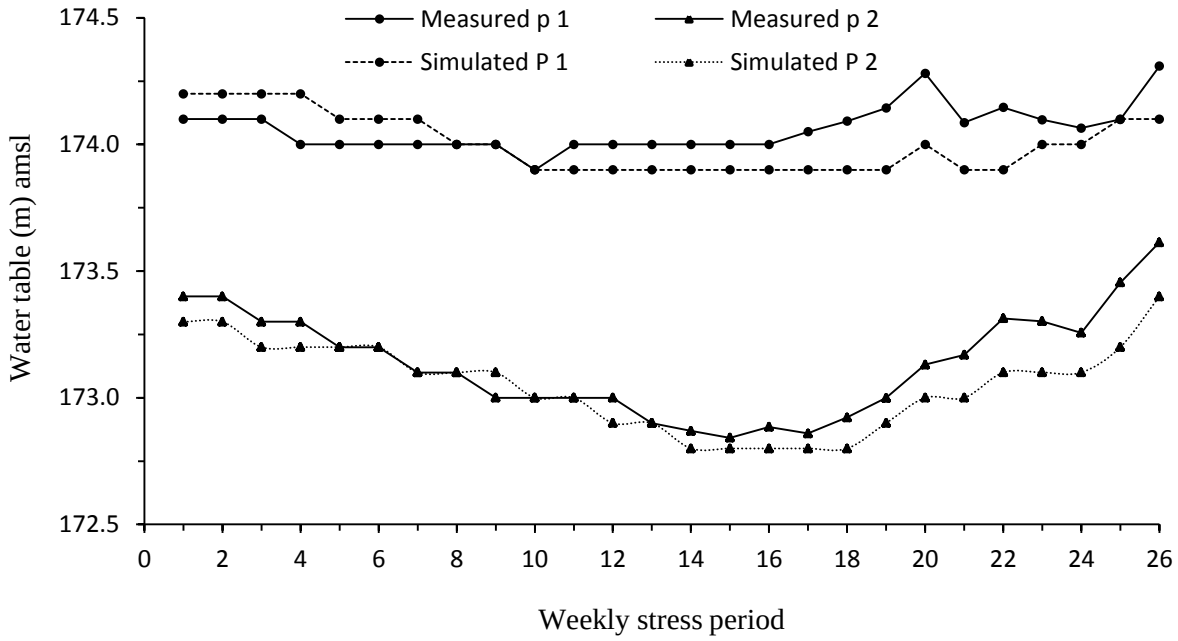

Figure 5.41: Observed and simulated weekly water table evolutions in two piezometers on the alluvial aquifer located 500 and 1,000 m away from River Benue during the period January to June 2012. amsl – above mean sea level.

5.5.3 Groundwater head

The water table gradient along the modelled cross-section is plotted in Figure 5.42 for February, April and June 2012. Groundwater heads decrease with distance away from River Benue. It is also clear that in February, groundwater levels were high, with lower groundwater levels in April, the peak period of the dry season. In June, groundwater levels began to rise as the rainy season approached and groundwater abstraction for irrigation slowly decreased.

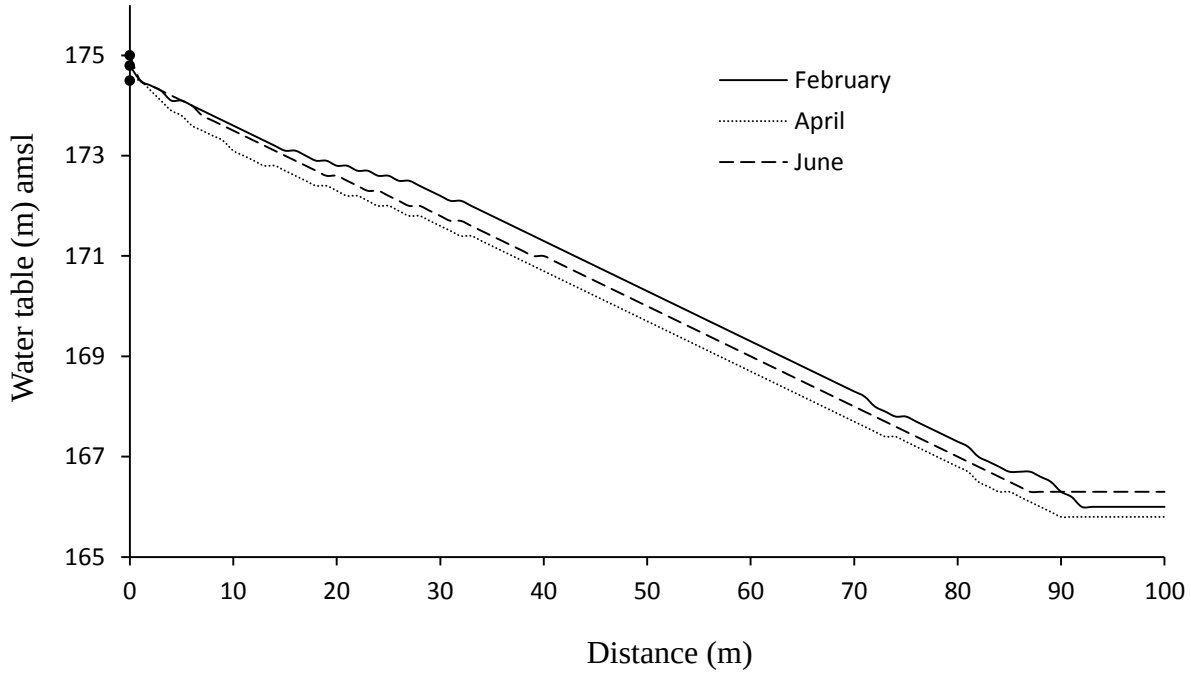

Figure 5.42: A cross-section of groundwater levels along the floodplain transects 1 flow from river to the floodplain for February, April and June year; black dots on the y-axis show observed river stage for each month.

5.5.4 Model water budget

Water budgets, giving the difference between modelled water inflows and outflows, are summarised in Figure 5.43 for the region. These estimates of the groundwater budget of the Lake Geriyo Irrigation Project are essential for water management planning for this area.

Evapotranspiration (ET) is envisaged in the model, as a function of the water table, representing drawdown that is induced directly by evapotranspiration from the model. For waters abstracted from wells for irrigation, the common assumption is that all this water is directly consumed by the arable crops/pasture, thus increasing evapotranspiration to levels close to the maximum (potential evapotranspiration). High rates of potential evapotranspiration result in no excess moisture, and hence none of the abstracted water is assumed to subsequently infiltrate and recharge the groundwater body (i.e. all the waters

abstracted are either evaporated, or replenish the soil moisture deficit). This assumption is commonly used in the United Kingdom (ENTEC, 2009).

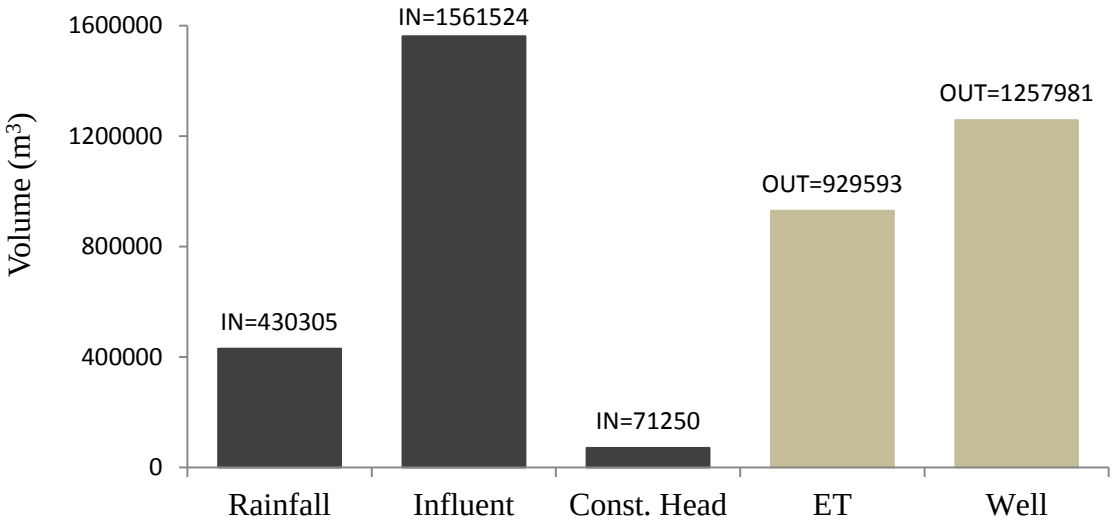

Figure 5.43: The volumetric water balance for the modelled area at the end of stress period 26: black histogram show flows into the system and olive-brown histogram flows from the system. **"**Rainfall" is the recharge from precipitation, "Influent" is seepage from the river to the floodplain, "Const. Head" is recharge from boundary constant head, "ET" is outflows from model evapotranspiration, Well is outflows from pumping wells.

The floodplain water budget includes the following fluxes: i. recharge through precipitation; ii. loss of water through evapotranspiration from the model, iii. groundwater abstraction by pumping wells and iv. influent (seepage from the river to the alluvial aquifer). Errors in the model water balance are shown in the lower panel of Figure 5.44, which illustrates the relationship between the timing of positive and negative water balance errors and recharge. While precipitation and model evapotranspiration were estimated using data from the local weather station (as described above), seepage to and from the river are estimated from the MODFLOW water budget calculations. These are defined for each stress period by the equation:

$$P + Inf_{RIV} + S_{OUT} + CH = ET + Wel_{IRR} + S_{IN} \quad 5.3$$

where inflows comprise precipitation (P), influent seepage from the river (Inf_{RIV}), water movements from storage (S_{OUT}) and flow of water from the Constant Head boundary (CH) and outflows are model evapotranspiration (ET), well abstraction (Wel_{IRR}) and water movement to storage (S_{IN}).

The relationship between the storage terms (In and Out) to recharge and river seepage (influent flow) are summarised in Table 5.18 and Figure 5.44. Together, these give an annotated summary of the water balance of the studied aquifer obtained from the transient state calibration over the 26 stress periods. The final transient state model produced a mass balance error of -0.03%. This is considered satisfactory as Anderson (1993) suggest that a model discrepancy of < 1% is acceptable.

As expected, the mass balance data shows that river seepage (influent flow) is the primary water inflow (1,561,524 m^3) representing ~75.6% of the total input to the alluvial aquifer while rainfall (430,305 m^3) represents ~20.9% of the total water inflow over the period. The constant head boundary provides a significant input (71,250 m^3) equivalent to ~ 3.5% of the total inflow. Model outputs are dominated by groundwater abstraction by pumping wells which total 1,257,981 m^3, representing 57.5% of the total outflow while model evapotranspiration (929,593 m^3) represents 42.5% of the total outflow.

When losses from the modelled area (via groundwater abstraction from pumping wells and model evapotranspiration) are subtracted from the recharge from: i. river seepage (influent flow); ii. recharge from rainfall and iii. recharge from the constant head boundaries, the volume of water leaving the aquifer is ~124,495 m^3. Over the period modelled, the amount of water withdrawal exceeds groundwater recharge.

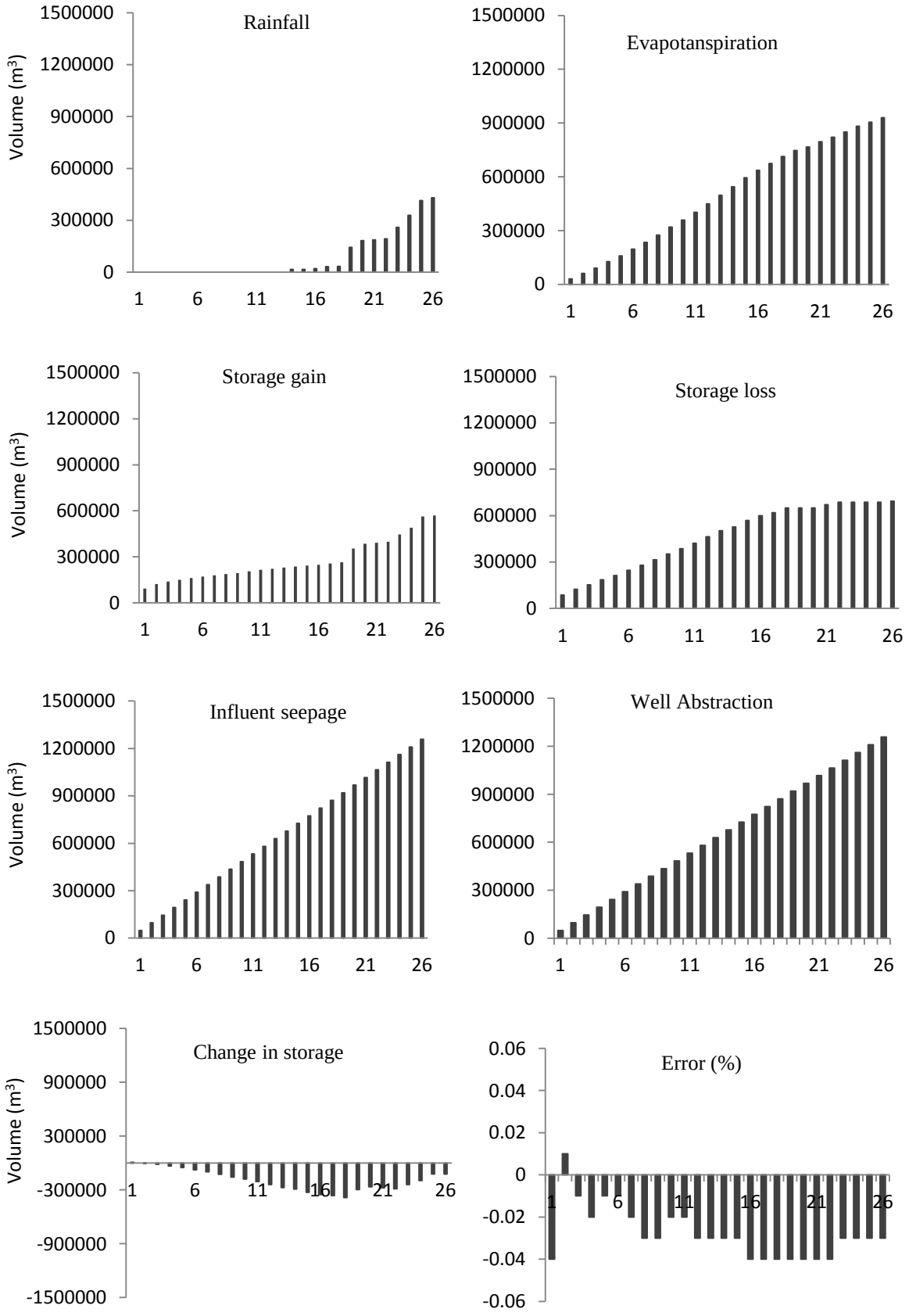

Figure 5.44: Detailed model of the floodplain cumulative water balance result for the floodplain shallow alluvial aquifers along 26 stress periods.

Table 5.18: The floodplain cumulative water balance results from the modelling

Stress period	Rainfall (m^3)	Influent (m^3)	Constant Head (m^3)	Evapotranspiration (m^3)	Well abstraction (m^3)	Balance (m^3)	Storage gain (m^3)	Storage loss (m^3)	Change in storage (m^3)	Error (%)
1	0	85617	991	30918	48383	7307	93446	86080	7366	-0.04
2	0	153506	2639	60970	96768	-1593	121919	123535	-1616	0.01
3	0	217401	4437	90487	145152	-13801	138742	152522	-13780	-0.01
4	0	279188	6410	126661	193536	-34599	150590	185089	-34499	-0.02
5	0	341053	8541	158633	241920	-50959	162239	213125	-50886	-0.01
6	0	401373	10870	197527	290304	-75588	171708	247209	-75501	-0.01
7	0	460803	13387	234150	338688	-98648	180284	278764	-98480	-0.02
8	0	519593	16099	274960	387072	-126340	187857	313957	-126100	-0.03
9	0	577909	19031	319621	435456	-158137	194589	352468	-157879	-0.03
10	0	640838	22121	359349	483840	-180230	206154	386137	-179983	-0.02
11	0	701364	25363	401797	532224	-207294	215024	422061	-207037	-0.02
12	0	761020	28803	450221	580608	-241006	222471	463152	-240681	-0.03
13	0	820127	32411	496306	628992	-272760	229453	501849	-272396	-0.03
14	16701	878726	36039	544244	677376	-290154	237104	526815	-289711	-0.03
15	16701	937010	39818	594299	725759	-326529	242681	568681	-326000	-0.03
16	19958	995008	43700	636102	774143	-351579	248905	599818	-350913	-0.04
17	32710	1052648	47533	674776	822526	-364411	255951	619693	-363742	-0.04
18	33818	1113336	51418	713909	870911	-386248	264710	650273	-385563	-0.04
19	143798	1171835	54472	747007	919294	-296196	354904	650273	-295369	-0.04
20	183298	1229347	57047	767087	967678	-265073	386037	650295	-264258	-0.04
21	186763	1286649	59870	795547	1016062	-278327	392521	670037	-277516	-0.04
22	192405	1341321	62899	820812	1064446	-288633	398589	686366	-287777	-0.04
23	258835	1396438	65550	849805	1112829	-241811	445373	686366	-240993	-0.03
24	328205	1451305	67762	882800	1161213	-196741	490459	686366	-195907	-0.03
25	414434	1506570	69449	904097	1209597	-123241	563844	686366	-122522	-0.03
26	430305	1561524	71250	929593	1257981	-124495	569745	693511	-123766	-0.03
Mean	86844	841597	35304	502372	653183	-191811	274050	465416	-191366	-0.03

The gain in storage, which is equivalent to recharge, is lower in January, February, March and April; and then higher in May and June. These correspond to the lower storage gain in January, February, March and April. Similarly, it corresponds with the higher storage gain in May and June. Model evapotranspiration increases with stress period, which shows decrease in the floodplain groundwater with stress period. River seepage (influent flow) to the floodplain system increases over the stress period, which corresponds with the period when water is abstracted by the alluvial aquifer. Changes in storage are negative for all the stress period except in stress period 1 when there was a positive change in storage. This reflects water loss from storage from the alluvial aquifer (as the water table falls), with the exception of stress period 1 when there was an increase in storage. As mentioned earlier the reason for choosing these time period January to June, is that this is the time irrigation is practiced along the River Benue floodplain. Farmers use a hand-augering method to extract groundwater from the shallow alluvial aquifers to irrigate their farms. Understanding the groundwater conditions along the floodplain for this time period will be useful for the water management for the irrigation activities.

5.5.5 Uncertainty and sensitivity analyses

The significance of the parameters hydraulic conductivity, specific yield and riverbed conductance were investigated by a sensitivity analyses. The hydraulic conductivity values in the range of 150 to 300 m/day were used, specific yield values in the range 0.1 to 0.3 were used and riverbed conductance values in the range 1,500 to 2,000 m^2/day were used. Sensitivity analysis was performed by changing these three key parameter values each at a time. It appeared that: Model heads are sensitive to low values of hydraulic conductivity (<150 m^2/day). The model river seepage to the floodplain was most sensitive to specific yield values (<0.1); for values above this, changes occurs between modelled and observed heads.

Riverbed conductance increased significantly at low values (<500 m^2/day), but field data do not indicate a low conductance term.

The sensitivity analyses indicate that aquifer specific yield and hydraulic conductivity are the most sensitive parameters, and that the river bed conductance is of secondary importance in controlling the river seepage to the floodplain groundwater. In particular, the model is more sensitive for the lower ranges of specific yield (<0.1). Acceptable estimates of the river seepage to the floodplain were obtained with S_y = 0.3, hydraulic conductivity values in the range of 250 to 300 m^2/day and the river bed conductivity in the range of 1,500 to 2,000 m^2/day.

Overall, model outputs are more sensitive to specific yield than to the hydraulic conductivity and less to riverbed conductivity. Since model outputs are sensitive to all these key parameters and the model was considered to be well calibrated, the uncertainty would be small when the calibrated model is used for predictions. However, the major driving force of the groundwater flow dynamics in the floodplain, which is the river seepage (influent flow), was not calibrated against any direct measurements. Model calibrations found strong correlation between the river seepage (influent flow) and specific yield. Therefore, model predictions would still be subject to uncertainty associated with the river seepage (influent flow). Future investigations should focus on obtaining data that are reliable to estimate the river seepage (influent flow) with more confidence.

5.5.6 Predictive scenarios

The input parameter values for model scenarios are shown in Tables 5.19, 5.20 and 5.21, including groundwater abstraction by pumping wells discussed below. Table 5.19 shows the lowest, mean and highest rainfall data for the period January to June (1960 – 2012); Table 5.20 shows the lowest, mean and highest evaporation data for the period January to June

(1960 – 2012); and Table 5.21 shows the lowest, mean and the highest River Benue gauge height for the period January to June (1960 – 2012). These parameters are used in the model to predict future scenarios.

Table 5.19: Rainfall in mm/day for the period 1960 – 2012

Month	Highest values	Mean values	Lowest values	Stress period
JAN	0.1258	0.0024	0.0000	1 – 4
FEB	0.0000	0.0000	0.0000	5 – 8
MAR	0.9000	0.1102	0.0161	9 – 13
APR	5.0533	1.4770	0.4133	14 – 17
MAY	7.0000	3.5278	0.9871	18 – 21
JUN	9.6700	4.4881	1.2100	22 – 26

Table 5.20: Evaporation in mm/day for the period 1960 – 2012

Month	Highest values	Mean values	Lowest values	Stress period
JAN	8.0797	6.8068	4.7613	1 – 4
FEB	12.6657	8.5542	5.9071	5 – 8
MAR	10.9487	9.3316	6.7419	9 – 13
APR	11.1867	8.7950	6.7333	14 – 17
MAY	9.6387	6.7904	4.2903	18 – 21
JUN	7.7927	5.1127	3.5813	22 – 26

Table 5.21: River gauge height in m for the period 1960 – 2012

Month	Highest values	Mean values	Lowest values	Stress period
JAN	2.74	1.79	1.31	1 – 4
FEB	2.77	1.65	0.52	5 – 8
MAR	2.47	1.65	0.52	9 – 13
APR	2.05	1.50	0.81	14 – 17
MAY	5.23	1.86	0.44	18 – 21
JUN	6.75	2.246	1.04	22 – 26

As the actual rate of groundwater extraction by pumping wells for irrigation for the floodplain is largely unknown, the pumping rates used for the pumping tests (Figure 5.34) during the fieldwork for determination of hydraulic conductivity were used. The rate for the pumping tests is similar to the extraction rate used by farmers to extract groundwater for

irrigation activities. Groundwater extraction was estimated considering the numbers of wells along transect 1 which is 40 wells (Figure 5.30). The rate of pumping was estimated at 172.8 m^3/day which is equivalent to the rate of pumping farmers irrigate their farms 6 hours per week.

5.5.7 Scenario 1 –River water stages

Three river water stages scenarios were used: low river water stage, average river water stage and high river water stage.

5.5.7.1 Low river water stage

Low values for the river stage observed during the 1966 drought were used to assess the amount of river seepage (Influent flow) to the floodplain during the dry season period.

The mass balance data, plotted in Figure 5.45A, shows that rainfall is the primary model input (425,958 m^3) representing 85.6% of the total inflow to the system and recharge from the constant head boundaries (71,250 m^3) represents 14.3% of the total inflow to the system. Input from river seepage (influent flow) (696 m^3) represents 0.1% of the inflow. Model outputs are dominated by model evapotranspiration (ET) amounts to 919,227 m^3 representing 99.5% of the total outflow and output from groundwater abstraction by pumping wells (4,838 m^3) represents 0.5% of the total outflow.

When losses from the model via model evapotranspiration (ET) and groundwater abstraction by pumping wells are subtracted from the recharge from rainfall, constant head boundaries and river seepage (influent flow), the amount that leaves the aquifer system is around -416,485 m^3. Thus, the amount of water withdrawal exceeds groundwater recharge. It was observed that an increase of 54% of water withdrawal from the system than the water losses from the model system. This shows that lowest river stages have a negative impact to the floodplain during the dry season period.

The negligible well output shown in Figure 5.45A is a threshold being reached, because of no water coming from the river to the floodplain during the dry season. At this threshold depth, it will be difficult to abstract the floodplain groundwater using hand-drilling method.

The gain in storage is low from January to April and higher in May and June (Figure 5.46 and Table 5.22). Similarly, losses in storage are lower in the period January to April and higher in May and June. These correspond to the low storage gain in the period January to April and higher storage gain in May and June. The river seepage (influent flow) is low throughout the modelled periods. These correspond to the groundwater well abstraction, which is low throughout the modelled period (Figure 5.46). These suggest that the level of the River Benue influenced recharge to the floodplain during the dry season period (January to June). Similarly, shallow alluvial aquifer wells in the floodplain become low due to the lower river water stage. Changes in storage are negative throughout the stress period. This shows storage loss.

During the dry season period, the flow of River Benue is controlled by the Lagdo Dam upstream in Cameroon. It is important to remember that the Yola region has no agreement with the Lagdo Dam to maintain a minimum flow in case of crisis.

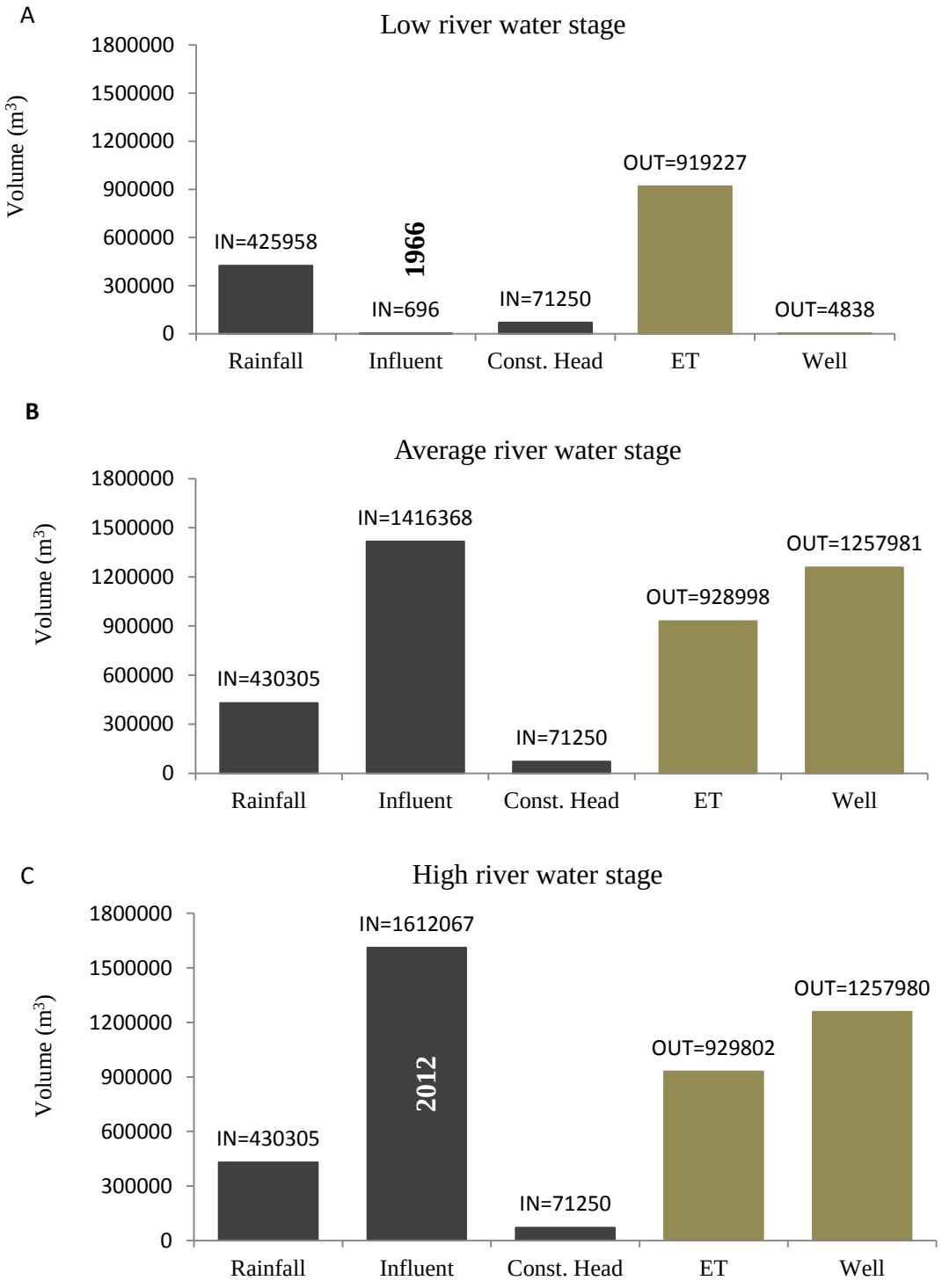

Figure 5.45: Output of the model mass balance for scenario 1 considering river regime at three different river water stages (low, average and high) at the end of stress period 26: A – 1966 drought; B – average river water stages for the period January to June (1960 to 2012); C – 2012 flood. Black histogram flows into the system and olive-brown histogram flows out of the system. Rainfall – recharge from rainfall; Influent – river seepage to the floodplain; Const. Head – recharge from Lake Geriyo; ET – outflows from model evapotranspiration; Well – outflows from pumping wells.

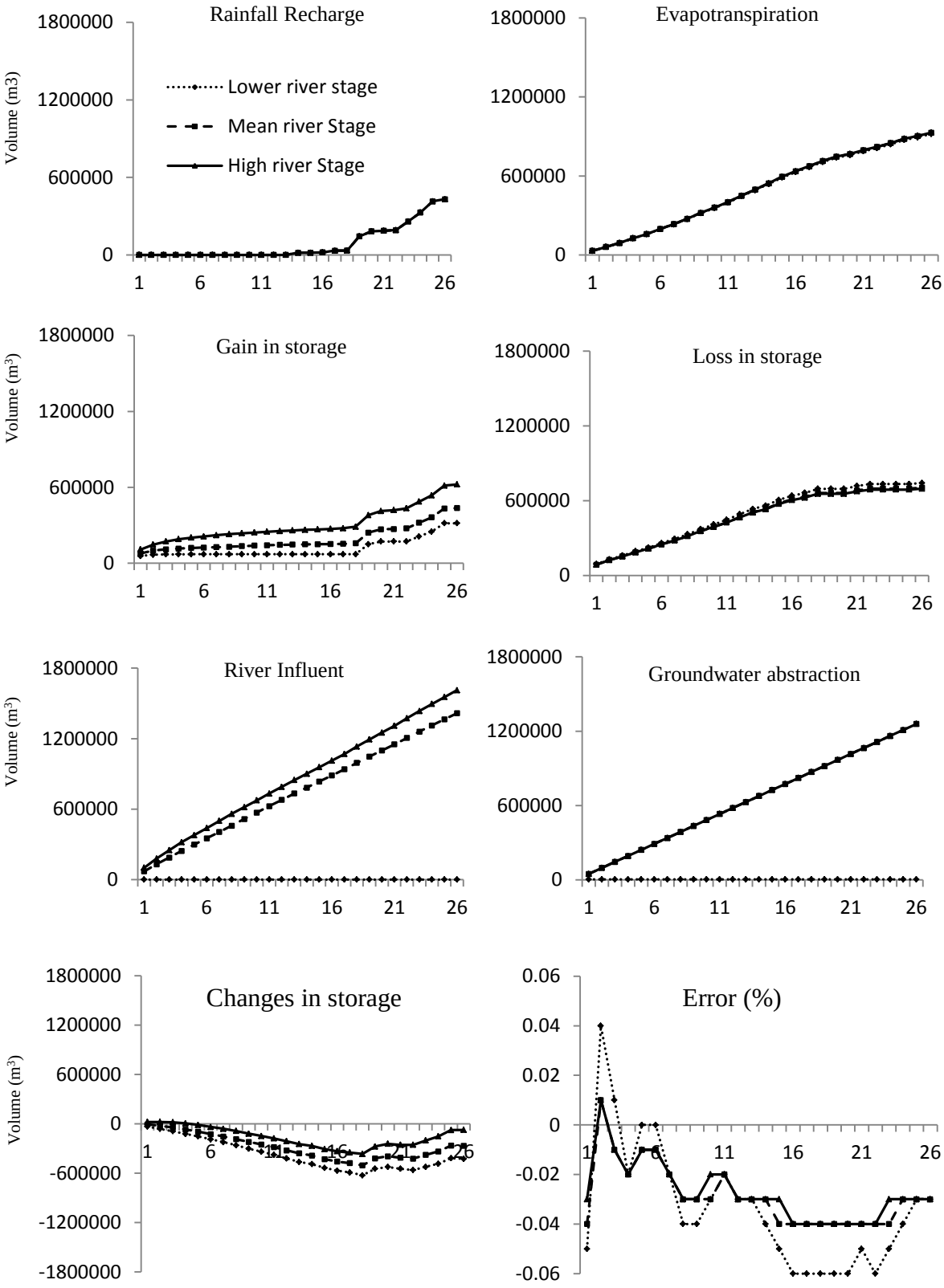

Figure 5.46: Comparison of the detailed cumulative model water balance result for scenario 1 river regime at three different river water stages (low, average and high). Low river water stage drought event in 1966; Average river water stages for the period January to June (1960 to 2012); High river water stage flood event in 2012.

Table 5.22: The cumulative water budget for the modelling scenario 1 – Low river water stage for the period January to June (1960 - 2012)

Stress period	Rainfall (m^3)	Influent (m^3)	Constant Head (m^3)	Evapotranspiration (m^3)	Well abstraction (m^3)	Balance (m^3)	Storage gain (m^3)	Storage loss (m^3)	Change in storage (m^3)	Error (%)
1	0	696	991	30640	4838	-24115	57144	90887	-33743	-0.05
2	0	696	2638	60385	4838	-52213	67379	129318	-61939	0.04
3	0	696	4437	89595	4838	-79624	70177	159500	-89323	0.01
4	0	696	6410	125393	4838	-113449	70597	193678	-123081	-0.02
5	0	696	8541	157028	4838	-142953	70716	223343	-152627	0
6	0	696	10870	195509	4838	-179105	70716	259492	-188776	0
7	0	696	13387	231738	4838	-212817	70716	293135	-222419	-0.02
8	0	696	16099	272108	4838	-250475	70716	330734	-260018	-0.04
9	0	696	19030	316283	4838	-291719	70716	371972	-301256	-0.04
10	0	696	22122	355575	4838	-327919	70716	408201	-337485	-0.03
11	0	696	25363	397553	4838	-366656	70716	446944	-376228	-0.02
12	0	696	28803	445437	4838	-411100	70716	491334	-420618	-0.03
13	0	696	32411	491004	4838	-453059	70716	533267	-462551	-0.03
14	16533	696	36039	538399	4838	-480293	70749	560472	-489723	-0.04
15	16533	696	39818	587884	4838	-525999	70749	606103	-535354	-0.05
16	19757	696	43700	629207	4838	-560216	70752	640202	-569450	-0.06
17	32379	696	47533	667435	4838	-581989	70871	662104	-591233	-0.06
18	33477	696	51417	706113	4838	-615685	70871	695797	-624926	-0.06
19	142345	696	54472	738823	4838	-536472	150210	695797	-545587	-0.06
20	181447	696	57047	758667	4838	-514639	172039	695818	-523779	-0.06
21	184877	696	59870	786789	4838	-536508	172039	717703	-545664	-0.05
22	190461	696	62898	811754	4838	-552861	172039	734025	-561986	-0.06
23	256221	696	65549	840400	4838	-513096	211756	734024	-522268	-0.05
24	324889	696	67761	872999	4838	-474815	250040	734024	-483984	-0.04
25	410248	696	69448	894040	4838	-408810	315916	734024	-418108	-0.03
26	425958	696	71250	919227	4838	-416485	315920	741711	-425791	-0.03
Mean	85966	696	35304	496923	4838	-370118	115988	495523	-379535	-0.03

5.5.7.2 Average river water stage

Mean river water stage recorded for the period January to June (1960 – 2012) were used to assess the amount of river seepage (influent flow) to the floodplain during the dry season period.

The mass balance data, plotted in Figure 5.45B, shows that river seepage (influent flow) is the primary model input (1,416,368 m^3) representing ~74.0% of the total inflow to the system and recharge from rainfall (430,305 m^3) represents ~22.0% of the total inflow to the system. A relatively significant input from the constant head boundaries (71,250 m^3) represents ~4.0% of the total inflow. Model outputs are dominated by groundwater abstraction by pumping wells amounts to 1,257,981 m^3 representing ~57.5% of the total outflow and model evapotranspiration (ET) amounts to 928,998 m^3 represents ~42.5% of the total outflow.

When losses from the model via groundwater abstraction by pumping wells and model evapotranspiration (ET) are subtracted from the recharge from river seepage (influent flow), recharge from rainfall and recharge from the constant head boundaries, the amount that leaves the aquifer system is ~-280,535 m^3. Thus, the amount of water withdrawal exceeds groundwater recharge. Note that an increase of 38% of water withdrawal from the system than the water losses from the normal model output is observed. This shows that mean river stages have a negative impact to the floodplain during the dry season period.

The increase in storage is lowest in January to April and higher in May and June (Figure 5.46 and Table 5.23). Losses in storage are lower in the period January to April and become higher in May and June. The river seepage (influent flow) is lowest in January and highest in June. The higher river seepage (influent flow) in June is due to high water abstractions for irrigation activities and the lower river seepage (influent flow) in January is due to the less irrigation activities. Changes in storage are negative for all the model period. These show water loss from the storage from the floodplain alluvial aquifers.

Table 5.23: The cumulative water budget for the modelling scenario 1 – Considering the river regime at the average river water stage for the period January to June (1960 – 2012)

Stress period	Rainfall (m^3)	Influent (m^3)	Constant Head (m^3)	Evapotranspiration (m^3)	Well abstraction (m^3)	Balance (m^3)	Storage gain (m^3)	Storage loss (m^3)	Change in storage (m^3)	Error (%)
1	0	70601	991	30916	48384	-7708	78517	86164	-7647	-0.04
2	0	130716	2639	60964	96768	-24377	99330	123730	-24400	0.01
3	0	188034	4437	90474	145152	-43155	109753	152888	-43135	-0.01
4	0	244130	6410	126639	193536	-69635	116094	185630	-69536	-0.02
5	0	297899	8541	158602	241920	-94082	120503	214512	-94009	-0.01
6	0	351872	10870	197482	290304	-125044	123917	248875	-124958	-0.01
7	0	405648	13387	234090	338688	-153743	127110	280685	-153575	-0.02
8	0	459232	16099	274882	387072	-186623	129795	316178	-186383	-0.03
9	0	515763	19031	319522	435456	-220184	135133	355060	-219927	-0.03
10	0	570711	22122	359229	483840	-250236	139109	389101	-249992	-0.03
11	0	625154	25363	401654	532224	-283361	142339	425444	-283105	-0.02
12	0	679346	28803	450049	580608	-322508	144881	467064	-322183	-0.03
13	0	733356	32411	496104	628992	-359329	147287	506252	-358965	-0.03
14	16701	783248	36039	544008	677376	-385396	149599	534552	-384953	-0.03
15	16701	834848	39818	594026	725759	-428418	150581	578469	-427888	-0.04
16	19958	886827	43700	635795	774143	-459453	151758	610545	-458787	-0.04
17	32710	938841	47533	674436	822527	-477879	153540	630748	-477208	-0.04
18	33818	993990	51418	713534	870911	-505219	157366	661899	-504533	-0.04
19	143798	1047075	54472	746601	919294	-420550	242175	661899	-419724	-0.04
20	183298	1099453	57047	766662	967678	-394542	268193	661921	-393728	-0.04
21	186763	1151839	59870	795092	1016062	-412682	270239	682109	-411870	-0.04
22	192405	1206571	62899	820332	1064446	-422903	274993	697039	-422046	-0.04
23	258835	1259839	65550	849295	1112830	-377901	319959	697039	-377080	-0.04
24	328205	1312414	67762	882255	1161213	-335087	362789	697039	-334250	-0.03
25	414435	1364409	69449	903529	1209597	-264833	432928	697039	-264111	-0.03
26	430305	1416368	71250	928998	1257981	-269056	436115	704439	-268324	-0.03
Mean	86844	752622	35304	502122	653183	-280535	191692	471782	-280089	-0.03

5.5.7.3 High river water stage

The high values for the river water stage recorded for the period January to June (1971 – 2012) were used to assess the amount of river seepage (i.e. influent flow) to the floodplain from the river during the dry season period.

The mass balance data, plotted in Figure 5.45C, show that river seepage (influent flow) is the primary model input (1,612,067 m^3) representing 76.2% of the total inflow water to the system and recharge from rainfall (430,305 m^3) represents 20.4% of the total inflow. A relatively significant input from the constant head boundaries (71,250 m^3) represents 3.4% of the total inflow. Model outputs are dominated by groundwater abstraction by pumping wells amounts to 1,257,980 m^3 representing 57.5% of the total outflow from the system and model evapotranspiration (ET) amounts to 929,802 m^3 represents 42.5% of the total outflow from the system.

When losses from the model via groundwater abstraction by pumping wells and model evapotranspiration (ET) are subtracted from the recharge from river seepage (influent flow), recharge from rainfall and recharge from the constant head boundaries, the amount that leaves the aquifer system is ~–74,160 m^3. Thus, the amount of water withdrawal exceeds groundwater recharge. Note that decrease of 25.4% of water withdrawal from the system than the water losses from the model is observed. This shows that higher river stages have a positive impact to the floodplain.

The water budget output for the highest river water stages for the period January to June (1971 – 2012) is shown in Figure 5.46 and Table 5.24. Gains in storage are lower between January and April and low in May and June. The highest storage gains in May and June are because the rainy season begins in these months, which will increase recharge. The losses in storage are lower in the period January to April and higher in May and June. Model evapotranspiration (ET) increases through the stress period. But June has especially the highest model evapotranspiration (ET). River seepage (influent flow) increases with the stress period, these correspond to the groundwater abstractions for irrigation. Changes in storage are negative in the period February to June except for January, which has positive change in storage, these shows water loss from the storage from the floodplain alluvial aquifers for the period February to June, except for January that shows gain in storage.

Table 5.24: The cumulative water budget for the modelling scenario 1 – High river water stage for the period January to June (1960 - 2012)

Stress period	Rainfall (m^3)	Influent (m^3)	Constant Head (m^3)	Evapotranspiration (m^3)	Well abstraction (m^3)	Balance (m^3)	Storage gain (m^3)	Storage loss (m^3)	Change in storage (m^3)	Error (%)
1	0	101099	991	30921	48384	22785	108860	86014	22846	-0.03
2	0	178541	2639	60977	96768	23435	146793	123383	23410	0.01
3	0	250310	4437	90500	145151	19096	171398	152283	19115	-0.01
4	0	318966	6410	126685	193536	5155	189916	184661	5255	-0.02
5	0	378114	8541	158666	241920	-13931	201855	215713	-13858	-0.01
6	0	438732	10870	197572	290304	-38274	211539	249726	-38187	-0.01
7	0	499147	13387	234205	338688	-60359	220943	281134	-60191	-0.02
8	0	559179	16099	275027	387072	-86821	229538	316119	-86581	-0.03
9	0	616384	19031	319701	435456	-119742	236322	355807	-119485	-0.03
10	0	674214	22122	359440	483840	-146944	242673	389370	-146697	-0.02
11	0	732026	25363	401898	532224	-176733	248557	425033	-176476	-0.02
12	0	789752	28803	450333	580608	-212386	253723	465785	-212062	-0.03
13	0	847352	32411	496428	628992	-245657	258874	504166	-245292	-0.03
14	16701	901439	36039	544375	677375	-267571	264098	531226	-267128	-0.03
15	16701	956738	39818	594438	725759	-306940	267419	573830	-306411	-0.03
16	19958	1012307	43700	636247	774143	-334425	271081	604840	-333759	-0.04
17	32710	1067844	47533	674925	822527	-349365	275863	624559	-348696	-0.04
18	33818	1132388	51418	714064	870911	-367351	288227	654892	-366665	-0.04
19	143798	1192608	54472	747166	919294	-275582	380136	654892	-274756	-0.04
20	183298	1251254	57047	767250	967678	-243329	412401	654914	-242513	-0.04
21	186763	1309413	59870	795714	1016062	-255730	419554	674472	-254918	-0.04
22	192405	1373931	62899	820985	1064446	-256196	433651	688992	-255341	-0.04
23	258835	1435220	65550	849986	1112830	-203211	486600	688992	-202392	-0.03
24	328205	1495042	67762	882992	1161213	-153196	536633	688992	-152359	-0.03
25	414435	1553768	69449	904296	1209597	-76241	613470	688992	-75522	-0.03
26	430305	1612067	71250	929802	1257980	-74160	622523	695953	-73430	-0.03
Mean	86844	872224	35304	502484	653183	-161295	307410	468259	-160850	-0.03

5.5.8 Scenario 2 – Pumping rates

Three pumping rate scenarios were used: high pumping rate, average pumping rate and low pumping rate.

5.5.8.1 High pumping rate

The high pumping rate simulates the hypothesised effects of population increase and the irrigation development plan of the Upper Benue Authority to boost agricultural production in the region. A high pumping rate, at levels was set at 100 % of the normal abstraction (172.8 m^3/day). This value was considered to assess groundwater levels across the floodplain.

The mass balance data, plotted in Figure 5.47A, show that river seepage (influent flow) is the primary model input (2,624,681 m^3) representing 84% of the total water inflow to the system. Recharge from precipitation (430,305 m^3) represents 13.7% of the inflow to the system with negligible input from constant head boundaries (3,5304 m^3) which represent 2.3% of total water inflow. Model output is dominated by groundwater abstraction by pumping wells, which amount to 2,515,962 m^3, representing 73% of the total outflow from the system and output from model evapotranspiration (ET) 928,722 is 27% of the total outflow.

When losses from the model via model evapotranspiration (ET) and groundwater abstraction by pumping wells are subtracted from the recharge from rainfall, river seepage (influent flow) and constant head boundaries, the amount that leaves the aquifer system is ~-318,448 m^3. Thus, the amount of water withdrawal exceeds groundwater recharge. Note that an increase of 44% of water withdrawal from the system than the water losses for the model is observed. This shows that high pumping rates have a negative impact to the floodplain.

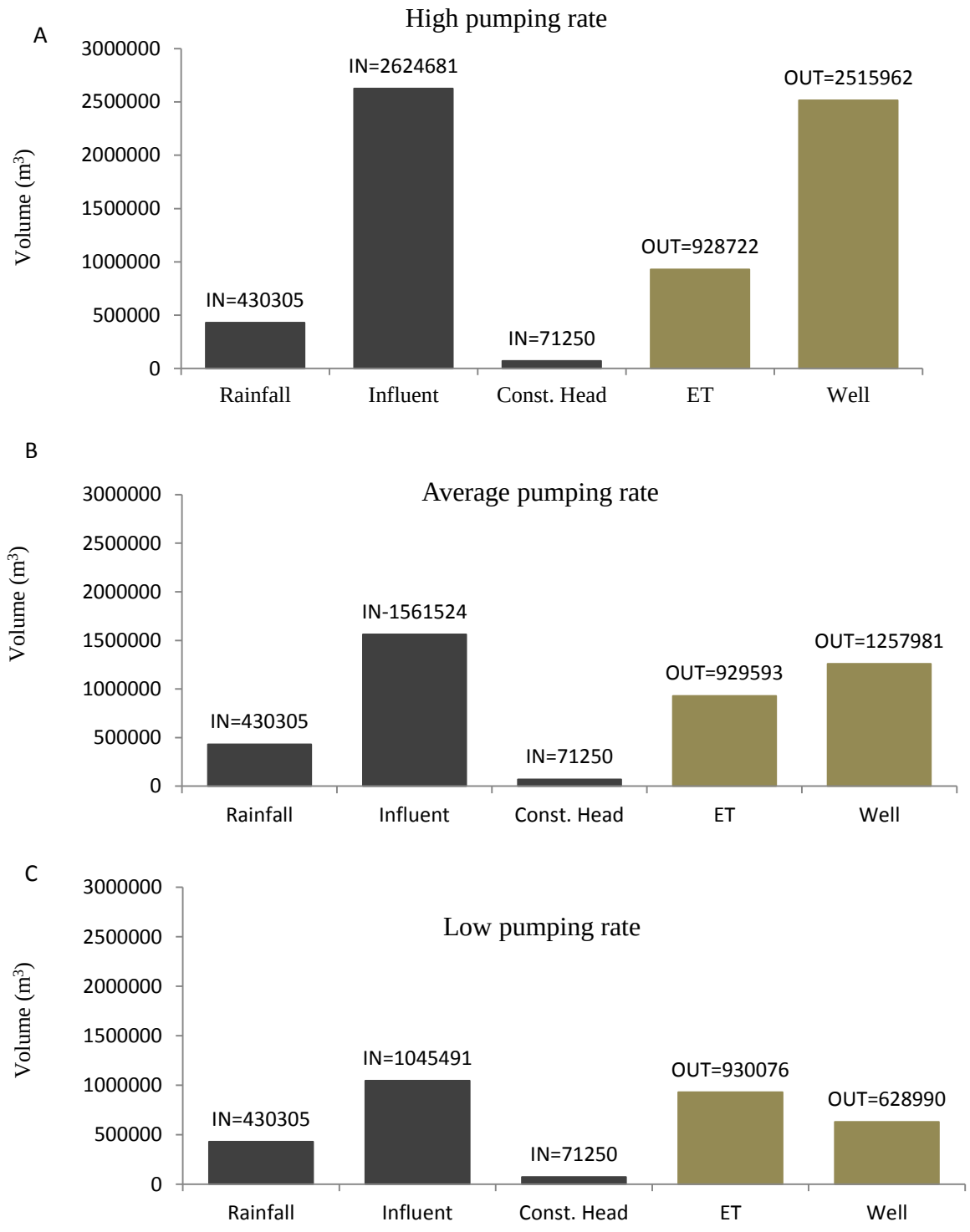

Figure 5.47: Output of the model mass balance for scenario 2 pumping rates at three different abstraction rates at the end of stress period 26: A – multiplying the normal pumping rate by 2 (172.8 m^3/day); B – multiplying the normal pumping rate by 1.5 (172.8 m^3/day); C – multiplying the normal pumping rate by 0.5 (172.8 m^3/day). Black histogram flows into the system and olive-brown histogram flows out of the system. Rainfall – recharge from rainfall; Influent – river seepage to the floodplain; Const. Head – recharge from Lake Geriyo; ET – outflows from evapotranspiration; Well – outflows from pumping wells.

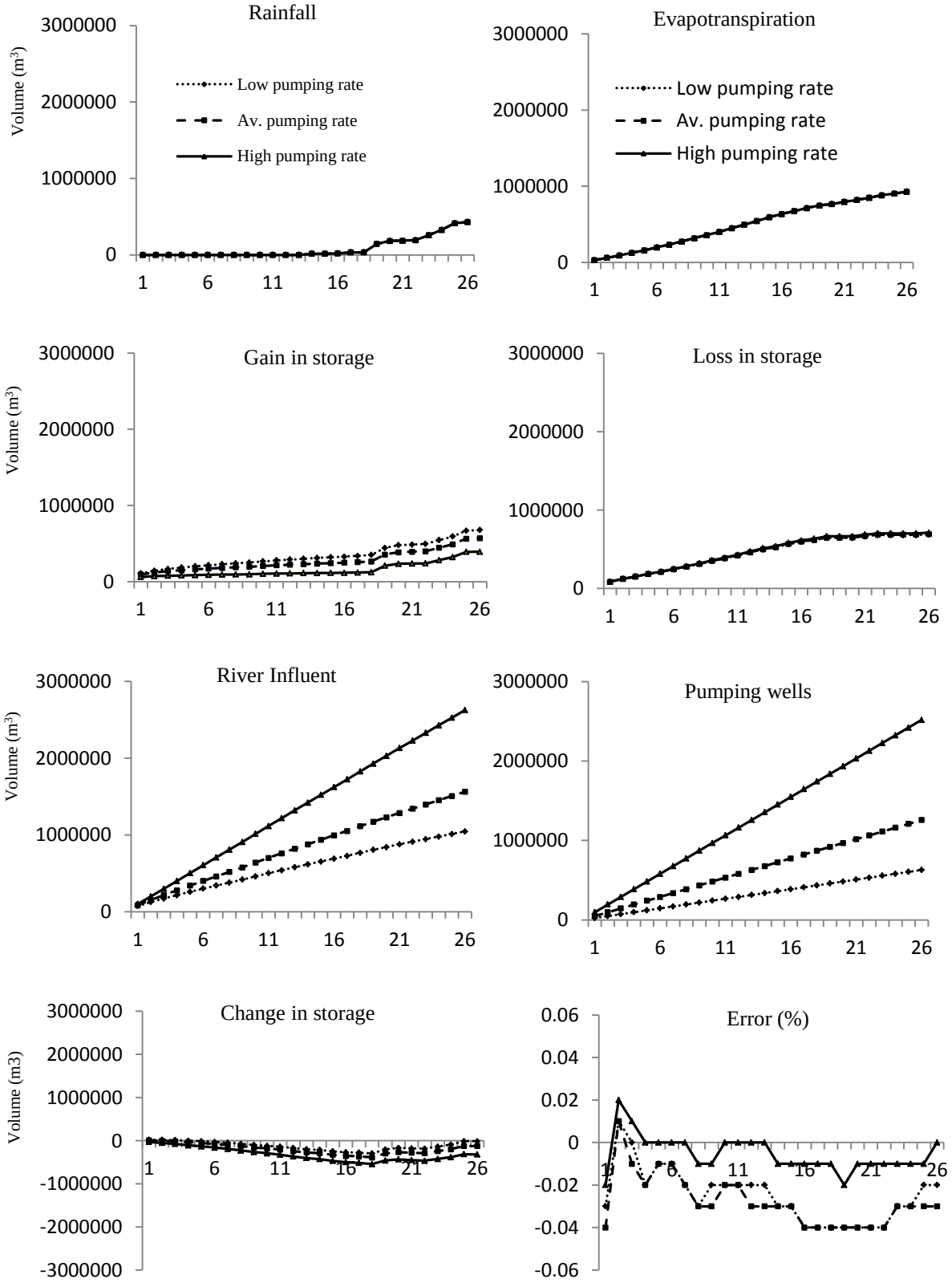

Figure 5.48: Comparison of the detailed cumulative model water balance result for scenario 2 considering the impact of groundwater abstraction by pumping wells at three different impacts, low, average and high pumping rates.

Table 5.25: The cumulative water budget for the modelling scenario 2 – High pumping rate for groundwater abstraction by pumping wells from the normal abstraction rate of 172.8 m^3/day

Stress period	Rainfall (m^3)	Influent (m^3)	Constant Head (m^3)	Evapotranspiration (m^3)	Well abstraction (m^3)	Balance (m^3)	Storage gain (m^3)	Storage loss (m^3)	Change in storage (m^3)	Error (%)
1	0	100145	991	30914	96768	-26546	59909	86414	-26505	-0.02
2	0	200290	2639	60955	193536	-51562	72725	124353	-51628	0.02
3	0	300434	4437	90459	290304	-75892	77947	153880	-75933	0.01
4	0	400579	6410	126614	387072	-106697	80511	187192	-106681	0
5	0	503039	8541	158568	483840	-130828	85108	215967	-130859	0
6	0	605490	10870	197437	580608	-161685	89224	250946	-161722	0
7	0	706964	13387	234035	677376	-191060	92324	283359	-191035	0
8	0	807730	16099	274815	774145	-225131	94473	319528	-225055	-0.01
9	0	908206	19031	319441	870913	-263117	96090	359134	-263044	-0.01
10	0	1013182	22122	359136	967681	-291513	102304	393778	-291474	0
11	0	1115649	25363	401546	1064449	-324983	105791	430747	-324956	0
12	0	1217484	28803	449926	1161216	-364855	108294	473076	-364782	0
13	0	1318994	32411	495966	1257984	-402545	110529	512982	-402453	0
14	16701	1420197	36039	543855	1354751	-425669	113179	538699	-425520	-0.01
15	16701	1521267	39818	593857	1451519	-467590	114649	582022	-467373	-0.01
16	19958	1622204	43700	635614	1548286	-498038	116486	614194	-497708	-0.01
17	32709	1722932	47533	674243	1645054	-516123	118941	634751	-515810	-0.01
18	33818	1826600	51418	713330	1741821	-543315	123449	666458	-543009	-0.01
19	143798	1928091	54472	746387	1838589	-458615	208270	666458	-458188	-0.02
20	183298	2028845	57047	766442	1935356	-432608	234267	666480	-432213	-0.01
21	186763	2129577	59870	794864	2032124	-450778	236567	686973	-450406	-0.01
22	192405	2227983	62899	820095	2128892	-465700	238680	703987	-465307	-0.01
23	258835	2327067	65550	849049	2225659	-423256	281067	703987	-422920	-0.01
24	328205	2426034	67762	881997	2322427	-382423	321895	703987	-382092	-0.01
25	414435	2525470	69449	903263	2419194	-313103	391077	703987	-312910	-0.01
26	430305	2624681	71250	928722	2515962	-318448	393219	711486	-318267	0
Mean	86844	1366505	35304	501982	1306366	-319695	156422	475955	-319533	-0.01

The storage gain is low from January to April and higher in May and June (Figure 5.47 and Table 5.25). Losses in storage are lower from January to April and higher in May and June. This corresponds to the low storage gain from January to April and higher storage gain in May and June. The river seepage (influent flow) increases with the modelled periods. This corresponds with the rate of groundwater abstraction, which increased with the modelled periods. These suggest that groundwater abstraction drains the floodplain alluvial aquifer and river during the dry season period (January to June). The changes in storage are negative throughout the modelled period, these shows water loss from the storage from the floodplain alluvial aquifers throughout the modelled period.

5.5.8.2 Mean pumping rate

Mean pumping rates were set at the normal abstraction rate (172.8 m^3/day). This value was considered to assess groundwater levels across the floodplain.

The mass balance data, plotted in Figure 5.47B, show that river seepage (influent flow) is the primary model input (1,561,524 m^3) representing 75.7% of the total inflow to the system and recharge from rainfall (430,305 m^3) represents 20.8% of the total inflow to the system. A relatively significant input from the constant head boundaries (71,250 m^3) represents 3.5% of the total inflow. Model outputs are dominated by groundwater abstraction by pumping wells amounts to 1,257,981 m^3 representing 57.5% of the total outflow and model evapotranspiration (ET) amounts to 929,593 m^3 represents 42.5% of the total outflow.

When losses from the model via groundwater abstraction by pumping wells and model evapotranspiration (ET) are subtracted from the recharge from river seepage (influent flow), recharge from rainfall and recharge from the constant head boundaries, the amount that leaves the aquifer system is ~-124,495 m^3. Thus, the amount of water withdrawal exceeds groundwater recharge. It was observed that no increase of water withdrawal from the system than water losses from the model system.

Table 5.26: The cumulative water budget for the modelling scenario 2 – Average pumping rate for groundwater abstraction by pumping wells from the normal abstraction of 172.8 m^3/day

Stress period	Rainfall (m^3)	Influent (m^3)	Constant Head (m^3)	Evapotranspiration (m^3)	Well abstraction (m^3)	Balance (m^3)	Storage gain (m^3)	Storage loss (m^3)	Change in storage (m^3)	Error (%)
1	0	85617	991	30919	48384	7305	93447	86080	7367	-0.04
2	0	153507	2638	60970	96768	-1593	121919	123535	-1616	0.01
3	0	217402	4437	90487	145152	-13800	138742	152522	-13780	-0.01
4	0	279189	6410	126661	193536	-34598	150590	185089	-34499	-0.02
5	0	341053	8541	158633	241920	-50959	162239	213125	-50886	-0.01
6	0	401373	10870	197527	290304	-75588	171708	247209	-75501	-0.01
7	0	460803	13387	234150	338688	-98648	180284	278764	-98480	-0.02
8	0	519593	16099	274960	387072	-126340	187857	313957	-126100	-0.03
9	0	577909	19031	319621	435456	-158137	194589	352468	-157879	-0.03
10	0	640838	22122	359349	483840	-180229	206154	386137	-179983	-0.02
11	0	701364	25363	401797	532224	-207294	215024	422061	-207037	-0.02
12	0	761020	28803	450221	580608	-241006	222471	463152	-240681	-0.03
13	0	820127	32411	496306	628991	-272759	229453	501849	-272396	-0.03
14	16701	878726	36039	544244	677375	-290153	237104	526815	-289711	-0.03
15	16701	937010	39817	594299	725759	-326530	242681	568680	-325999	-0.03
16	19958	995008	43700	636102	774143	-351579	248904	599818	-350914	-0.04
17	32710	1052648	47533	674776	822527	-364412	255951	619693	-363742	-0.04
18	33818	1113336	51417	713909	870911	-386249	264710	650273	-385563	-0.04
19	143797	1171835	54472	747007	919294	-296197	354904	650273	-295369	-0.04
20	183298	1229347	57047	767087	967678	-265073	386037	650295	-264258	-0.04
21	186763	1286649	59870	795547	1016062	-278327	392521	670037	-277516	-0.04
22	192405	1341321	62899	820812	1064446	-288633	398589	686366	-287777	-0.04
23	258835	1396438	65550	849805	1112830	-241812	445373	686366	-240993	-0.03
24	328205	1451305	67762	882800	1161213	-196741	490459	686366	-195907	-0.03
25	414435	1506570	69449	904097	1209597	-123240	563844	686366	-122522	-0.03
26	430305	1561524	71250	929593	1257981	-124495	569745	693511	-123766	-0.03
Mean	86844	841597	35304	502372	653183	-191811	274050	647775	-191366	-0.03

The gain in storage is lower between January and April and higher in May and June (Figure 5.48 and Table 5.26). Losses in storage are lower from January to April and higher in May and June. Low storage loss in the period January to April corresponds with the lower storage gain in the period January to April, similarly the higher storage loss in May and June, corresponds to the higher storage gain in May and June. Changes in storage are negative throughout the modelled period except for stress period 1, when there was a negative changes in storage.

5.5.8.3 Low pumping rate

Low pumping rate scenario was set by multiplying 0.5 times the normal pumping rate (172.8 m^3/day) that is reducing the groundwater abstractions by half. This low pumping rate value was considered to assess hydraulic head across the floodplain alluvial aquifers.

The mass balance data, plotted in Figure 5.47C, show that river seepage (influent flow) is the primary model input (1,045,491 m^3) representing 67.6% of the total inflow to the system and recharge from rainfall (430,305 m^3) represents 27.8% of the total inflow to the system. A relatively significant input from the constant head boundaries (71,250 m^3) represents 4.6% of the total inflow. Model outputs are dominated by groundwater abstraction by model evapotranspiration (ET) amounts to 930,076 m^3 represents 59.7% of the total outflow and pumping wells amounts to 628,990 m^3 representing 40.3% of the total outflow.

When losses from the model via model evapotranspiration (ET) and groundwater abstraction by pumping wells are subtracted from the recharge from river seepage (influent flow), recharge from rainfall and recharge from the constant head boundaries, the amount that leaves the aquifer system is ~-12,020 m^3. Thus, the amount of groundwater withdrawal exceeds groundwater recharge. It was observed that a decrease of 82.4% of water withdrawal from the system than the water losses from the model system.

Table 5.27: The cumulative water budget for the modelling scenario 2 – Low pumping rate for groundwater abstraction by pumping wells from the normal abstraction of 172.8 m^3/day

Stress period	Rainfall (m^3)	Influent (m^3)	Constant Head (m^3)	Evapotranspiration (m^3)	Well abstraction (m^3)	Balance (m^3)	Storage gain (m^3)	Storage loss (m^3)	Change in storage (m^3)	Error (%)
1	0	74886	991	30921	24192	20764	106839	86021	20818	-0.03
2	0	126839	2639	60977	48384	20117	143482	123402	20080	0.01
3	0	173349	4437	90499	72576	14711	167025	152314	14711	0
4	0	216881	6410	126681	96768	-158	184623	184710	-87	-0.02
5	0	259987	8541	158663	120960	-11095	201577	212635	-11058	-0.01
6	0	301118	10870	197570	145152	-30734	215836	246526	-30690	-0.01
7	0	341009	13387	234206	169344	-49154	228917	277952	-49035	-0.02
8	0	379979	16099	275032	193536	-72490	240640	312947	-72307	-0.03
9	0	418242	19031	319712	217728	-100167	251255	351227	-99972	-0.02
10	0	461013	22121	359458	241920	-118244	266639	384706	-118067	-0.02
11	0	501313	25363	401927	266112	-141363	279172	420355	-141183	-0.02
12	0	540589	28803	450377	290304	-171289	290043	461092	-171049	-0.02
13	0	579175	32411	496487	314496	-199397	300314	499438	-199124	-0.02
14	16701	617126	36039	544453	338688	-213275	311246	524175	-212929	-0.03
15	16701	654647	39818	594538	362880	-246252	319763	565589	-245826	-0.03
16	19958	691780	43700	636367	387072	-268001	328940	596387	-267447	-0.04
17	32710	728460	47533	675066	411264	-277627	338977	616052	-277075	-0.04
18	33818	768190	51418	714226	435455	-296255	350541	646238	-295697	-0.04
19	143798	805685	54472	747347	459647	-203039	443893	646238	-202345	-0.04
20	183298	842078	57047	767441	483839	-168857	478078	646260	-168182	-0.04
21	186763	878167	59870	795922	508031	-179153	487248	665736	-178488	-0.04
22	192405	911490	62899	821207	532223	-186636	495785	681720	-185935	-0.04
23	258835	945151	65550	850223	556415	-137102	545276	681720	-136444	-0.03
24	328205	978487	67762	883245	580607	-89398	592990	681720	-88730	-0.03
25	414435	1012172	69449	904559	604799	-13302	668963	681720	-12757	-0.02
26	430305	1045491	71250	930076	628990	-12020	677187	688661	-11474	-0.02
Mean	86844	586666	35304	502584	326592	-120362	342894	462905	-120011	-0.03

The low well output shown in Figure 5.47C is because less water is being abstracted from the alluvial aquifer, suggesting that the floodplain water table depth will remain sustainable for abstraction using hand drilling techniques.

Gain in storage is lower from January to April and higher in May and June (Figure 5.48 and Table 5.27). Losses in storage are lower from January to April and higher in May and June. Low storage loss from January to April corresponds with the lower storage gain in the period January to April. River seepage (Influent flow) increases throughout the modelled period, these correspond to the water abstractions for irrigation activities that increase throughout the stress period. Changes in storage are negative throughout the modelled period, except in stress periods one to three that have positive change in storage. These shows water loss from the storage from the floodplain alluvial aquifers, except stress periods one to three which shows water gain to the floodplain aquifers.

5.5.9 Scenario 3 – Global climate change scenarios

The three global climate change scenarios are: i. Low precipitation and high evaporation, lower river water stage, and high pumping rate or in brief, the drought scenario; ii. Average precipitation, evaporation, and river water stages, and normal pumping rate, iii. High precipitation and low evaporation, high river water stages and low pumping rates.

5.5.9.1 Drought scenario

The drought scenarios are: low precipitation and high evaporation for the drought event that occurred in 1966 in the region, lower river water stage observed during the 1966 drought, and high pumping rate by multiplying pumping rate by 100% were used to assess the hydraulic head across the alluvial aquifer.

The mass balance data shows that constant head boundaries (110,541 m^3) representing 98.9% of the total inflow to the floodplain system while input from river seepage (influent flow) (696 m^3) represents 0.6% of the total inflow to the floodplain (Figure 5.49A). Input from rainfall represents 0.5% of the inflow to the floodplain. Model output is dominated by model evapotranspiration (ET) amounts to 1,420,806 m^3 representing 99.5% of the total outflow from the system and output from groundwater abstraction by pumping wells (7257 m^3) represents 0.5% of the total outflow.

When losses from the model through model evapotranspiration (ET) and groundwater abstraction by pumping wells are subtracted from the recharge from constant head boundaries and rainfall, the amount that leaves the aquifer system is around -1,316,323 m^3. Thus, the amount of water withdrawal exceeds groundwater recharge. It was observed that an increase of 82.8% of water withdrawal from the floodplain than the water losses from the model system. This shows that the drought scenario have a severe impact to the floodplain groundwater during dry season period. This is the period farmers abstract the shallow wells on the floodplain for irrigation.

The gain in storage is low in all stress periods (Figure 5.50 and Table 5.28). Similarly, loss in storage is higher for all stress periods except May and June. This corresponds to low gain in storage for all stress periods. The river seepage (influent flow) is low throughout the modelled period. These correspond to the wells abstraction, which was low throughout the modelled period (Figure 5.49). This suggests that the drought scenario have an impact to both River Benue and the floodplain groundwater during the dry season period (January to June) in the region. Changes in storage are negative for all the stress period these shows storage loss for all the stress period.

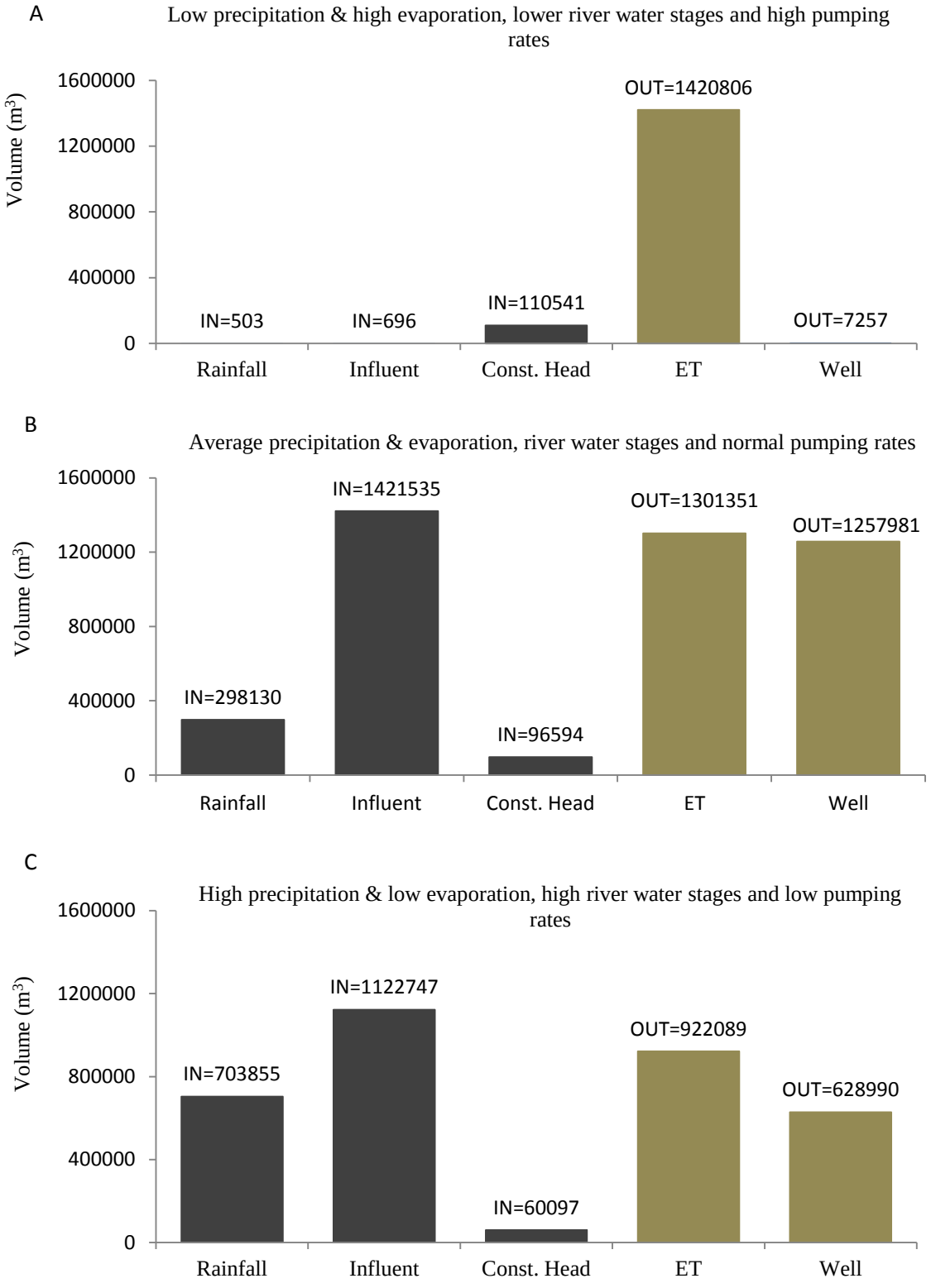

Figure 5.49: Output of the model mass balance for scenario 3 global climate change at three different scenarios at the end of stress period 26: A – low precipitation & high evaporation, lower river water stages and high pumping rates; B – average precipitation & evaporation, river water stages and normal pumping rates; C – high precipitation & low evaporation, high river water stages and low pumping rates.

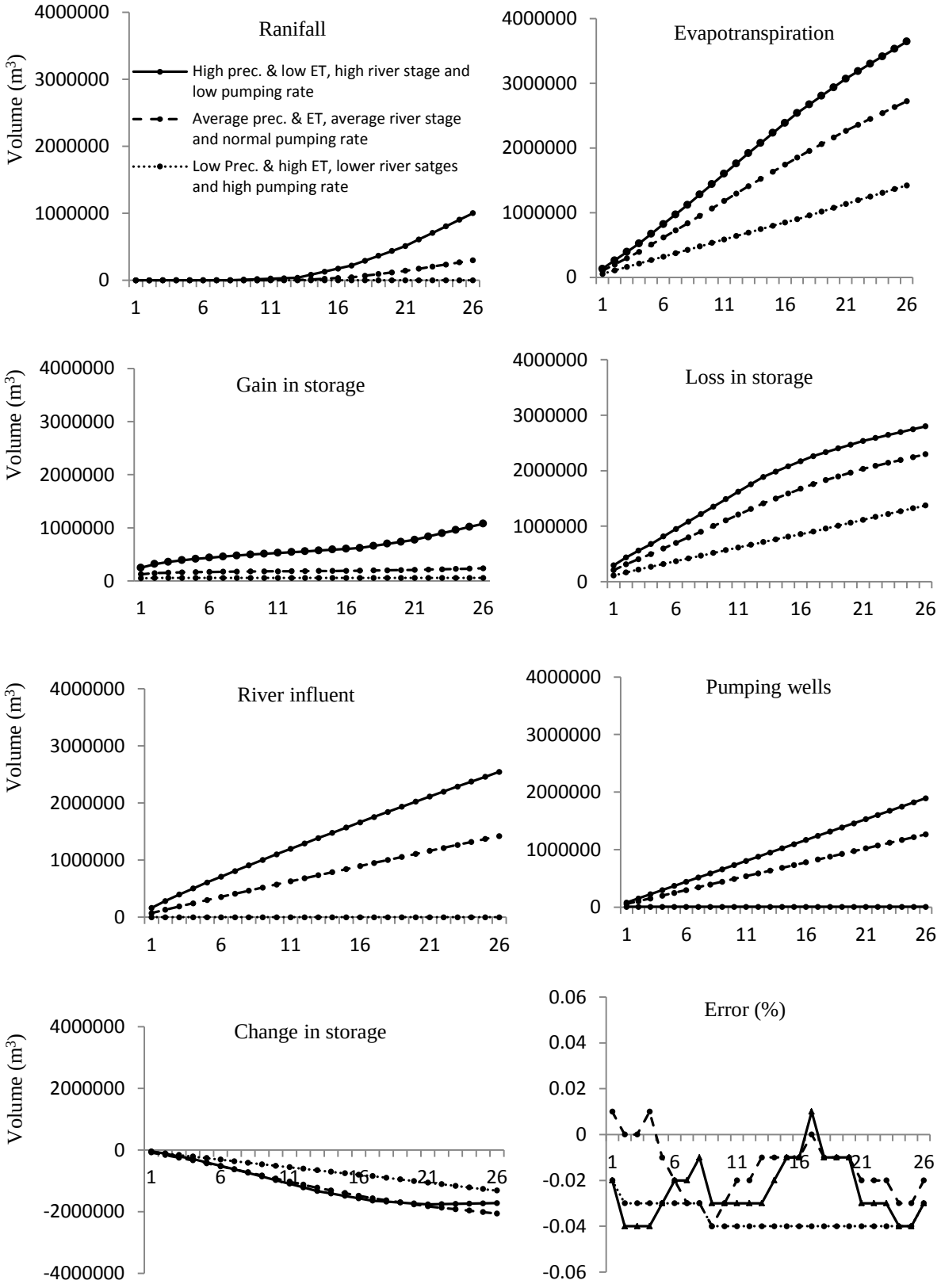

Figure 5.50: Comparison of the detailed cumulative model water balance result for scenario 3 – Global climate change scenarios. i. low precipitation & high evaporation, lower river water stages and high pumping rates in smallest dotted lines; ii. average precipitation & evaporation, river water stages and normal pumping rates in black dotted lines; and iii. high precipitation & low evaporation, high river water stages and low pumping rates in black lines.

Table 5.28: The cumulative water budget for the modelling scenario 3 – Low precipitation & high evaporation, lower river water stages and high pumping rates

Stress period	Rainfall (m^3)	Influent (m^3)	Constant Head (m^3)	Evapotranspiration (m^3)	Well abstraction (m^3)	Balance (m^3)	Storage gain (m^3)	Storage loss (m^3)	Change in storage (m^3)	Error (%)
1	0	696	1183	53348	7257	-58726	51548	110252	-58704	-0.02
2	0	696	3241	106622	7257	-109942	56523	166421	-109898	-0.03
3	0	696	5606	159875	7257	-160830	57181	217947	-160766	-0.03
4	0	696	8218	213107	7257	-211450	57275	268640	-211365	-0.03
5	0	696	11067	266319	7257	-261813	57275	318981	-261706	-0.03
6	0	696	14147	319510	7257	-311924	57275	369072	-311797	-0.03
7	0	696	17447	372680	7257	-361794	57275	418921	-361646	-0.03
8	0	696	20952	425830	7257	-411439	57275	468544	-411269	-0.03
9	0	696	24651	478960	7257	-460870	57275	517955	-460680	-0.04
10	0	696	28529	532069	7257	-510101	57275	567165	-509890	-0.04
11	0	696	32573	585158	7257	-559146	57275	616189	-558914	-0.04
12	0	696	36772	638227	7257	-608016	57275	665038	-607763	-0.04
13	0	696	41116	691277	7257	-656722	57275	713722	-656447	-0.04
14	0	696	45596	744306	7257	-705271	57275	762250	-704975	-0.04
15	0	696	50204	797315	7257	-753672	57275	810632	-753357	-0.04
16	0	696	54932	848199	7257	-799828	57275	856771	-799496	-0.04
17	0	696	59775	898172	7257	-844958	57275	901881	-844606	-0.04
18	0	696	64812	957573	7257	-899322	57275	956215	-898940	-0.04
19	0	696	70045	1016321	7257	-952837	57275	1009695	-952420	-0.04
20	0	696	75440	1075042	7257	-1006163	57275	1062989	-1005714	-0.04
21	0	696	80981	1133297	7257	-1058877	57275	1115675	-1058400	-0.04
22	101	696	86655	1191339	7257	-1111144	57275	1167935	-1110660	-0.04
23	203	696	92454	1249230	7257	-1163134	57275	1219922	-1162647	-0.04
24	303	696	98372	1306594	7257	-1214480	57275	1271258	-1213983	-0.04
25	403	696	104402	1363933	7257	-1265689	57275	1322459	-1265184	-0.04
26	503	696	110541	1420806	7257	-1316323	57275	1373086	-1315811	-0.03
Mean	58	696	47681	724812	7257	-683634	57022	740370	-683348	-0.04

5.5.9.2 Mean precipitation, evaporation and river water stages, and normal pumping rate.

This scenario is: average precipitation and evaporation values recorded during the period January to June (1960 – 2012), average river water stages values recorded for the period January to June (1960 – 2012) and normal pumping rate (172.8 m^3/day). The above informations were used to assess the hydraulic head across the floodplain alluvial aquifers.

The mass balance data, plotted in Figure 5.49B, shows that river seepage (influent flow) is the primary model input (1,421,535 m^3) representing 78.3% of the total inflow to the system and recharge from rainfall (298,130 m^3) represents 16.4% of the total inflow to the system. A relatively significant input from the constant head boundaries (96,594 m^3) represents 5.3% of the total inflow to the system. Model outputs are dominated by model evapotranspiration (ET) (1,301,351 m^3) representing 51% of the total outflow from the system and groundwater abstraction by pumping wells (1,257,981 m^3) represents 49% of the total outflow from the system.

When losses from the model through model evapotranspiration (ET) and groundwater abstraction by pumping wells are subtracted from the recharge from river seepage (influent flow), recharge from rainfall and recharge from constant head boundaries, the amount that leaves the floodplain aquifer system is ~-743,073 m^3. This shows that the amount of water withdrawal exceeds groundwater recharge. An increase of 71.4% of water withdrawal from the system than the water losses from the model, these show that average combinations of scenarios have a negative impact to the floodplain groundwater.

Table 5.29: The cumulative water budget for the modelling scenario 3 – Average precipitation & evaporation, average river water stages and normal pumping rates

Stress period	Rainfall (m^3)	Influent (m^3)	Constant Head (m^3)	Evapotranspiration (m^3)	Well abstraction (m^3)	Balance (m^3)	Storage gain (m^3)	Storage loss (m^3)	Change in storage (m^3)	Error (%)
1	17	70658	1112	45351	48383	-21947	74573	96564	-21991	0.03
2	33	130907	3022	90693	96768	-53499	91273	144859	-53586	0.03
3	50	188410	5187	136022	145152	-87527	99405	187064	-87659	0.03
4	66	244699	7555	181341	193536	-122557	105406	228138	-122732	0.04
5	66	300288	10221	238274	241920	-169619	109733	279475	-169742	0.02
6	66	355414	13191	295187	290304	-216820	113451	330339	-216888	0.01
7	66	410189	16425	352079	338688	-264087	116698	380799	-264101	0
8	66	464694	19896	408952	387072	-311368	119536	430864	-311328	0
9	830	519014	23622	470968	435456	-362958	121820	484821	-363001	0
10	1594	573187	27589	532961	483840	-414431	123825	538383	-414558	0.01
11	2357	627235	31769	594929	532224	-465792	125641	591642	-466001	0.02
12	3121	681176	36141	656872	580608	-517042	127301	644633	-517332	0.02
13	3884	735027	40692	718792	628992	-568181	128824	697374	-568550	0.03
14	14121	788726	45302	777131	677376	-606358	130936	737748	-606812	0.03
15	24356	842286	49952	835452	725759	-644617	132839	777997	-645158	0.03
16	34592	895747	54671	893757	774143	-682890	134582	818097	-683515	0.03
17	44827	949127	59464	952045	822527	-721154	136189	858049	-721860	0.04
18	69275	1002278	64109	997039	870911	-732288	140280	873234	-732954	0.03
19	93723	1055211	68588	1042029	919294	-743801	143899	888322	-744423	0.03
20	118170	1107999	72976	1087015	967678	-755548	147196	903321	-756125	0.03
21	142618	1160672	77307	1131998	1016062	-767463	150236	918232	-767996	0.02
22	173721	1213144	81451	1165866	1064446	-761996	156966	919432	-762466	0.02
23	204823	1265427	85406	1199735	1112829	-756908	163289	920605	-757316	0.02
24	235925	1317572	89232	1233606	1161213	-752090	169315	921746	-752431	0.01
25	267028	1369604	92956	1267477	1209597	-747486	175092	922860	-747768	0.01
26	298130	1421535	96594	1301351	1257981	-743073	180657	923948	-743291	0.01
Mean	66674	757316	45170	715651	653183	-499673	131499	631483	-499984	0.02

The water budget output for the average values for combinations of scenarios is shown in Figure 5.50 and Table 5.29. The gain in storage is lower for all stress periods. Losses in storage are higher from February to June and lower in January. River seepage (influent flow) increases throughout the stress period. These correspond to the wells abstraction that increases throughout the stress period. The changes in storage are negative throughout the stress period, these shows water loss from the storage from the floodplain aquifers for all the stress period.

5.5.9.3 High precipitation and low evaporation, high river water stages and low pumping rate.

This scenario is: high precipitation and low evaporation values recorded during the period January to June, 2012 for the flood event that occurred that year, high river water stages values recorded for the period January to June (1971 – 2012) and low pumping rates was set by multiplying the normal pumping rate (172.8 m^3/day) by 0.5 that is reducing the groundwater abstraction by half. The above informations were used to assess the hydraulic head across the floodplain alluvial aquifers.

The mass balance data, plotted in Figure 5.49C, shows that river seepage (influent flow) is the primary model input (1,122,747 m^3) representing 59.5% of the total inflow to the system and recharge from rainfall (703,855 m^3) represents 37.3% of the total inflow to the system. Input from the constant head boundaries (60,097 m^3) represents 3.2% of the total inflow to the system. Model outputs are dominated by model evapotranspiration (ET) (922,089 m^3) representing 59.5% of the total outflow from the system and groundwater abstraction by pumping wells (628,990 m^3) represents 40.5% of the total outflow from the system.

When losses from the model through model evapotranspiration (ET) and groundwater abstraction by pumping wells are subtracted from recharge from river seepage (influent flow), recharge from rainfall and recharge from the constant head boundaries, the amount that enters the floodplain aquifer system is ~335,620 m^3. Thus, the amount of groundwater recharge exceeds groundwater withdrawal. It was note that an increase of 73% of water recharge to the system than the water losses from the model. This shows that the high precipitation scenario values have a positive impact to the floodplain groundwater. Recharge to the aquifers raises the floodplain groundwater. The output suggests that the floodplain groundwater will sustainable for abstraction using hand-drilling techniques.

The water budget output for the high precipitation scenario is shown in Figure 5.50 and Table 5.30. The low rate of storage loss from January to April corresponds with the lower storage gain for the same time period, similarly higher storage gain in May and June correspond with the higher storage loss in May and June. River seepage (influent flow) increases throughout the stress period, which corresponds, with increase in water abstraction for irrigation throughout the modelled period. The changes in storage are negative for all the stress period, except June show positive change in storage. These shows water loss from the storage from the alluvial aquifers for all the stress period, except June, which shows water gain to the storage to the floodplain alluvial aquifers.

Table 5.30: The cumulative water budget for the modelling scenario 3 – High precipitation & low evaporation, high river water stages and low pumping rates

Stress period	Rainfall (m^3)	Influent (m^3)	Constant Head (m^3)	Evapotranspiration (m^3)	Well abstraction (m^3)	Balance (m^3)	Storage gain (m^3)	Storage loss (m^3)	Change in storage (m^3)	Error (%)
1	872	90600	991	31732	24192	36539	122526	85935	36591	-0.03
2	1743	152852	2644	63467	48384	45388	169172	123684	45488	-0.04
3	2615	207887	4459	95204	72576	47181	200816	153483	47333	-0.04
4	3487	258865	6405	126941	96768	45048	226232	180979	45253	-0.05
5	3487	307195	8561	166312	120960	31971	247692	215611	32081	-0.02
6	3487	353618	10940	205679	145152	17214	267069	249840	17229	0
7	3487	398568	13515	245042	169344	1184	284854	283749	1105	0.01
8	3487	442343	16267	284399	193536	-15838	301335	317347	-16012	0.02
9	9724	485147	19177	329314	217728	-32994	316765	349854	-33089	0.01
10	15961	527136	22229	374221	241920	-50815	331261	382093	-50832	0
11	22198	568429	25416	419123	266112	-69192	344886	414012	-69126	-0.01
12	28435	609121	28725	464018	290304	-88041	357771	445668	-87897	-0.01
13	34672	649286	32150	508907	314496	-107295	370005	477078	-107073	-0.02
14	69691	688806	35450	553737	338688	-98478	385335	483679	-98344	-0.01
15	104711	727709	38595	598570	362879	-90434	399833	490221	-90388	0
16	139730	766104	41662	643406	387071	-82981	413685	496708	-83023	0
17	174749	804054	44677	688244	411263	-76027	426979	503132	-76153	0.01
18	223259	841418	47412	716819	435455	-40185	462879	503132	-40253	0
19	271769	878208	49849	745401	459647	-5222	497898	503132	-5234	0
20	320279	914522	52083	773991	483839	29054	532232	503132	29100	0
21	368789	950418	54151	802589	508030	62739	565976	503132	62844	-0.01
22	435802	985790	55888	826469	532223	118788	622062	503132	118930	-0.01
23	502816	1020644	57291	850359	556414	173978	677289	503132	174157	-0.01
24	569829	1055060	58438	874259	580606	228462	731810	503132	228678	-0.01
25	636842	1089084	59365	898169	604798	282324	785706	503132	282574	-0.01
26	703855	1122747	60097	922089	628990	335620	839038	503132	335906	-0.01
Mean	179068	649831	32555	508018	326591	26846	418504	391587	26917	-0.01

5.5.10 Summary for the scenarios

It was observed that the high river water stages in River Benue with normal pumping rates have a positive impact on the floodplain water table. This suggests that the floodplain water table remains within reach with the hand drilling methods.

It was also observed that the low water levels in River Benue, high rate of groundwater abstractions during the dry season period and drought scenario leads to a significant fall in the floodplain water table.

In general, hand-drilling methods can only be used to abstract groundwater from the alluvial aquifer from depths of less than 40 m. If the groundwater table falls below 40 m, it will be very difficult to extract groundwater using hand-drilling techniques. However, in the present study, 20 m depth of impermeable layer was considered and this depth is within the limit of hand drilling. One of the measures, which could be taken, is to avoid excessive water abstractions from the floodplain. This could be controlled by the UBRBDA Yola.

The modelling simulations suggest that alluvial groundwaters are within the limit for abstracting with the hand drilling techniques at present. However, in the future, if the scenarios of low river water stages, high pumping rates and drought occur, then the hand drilling method is likely to be no longer suitable for abstracting floodplain groundwaters.

CHAPTER SIX - DISCUSSION

6.1 Introduction

This chapter discusses the results obtained from the surface elevation, sedimentological, hydrogeological and groundwater modelling work, as presented in previous chapters and this is in the frame of other similar research.

6.2 Elevation height

The surveyed elevation profiles of the floodplain indicate a higher elevation (see Figure 5.1) than the available topographic map (see Figure 2.1). The irregular variations in the heights between the topographic levels obtained from Upper Benue River Benue Development Authority (UBRBDA) and those one obtained in the field may have several causes: the differences in the surveying instruments used, the number of points surveyed and the evolution of the floodplain morphology in the time between the two surveys (38 years).

1) The survey instrument used by the UBRBDA was a theodolite ranging pole method, which gives high error reading. In contrast, the instrument used for the fieldwork is a more advanced surveying method, using a ProMark3 GPS dual frequency instrument that gives readings in vertical accuracy between 0.01 m (see Figure 3.1).

2) In addition, the present study was undertaken with a specific purpose that required a more dense point network than the general topographic map.

3) Several flood events were recorded in the past in the region, including those recorded in 1977, 1981, 1989, 1993, 2004 and 2012 (see Table 4.3). These flood events cause changes to the floodplain sediment deposition. The changes may include local erosion and/or deposition

on the floodplain. Therefore, understanding these differences in the surface elevations of the floodplain are important (Sander, 2001).

These will enable an up-to-date suitable topographic map of the floodplain to be generated, which is necessary for the groundwater model. As discussed in section 2.4.3, one of the criteria for assessing the suitability of the hand drilling techniques is the floodplain geomorphology. The floodplain surface elevation shown in Figure 5.1 is suitable for application using hand-drilling techniques.

Surface elevation could also help identify suitable locations to drill a well on the floodplain. Generally low elevations will be closer to the top of the aquifers. On the low surface, more infiltration of rainfall is possible to recharge the shallow alluvial aquifers, which can be abstracted with the hand drilling techniques. On the high surface, there is a longer distance between the ground surface and the top of groundwater.

6.3 Sedimentology

This section discusses the sedimentology of the alluvial floodplain sediment in the frame of other studies.

6.3.1 The particle size analysis of the alluvial floodplain

The River Benue is an example of braided stream (Miall, 1977), where the alluvial deposits are composed of fine-grained sand and sandy silt (see Figure 5.2). The sand-rich deposits may be formed in braided riverbed when sediment influx was high, especially from high flooding events (Brooks, 2003). Braided rivers typically have high flood velocities and material is transported during peak flow (Miall, 1977). Similar deposition processes were reported by Haschenburger and Cowie (2009) on the braided Ngaruroro River, New Zealand.

In that case, lateral migration and formation of coarser-grained layers during large floods are mechanisms that initiate floodplain development by the braided-rivers.

The sedimentology of the floodplain was found to vary considerably across the areas surveyed through resistivity sounding and coring. Distinct coarser sand units with differing sizes were revealed by the coring and resistivity sounding surveys (see Figures 5.24 to 5.29), indicating deposits with different sediment composition possibly from different migration patterns resulting from the river flows. River Benue has a large bed load as well as suspended load due to high flooding events and the 1977, 1981, 1989, 1993, 2012 flood events, and very high rainfall usually in August and September each year. This accounts for significant sediment transport. Part of these loads is deposited on the floodplain due to a very high discharge of the river, giving rise to thick sandy-silt sequences in the plains. Sinha (1995) reported similar causes for deposition on a semi-arid alluvial floodplain in North Bihar, India.

Marriott (1992) and Walling et al. (2004) reported that river outcrop sediments are consistently coarser, while sediment at a distance from river is finer. Their findings are contrary to what was observed in the present study, as the alluvial sediment depositions in the core tops are more complex. It varies spatially across the floodplain at different locations and depths (Figures 5.2). This is unsurprising as the studies by Marriott and Walling et al., were carried out on meandering rivers with single stable channels, whereas the Benue is a braised river system with unstable channels. For example, in the borehole tops at locations 8 and 11 (Figure 5.2) away from the River Benue, the majority of the sediments were coarse, with some fine sandy silt, which show flood deposits. The very coarse sediments of core borehole 8 shows the near-surface aquifer, while that of borehole 11 are representative of depressions created by Lake Geriyo Basin that occur between alluvial ridges (for location of Lake Geriyo see Figure 5.1).

Coarser sediments/soils dominated by sand and sandy silt are typically permeable and therefore transmit water easily. These types of sediments are a common feature of floodplain deposits as defined by Baker (1987). As reported by Grenfell et al. (2009) floodplain sediment are finer while river outcrop sediment are coarser because of the decrease in water energy away from the main flow. However, coarser alluvial sediments in the present study vary across the floodplain at different location and depth (see Figure 5.2, the floodplain sedimentology).

Hand drilling can only penetrate unconsolidated formations such as sand, sandy silt and clayey silt (see section 2.4.1). The floodplain sedimentology consists mainly of these types of formations. The floodplain sedimentology shows that the formations are suitable for the application of the low-cost hand drilling technique. This is because the floodplain sediment consists mainly of sandy silt formations as shown in Figure 5.2 (the visual sedimentology).

6.3.2 Loss on ignition (LOI) for the floodplain sediment

6.3.2.1 Moisture content loss to 105 ˚C

Despite the limitations previously highlighted, moisture content (MC) clearly increases with depth (see Figures 5.8 and 5.22) as expected. Because the samplings were carried out during the dry season and due to the high evaporation in the region, the top surface is drier while in the subsurface (a few metres deep), the sediment becomes softer as it approaches aquifer formations.

6.3.2.2 Loss on ignition at 550 ˚C

Variation in sediment LOI at 550 ˚C will reflect factors such as the trapping potential of the depositional environment (Dean, 1974, Heiri et al., 2001, Shuman, 2003, Santisteban et al., 2004, Volk and Costa, 2010, Beasy and Ellison, 2013).

Generally, the LOI at 550 ˚C are low (<10%) this may reflect loss of moisture bond within a clayey silt of the floodplain sediment (see Figures 5.10, 5.11 and 5.12). However, some locations have slightly higher amount of LOI at 550 ˚C (see Figure 5.11, location R.B. Cam, Figure 5.10, boreholes 7, 10 and 12). These locations tend to be relatively low in elevation. Locations that have low amount of LOI at 550 ˚C tend to be high at higher elevations (see Figure 5.10, locations boreholes 3, 4, 6, 8 and 10). The lowest LOI at 550 ˚C in the sediment were in locations away from the river (see Figure 5.10, locations Boreholes 4, 6, 8 and 10). The highest LOI at 550 ˚C in the sediment were in locations closer to the river with lower elevation (see Figure 5.10, location boreholes 3, 5 and 7). This LOI is thus presumably both influenced by a flow from the river, and accumulation of LOI at 550 ˚C in small wet depressions (as observed at boreholes 4, 6, 6 and 10 away from the river.).

Similar findings were reported by Asselman and Middlekoop (1995) and by Walling et al. (1997) where both studies observed less than 10% of LOI at 550 ˚C in sandy floodplain alluvial sediment on the River Ouse, UK. These two studies are consistent to what was observed in the present study.

Other possible causes for the low values of LOI at 550 ˚C in the alluvial sediment is the use of chemical fertilizer instead of organic manure, because using fertilizer will only supplement nutrient supply to crops (this chemical fertilizer leaves no residue). Also burning the irrigated land may contribute to low LOI at 550 ˚C in sediment, because the crop residue, which could decay thereby increasing the amount of LOI at 550 ˚C in the sediments, is burnt.

6.3.2.3 Loss on ignition at 950 ˚C

As reported by Obiefuna and Orazulike (2011b), the mineralogical composition of Yola Bima sandstone consists of quartz (65%), feldspars (14%), mica (9%), iron oxide (5%) and calcite

(3%). This calcite may be the source of the LOI at 950 ˚C in the alluvial floodplain sediments. However, the LOI at 950 ˚C is extremely low (<5%) and no trend is evident.

A study by Volk and Costa (2010) on alluvial floodplain sediment in Central Ohio, USA showed that total LOI at 950 ˚C values less than 5%, are interpreted to have essentially zero LOI at 950 ˚C. This finding is similar to what was obtained in the present study (Figures 5.10, 5.11 and 5.12). Therefore, the total LOI at 950 ˚C in the present sediment samples may be assumed to be close to zero.

6.3.3 Magnetic susceptibility

The statistical correlation shows that the magnetic susceptibility (MS) values are slightly higher in coarser sand and sandy silt sediments (see Table 5.8). This differences in the MS could be related to the process of sediment deposition by flooding (Dearing, 1999), though, some clayey silt sediments show higher values of the MS (see Figure 5.12, locations D, F and I; Figure 5.13, locations K, L, O and Q; Figure 5.15, location boreholes 1 and 5). The source of MS (whatever size it is) is largely the volcanic intrusions that are found upstream along Benue and Faro Rivers in Cameroon (see Figure 2.4). Fire resulting from burning the irrigated areas could also influence the amount of MS in the sediment of the floodplain. A study by Litton ans Santetices (2003) on the woodland area in Chile have shown the expected fire effects are concentrated in the top soil surface.

It was hypothesised before fieldwork that the volcanic fields found along Benue and Faro Rivers in Cameroon (see Figure 2.4) might have left a strong impact on the sediment of Benue and Faro Rivers in Cameroon that contributes sediment to the Nigerian portion of the river. However, it does not seem to be the case, because the MS is generally low in the alluvial sediments of the floodplain (see Figures 5.13, 5.14 and 5.15). The MS method tells us

the preliminary understanding of the floodplain alluvial sediment. The main result is the rather homogenous nature of the MS values, hence of the source of the sediment.

6.3.4 Field Shear Strength

The values of the preliminary field measurements using the Field Shear Vane Tester (FSVT) on the floodplain help establish places that are more suitable locations for drilling, especially using hand drilling method. The availability of equipment meant that it was only possible to examine the top 3 metres of floodplain soil and sediment. This is the first such study on the Benue floodplain.

No clear correlation between shear strength forces in relation to hand drilling exist in literature (see section 2.4.5). Some studies however report values of shear strength forces on the alluvial sediment in relation to the types of the *in-situ* sediment formations (for example Schjønning, 1986; Hubbell, 2003; Eijkelamp, 2009).

In the present study, the lower shear strength forces on floodplain sediment range between 15 and 95 kPa (see Figure 5.16), which is assumed to be within the limit for drilling with human power. The higher shear strength forces on the floodplain sediment are in the range between 100 and 160 kPa (see Figure 5.16), which is assumed to be slightly above the limit of force to be applied with human power. Perhaps these were drilled shortly after the wet season, when the soil was wetter and weaker. These assumptions are based on the ranges of the shear strength forces on the floodplain sediment obtained in the present study since there are no criteria in literature to support this assumption.

Currently hand made wells occur in all these areas, therefore also in areas about the recommended limit of 100 kPa. The relation of the shear strength forces to the hand drilling in the present study should be viewed as preliminary findings. Further studies are required to

know the cut off point for the shear strength forces on alluvial sediment in relation to the hand drilling method.

Sediment properties, particularly the floodplain sediment formations and location, appear to influence the variations in shear strength. For example, borehole location 5 (see Figure 5.16) closer to the river shows high shear forces on sediments despite moisture from the river. This is due to the nature of the sedimentary formation, which are mostly clayey silt and sandy silt in that particular core, and clayey silt and sandy silt formations tend to show slightly high shear strength because of their plasticity (Kilic et al., 2006). Similarly, borehole locations 8 and 11 at distances of 1,500 and 2,500 m away from the river respectively show low shear forces on sediments. This is due to mainly sandy sediment formation. Generally sandier formations show low shear strength, because sand sediments have less or even no plasticity.

The FSVT provides some useful information regarding the strength behaviour of the floodplain sediments, for example the identification of some possible zones and locations more suitable for the application of the low-cost hand drilling methods, in southeast, northwest and southwest (see Figure 5.17) on the floodplain. Identifying softer and harder zones and locations in the floodplain will give farmers an easies means of drilling for extracting groundwater for the irrigation activities.

The results from the research on the Benue floodplain show that hand drilling is taking place in parts of the floodplain where, according to the literature, shear strengths are close to the limits of suitability (>100 kPa) perhaps due to coring during the wet . It is necessary to note that any change towards harder sediment/soil will not allow further hand drilling but requires a move to motorised drilling.

6.4 Groundwater

This section discusses the results of the floodplain groundwater.

6.4.1 Resistivity soundings

Two studies by Nur and Kujir (2006) and Arabi et al. (2010) in the River Benue 10 km upstream of the study site used vertical electrical sounding (VES) to find groundwater along the floodplain. They obtained resistivity values between 600 and 896 Ωm. Their results are within the range of what was obtained in the present study.

The average resistivity of the surface, middle and saturated layers ranged from 160 to 328, 702 to 1,460 and 49 to 185 Ωm respectively (see Table 5.12 and Table E, Appendix E). Similar resistivity values in the range of 20 to 2862 Ωm were found by Okiongbo and Odubo (2012) in southern part of Nigeria on similar alluvial floodplain indicating a good groundwater potential. Khalil and Santos (2013) reported resistivity values on the alluvial floodplain of Wadi El Natrun, Egypt, which was similar to the alluvial floodplain in the present study. In their study three subsurface layers were observed using VES that show good groundwater potential.

The floodplain groundwaters explored here (between 5 and 20 m depth) were within the range for the application of the hand-drilling methods (see Figures 5.24 to 5.29). As reported in literature hand drilling techniques enable abstraction of shallow alluvial groundwaters to a depth of 40 m (RWSN, 2013; Weight et al., 2013).

6.4.2 Perched water tables

Although the identification of the perched aquifers is not directly related to the aims of the present study, it is a useful finding and is very important to the farmers. Perched aquifers are frequently observed on alluvial floodplains (see section 2.2.9.2). Park et al. (2007) identified

perched aquifers from VES along the alluvial floodplain of Geum River in semi-arid environments in Korea. Robinson et al. (2005) identified 33 perched aquifers along the semi-arid region of the Pajarito Plateau by using electrical geophysics and direct water-level measurements.

In the present study, Direct observation of water tables in drill holes and resistivity soundings were combined three possible perched aquifer formations were observed at boreholes 2 and 8, and resistivity location 22 (see Figures 5.30, 5.32 and 5.33). The anomaly observed at borehole 8 where drilling and resistivity were used, requires further investigation in order to justify the presence of perched aquifer in that location. Similarly, at location 22 it requires drilling to justify the existence of perched aquifer. The present data are somehow inconclusive to show the existence of perched aquifer in the floodplain. The anomalous resistivity values are possibly influenced by polluted water (see Table 2.5) which may have high resistivity values. However, the question remains to ask what might cause the contamination of water at that single location. This requires further investigation, especially at borehole 8 to check the water quality at that location.

6.4.3 Hydraulic conductivity

It was observed that the laboratory hydraulic conductivity for the alluvial sediments is lower than the field-determined average values (see Tables 1F and 2F in Appendix F). This is consistent with findings by Herzog and Morse (1984) and White (1988). The lower values, derived in the laboratory, for the hydraulic conductivity of alluvial sediments were for artificially compacted samples. The higher values for field permeability probably are due to the presence of fissures, as well as more permeable clean sand and gravel beds across the floodplain. However, laboratory samples remain a valuable source of material: as they were compacted in the same way, the data are comparable within the dataset.

The differences in the ranges arise from types of sediments formation in the floodplain. The presence of LOI at 550 ˚C in the sediments could also reduce the rate of flow: high amount of LOI at 550 ˚C in sediments lowers flow rate. However, the Benue sediments have low quantities of LOI at 550 ˚C and LOI at 950 ˚C (see Figures 5.0, 5.11 and 5.12). Therefore, it is expected to have a high rate of water flow through the alluvial floodplain. These will enable the recharge of the shallow alluvial aquifers of the floodplain for easy abstraction using the low-cost hand drilling methods. Wells in locations with high aquifer recharge produce more water than low recharging aquifers (MacDonald et al., 2009; Calow et al., 2011; MacDonald et al., 2011; Baffour et al., 2013).

As discussed in section 2.4.2, criteria for permeability suitability for hand drilling techniques is based on the permeable formations. The hydraulic conductivity values obtained from both laboratory and pumping test show high rates of water flow through the floodplain sediment.

The literature suggests that field hydraulic conductivity provides a better estimate than the laboratory hydraulic conductivity, because field hydraulic conductivity gives real groundwater flows (Taylor et al., 1987; Chimungu et al., 2010). Hence, in order to get better estimate for the rate of groundwater flow with the model the field hydraulic conductivity obtained by pumping tests was used.

The high hydraulic conductivity value of 4.01×10^{-1} m/s obtained in the present study is significantly higher than that reported by Zume and Tarhule (2011) of 7.52×10^{-4} m/s on a similar floodplain in Oklahoma, USA, and with those reported by Campos (2009) and Abdalla and Scheytt (2012) 4.05×10^{-4} m/s and 9.3×10^{-4} m/s respectively on the alluvial floodplain in semi-arid areas of Nile Basin in Egypt. The high value of hydraulic conductivity in the present study indicates that the alluvial sediments across the floodplain are permeable which allows high flow of water for recharging the shallow aquifers.

6.5 Linking sedimentology to the model

Any numerical model is an approximate representation of a field situation (Anderson and Woessner, 1992). A simple groundwater conceptual numerical model was developed (see Figure 6.1A) to represent a real situation of the floodplain groundwater system (see Figure 6.1B). The model however needs to assume that the floodplain is homogenous, i.e. groundwater flows uniformly through the system; while the real situation of the floodplain is often heterogeneous, i.e. groundwater flow is not uniform through the system. Quantifying parameter heterogeneity in the floodplain sediment is very difficult. The uncertainty that this heterogeneity may introduce to the floodplain groundwater is a divergence in the flow direction (Kumar et al., 2009).

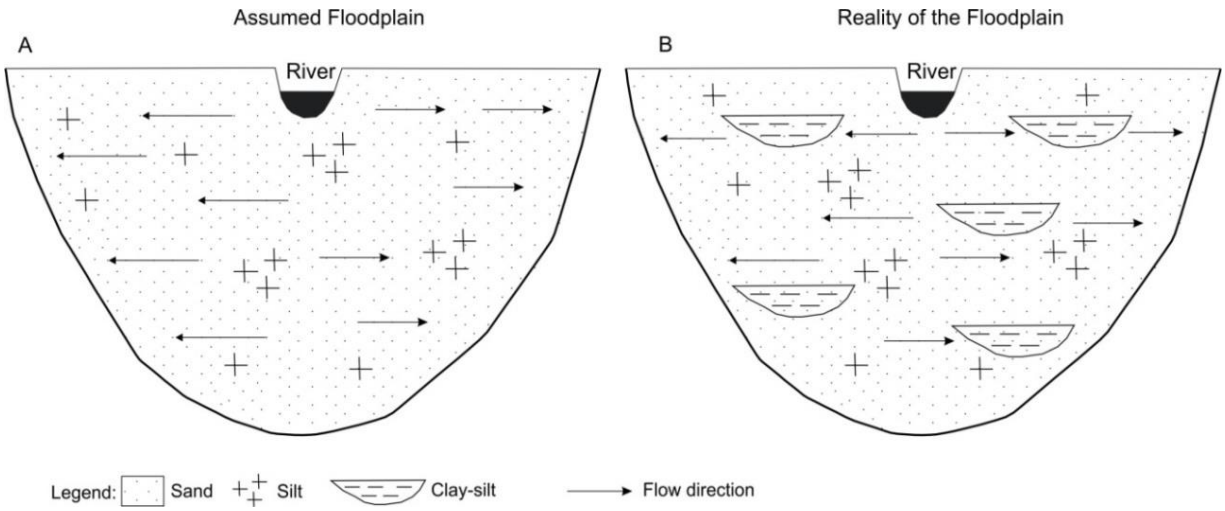

Figure 6.1: Schematic diagram showing assumed floodplain and field reality of the floodplain.

The following results from the field sedimentology survey were also used for the modelling process and show that the expected heterogeneity is minor.

a. The result of the particle size distribution of the floodplain are higher values for sand and sandy silt than clayey silt sediment, in the ratios of 46% sand, 52% sandy silt and 2% clayey silt (see section 5.3.2 particle size analysis result). This suggests that the

water flows through the system are rather homogenous since the sediment of the floodplain is coarse and this allows high flow of water through the system.

b. The hydraulic conductivity results obtained from both laboratory analysis and pumping tests revealed that the floodplain sediment formations have a high rate of water flow through the system (see Tables F1 and F2, Appendix F). This high values of hydraulic conductivity suggests that the floodplain sediment is permeable that allows high flow of water through the system for recharging the shallow alluvial groundwater.

c. The resistivity results obtained from the twenty four electrical soundings revealed the potentiality of the shallow alluvial floodplain aquifers (see Figures 5.24 to 5.29 resistivity soundings results). The potentiality of these shallow aquifers is an indication of homogeneity of the floodplain alluvial formations.

d. Magnetic susceptibility result reveals that the main source for the sediments in the floodplain is likely from sedimentary, and to some extend igneous, materials, upstream of the study site. The clustering of the data versus grain size shows that the floodplain alluvial sediments are from the same source (see Figure 5.21).

6.6 Groundwater model

All numerical groundwater flow models have limitations that are typically associated with the quality and quantity of data, assumptions and simplifications used to develop the model and the scale of the model. In the present study, some of the model data input was based on limited information and hence there were a number of assumptions. For example, assumptions were made concerning the quantities of groundwater abstracted by pumping wells and the riverbed conductance. Model calibration could also be affected by the distribution of the water level across the floodplain. The transient model does a reasonable

job of matching the groundwater level distribution in the alluvial floodplain. However, given the assumptions and limited data, it is unlikely that the model will fully represent local groundwater flows, although the model provides a reasonable insight into the groundwater system in terms of water budgets and groundwater flow directions. It should be viewed as a basic model that could be improved and needs more investigation to understand fully groundwater movement across the floodplain. Significantly, though, this is the first groundwater model developed for Adamawa Province in northeastern Nigeria.

The main direction of horizontal groundwater flow in the model is from northeast to southwest (see Figure 5.42, cross-section of the floodplain groundwater levels), from the River Benue towards the floodplain. This was expected from the conceptual model, as groundwater flows preferentially along the steepest hydraulic gradient (Bradley, 1996). The modelling covered the dry season period (January to June) only, with high water losses due to evaporation, and abstraction for irrigation lowered the floodplain water table. Therefore, it is expected that the direction of water flow is towards the floodplain from the river (the flow of the River Benue is perennial and the river flow is maintained by discharge from the Lagdo Dam upstream during the dry season period). A similar flow direction was observed on the floodplain of Helwan, Nile Basin in Egypt (Abdalla and Scheytt, 2012) where the direction of the groundwater flow is also towards the floodplain from the river.

In the process of model calibration, the two observation wells show slight differences between observed and modelled data at some stress periods (see Figure 5.41). These discrepancies are possibly due to numerical instability at the beginning of the model simulation as the initial heads were derived from head data observed in January to June 2012. It may also be attributed to the effects of intensive irrigation locally, and some discrepancies may arise due to errors in determining surface elevations across the floodplain.

This study has led to the successful development of a transient state groundwater flow model, which was calibrated against existing groundwater level data monitored locally in the floodplain (see Figure 5.37 the monitored water levels). The modelling results provide clear evidence of variations in the water seepage through the riverbed and the alluvial aquifer (see Figure 5.43, the volumetric water balance for the floodplain modelled area). The model is useful in quantifying water flow, and enabling the examination of specific scenarios that have important water resource implications.

Globally several groundwater studies using MODFLOW have been used for assessing the response of the alluvial aquifers in semi-arid floodplains environments. Zume and Tarhule (2011) investigated groundwater flow along alluvial floodplain in a semi-arid region of northwestern Oklahoma, USA. Their results showed that over-pumping and low precipitation lowers the groundwater table in the floodplain. Falke et al. (2011) also investigated impact of groundwater pumping in alluvial aquifers of a semi-arid floodplain of Arikaree River, eastern Colorado, USA, using MODFLOW, finding a reduction in the floodplain groundwater by 12 m during the dry season period. Dent et al. (2007) and Kulatunga (2009) assessed the groundwater using MODFLOW along alluvial floodplain of upper Murray-Darling Basin in a semi-arid area of Australia. They found that a combination of increased pumping and below average rainfalls in 2005 increased river leakage and decreased aquifer storage. Their findings are consistent with what was obtained in the present study, where river low water stages and over pumping from wells during the dry season period lowered the shallow alluvial aquifers on the floodplain beyond extraction with hand-drilling technique (see Figures 5.45A and 5.47A). Dawoud et al. (2005) and Mohammed and Hua (2010) used MODFLOW to model the groundwater flow along the alluvial floodplain semi-arid area of Western Nile Basin, Egypt. Their findings show that over-abstraction from wells lowers the floodplain groundwater by 20% of the floodplain water levels. Similarly, a lowering of

floodplain groundwater due to over-abstraction was observed on a semi-arid alluvial floodplain in the irrigation district of the upper Yellow River basin, China (Xu et al., 2011). This is consistent with what was observed from the pumping scenario in the present study (see Figures 5.47A). Baffour et al. (2013) used MODFLOW to simulate groundwater on the semi-arid floodplain of the Beseas Inland Valley in Ghana. Their results show a decline in simulated hydraulic heights in the dry season period by 0.2 m, which is consistent to what was obtained in the present study.

6.6.1 Groundwater – surface water interaction

The study developed a numerical model of the floodplain aquifer based on historical and fieldwork data gathered as part of this study, including water level monitoring (see Figure 5.37) and pumping tests data (see Table 5.14). The model was used to evaluate the potential impacts of recharge variability on River Benue aquifer dynamics and groundwater withdrawal, including stream – aquifer interaction.

The floodplain aquifers are mostly fed by seepage from the River Benue and locally fed by Lake Geriyo during the dry season. Simulated seepage to the floodplain alluvial aquifer was determined weekly (see Figure 5.31, for locations of River Benue and Lake Geriyo). The simulated river seepage (influent flow) to the floodplain is estimated at ~1,561,524 m^3 and groundwater discharge to the river is zero (see Figure 5.43, the volumetric water balance for the floodplain modelled area). The simulation was considered for the dry season period (January to June), at this time the floodplain alluvial aquifers mostly depend on the river seepage, and this was maintained by a dam built upstream in Cameroon. Lake Geriyo has water all the year round, partially contributing to the floodplain during the dry season period, the modelling results show that there is continuous flow from Lake Geriyo to the alluvial groundwaters occurs (see outputs from constant head in Figure 5.43).

6.6.2 Prediction of future conditions

The main scenario is that the seepage (influent flow) through the river bed to the alluvial aquifers during the peak dry season period may be influenced by factors such as 1) changes river regime (more or less water released) due to regulation of Lagdo Dam, 2) impact of increased groundwater abstraction by pumping wells for irrigation (due to population increase), and 3) impact of global climate change. Because in the study area surface waters are hydraulically connected with the floodplain Quaternary aquifer system, any change in the surface water inflow will lead to change in water level in this surface water body, which has direct impact on the floodplain groundwater.

The calibrated model is used for predicting future conditions of the water levels of the alluvial floodplain. Transient state groundwater flow was simulated for three different combinations of scenarios. These are discussed in the following sections.

6.6.2.1 River water stage scenario

Low-flow in the river during the dry season period has led to significant water-table drawdown in floodplains in semi-arid regions of Australia (McCallum et al., 2013). Similarly, a study by Ahmed and Umar (2009) showed that low river water stages led to a reduction in groundwater levels in shallow alluvial aquifers across the floodplain of the Uttar Pradesh River, India.

The low river water stage scenario shows much variation in hydraulic head across the floodplain (see Figure 5.45A). Water levels in the River Benue during the dry season are maintained by the Lagdo Dam located 250 km upriver of the catchment and this recharges the shallow alluvial aquifer. If this does not continue, low river water levels would have a significant impact on the shallow alluvial aquifers of the floodplain aquifer.

The likely consequence of this is that the floodplain water table would be lowered to a point where groundwater extraction using the low-cost hand drilling methods is no longer possible. This is the critical point for farmers. It was originally hypothesised that model simulations using low river stage would have a negative impact on the floodplain water table, and the results were as expected.

The high river water stage scenario shows positive impact contributing approximately 82.4% of the river seepage (influent flow) to the floodplain (see Figure 5.45C). This raises groundwater levels across the floodplain, making it easier for low-cost hand drilling to abstract the floodplain alluvial groundwater for irrigation.

A threshold was reached at low river water stages: negligible water inflow to the system was observed (see Figure 5.45A). This led to a critical depth (beyond 40 m deep) to abstract the shallow alluvial aquifers using the hand drilling techniques. This is consistent with what was modelled by Merz (2012) in the semi-arid of the Murray River Australia, reduced stream flows might reduce the recharge volume into aquifers via alluvial floodplains.

Elsewhere, the impacts of dam construction have been reported to pose a threat to groundwater levels downstream during the dry season period. Abu-Zeid and El-Shibini (1997) showed that the post construction of the Aswan High Dam in Egypt has caused a reduction of the floodplain groundwater level in the range of 0.7 to 0.3 m. Similarly, Sun et al. (2012) showed that the impacts of the Three Gorges Dam in China caused a severe reduction in groundwater level downstream in the range between 3.30 and 3.02 m.

In brief, the river water stage scenario result shows that if the Cameroon Government were to change the mode of operation of the Lagdo Dam, for example, by diverting flow to the other source, this will have a severe impact on the study site, since at low river water stages in River Benue during the dry season period, the floodplain groundwater abstraction is beyond

the limit with the hand drilling method as shown in Figure 5.45A. Therefore, the river water stage scenario shows that the shallow alluvial floodplain groundwater will be sustainable for abstraction using hand-drilling method if constant flow of water is maintained in River Benue during the dry season period.

6.6.2.2 Pumping rates scenario

Groundwater abstraction has led to a reduction of baseflow in different semi-arid regions worldwide (Winter et al., 1998). Rai and Manglik (2012) showed that pumping rates have significant effects on the floodplain groundwater table. Over-exploitation produced stress on the sustainability of groundwater systems in arid and semi-arid regions (Vrba and Gun, 2004; Shamsudduha et al., 2011; Huang et al., 2013).

The model simulations indicate that any reduction in groundwater abstraction rates will have a positive impact on the alluvial aquifer (see Figure 5.47C). When the floodplain water levels are higher, groundwater abstraction is easier for farmers. However, when abstraction rates are increased, both the river levels and the floodplain water table fall (see Figure 5.47A) to points below which continued abstraction is no longer possible via the hand drilling methods. This is the critical depth for the farmers as hand drilling can only abstract the shallow groundwater of the alluvial floodplain to depths not exceeding 40 m below the surface (RWSN, 2012 and 2013). This poses a threat to the sustainability of irrigation. The Upper Benue Authorities should monitor this threat very closely.

The pumping well scenario was simulated at three different pumping rates in order to find a threshold. Simulation at a decrease of 50% pumping rate showed a decrease of 82.4% of water flow to the system (see Figure 5.47C). Simulation at an increase of 100% pumping rate showed significant fall of the floodplain groundwater (see Figure 5.47A), where a threshold

was observed. At this threshold, the floodplain water table falls to the points below which continued abstraction is no longer possible via the low-cost hand drilling methods.

Elsewhere, there are examples of instances where this threshold has been exceeded: over-exploitation of groundwaters in semi-arid regions of eastern Ethiopia has influenced aquifers across the floodplain (Alemayehu et al., 2007) and similarly, in a semi-arid alluvial floodplain aquifer in India (Rejani et al., 2008). Van Oel et al. (2013) showed that over-pumping lowered the groundwater level by 0.8 m on the alluvial floodplain in semi-arid of Kenya. Similarly, Arabi (2012) showed that over-exploitation lowered the shallow alluvial aquifers along the western floodplain in Nile Basin of Egypt.

Therefore, in order to continually use the low-cost hand drilling methods for abstracting the shallow alluvial groundwater across the floodplain, high pumping rates should be reduced. Alternatively, the amount of water being pumped from wells should be controlled and water wastage should be minimised. Farmers should be advised on how to use the water properly according to their irrigated crops demand for sustainability of the floodplain shallow alluvial aquifers.

6.6.2.3 Global climate change scenario

Globally the impact of climate change has led to a reduction of the alluvial floodplain shallow groundwater in many semi-arid environments (Zume and Tarhule, 2011). In a study by Kirby et al. (2013), working on the floodplain of Murray-Darling Basin, Australia, showed that climate change decreased groundwater level by 12%. Cao et al. (2013), working on an alluvial floodplain in the semi-arid area of North China, reported that climate change has led to depletion of the groundwater by 4 m per year. A similar study by Virdi et al. (2013) reported that climate change had led to the reduction of the alluvial floodplain groundwater by 70% per year in the semi-arid area in North America, U.S.A. This suggested that the

impact of the climate change has been the cause of depleting the alluvial floodplain shallow groundwater in many arid and semi-arid environments around the world.

In the present study, despite a minor increase of precipitation in the last few years (see Chapter Four) and a minor increase of precipitation forecasted by IPCC 2013, droughts remain very likely and are included as one of three possible scenarios. The present study site is indeed close to the Sahel region, which is prone to droughts.

It is hypothesised that simulating the drought data could show a greater negative impact on the floodplain by lowering the floodplain water table to depths beyond which continued groundwater extraction using hand drilling method becomes no longer possible. The results (see Figure 5.49A) show severe negative impact to the floodplain. The simulation shows that both the river levels and the floodplain water table fall (see Figure 5.49A) to points below which continued abstraction becomes no longer possible through the hand drilling methods. However, the scenario with high precipitation shows that the floodplain shallow alluvial groundwater will not fall below abstraction with the hand drilling techniques.

The model shows severe negative impacts in the region. The global climate change scenario shows that the shallow alluvial floodplain groundwater will only be in the limit of abstraction with the hand drilling if no droughts (even only one year long) occur in the region.

6.7 Long-term sustainability of the floodplain groundwater resources

The following are measures to be taken for the long-term sustainability of the floodplain shallow alluvial aquifers use for the application of the hand-drilling methods.

1. Water flow in the River Benue recharges the floodplain groundwater particularly during the dry season period. However, an obvious need to have a mutual agreement between the Cameroonian and Nigerian Governments exists in order to allow a

constant release of water from Lagdo Dam to maintain flow in River Benue (see section 2.3.2.2). Constant flow in River Benue will contribute to ensure the future sustainability of the floodplain groundwater.

2. During the fieldwork survey campaign, it was observed that some farmers are over-exploiting the shallow groundwater of the floodplain, in excess of what their crops need (see section 3.5.3, paragraph 4). Enforcement of some regulatory measures by the Upper Benue Basin Authority is needed on River Benue groundwater pumping to avoid misuse of groundwater resources of the floodplain. However, normal pumping rates for abstracting the floodplain groundwater will ensure the sustainability of the floodplain groundwater.

3. The present research has obtained useful findings from the floodplain sedimentology, groundwater and modelling. However, delivering the findings to the farmers is of paramount importance. The Upper Benue River Basin Development Authority with the head office in Yola is responsible for the management of Lake Geriyo Irrigation Project the study site. Since at the beginning of this research work, I was in contact with the authority for advice and collection of meteorological and hydrological data (see Chapter Four). The findings of this research work will be passed on to the authority of the Upper Benue Basin, Yola and the authority will then disseminate the information to the farmers.

6.8 Type of hand drilling technique

Among the various types of the hand drilling techniques discussed in the literature (see section 2.5), augering and jetting methods are already being used by the farmers for irrigation. Based on the assessment and interview with the farmers during the fieldwork survey (see section 3.4.1.2, paragraph 1), more farmers preferred the augering technique than

the jetting method. This is because the augering method requires only human power for the drilling operation, which could easily be affordable to the irrigation farmers. In comparison the jetting technique, being more mechanical, requires a pumping machine for the operation, which is often too expensive to the irrigation farmers.

Other techniques, for example, hand percussion, sludging, Rota sludge, Baptist drilling, EMAS hand-drilling, Banka hand drilling, pounder rig and Water for all International (see section 2.5) could also be applied on the alluvial floodplain of River Benue.

It is important to note that the farmers are already working to the limit of the usability of the augering method in the dry season, which is the season for drilling and that any change towards harder sediment will require the need to change to motorised drilling.

CHAPTER SEVEN - CONCLUSIONS AND RECOMMENDATIONS

7.1 Introduction

This chapter presents the key findings in relation to the aims of the research as well as the conclusions and recommendations from the results obtained from the surface elevation, sedimentology, groundwater investigation and groundwater modelling along the alluvial floodplain. The study represents the first investigation of its type in the Upper Benue Basin, NE Nigeria, for the application of the hand-drilling techniques. The study also, for the first time, assesses the groundwater sustainability along the floodplain of the alluvial shallow aquifer by understanding how and why irrigation by hand drilled wells work as well as what are the threats by modelling the groundwater resource and considering different drilling techniques and extraction scenarios.

7.2 Key findings

The aims of this research work were to assess the suitability for hand drilling techniques, the best methods for water abstraction in the floodplain and the sustainability of water resources of the floodplain.

7.2.1 Suitability for hand drilling techniques

Suitability of hand drilling techniques is based on the geological, permeability, water depth, geomorphological and shear strength requirements. Geological suitability is related to the types of sediment present. Hand drilling techniques are suitable only on unconsolidated sediment formations such as soft sand, silt and clay (see section 2.4.1). The floodplain sediment consists mainly of sand and sandy silt formations (see section 5.3.1, Figure 5.2 visual floodplain sedimentology) that are potentially very suitable for application of hand drilling techniques. Suitability based on permeability is related to the types of sediment that

allows free flow of water to recharge the floodplain aquifers. Sand and sandy silt formations are dominant across the floodplain (see Figures 5.2, 5.3, 5.4, 5.5 and 5.6), which are permeable formations and allow easy flow of water through the formation to recharge the shallow alluvial aquifer. Suitability according to the water depth is related to the depth where the floodplain groundwater level can be exploitable and reached by hand drilling. Hand drilling techniques are suitable when exploiting the floodplain groundwater usually not deeper than 40 m deep (RWSN, 2013). The floodplain groundwater obtained from both drilling logs and resistivity soundings ranges between 5 and 20 m depth (see section 5.4.1, Figure 30). The depths of the groundwater levels across the floodplain are therefore currently within the depth for abstraction with the hand drilling techniques. Geomorphological suitability is related to the surface elevation of the floodplain. Low lying surfaces and areas that are relatively flat, as the case in the present study, are suitable for hand drilling to abstract the shallow alluvial aquifers.

7.2.2 Identification of suitable zones along the floodplain

The Field Shear Vane Tester has identified some more suitable locations/zones (see Figure 5.17) along the floodplain for the application of the low-cost hand drilling method. This will ease drilling using the hand drilling for abstracting shallow groundwater from the alluvial aquifers, especially during the dry season period. In the present study, the lower shear strength forces on floodplain sediment (between 15 and 95 kPa, see Figure 5.16) are assumed to be within the limit for drilling with human power. The higher shear strength on the floodplain sediment (between 100 and 160 kPa, see Figure 5.16), are assumed to be slightly above the limit of force to be applied with human power. This indicates that the augering method presently used has probably reached its limit in several locations. Any increase in the shear strength requirements would force the farmers to use more powerful, but also more costly, drilling equipment.

7.2.3 Possible perched aquifer formation

The discovery of possible perched aquifers in the floodplain is detrimental to the farmers. The research has identified perhaps as much as three possible perched aquifer formations between 6 and 7 m depth (see Figures 5.30, 5.32, 5.33 and Table 5.13). They may mislead the farmers, as their yield would be short term only.

7.2.4 Sustainability of water resources of the floodplain

Although, at present, augering is a suitable method to extract the floodplain groundwater for irrigation, the present research explains why, in the future, the hand drilling method may not remain sustainable. Three types of threat have been identified:

a. Low water stages in River Benue during the dry season period due to the operation of the Lagdo Dam upstream (see Figure 5.45A). This could lower the floodplain groundwater beyond the extraction by depth achievable by low-cost hand drilling methods.

b. Over pumping of the floodplain shallow alluvial aquifers during the dry season period for domestic use and irrigation activities due to population increase (see Figure 5.47A). This may lower the floodplain groundwater beyond extraction with the augering method.

c. The drought scenario (see Figure 5.49A) has severe negative impact to the alluvial floodplain groundwater. This will lower the floodplain groundwater beyond extraction with the low-cost hand drilling method.

d. In addition in these three scenarios, an indirect impact will be the drying of the soil surface leading to increased shear strength and hence less suitable conditions for drilling.

7.3 Conclusions

The following are conclusions derived from the initial objectives of this study.

The first objective of this study was to scientifically characterise the sedimentology of cores and of River Benue outcrops using laser granulometry and examine why they are suitable for the application of the low-cost hand drilling techniques. This was achieved as follows:

- The particle size distribution of the alluvial floodplain revealed that the sediments consists more of sand and sandy silt deposit formations than clayey silt, with an average ratio of 46% sand, 52% sandy silt and 2% clayey silt (see section 5.3.2). These types of sediments are suitable for hand drilling techniques. Moreover sand and sandy silt formations readily allow groundwater flow to recharge the floodplain's shallow alluvial aquifer and easy drilling using the low-cost hand drilling methods for abstracting the shallow alluvial aquifers on the floodplain. Although farmers are already drilling on the alluvial floodplain, no scientific studies of the alluvial sediment are available to show its suitability for hand drilling method. The present study has highlighted a concern with the shear strength presently required. The values obtained are often above the range normally recommended for hand drilling.

The second objective of this study was to quantify the maximum drilling depths required for irrigation at the peak period of the dry season for the application of hand drilling techniques. This was achieved as follows:

- The maximum depth to the aquifer formations on the alluvial floodplain ranges between 5 to 20 m deep (see Figure 5.2 the alluvial floodplain sedimentology) during the dry season period. The shallow alluvial groundwaters in the wells were also compared to resistivity soundings (see Figures 5.24 to 5.29 resistivity soundings results). These depth ranges (5 – 20 m) are within the limit of the hand drilling method for abstracting the

groundwater on the floodplain. As reported by RWSN (2012), the hand drilling methods can abstract the shallow aquifers of the alluvial floodplain up to depth of 40 m deep.

The third objective of this study was to critically compare the types of sediment in the floodplain to the aquifer potential for the application of hand drilling techniques. This was achieved as follows:

- The integration of sedimentological log data with surface geoelectric studies (see Figures 5.24 to 5.29) delineates the aquifer potential across the floodplain and provides continuity for understanding the subsurface location of the shallow aquifer systems.

The fourth objective of this study was to establish the hydrogeology of the floodplain to improve the planning and effectiveness of abstraction sites for irrigation of the low-cost hand drilling techniques. This was achieved as follows:

- The hydraulic conductivity obtained from both pumping tests and laboratory analysis (see Tables F1 and F2, Appendix F) has shown that the sediments of the floodplain alluvial aquifers are permeable, and these allowed free flows of water through the formations to recharge the aquifer system. One of the requirements of hand drilling is that the formation should be permeable for easy pumping from wells. Mean hydraulic conductivity of $1.18\ 10^{-1}$ m/s across the alluvial floodplain (see Table 5.14), which suggests that the floodplain sediments are suitable in terms of permeability criteria.

The fifth objective of this study was to develop a transient state model and calculate the water balance of the floodplain. This was achieved as follows:

- A transient numerical model was developed and calibrated against two monitored wells in the floodplain located 500 and 1,000 m from River Benue and returned reasonable estimates of hydraulic heads along the model transects (see Figure 5.41). The results indicate that the river seepage (influent flow) is the primary source of inflow to the

modelled aquifer (~75.6%), and under normal pumping conditions, groundwater discharge by the pumping wells constitutes the largest outflow from the aquifer (~57.5%) (see Figure 5.43).

The sixth objective of this study was to quantify the flux exchange between the groundwater and the river in the groundwater – surface water interaction. This was achieved as follows:

- The exchange of flow between the floodplain aquifer and the River Benue has been modelled to find out the flux exchange between the shallow alluvial aquifers of the floodplain and River Benue. The interaction mainly depends on the difference of the water in the river water stages and the floodplain. The simulated seepage to the floodplain alluvial aquifer was determined on a weekly basis. The simulated river seepage (influent flow) to the floodplain is ~425,958 m^3 and groundwater discharge to the river is zero (see Figure 5.45A).

The seventh objective of this study was to critically examine long-term water level variations in the alluvial aquifer of the floodplain and their relationship to climate conditions. This was achieved as follows:

- The predictive scenario was simulated for the regional climate change. The impact of this scenario on groundwater levels and stream – aquifer interactions was compared with the current situation (using observed data). The results show that the drought scenario shows an immediate severe negative impact to the alluvial floodplain groundwater (see section 5.5.9.1, Figure 5.49A). The drought scenario showed groundwater withdrawal exceeded rates of groundwater recharge, reducing water-tables below the limit of groundwater abstraction achievable using the hand drilling method.

The eighth objective of this study was to critically assess how the operation of the Lagdo Dam in Cameroon upstream and abstraction rates will influence the water table of the floodplain. This was achieved as follows:

- Two predictive scenarios were simulated: i. decreased river stage; and ii. increased groundwater abstraction. The results of these two scenarios (river stage and groundwater abstraction) indicate negative impacts on the floodplain aquifer (see Figures 5.45A and 5.47A). These scenarios lower groundwater levels beyond that where abstraction using the hand drilling is possible.

In summary, the information obtained is going to be relevant to the development of an effective water scheme for irrigation activities along the floodplain and possibly beyond nearby areas underlain by similar geological formation, and it will constitute a background information and useful guide for a more elaborate groundwater development programme in the area, such as those planned by the Upper Benue River Basin Development Authority, Yola. Any shift in the floodplain will have to take in account unconfined and confined aquifers, climate change and any possible changes in the management of the Lagdo Dam, which is presently out of the control of Nigeria.

7.4 Recommendations

This section presents the recommendations for new research questions for future studies in the study area and other similar alluvial floodplain, and some specific recommendations for the farmers.

7.4.1 New research questions

This study provides considerable insights into the sedimentology and hydrogeology of the floodplain, and water budgets and groundwater flow directions during the dry season period (January to June) and reaches useful findings from the scientific point of view. Further study in the future is nevertheless required on the floodplain sedimentology and groundwater modelling and will be useful to the Lake Geriyo Irrigation Project, Yola and similar alluvial floodplains.

1. Further studies are needed to obtain more data on shear strength distribution in the alluvial floodplain. Shear strengths were obtained to 3 m depth on the alluvial of the floodplain. However, it would be appropriate to determine shear strength to the maximum depth reached by augering hand drilling, i.e. at 18 m depth, to become immediately relevant to the choice of the drilling equipment.

2. In the present study, shear strength forces on the floodplain in relation to the hand drilling techniques were only based on the value range of the shear strength forces on the floodplain sediment. This is because no information in literature is available to show correlation of shear strength forces in relation to hand drilling. A study to establish a good correlation of shear strength forces in relation to hand drilling is required. New shear strength measurements should be made in a way that can be more directly useful for estimating shear strengths required for hand drilling method, such as using a vane mimicking a drill bit.

3. There are variations in the hydraulic conductivity values at different borehole locations in the field; this could be due to limited numbers of tested wells. This may be improved with more pumping tests, which may provide a more precise estimate for the aquifer parameters of the floodplain.

4. Much more work is required to reach conclusive data on the possible presence of perched aquifers, especially to explain the contradiction in borehole site 8 and to compute data by a well in resistivity 22 site (see Figures 5.30, 5.32 and 5.33).

5. No observed quantitative data are available on groundwater abstraction by pumping wells for irrigation. Therefore, they were not sufficiently precisely estimated in the model. Such data are essential to estimate the significance of groundwater abstraction relative to groundwater balance and to predict the effect of groundwater abstraction on groundwater levels of the floodplain.

6. Groundwater level measurements were only obtained for a three year period. However, groundwater level measurement by piezometer installation should continue in order to obtain longer term records of groundwater level changes on the floodplain as inputs to a groundwater model and monitor trends.

7. This study only considered one layer modelling. In order to more accurately quantify the groundwater source along the floodplain, two, three and four layer modelling is needed.

8. The present study has not considered soil water balance of the floodplain. Future studies to model the floodplain soil water balance are required.

7.4.2 Recommendations for the farmers

The following are recommendations for the farmers and the Upper Benue River Basin Development Authority (UBRBDA) for proper utilisation of the floodplain groundwater.

1. In the floodplain, many boreholes fail after a short period of use (see section 3.4.1.2, paragraph 3). This may be due to possible perched aquifer locations. Therefore, the farmers using the wells in those locations should be advised to drill their tube wells deeper in order to get to actual groundwater level, which will be longer lasting.

2. Farmers are advised to utilise the floodplain groundwater according to their crop demand (see section 3.5.3, paragraph 4). Excessive over-exploitation of the shallow alluvial aquifers will lower the floodplain groundwater beyond extraction by the hand-drilling techniques, especially in dry years, and increase shear strength.

REFERENCES

Aas, G., Lacasse, S., Lunne, T. and Høeg, K. (1989) "Use of in situ tests for foundation design on clay". *Proceedings in Situ 86 use of in situ tests in Geotechnical Engineering, ASCE, New York*, pp. 1 – 30.

Abaje, I.B., Ati, O.F., Iguisi, E.O. and Jidauna, G.G. (2013) "Droughts in the Sudano-Sahelian Ecological Zone of Nigeria: Implications for Agriculture and Water Resources Development". *Global Journal of Human Social Science Geography, Geo-Sciences and Environmental*, vol. 13, no. 2, pp. 1 – 10.

Abbott, R. (2005) "Loss on ignition (LOI) procedures". *S.O.P – Loss on Ignition*, pp. 1 – 5.

Abdalla, F.A. and Scheytt, T. (2012) "Hydrochemistry of surface water and groundwater from a fractured carbonate aquifer in the Helwan area, Egypt". *Journal of Earth System Science*, vol. 121, no. 1, pp. 109 – 124.

Abu-Hassanein, Z., Benson, C. and Blotz, L. (1996) "Electrical Resistivity of Compacted Clay". *Journal of Geotechnical Engineering*, vol. 122, no. 5. pp. 397 – 406.

Abu-Zeid, M.A. and El-Shibini, F.Z. (1997) "Egypt's High Aswan Dam". *Water Resources Development*, vol. 13, no. 2, pp. 209 – 217.

Adanu, E.A. (1991) "Sources and recharge of groundwater in the basement terrain in the Zaria-Kaduna area, Nigeria: applying stable isotopes". *Journal of African Earth Sciences*, vol. 13, no. 2, pp. 229 – 234.

Adebayo, A.A. (1997) "The Agroclimatology of Rice Production in Adamawa State". *Ph.D. Thesis, Department of Geography. Federal University of Technology, Minna, Nigeria*, pp. 1 – 356.

Adebayo, A.A. (1999) "Climate: Sunshine, Temperature, Evaporation and Relative Humidity. In Adamawa State in Maps, Edited by Adebayo and Tukur". *Paraclete publisher, Yola, Nigeria*, pp. 20 – 26.

Adebayo, A.A. and Tukur, A.L. (1999) "Adamawa State in Maps". *Paraclete publishers, Yola, Nigeria*. pp. 1 – 112.

Adebayo, A.A. and Umar, A.S. (1999) "Hydrology and Water Resources: In Adamawa State in Maps, Edited by Adebayo and Tukur". *Paraclete publisher, Yola, Nigeria*, pp. 17 – 19.

Adejumo, T.E. (2012) "Shear Strength parameters of organic clay soils of Ikoyi, Lagos Nigeria". *Electronic Journal of Geotechnical Engineering*, vol. 17, pp. 2135 – 2144.

Adekile, D. and Olabole, O. (2009) "Hand Drilling in Nigeria". *Why kill an ant with a sledgehammer. Rural Water Supply Network. Field Note. UNICEF*, vol. 1, pp. 3 – 7.

Adelana, S.M.A., Olasehinde, P.I. and Bale, R.B. (2008) "An overview of the geology and hydrogeology of Nigeria". *In Applied Groundwater Studies in Africa Edited by Adelana and MacDonald*, pp. 171 – 197.

Afolaya, A.A. and Adelekan, I.O. (1998) "The role of climatic variations on immigration and human health in Africa". *The Environmentalist*, vol. 18, pp. 213 – 218.

Ahmed, I. and Umar, R. (2009) "Groundwater flow modelling of Yamuna – Krishni interstream, a part of central Ganga Plain Uttar Pradesh". *Journal of Earth System Science*, vol. 118, no. 5, pp. 507 – 523.

Aizebeokahi, A.P. (2011) "Potential impacts of climate change and variability on groundwater resources in Nigeria". *African Journal of Environmental Science and Technology*, vol. 5, no. 10, pp. 760 – 768.

Ajami, H., Meixner, T., Maddock, T., Hogan, J.F. and Guertin, D.F. (2011) "Impact of land-surface elevation and riparian evapotranspiration seasonality on groundwater budget in MODFLOW models". *Hydrogeology Journal*, vol. 19, pp. 1181 – 1188.

Akkeringa, J. E. (2006) "A reliable Banka".*GeoDrilling International*, pp. 1 – 2. Available online at http://www.conrad-stanen.com/Banka. Last accessed on 5th December 2010.

Alemayehu, T., Furi, F. and Legesse, D. (2007) "Impact of water over-exploitation on highland lakes of eastern Ethiopia". *Environmental Geology*, vol. 52, pp. 147 – 154.

Al-Fares, W. (2011) "Contribution of the geophysical methods in characterising the water leakage in Afamia B dam, Syria". *Journal of Applied Geophysics*, vol. 75, pp. 464 – 471.

Ali, A., Ahmadou, D., Mohamadou, B.A., Saidou, C. and Tenin, D. (2010) "Determination of Minerals and Heavy Metals in Water, Sediments and Three Fish Species (Tilapia nilotica, Silurus glanis and Arius park ii) from Lagdo Lake, Cameroon". *Journal of Fisheries international*, vol. 5 no. 3, pp. 54 – 57.

Alkali, A.G. (1995) "River-Aquifer Interaction in the Middle Yobe River Basin, North East Nigeria". *PhD Theses, Silsoe College, Cranfield University.*

Allen, D.M., Mackie, D.C. and Wei, M. (2004) "Groundwater and climate change: A sensitivity analysis for the Grand Forks aquifer, southern British Columbia". *Hydrogeology Journal*, vol. 12, pp. 270 – 290.

Allen, J.R.L. and Thornley, D.M. (2004) "Laser granulometry of Holocene estuarine silts: effects of hydrogen peroxide treatment". *The Holocene*, vol. 14, no. 2, pp. 290 – 295.

Allen, T. (1997) "Particle size measurement". Volume 1, 5th edition". *London: Chapman and Hall.*

Alley, W.M., Reilly, T.E. and Franke, O.E. (1999) "Sustainability of groundwater resources". *US Geological Survey Circulation*, pp. 1 – 1186.

Allix, P. (1983) "Environments me'sozoiques de la partie nord-orientale du fosse dela Benue (Nigeria)".*Stratigraphe, sedimentologie, evolution geodynamique. Trav. Lab. Sci. Terre, St. Jerome, Marseille* (B), vol. 21, pp. 1 – 200.

Alvarez, M.D.P., Travatto, M.M., Hermández, M.A. and González, N. (2012) "Groundwater flow model, recharge estimation and sustainability in an arid region of Patagonia, Argentina". *Environmental Earth Science*, vol. 66, pp. 2097 – 2108.

Amogu, O., Descroix, L., Yero, K.S., Breton, E.L., Mamadou, I., Ali, A., Vischel, T., Bader, J.C., Moussa, I.B., Gautier, E., Boubkraoui, S. and Belleudy, P. (2010) "Increasing River Flows in the Sahel". *Water*, vol. 2, pp. 170 – 199.

Anderson, E.K. and Brakenridge, R.M. (2007) "Nigeria and Cameroon – Benue River – Rapid Response Inundation Map 1". *Fl-2007-000141-NGA*. Available online at http://www.reliefweb.nit/rw/RWB.NSF.Last accessed on 29th January 2011.

Anderson, M.P. and Woessner, W.W. (1992) "Applied groundwater modelling, Simulation of flow and Advective transport". *Academic Press, San Diego*, pp. 1 – 381.

Anderson, M.P. and Woessner, W.W. (2002) "Model execution and the calibration process". *Applied Groundwater Modelling*, pp. 214 – 274.

Anderson, P.F. (1993) "A manual of instructional problems for the U.S.G.S MODFLOW model". U.S. *Environmental Protection Agency*.

Ankidawa, B.A. (2011) "Prediction of flood return period in Adamawa State, Nigeria". *LAP LAMBERT Academic Publishing GmbH& Co. KG Dudweiler Landstr, 99,66123 Saarbrucken, Germany*, pp. 1 – 62.

Apata, T.G., Rahji, M.A.Y., Samuel, K.D. and Igbalajoli, O.A. (2009) "The Persistence of small farmers and poverty levels in Nigeria: An Empirical Analysis". *III EAAEE-TAAE Seminar Small Farms: decline or persistence, University of Kent, Canterbury, UK.*

Arabi, N.E. (2012) "Environmental management of groundwater in Egypt via artificial recharge extending the practice to soil aquifer treatment (SAT)". *International Journal of Environmental and Sustainability*, vol.1, no.3, pp. 66 – 82.

Arabi, S.A., Dewu, B.B.M., Muhammad, A.M., Ibrahim, M.B. and Abafoni, J.D. (2010) "Determination of weathered and fractured zones in part of the basement complex of north-eastern Nigeria". *Journal of Engineering and Technological Resources*, vol. 2, no. 11, pp. 213 – 218.

Ariyo, S.O. and Adeyemi, G.O. (2009) "Role of Electrical Resistivity Method for Groundwater Exploration in Hard Rock Areas: A case study from Fidiwo/Ajebo Areas of South-western Nigeria". *The Pacific Journal of science and Technology*, vol. 10, no. 1, pp. 483 – 486. Available online at http://www.akamaiuniversity.us/PJST.htm.Last accessed on 29th March 2011.

Arsenault, N. Rose, C., Azulay, A. and Phillips, J. (2007) "People and place curriculum resources on human-environment interactions". *Hemispheres*, pp. 39 – 56.

Arshad, M., Cheema, J.M. and Ahmed, S. (2007) "Determination of lithology and groundwater quality using electrical resistivity survey". *International Journal of Agricultural Biology*, vol. 9, pp. 143 – 146.

Asfahani, J. (2013) "Groundwater potential estimation using vertical electrical sounding measurements in the semi-arid Khanasser Valley region, Syria". *Hydrological Science Journal*, vol. 58, no. 2, pp. 468 – 482.

Ashafa, T. (2009) "Mineral Resources of Adamawa State": *Napad Adamawa,* pp. 1. Available on line at. http://www.nepadadamawa.org/adamawa-state/mineral-resources. Last accessed on 20th November 2010.

Asselman, N.E.M. and Middlekoop, H. (1995) "Floodplain sedimentations, quantities, patterns and processes". *Earth Surface Processes Land*, vol. 20, pp. 481 – 499.

Ati, O.F., Iguisi, E.O. and Afolayan, J.O. (2007) "Are WE Experiencing Drier Conditions in the Sudano-Sahelian Zone of Nigeria". *Journal of Applied Science Research*, vol. 3, no. 12, pp. 1746 – 1751.

Ayonghe, S.N. (2001) "A quantitative evaluation of global warming and precipitation in Cameroon from 1930 to 1995 and projections to 2060: Effects on environment and water resources". *Bamemda: Unique Printers*, pp. 142 – 155.

Baalousha, H.M. (2012) "Modelling Surface – Groundwater interaction in the Ruatainwha Basin, Hawke's Bay, New Zealand". *Environmental Earth Sciences*, vol. 66, pp. 285 – 294.

Baffour, N.K., Ofori, E., Mensah, E., Agyare, W.A. and Atta-Darkwa, T. (2013) "Modelling groundwater flow to the Besease Inland Valley Bottom in Ghana". *Global Journal of Biology, Agriculture and Health Sciences*, vol. 2, no. 1, pp. 52 – 60.

Baker, V.R. (1987) "Paleoflood hydrology and extraordinary flood events". *Journal of Hydrology*, vol. 96, pp. 79 – 99.

Ball, P. and Danert, K. (1999) "Field Trials of the Prototype Pounder Rig, Uganda, 20th August – 13th November, 1999". *Report of DFID KAR Project R7126 Private Sector Participation in Low-cost Water Well Drilling, Cranfield University*, pp. 1 – 43.

Bansal, R.K., Das, S.K. (2011) "Response of an unconfined sloping aquifer to constant recharge and seepage from the stream of varying water level". *Water Resources Management*, vol. 25, pp. 893 – 911.

Barber, W. and Jones, D.G. (1958) "The Geology and Hydrology of Maiduguri, Bornu Province". *Record of Geological Survey of Nigeria*, pp. 5 – 20.

Barron, O.V., Barr, A.D. and Donn, M.J. (2013) "Effect of urbanization on the water balance of a catchment with shallow groundwater". *Journal of Hydrology*, vol. 485, pp. 162 – 176.

Bassoullet, P. and Le Hir, P. (2007) "In situ measurements of surficial mud strength: A new vane tester suitable for soft intertidal muds". *Continental Shelf Research*, vol. 27, pp. 1200 – 1205.

Bates, B.C., Kundzewicz, Z.W., Wu, S. and Palutikof, J. (2008) "Climate Change and Water". *Technical Paper of the Intergovernmental Panel on Climate Change, IPCC Secretariat, Geneva*, pp. 1 – 210.

Beasy, K.M. and Ellison, J.C. (2013) "Comparison of three methods for the quantification of sediment organic in salt marshes of the Rubicon Estuary, Tasmania, Australia". *International Journal of Biology*, vol. 5, no.4, pp. 1 – 13.

Beierle, B.D., Oureux, S.F., Cockburn, J.M.H. and Spooner, I. (2002) "A new method for visualizing sediment particle size distributions. *Journal of Paleolimnology*, vol. 27, pp. 279 – 283.

Bello, A.A. and Makinde, V. (2007) "Delineation of the aquifer in the south-western part of the Nupe Basin, Kwara State, Nigeria". *Journal of American Science*, vol. 3, pp. 36 – 44.

Bengtsson, L. and Enell, M. (1986) "Chemical analysis: In Berglund, B. E. (ed), Handbook of Holocene Palaeoecology and Palaeohydrology". *John Wiley and Sons Ltd., Chichester*, pp. 423 – 451.

Benson, C. and Clay, E.J. (1998) "The impact of drought on sub-Saharan economies". *World Bank Technical Paper No. 401, World Bank, Washington DC, U.S.A*, pp. 1 – 95.

Biggs, E.M. (2009) "Changes in hydrological extremes and climate variability in the Severn Uplands". *University of Southampton*, School of Geography, *Doctoral Thesis*, pp. 1 – 294.

Bill, S.A. (2011) "Simple Low-cost Manual Water Drilling: An Instruction Manual". *Simple Well Drilling Website*, pp. 1 – 56. Available online at www.manualwelldrilling.org.Last accessed on 19th June 2011.

Binod, J. (2008) "Constant and Falling Head Permeability". *Cal State Fullerton, Civil and Environmental Engineering*, pp. 1 – 8.

Biswas, A.K. (2012) "Impacts of large dams: issues, opportunities and constraints". *Springer-Verlag Berlin Heidelberg*, pp. 1 – 18.

Biswas, A.K. and Tortajada, C. (2012) "Impacts of the High Aswan Dam". *Springer-Verlag Berlin Heidelberg*, pp. 379 – 395.

Blott, S. (2011) "Gradistat version 8.0: A Grain Size Distribution and statistic Package for the Analysis of Unconsolidated Sediments by Sieving or Laser Granulometer". *Kenneth Pye Associated Ltd, UK*.

Blott, S.J., Croft, D.J., Pye, K., Saye, S.E. and Wilson, H.E. (2004) "Particle size analysis by laser diffraction. In: Fororensic Geoscience – Principles, Techniques and Application (Eds K. Pye and D. Croft)". *Geological Society of London Special Publication*, vol. 232, pp. 63 – 73.

Blott, S.J. and Pye, K. (2006) "Particle size distribution analysis of sand-size particles by laser diffraction: an experimental investigation of instrument sensitivity and the effects of particle shape". *Sedimentology*, vol. 53, pp. 671 – 685.

Bob, E. (1994) "Low technology drilling. Affordable water supply and sanitation". *20th WEDC Conference. Colombo, Sri Lanka*, pp. 216 – 219.

Bob, E. and Rod, S. (1994) "Simple drilling methods, WEDC, Loughborough University Leicestershire". *Le 113 TU UK*, pp. 41 – 44. Available online at www.iboro.ac.uk/departments/cv/wedc. Last accessed on 25th November 2010.

Bob, M.C. (2008) "Monitoring well design and construction guidance manual". *Florida Department of Environmental Protection Bureau of Water Facilities Regulation. 2600 Blair-stone Road. Tallassee, Florida*, pp. 1 – 73.

Bradley, C. (1994) "The hydrology of a floodplain wetland, Narborough Bog, Leicestershire". *Ph.D. Thesis, University of Leicester*, pp. 1 – 320.

Bradley, C. (1996) "Transient modelling of water-table variation in a floodplain wetland, Narborough Bog, Leicestershire". *Journal of Hydrology*, vol. 185, pp. 87 – 114.

Bradley, C. (1997) "The hydrological basis for conservation of floodplain wetlands: implications of work at Narborough Bog, UK". *Aquatic Conservation*, vol. 7, pp. 41 – 62.

Bradley, C. (2002) "Simulation of the annual water table dynamics of a floodplain wetland, Narborough Bog, UK". *Journal of Hydrology*, vol. 281, pp. 150 – 172.

Bradley, C. and Petts, G.E. (1995) "Observations and modelling of influent seepage from the River Wolf, Devon: In. Modelling River-Aquifer Interactions (Edited by P.L. Younger)". *British Hydrological Society Occasional Paper* 6, pp. 17 – 26.

Braide, S.P. (1992) "Studies on the Sedimentation and Tectonics of the Yola arm of the Benue Trough. Facies Architecture and their Tectonic significance". *Journal of Mining Geo*logy, vol. 28, no. 1, pp. 23 – 31.

Brassington, R. (2006) "Field Hydrogeology Third Edition". *John Wiley and Sons Chichester*, pp. 1 – 248.

British Broadcasting Cooperation (BBC) News (2012) "Flood in Adamawa State 2012". Available online at http://www.bbc.co.uk/news/world-africa-19655162). Last accessed on 24th August 2012.

British Standard, 1377-1 (1990) "Methods of test for Soils for Civil Engineering Purposes-Part 1: General requirements and sample preparation". *British standard Publication*, pp. 1 – 64.

British Standard, EN 1997 – 2 (2007) "Eurocode 7 – Geotechnical design – Part 2: Ground investigation and testing". *British Standard Publication*, pp. 1 – 96

British Standard, EN ISO 14688-1 (2002) "Geotechnical investigation and testing-identification and classification of soil". *British Standard Publication*, pp. 1 – 12.

British Standard, EN ISO 22282-4 (2012) "Geotechnical investigation and testing-Geohydraulic testing. Part 4: Pumping tests". *British Standard Publication*, pp. 1 – 34.

British Standard, EN ISO 22475 – 1 (2006) "Geotechnical investigation and testing – sampling methods and groundwater measurements". *British Standard Publication*, pp. 1 – 134.

Brodie, R.S., Hostetler, S. and Slatter, E. (2007) "Comparison of daily percentiles of stream flow and rainfall to investigate stream-aquifer connectivity". *Journal of Hydrology*, vol. 349, pp. 56 – 67.

Brooks, G.R. (2003) "Alluvial deposits of a mud-dominated stream: the Red River, Mantoba, Canada". *Sedimentology*, vol. 50, pp. 441 – 458.

Brouyère, S., Carabin, G. and Dassargues, A. (2004) "Climate change impacts on groundwater: Modelled deficits in a chalky aquifer, Geer Basin, Belgium". *Hydrogeology Journal*, vol. 12, pp. 123 – 134.

Brunke, M. and Gonser, T. (1997) "The ecological significance of exchange processes between rivers and groundwater". *Freshwater Biol*ogy, vo. 37, pp. 1 – 33.

Burazer, M., Zitko, V., Radakovic, D. and Parezanovic, M. (2010) "Using geophysical methods to define the attitude and elevation of water-bearing strata in the Miocene sediments of the Pannonian Basin". *Journal of Applied Geophysics*, vol. 72, pp. 242 – 253.

Burrows, R.G. (2006) "Design of a low-cost, hand operated drill rig appropriate for adoption by sub-Saharan Africa's Private Sector". *Cranfield University*, pp. 1 – 92.

Butler, D.K. (2003) "Implications of magnetic backgrounds for unexploded ordnance detection". *Journal of Applied Geophysics*, vol. 54, pp. 111 – 125.

Calow, R., Bonsor, H., Jones, L., O'Meally, S., Mur, N. (2011) "Climate change, water resources and wash". *British Geological Survey*, pp. 1 – 69.

Calow, R.C., Robins, N.S., MacDonald, D.M.J., Orpen, W.R.G., Membezeka, P., Andrews, A.J. and Appiah, S.O. (1997) "Groundwater management in drought prone areas of Africa". *Journal of Water Resources Development*, vol. 13, pp. 241 – 261.

Campos, E.H. (2009) "A groundwater flow model for water related damages on historic monuments – case study West Luxor, Egypt". *Vatten*, vol. 65, pp. 247 – 254.

Cancelliere, A., Mauro, G.D., Bonaccorso, B. and Rossi, G. (2007) "Stochastic forcasting of drought indices". *Water Science and Technology Library*, vol. 62, pp. 83 – 100.

Cao, G., Zheng, C., Scanlon, B.R., Liu, J. and Li, W. (2013) "Use of flow modeling to assess sustainability of groundwater resources in the North China Plain". *Water Resources Research*, vol. 49, pp, 159 – 175.

Carmichael, V., Fyfe, J. and Simpson, M. (2008) "Guide to conducting well pumping tests". *Britsih Columbia Ministry of Environment*, pp. 1 – 8.

Carter, J.D., Barber, W. and Tait, E.A. (1963) "The Geology of parts of Adamawa, Bauchi and Bornu Provinces in North-Eastern Nigeria". *Geological Survey of Nigeria Bulletin*, vol. 30, pp. 1 – 109.

Carter, J.T.V., Gotkowitz, M.E. and Anderson, M.P. (2011) "Field verification of stable perched groundwater in layered bedrock uplands". *Ground Water*, vol. 49, no. 3, pp. 383 – 392.

Carter, R.C. (2005) "Human powered drilling technologies: An overview of human-powered drilling technologies for shallow small diameter well construction, for domestic and agricultural water supply". *First Edition, May 2005. Cranfield University Silsoe*, vol. 1, pp. 1 – 18.

Carter, R.C. and Alkali, A.G. (1996) "Shallow groundwater in the northeast arid zone of Nigeria". *Quarterly Journal of Engineering Geology*, vol. 29**,** pp.341 – 355.

Carter, R.C., Chilton, Danert, K. and Olschewski (2010) "Siting of Drilled Water Wells – A Guide for Project Managers". *Rural Water Supply Network*, pp. 1 – 16. Available online at http://www.rwsn.ch/documentation/skatdocumentation. Last accessed on 13th March 2010.

Ceglar, A., Zalika, C. and Lucka, K. (2008) "Analysis of meteorological drought in Slovenia with two drought indices, BALWOIS 2008 – Ohrid, Republic of Macedonia".

Census (2006) "Population of the Federal Republic of Nigeria, Adamawa State statistical Tables". *National Population Commission Final Results of Population of Nigeria*.

Chambers, J.F., Wilkinson, P.B., Penn, S., Meldrum, P.I., Kuras, O., Loke, M.H. and Gunn, D.A. (2013) "River terrace sand and gravel deposit reserve estimation using three-dimensional electrical resistivity tomography for bedrock surface detection". *Journal of Applied Geophysics*, vol. 93, pp. 25 – 32.

Cheelham, M.D., Keene, A.F., Bush, R.T., Sullivan, L.A. and Erskine, W.D. (2008) "A comparison of grain – size analysis methods for sand- dominated fluvial sediments". *Sedimentology,* vol. 55, pp. 1905 – 1913.

Chen, X. and Chen, X. (2003) "Stream water infiltration, bank storage, and storage zone changes due to stream-stage fluctuations". *Journal of Hydrology,* vol. 280, pp. 246 – 264.

Cheo, A.E., Voit, H.J. and Mbua, R.L. (2013) "Climate change and the vulnerability of water resources in northern Cameroon". Available online at http://www.tropentag.de/2012/abstracts/full/141. Last accessed on 15th March 2013.

Chimungu, J.G., Hensley, M. and Vans Rensburg, L.A. (2010) "Comparison of field and laboratory measured hydraulic conductivity properties of selected disgnostic soil horizons". *Second RUFORUM Biennial Meeting 20 – 24 September 2010, Entebbe, Uganda*, pp. 1327 – 1330.

Chung, S.G., Hong, Y.P., Lee, J.M. and Min, S.C. (2012) "Evaluation of the Undrained Shear Strength of Busan Clay". *Journal of Civil Engineering,* vol. 16, no. 5, pp. 733 – 741.

Chung, S.G., Kim, G.J. and Kim, M.S. (2007) "Undrained Shear Strength from Field Vane Test on Busan Clay". *Marine Georesources and Geotechnology*, vol. 25, pp. 167 – 179.

CILAS (2004) "Particle Size Analyzer CILAS 920, 930e, 1064 and 1180 User Manual". *8 Avenue Buffon BP 6319 ZI LA Source 45063 ORLEALNS cedex France*, pp. 1 – 81. Available online at http://www.particle-size-analyzer.com. Last accessed on 1st April 2011.

Coker, J.O. (2012) "Vertical electrical sounding methods to delineate potential groundwater aquifers in Akolo area, Ibadan, South-western, Nigeria". *Journal of Geology and Mining Resources*, vol. 4, no. 2, pp. 35 – 42.

Conway, D. (2011) "Adapting climate research for development in Africa". *WIREs Climate Change*, vol. 2, pp. 428 – 450.

Cratchley, C.R. (1960) "Geological Survey of the South Western part of the Chad Basin". *C.C.T.A. Publication*, pp. 1 – 31.

Dai, A., Lamb, P.J., Trenberth, K.E., Hulme, M., Jones, P.D. and Xie, P. (2004) "The recent Sahel drought is real". *Journal of International Climatology*, vol. 24, pp. 1323 – 1331.

Dakhnov, V.M. (1962) "Geophysical well logging". *Quarterly Colorado School of Mines,* vol. 57, no. 2, pp. 1 – 445.

Danert, K. (2003) "Technology Transfer for Development: Insights from the Introduction of Low-cost Water Well Drilling Technology to Uganda". *Unpublished PhD Thesis, Institute of Water and Environment, Cranfield University at Silsoe*, pp. 1 – 295.

Danert, K. (2009) "Hand Drilling Directory". *Cost Effective Boreholes. Rural Water Supply Network*, pp. 1 – 37. Available online at http://www.rwsn.ch/documentation. Last accessed on 20th December 2010.

Danert, K. (2013) "Experiences and Ideas from RWSN's Sustainable Groundwater Community 2013". *Rural Water Supply Network*, pp. 1 – 34. Available online at http://www.rwsn.ch/documentation. Last accessed on 22ndAugust 2013.

Dark, P. and Allen, J.R.L. (2005) "Seasonal depositional of Holocene banded sediments in the Severn Estuary levels (southwest Britain): Palynological evidence". *Quaternary Science Reviews*, vol. 24, pp. 11 – 33.

Davis, R.E. and Christenson, S.C. (1981) "Geohydrology and numerical simulation of the alluvium and terrace aquifer along the Beaver – North Canadian River from the Pan-handle to Canton Lake, Northwestern Oklahoma". *U.S. Geological Survey, Open-file Report*, pp. 81 – 483.

Dawoud, M.A., Darwish, M.M. and El-Kady, M.M. (2005) "GIS – based groundwater management model for Western Nile Delta". *Water Resources Management*, vol. 19, pp. 585 – 604.

De Carlo, L., Perri, M.T., Caputo, M.C., Deiana, R., Vurro, M. and Cassiani, G. (2013) "Characterization of a dismissed landfill via electrical resistivity tomography and mise-à-la-masse method". *Journal of Applied Geophysics*, vol. 98, pp. 1 – 10.

Dean, W.E. (1974) "Determination of Carbonate and Organic Matter in Calcareous sediments and sedimentary rocks by loss on ignition: comparison with other methods". *Journal of Sedimentary Petrology*, vol. 44, pp. 242 – 248.

Dearing, J.A. (1999) "Environmental magnetic susceptibility using the Bartington MS2 system". *Chi Publisher, Kenilworth, UK*, pp. 1 – 54. Available online at www.bartington.com.Last accessed on 18th November 2010.

Dearing, J.A., Hu, Y., Doody, P., James, P.A. and Brauer, A. (2001) "Preliminary reconstruction of sediment-source linkages for the past 6000 yrs at the Petit Lae d'Annecy, France, based on mineral magnetic data". *Journal of Paleolimnology*, vol. 25, pp. 245 – 258.

Dent, B., Merrick, N., Kelly, B., Milne-Home, W. and Yates, D. (2007) "Groundwater knowledge and gaps in the Lachlan catchment management area". *National Centre for Groundwater Management University of Technology, Sydney, Australia*, pp. 1 – 43.

Dettinger, M., Redmond, K. and Cayan, D. (2004) "Winter Orographic Precipitation Ratios in the Sierra Nevada – Large – Scale Atmospheric Circulations and Hydrologic Consequences". *Journal of Hydrometeorology*, vol. 5, pp. 1102 – 1116.

Deve, D.O. (2000) "Rainfall variation and water resources management in the semi-arid zone of Nigeria". *Journal of Nigeria Meteorological Society*, vol. 3, no. 3, pp. 6 – 11.

Di Stefano, C., Ferro, V. and Mirabile, S. (2010) "Comparison between grain – size analysis using laser diffraction and sedimentation methods". *Biosystems Engineering*, vol. 106, pp. 205 – 215.

Dietmar, K. (2006) "Particle World. Technical paper on QUANTACHROME particle analysis techniques". *1st English Issue*, pp. 3. Available online at www.quantahrome.de. Last accessed on 25th November 2010.

Dor, N., Syafalni, S., Abustan, I., Rehman, M.T.A., Nazri, A.A., Mostafa, R. and Mejus, L. (2011) "Verification of surface-groundwater connectivity in an irrigation canal using geophysical, water balance and stable isotope approaches". *Water Resources Management*, vol. 25, pp. 2837 – 2853.

Driscoll, F.G. (1986) "Groundwater and Wells, 2nd edition". *St. Paul, Minn., Johnson Filtration Systems Inc.*, pp. 1 – 1089.

Druyan, L.M. (1991) "The Sensitivity of Sub-Saharan Precipitation to Atlantic SST". *Climatic Change*, vol. 18, pp. 17 – 36.

Dyer, K.R. (1979) "Estuaries and estuarine sedimentation. In K.R. Dyer (ed.): Estuarine hydrograph and sedimentation". *Cambridge: Cambridge University Press*, pp. 1 – 18.

Eastoe, C.J., Hutchison, W.R., Hibbs, B.J., Hawley, J. and Hogan, J.F. (2010) "Interaction of a river with an alluvial basin aquifer: stable isotopes, salinity and water budgets". *Journal of Hydrology*, vol. 395, no. (1-2), pp. 67 – 78.

Edmunds, W.M. and Gaye, C.B. (1994) "Estimating the spatial variability of groundwater recharge in the Sahel using chloride". *Journal of Hydrology*, vol. 156, pp. 47 – 59.

Eduvie, M.O. (2000) "Groundwater Assessment and Development in the Bima sandstone: A case study of Yola – Jimeta area". *Water Resources Journal of the Nigerian Association of Hydrogeologists (NAH)*, vol. 2, pp. 31 – 38.

Eijkelkamp (2009) "Field Inspection Vane Tester – Operating Instructions". *Agrisearch Equipment*, pp. 1 – 3. Available online at http://www.eijkelkamp.com. Last accessed on 4th April 2011.

Eke, K.T. and Igboekwe, M.U. (2011). "Geoelectric investigation of groundwater in some villages in Ohafia Locality, Abia State, Nigeria". *British Journal of Applied Science and Technology*, vol. 1, no. 4, pp. 190 – 203.

Ekpoh, I.J. and Nsa, E. (2011) "Extreme climate variability in North-western Nigeria: An Analysis of Rainfall Trends and Patterns". *Journal of Geography and Geology*, vol. 3, no. 1, pp. 51 – 62.

ELE International (2006) "Operation Instructions H-60 Field Inspection Vane Tester". *ELE International, a division of Danaher UK industries Ltd*, pp. 1 – 5. Available online at http://www.ele.com. Last accessed on 4th April 2011.

Elkrail, A. and Long-Cang, S. (2009) “Surface water and Groundwater Interaction in Alluvial Plain”. *Journal of Applied Sciences in Environmental Sanitation*, vol. 4, no. 3, pp. 253 – 262.

El-Shinnawy, I.A., Abdel-Meguid, M., Nour Eldin, M.M. and Bakry, M.F. (2000) “Impacts of Aswan High Dam on the aquatic weed ecosystem”. *.ICHEM2000, Cairo University Egypt*, pp. 534 – 541.

Emiroglu, S., Rey, D. and Petersen, N. (2004) “Magnetic properties of sediment in the Ria de Arousa (Spain): dissolution of iron oxides and formation of iron sulphides”. *Physics and Chemistry of the Earth*, vol. 29, pp. 947 – 959.

ENTEC (2009) “Site Option Plan: Ant Broads and Marshes SSSI / Alderfen Broad SSSI. Final Report for the Environment Agency”. *Habitat Directive Review of Consents, Stage 4, June 2009*, Volume 1, 187pp.

Falke, J.A., Fausch, K.D., Magelky, R., Aldred, A., Durnford, D.S., Riley, L.K. and Oad, R. (2011) “The role of groundwater pumping and drought in shaping ecological futures for stream fishes in a dry land river basin of the Western Great Plains, USA”. *Ecohyrology*, vol. 4, no. 5, pp. 682 – 697.

Faybishenko, B. (2000) “Vadose zone characterization and monitoring: current technologies, applications and future developments. In: Looney, B.B. and Falta, R.W. (eds) vadose zone science and technology solutions”. *Battelle Press, USA*, vol. 1, pp.1 – 589.

Federal Republic of Nigeria (2003) “National Action Program (NAP) to combat desertification and mitigate the effect of drought towards the implementation of the United Nations convention to combat desertification and mitigate the effect of drought in the country”.

Federal Surveys of Nigeria Topographic Sheet.48 (1974) “Topographical Map of the Study Area”. *Federal Surveys of Nigeria Topographic Sheet. 48*.

Fetter, C.W. (1994) “Applied Hydrogeology, third edition”. *Macmillan College Publishing Company, New York*, pp. 1 – 691.

Fikri, M.N. and Azahar, S.B. (2011) Non – quantitative correlation of soil resistivity with some soil parameters”. *Institute of Electrical and Electronics Engineers*, 1 – 4.

Fitts, C. (2002) “Groundwater Science First Edition”. *Elsevier, USA*, pp. 1 – 450.

Flialova, H., Maier, G., Petrovsky, E., Kapicka, A., Boyko, T. and Scholger, R. (2006) “Magnetic properties of soils from sites with different geological and environmental settings”. *Journal of Applied Geophysics*, vol. 59, pp. 273 – 283.

Foguet, A.P., Ledesma, A. and Huerta, A. (1998) “Analysis of the Vane test considering size and time effects”. *International Journal for Numerical and Analytical Methods in Geomechanics*, pp. 1 – 40.

Forsyth, A.M., Ramudu, E., Hindal, H.L. and Lazarus, D.R. (2010) "A Manual Well drilling Pilot Project: Implementing the water for all international method". *International Journal for Service Learning in Engineering*, vol. 5, no. 1, pp. 128 – 147.

Franke, O.L., Reilly, T.E. and Bennett, G.D. (1987) "Defination of boundary and initial conditions in the analysis of saturated groundwater flow systems – an introduction". Boo 3 Applications of Hydraulics, U.S. Geological Survey, pp. 1 – 22.

Freeze, R.A. and Cherry, J.A. (1979) "Groundwater". *Prentice Hall, Englwood cliffs, NJ*., pp. 1 – 604.

Fussi, F. (2011) "Mapping of suitable zones for manual drilling as a possible solution to increase access to drinking water in Africa". *6th Rural Water Supply Network Forum 2011, Uganda*, pp. 1 – 8.

Gemail, Kh.S., El-Shishtawy, A.M., El-Alfy, M., Ghoneim, M.F. and abd El-Bary, M.H. (2011) "Assessment of aquifer vulnerability to industrial waste water using resistivity measurements. A case study along El-Gharbyia main drain Nile Delta, Egypt". *Journal of Applied Geophysics*, vol. 75, pp. 140 – 150.

Geonor (2005) "Field Inspection Vane Tester". *RocTest TELEMAC*, pp. 1. Available online at http://www.esands.com.Last accessed on 5th April 2011.

Giannini, A., Saravanan, R. and Chang, P. (2003) "Oceanic forcing of Sahel rainfall on interannual to interdecadal time sclales". *Science*, vol. 302, pp. 1027 – 1030.

Gidahatari (2013) "Why is MODFLOW better than other softwares for groundwater modelling". Available online at http://gidahatari.com/. Last accessed on 8th December 2013.

Google Earth (2011) "Google Earth Image". *US Department of State Geographer, MapLink/Tele Atlas Europa Technologies*.

Google Earth (2013) "Google Earth Image". *US Department of State Geographer, MapLink/Tele Atlas Europa Technologies*.

Goswami, D., Kalita, P.K. and Mehert, E. (2010) "Modeling and Simulation of Baseflow to Drainage Ditches during Low-flow Periods". *Water Resources Management*, vol. 24, pp. 173 – 191.

Grapes, T.R., Bradley, C. and Petts, G.E. (2005) "Dynamics of river – aquifer interactions along a chalk stream: the River Lambourn, UK". *Hydrological Processes*, vol. 19, pp. 2035 – 2053.

Grapes, T.R., Bradley, C. and Petts, G.E. (2006) "Hydrodynamics of floodplain wetlands in a chalk catchment: The River Lambourn, UK". *Journal of Hydrology*, vol. 320, pp. 324 – 341.

Grenfell, S.E., Ellery, W.N. and Grenfell, M.C. (2009) "Geomorphology and dynamics of the Mfolozi River floodplain, KwaZulu-Natal, South Africa". *Geomorphology*, vol. 107, pp. 226 – 240.

Griffiths, D.V. and Lane, P.A. (1990) "Finite Element Analysis of the Shear Vane Test". *Computer and Structures*, vol. 37, no. 6, pp. 1105 – 1116.

Guggenmos, M. (2010) "Groundwater and surface water interaction, Wairarapa valley, New Zealand". *Unpublished M.Sc thesis, Victoria University of Wellington, New Zealand*, pp. 1 – 246.

Guiraud, M. (1990) "Mecanime de formation du basin sur decrochements multiples de la Haute-Benue (Nigeria): facies et geometrie des corps sedimentares". *Member Habilitation, University Montpellier*, pp. 1 – 445.

Guiraud, M. (1991) "Mecanisme de formation du basin cretace sur decrochements multiples de la Haute-Benue (Nigeria)". *Bulletin Centres Recharge Exploration Production Elf-Aquitaine*, vol. 15, pp. 11 – 67.

Gupta, A.D. and Onta, P.R. (1997) "Sustainable groundwater resources development". *Hydrological Sciences Journal*, vol. 42, no. 4, pp. 565 – 582.

Guttman, N.B. (1998) "Comparing the Palmer drought severity index and the standardized precipitation index". *Journal of American Water Resources Association*, vol. 34, no. 1, pp. 113 – 121.

Harbaugh, A.W. (2005) "MODFLOW – 2005, the U.S. Geological Survey modular groundwater model – the Groundwater Flow Process". *U.S. Geological Survey Techniques and Methods 6-A16*, pp. 1 – 253.

Harbaugh, A.W. (2010) "A data-input program (MFI2005) for the U.S. Geological Survey modular groundwater model (MODFLOW-2005) and parameter estimation program (UCODE_2005*)". U.S. Geological Survey Open-File Report 2010-1057*, pp. 1 – 35.

Harbaugh, A.W., Banta, E.R., Hill, M.C. and McDonald, M.G. (2000) "MODFLOW-2000, the U.S. Geological Survey Modular Groundwater Model-Users guide to modularization concepts and the groundwater flow process". *U.S. Geological Survey Open-File Report 00-92*, pp. 1 – 121.

Harleman, D.R.E., Mehthorn, P.E. and Rumer, R.R. (1963) "Dispersion-permeability correlation in porous media". *Journal of Hydraulic Division American Society of Civil Engineers*, vol. 89, pp. 67 – 85.

Haschenburger, J.K. and Cowie, M. (2009) "Floodplain stages in the braided Ngaruroro River, New Zealand". *Geomorphology*, vol.103, pp. 466 – 475.

Hayes, M.J., Svoboda, M., Wilhite, D.A. and Vanyarkho, O. (1999) "Monitoring the 1996 drought using the SPI". *Bulletin American Meteorological Society*, vol. 80, pp. 429 – 438.

Hazen, A. (1893) "Some physical properties of sand and gravels". *Massachusetts State Board of Health, 24th Annual Report*.

Heiri, O., Lotter, A.F. and Lemcke, G. (2001) "Loss on ignition as a method for estimating organic and carbonate content in sediments: reproducibility and comparability of results. *Journal of paleolimnology*, vol. 25, pp. 101 – 110.

Hendrickx, J., Jan, M.H., Bruce, J., Harrison, Remke, L., VanDam, B.U., Dave, L., Norman, Christian, D., Dezoe, B.U., Antwi, R.D., Asiamah, C.R., Paul, V. and Jan, F. (2005) "Magnetic soil properties in Ghana". Available online at http://www.ces.nmt.edu/hydro/landmine. Last accessed on 16th July 2011.

Herzog, B.L. and Morse, W.J. (1984) "A comparison of laboratory and field determined values of hydraulic conductivity at a waste disposal site". *Proceedings of the Seventh Annual Madison Waste Conference*, pp. 30 – 52.

Hess, T.M. (1998) "Trends in reference evapo-transpiration in the North East Arid Zone of Nigeria, 1961-91".*Journal of Arid Environments*, vol. 38 no. 1, pp. 99 – 115.

Hess, T.M., Stephens, W. and Maryah, U.M. (1995) "Rainfall trends in the North East Arid Zone of Nigeria 1961-1990".*Agricultural and Forest Meteorology*, vol. 74, pp. 87 – 97.

Holden, J. (2012) "An Introduction to Physical Geography and the Environment". *Third Edition, Perarson Education Ltd*, pp. 1 – 317.

Holman, I.P. (2006) "Climate change impacts on groundwater recharge-uncertainty, the way forward". *Hydrogeology Journal*, vol. 14, pp. 637 – 647.

Hsu, K.C., Wang, C.K., Chen, K.C., Chen, C.T. and Ma, K.W. (2007) "Climate-induced hydrological impacts on the groundwater system of the Pingtung Plain, Taiwan". *Hydrogeology Journal*, vol. 15, no. 5, pp. 903 – 913.

Huang, Q., Wang, J., Rozelle, S., Polasky, S. and Lie, Y. (2013) "The effects of well management and the nature of the aquifer on groundwater resources". *American Journal of Agriculture Economic*, vol. 95, no. 1, pp. 94 – 116.

Hubbell (2003) "Helical screw foundation system design manual for new construction". *Change*, pp. 1 – 19.

Idowu, O.A. (2007) "Hydrological Processes of Interaction between Surface Water and Groundwater – A Review". *ASSET Series, an International Journal*, vol. 6, no. 2, pp. 172 – 190.

Igboekwe, M.U., Lucky, E.E. and Akankpo, A.O. (2012) "Determination of aquifer characteristics in Eket, Akwa Ibom State, Nigeria, using the vertical electrical sounding methods". *International Journal of Water Resources and Environmental Engineering*, vol. 4, no. 1, pp. 1 – 7.

International Organization for Standardization (2009) "Geotechnical investigation and testing – Field testing". *Draft International Standard ISO/DIS* 22476-9, pp. 1 – 24. Available online at http://www.iso.org. Last accessed on 6th August 2011.

Ishaku, J.M. (2011) "Assessment of groundwater quality index for Jimeta–Yola area, North-eastern Nigeria". *Journal of Geology and Mining Research*, vol. 3, no. 9, pp. 219 – 231. Available online at http://www.academicjournals.org/JGMR. Last accessed on 14th December 2011.

Ishaku, J.M. and Ezeigbo, H.I. (2000) "Water quality of Yola, northern Nigeria". *Water Resources–Journal of the Nigerian Association of Hydrogeologists*, vol. 1, pp. 39 – 48.

Itmsoil (2012) "Instrumentation and Monitoring MAlog User Manual". *Itmsoil holding Ltd*, pp. 1 – 60.

Izinyon, O.C. and Ajumka, H.N. (2013) "Probability distribution models for flood prediction in Upper Benue River Basin – Part II". *Civil and Environmental Research*, vol. 3, no. 2, pp. 62 – 74.

Jackson, P. (1975) "An Electrical resistivity method for evaluating the In-situ porosity of clean marine sands". *Marine Geotechnology*, vol. 1, no. 2, pp. 91 – 115.

Jaw, S.W. and Hashim, M. (2013) "Locational accuracy of underground utility mapping using ground penetrating radar". *Tunneling and Underground Space Technology*, vol. 35, pp. 20 – 29.

Jeng, Y., Lin, C.H., Li, Y.W., Chen, C.S. and Yu, H.M. (2011) "Application of sub-image multire solution analysis of ground penetrating radar data in a study of shallow structure". *Journal of Applied Geophysics*, vol. 73, pp. 251 – 260.

Jonas, A. (2008) "An environmental magnetic study of a marine sediment core from Disko Bugt, West Greenland: Implications for ocean current variability", *Unpublished M.Sc Thesis, Department of Geology Land University*.

Junger, E.P. (1996) "Assessing the unique characteristics of close-proximity soil samples: just how useful is soil evidence". *Journal of Forensic Science*, vol. 41, pp. 27 – 34.

Jyrkama, M.I. and Sykes, J.F. (2007) "The impact of climate change on spatially varying groundwater recharge in the Grand River Watershed, Ontario". *Journal of Hydrology*, vol. 338, no. (3-4), pp. 237 – 250.

Kamga, F.M. (2001) "Impact of greenhouse gas induced climate change on the runoff of the Upper Benue River (Cameroon)". *Journal of Hydrology*, vol. 252, pp. 145 – 156. Available online at http://www.elsevier.com/locate/jhydrol.Last accessed on 2nd March 2011.

Kane, C.H., Fussi, F., Diene, M. and Sarr, D. (2013) "Feasibility study of boreholes hand drilling in Senegal – identification of potentially favorable areas". *Journal of Water Resource and Protection*, vol. 5, pp. 1219 – 1226.

Kelbe, B.E. and Germishuyse, T. (2000) "Conceptualization of the surface water – groundwater processes in South Africa ". *Draft of Proceeding of a Workshop on Surface Water – Groundwater Interaction held in Pietermaritzburg, South Africa*.

Kelly, W.E. and Stanislav, M. (1993) "Applied Geophysics in Hydrogeological and Engineering Practice". *Elsevier, Amsterdam*, pp. 1 – 292.

Khalil, M.A. and Santos, F.A.M. (2013) "2D and 3D resistivity inversion of Schlumberger vertical electrical soundings in Wadi El Natrun, Egypt: A case study". *Journal of Applied Geophysics*, vol. 89, pp. 116 – 124.

Khalil, M.H. (2006) "Geoelectric resistivity sounding for delineating salt water intrusion in the Abu Zenima Area, West Sinai, Egypt". *Journal of geophysics Engineering*, vol. 3, pp. 243 – 251.

Kilic, R.1., Ulamis, K.1. and Atalar, C. (2006) "Engineering Geology Assessment of the Quaternary Alluvium and Pliocene Deposits in North-western Ankara (Kazan-Ankara, Turkey)". *The Geological Society of London 2006, IAEG2006 Paper number 342*, pp. 1 – 6.

Kirby, J.M., Mainuddin, Md., Ahmad, M.D. and Gao, L. (2013) "Simplified monthly hydrology and irrigation water use model to explore sustainable water management options in the Murray-Darling Basin". *Water Resources Management*, vol. 27, pp. 4083 – 4097.

Kirsby, M.E., Lund, S.P. and Poulsen, C.J. (2005) "Hydrologic variability and the onset of modern El Nino-Southern oscillation: a 19 250-year record from Lake Elsinore, southern California". *Journal of Quaternary Science*, vol. 20, pp. 239 – 254.

Kirtman, B., Power, S.B., Adedoyin, J.A., Boer, G.J., Bojariu, R., Camilloni, I., Doblas-Reyes, F.J., Fiore, A.M., Kimoto, M., Meehl, G.A., Prather, M., Sarr, A., Schär, C., Sutton, R., van Oldenborgh, G.J., Vecchi, G. and Wang, H.J. (2013) "Near-term Climate Change: Projections and Predictability. In: Climate Change 2013: The Physical Science Basis. Contribution of Working Group I to the Fifth Assessment Report of the Intergovernmental Panel on Climate Change [Stocker, T.F., D. Qin, G.K. Plattner, M. Tignor, S.K. Allen, J. Boschung, A. Nauels, Y. Xia, V. Bex and P.M. Midgley (eds.)]". *Cambridge University Press, Cambridge, United Kingdom and New York, NY, USA*, pp. 1 – 76.

Knox, J.W., Hess, T.M., Daccache, A. and Wheeler, T. (2012) "Climate change impacts on crop productivity in Africa and South Asia". *Environmental Research Letters*, vol. 7 no.3, pp. 1 – 8.

Kresic, N. (1997) "Qualitative solutions in hydrogeology and groundwater modelling". *Lewis Publishers, USA*, pp. 1 – 461.

Kulatunga, N. (2009) "Upper Murray alluvium, groundwater management area 015: Albury to Corowa, groundwater resources status report – 2008". *NSW Department of Water and Energy, Sydney, Australia*, pp. 1 – 41.

Kumar, C.P. (2012) "Groundwater modelling software – capabilities and limitations". *IOSR Journal of Environmental Science, Toxicology and Food Technology*, vo. 1, no. 2, pp. 46 – 57.

Kumar, M., Duffy, C. J. and Salvage, K. M. (2009) "A second-order accurate, finite volume-based, integrated hydrologic modeling (FIHM) framework for simulation of surface and subsurface flow". *Vadose Zone Journal*, vol. 8, pp. 873 – 890.

Kumar, M., Ramanathan, A.L., Rao, M.S. and Kumar, B. (2011b) "Identification of aquifer – recharge zones and sources in an urban development area (Delhi, India), by correlating isotopic tracers with hydrological features". *Hydrogeology Journal*, vol. 19, pp. 463 – 474.

Kumar, P.B. and Alamgir, M. (2013) "Western Murray porous rock on lower Darling alluvium groundwater sources". *Groundwater Status Report, NSW Department of Primary Industries, Office of Water, Australia*, pp. 1 – 72.

Kumar, S., Halder, S. and Singhal, D.C. (2011a) "Groundwater Resources Management through Flow Modelling in Lower part of Bhagirathi-Jalangi Interfluve, Nadia, West Bengal". *Journal Geological Society of India*, vol. 78, pp. 587 – 598.

Labas, J., Vuik, R., Van der Wal, A. and Naugle, J. (2010) "Augering Technical Training Handbook on Affordable manual wells drilling". *Published by the PRACTICA Foundation*, pp. 1 – 78. Available online at www.practicafoundation.nl. Last accessed on 15th December 2010.

Lachaal, F., Mlayah, A., Bedir, M., Tarhouni, J. and Leduc, C. (2012) "Implementation of a 3-D groundwater flow model in a semi-arid region using MODFLOW and GIS tools: The Zeramdine-Beni Hassen Miocene aquifer system (east-central Tunisia)". *Computers and Geosciences*, vol. 48, pp. 187 – 198.

Lamb, P.J. (1978) "Large-scale Tropical Atlantic surface circulation patterns associated with sub-Saharan weather anomalies". *Tellus*, vol. 30, pp. 240 – 251.

Lamb, P.J. (1983) "West African water variations between recent contrasting sub-Saharan droughts". *Tellus*, vol. 35, pp. 198 – 212.

Lamb, P.J. and Peppler, R.A. (1992) "Further case studies of tropical Atlantic surface atmospheric and oceanic patterns associated with sub-Saharan drought". *Journal of Climate*, vol. 5, pp. 476 – 488.

Lange, J. (2005) "Dynamics of transmission losses in a large arid stream channel". *Journal of Hydrology*, vol. 306, pp. 112 – 126.

Laven, M., Verosub, K. and Southard, R. (1989) "Environmental magnetic susceptibility". *Chi publishing, Kenilworth*, UK.

Le Barbe, L., Label, T. and Tapsoba, D. (2002) "Rainfall variability in West Africa during the years 1950 – 1990", *.American Meteorological Society*, pp. 187 – 202.

Ledger, P.M., Edward, K.J. and Schofield, J.E. (2013) "Shieling activity in the Norse Eastern Settlement: Palaeoenvironment of the Mountain Farm, Vatnahverfi, Greenland". *The Holocene*, vol. 0, pp. 1 – 13.

Lees, J.A., Flower, R.J., Ryves, D., Vologina, E. and Sturm, M. (1998) "Identifying sedimentation patterns in Lake Baikal using whole core and surface scanning magnetic susceptibility". *Journal of Paleolimnology*, vol. 20, pp. 187 – 202.

Litton, C.M. and Santelices, R. (2003) "Effect of wild-fire on soil physical and chemical properties in a Nothofagus glauca forest, Chile". *Revista Chilena Historia Hatural*, vol 76, no. 4, pp. 529 – 542.

Loke, M.H. (2010) "Tutorial – 2D and 3D Electrical Imaging Surveys", pp. 1 – 157. Available online at http://www.geoelectrical.com. Last accessed on 5th April 2011.

Long, A.J., Plater, A.J., Waller, M.P. and Innes, J.B. (1996) "Holocene coastal sedimentation in the eastern English channel: new data from the Romney Marsh region, United Kingdon". *Marine Geology*, vol. 136, pp. 97 – 120.

Love, D., Moyse, W. and Ravengai, S. (2006) "Livelihood challenges posed by water quality in the Mzingwane and Thuli river catchment, Zimbabwe". *7th Water Net/WARFSA/GWP-SA Symposium, Lilongwe, Malawi, November 2006*.

Luckey, R.R., Gutentang, E.D., Heimes, F.J. and Weeks, J.B. (1986) "Digital simulation of groundwater flow in the High Plains aquifer in parts of Colorado, Kansas, Nebraska, New Mexico, Oklahoma, South Dakota, Texas, and Wyoming". *USGS, Professional Paper 1400-E*, pp. 1 – 44.

MacCarthy, M.F., Buckingham, J.W. and Mihelcic, J.R. (2013) "EMAS Household Water Supply Technologies in Bolivia". *Rural Water Supply Network Field Note No 2013-4*, pp. 1 – 12.

MacDonald, A.M., Bonsor, H.C., Calow, R.C., Taylor, R.G., Lapworth, D.J., Maurice, L., Tucker, J. and O'Dochartaigh, B.E. (2011) "Groundwater resilience to climate change in Africa". *British Geological Survey Open Report*, pp. 1 – 32.

MacDonald, A.M., Bonsor, H.C., Dochartaigh, B.É.Ó. and Taylor, R.G. (2012) "Quantitative maps of groundwater resources in Africa". *Environmental Research Letters*, vol. 7 pp. 1 – 7.

MacDonald, A.M., Calow, R.C. and Chilton, P.J. (2005) "Developing groundwater: a guide to rural water supply". *Practical Action Publishing, Rugby, UK*, pp. 1 – 358.

MacDonald, A.M., Calow, R.C., MacDonald, D.M.J., Darling, W.G. and O'Dochartaigh, B.E. (2009) "What impact will climate change have on rural groundwater supplies in Africa" *Hydrological Sciences Journal*, vol. 54, no. 4, pp. 690 – 703.

Maclay, R.W. and Land, L.F. (1988) "Simulation of flow in the Edwards aquifer, San Antonio region, Texas, and refinement of storage and flow concepts", *USGS, Water Supply Paper 2336-A*, pp. 1 – 48.

Maduabuchi, C.M. (2002) "Case studies on transboundary aquifers in Nigeria". *Proceedings of the International Workshop Tripoli, Libya,* pp. 135 – 141.

Magellan Professional (2007) "ProMark3 Reference Manual". pp. 1 – 292. Available online at http://professional.magellangps.com/en/support/rma.asp. Last accessed on 3rd June 2012.

Magilligan, F.J. (1992) "Sedimentaology of a fine-grained aggrading floodplain". *Geomorphology*, vol. 4, pp. 393 – 408.

Makaske, B., Smith, D.G. and Berendsen, H.J.A. (2002) "Avulsions, channel evolution and floodplain sedimentation rates of the anastomosing upper Columbia River, British Columbia, Canada". *Sedimentology,* vol. 49, pp. 1049 – 1071.

Mansell, M.G. and Hussey, S.W. (2005) "An investigation of flows and losses within the alluvial sands of ephemeral rivers in Zimbabwe". *Journal of Hydrology,* vol. 314, pp. 192 – 203.

Marriott, S. (1992) "Textural analysis and modelling of a floodplain deposit: River Severn, UK". *Earth Surface Processes and Landforms*, vol. 17, pp. 687 – 697.

Masch, F.D. and Denny, K.J. (1966) "Grain-size distribution and its effect on the permeability of unconsolidated sands". *Water Resources Research*, vol. 2, pp. 665 – 677.

Maxey G.B. (1964) "Hydrostratigrapic units". *Journal of Hydrology*, vol. 2, pp. 124 – 129.

Mbiimbe, E.Y., Ezeigbo, H.I. and Dike, E.F.C. (2008) "Groundwater Potential of Numan and Environs, Adamawa State, North-Eastern, Nigeria". *Continental Journal of Earth Science*, vol. 3, pp. 59 – 70.

McCallum, A.M., Andersen, M.S., Giambastiani, B.M.S., Kelly, B.F.J. and Acworth, R.I. (2013) "River-aquifer interactions in a semi-arid environment stressed by groundwater abstraction". *Hydrological Processes*, vol. 27, pp. 1072 – 1085.

McDonald, M.G. and Harbaugh, A.W. (2005) "A modular three-dimensional finite-difference groundwater flow model". *U.S. Geological Survey MODFLOW Manual*, pp. 1 – 201.

McDonald, M.G. and Harbaugh, A.W. (1988) "A modular three-dimensional finite-difference groundwater flow model". *U.S. Geological Survey Techniques of Water-Resources Investigation, book 6, chap. A1*, pp. 1 – 586.

McDonald, M.G. and Harbaugh, A.W. (1996) "User's Documentation for MODFLOW-96, an update to US Geological Survey Modular Finite–Difference Groundwater Flow Model". *US Geological Survey open-file Report*, pp. 1 – 485.

McKee, T.B., Doesken, N.J. and Kleist, J. (1993) "The relationship of drought frequency and duration of time scales". *Presented at the Eighth Conference on Applied Climatology, American Meteorological Society: Anahein, CA*, pp. 179 – 186.

McLaren, P. (1981) "An interpretation of trends in grain size measures". *Journal of Sedimentary Petrology*, vol. 51, no. 2, pp. 611 – 624.

McManus, J. (1988) "Grain size determination and interpretation. In M. Tucker (ed.) Techniques in Sedimentology". *Oxford Blackwell Scientific* Publications, pp. 63 – 85.

Mehl, S.W. and Hill, M.C. (2005) "MODFLOW-2005, the U.S. Geological Survey Modular groundwater model-Documentation of shared node local grid refinement (LGR) and the boundary flow and head (BFH) Package". *U.S. Geological Survey Techniques and Methods 6-A12*, pp. 1 – 68.

Mehl, S.W., Hill, M.C. and Leake, S.A. (2006) "Comparison of local grid refinement methods for MODFLOW". *Ground Water,* vol. 44, no. 6, pp. 792 – 796.

Merz, S.K. (2012) "Synthesis of groundwater – surface water connectivity knowledge for the Murray – Darling Basin". *Murray-Darling Basin Authority Australia*, pp. 1 – 75.

Miall, A.D (1977) "A review of the braided-river depositional environment" *Erath Science Reviews*, vol. 13, pp. 1 – 62.

Middlemis, H. (2000) "Groundwater flow modelling guideline: Murray-Darling Basin Commission". *Aquaterra Consulting Pty Ltd*. Available online at www.mdbc.gov.au. Last accessed on 13th January 2013.

Mogren, S., Batayneh, A., Elwadi, E., Al-Bassam, A., Ibrahim, E. and Qaisy, S. (2011) "Aquifer boundaries explored by geoelectrical measurements in the Red Sea coastal plain of Jazan area, Southwest Saudi Arabia". *International Journal of Physical Sciences*, vol. 6, no. 15, pp. 3688 – 3696.

Mohammed, R.F. and Hua, C.Z. (2010) "Regional groundwater flow modeling in Western Nile Delta, Egypt". *World Rural Observations*, vol. 2, no. 2, pp. 37 – 42.

Mohr, K.I. and Thorncroft, C.D. (2006) "Intense convective systems in West Africa and their relationship to the African easterly jet". *Quaternary Journal of Research Meteorological Society*, vol. 132, pp. 163 – 176.

Molua, E. and Lambi, C.M. (2006) "Climate, Hydrology and Water Resources in Cameroon". *CEEPA Discussion Paper No. 33, CEEPA, University of Pretoria*, pp. 1 – 37.

Moore, J.R., Boleve, A., Sanders, J.W. and Glaser, S.D. (2011) "Self-potential investigation of Moraine dam seepage". *Journal of Applied Geophysics*, vol. 74, no. 4, pp. 277 – 286.

Moussa, D., Nola, M., Gake, B., Ebang, M.D. and Njine, T. (2011) "Faecal contamination of well water in Garoua (Cameroon): Importance of household storage and sanitary hygiene". *International Journal of Research in Chemistry and Environment*, vol. 1, no. 2, pp. 97 – 103.

National Climatic Data Center (2013) "U.S. Standardized Precipitation Index" available online at http://www.ncdc.noaa.gov/oa/climate/research/prelim/drought/spi.html. Last accessed on 20th February 2013.

Naugle, J. (1991) "Hand Augered Garden Wells". Lutheran *World Relief, Niamey, Niger*, pp. 1 – 29.

Naugle, J. (1996) "Hand Augered Garden Wells, Lutheran World Relief (3rd edition)", pp. 1 – 63. Available online at http://www.enterpriseworks.org/pubs. Last accessed on 8th March 2011.

Nawrocksi, W.J., Polechenska, O. and Werner, T. (2009) "Magnetic susceptibility and selected geochemical mineralogical data as proxies for Early to Middle Franian (Late Devonium) carbonate depositional settings in the Holy cross Mountains, southern Poland". *Palaeogeography, Palaeoclimatology, Palaeoecology*, vol. 269, pp. 176 – 188.

Ndlovu, S., Mpofu, V., Manatsa, D. and Muchuweni, E. (2010) "Mapping Groundwater Aquifers using Dowsing Slimgram Electromagnetic Survey Method and Vertical Electrical Sounding Jointly in the Granite Rock Formation: A Case of Matshetshe Rural Area in Zimbabwe". *Journal of Sustainable Development in Africa*, vol. 12, no. 5, pp. 199 – 208.

Nejad, H.T. (2009) "Geoelectric Investigation of the Aquifer Characteristics and Groundwater Potential in Behbahan Azad University Farm, Khuzestan Province, Iran". *Journal of Applied Sciences*, vol. 9, no. 20, pp. 3691 – 3698.

Neukum, C. and Azzam, R. (2012) "Impact of climate change on groundwater recharge in a small catchment in the Black Forest, Germany". *Hydrogeology Journal*, vol. 20, pp. 547 – 560.

Niang, A.J., Ozer, A. and Ozer, P. (2008) "Fifty years of landscape evolution in south-western Mauritania by means of aerial photos". *Journal of Arid Environments*, vol. 72, pp. 97 – 107.

Nicholson, S.E. (1979) "Revised rainfall series for the West African sub-Tropics". *Monthly Weather Review*, vol. 107, pp. 620 – 623.

Nicholson, S.E. (2013) "The West African Sahel: A review of recent studies on the rainfall regime and its interannual variability". *Hindawi Publishing Corporation ISRN Meteorology*, pp. 1 – 33.

Nicholson, S.E. and Palao, J.M. (1993) "A re-evaluation of rainfall variability in the Sahel, Part I. characteristics of rainfall fluctuations". *International Journal of Climatology*, vol. 13, pp. 371 – 389.

Nielsen, D.M (1991) "Practical handbook of groundwater monitoring". *Chelsea, Michigan: Lewis*, pp. 1 – 717.

Nigerian Geological Society (2006) "Geological Map of the Study Area". *Nigerian Geological Society*.

Niswonger, R.G. and Fogg, G.E. (2008) "Influence of perched groundwater on base flow". *Water Resources Research*, vol. 44, no. 3, pp. 1 – 5.

Niwas, S. and Celik, M. (2012) "Equation estimation of porosity and hydraulic conductivity of Ruhrtal aquifer in Germany using near surface geophysics". *Journal of Applied Geophysics*, vol. 84, pp. 77 – 85.

Njitchoua, R., Fontes, J.Ch. and Zuppi, G.M. (1995) "Use of chemical and isotopic tracers in studying the recharge processes of the upper Cretaceous aquifer of the Garoua basin, northern Cameroon". *Proceedings of the Vienna Symposium IAHS Publication*, vol. 232, pp. 363 – 372.

Nur, A. and Kujir, A.S. (2006) "Hydro-Geoelectrical Studying in the North Eastern part of Adamawa State, Nigeria". *Journal of Environmental Hydrology*, vol. 14, pp. 1 – 7.

Nur, A., Obiefuna, G.I. and Bassey, N.E. (2001) "Interpretation of Geological data of the Federal University of Technology, Yola". *Journal of Environmental Hydrology*, vol. 9, no. 3, pp. 1 – 10.

Obiefuna, G.I. and Orazulike, D.M. (2010) "Geology and Hydrogeology of Groundwater Systems of Yola Area, Northeast, Nigeria". *Journal of Environmental Sciences and Resource Management*, vol. 2, pp. 37 – 63.

Obiefuna, G.I. and Orazulike, D.M. (2011a) "Geochemical and Mineralogical Composition of Bima Sandstone Deposit, Yola Area, NE Nigeria". *Resources Journal of Environmental Earth Science*, vol. 3, no. 2, pp. 95 – 102.

Obiefuna, G.I. and Orazulike, D.M. (2011b) "The Hydrochemical Characteristics and Evolution of Groundwater in Semiarid Yola Area, Northeast, Nigeria". *Resources Journal of Environmental Earth Science*, vol. 3, no. 4, pp. 400 – 416.

Obiefuna, G.I., Nur, A., Baba, A.U. and Bassey, N.E. (1999) "Geological and geotechnical assessment of selected gully sites, Yola area, Northeast, Nigeria". *Journal of Environmental Hydrology*, vol. 7, pp. 1 – 13.

Ochoe, B., Davis, M. and Engel, J. (2008) "Water well drilling in alluvial soils". *Water boys, DRLG*, pp. 1 – 33. Available online at http://www.undg-policynet.org. Last accessed on 14th December 2010.

Ojo, O., Oni, F. and Ogunkunle, O. (2003) "Implication of climatic variability and climate change on water resources management in West Africa". *IAH Publication*, pp. 37 – 47.

Okiongbo, K.S. and Odubo, E. (2012) "Geoelectric sounding for the determination of aquifer transmissivity in parts of Bayelsa State, South South Nigeria". *Journal of Water Resource and Protection*, vol. 4, pp. 346 – 353.

Okolie, E.C., Atakpo, E. and Okpikoro, F.E. (2010) "Application of linear Schlumberger configuration in delineation of formation strata and groundwater distribution in Ifon Ondo State, Nigeria". *International Journal of the Physical Sciences*, vol. 5, no. 6, pp. 642 – 650.

Oldfield, F., Maher, B.A., Donoghue, J. and Pierce, J. (1985) "Particle-size related, mineral magnetic source sediment: linkages in the Rhode River catchment, Maryland, USA". *Journal of the Geological Society of London,* vol. 142, pp. 1035 – 1046.

Onu, N.N. (2003) "Estimation of the relative specific yield of aquifers from geo-electrical sounding data of the coastal plains of south-eastern Nigeria". *Journal of Technology Education Nigeria*, vol. 8, pp. 69 – 83.

Onugba, A. and Aboh, H.O. (2009) "The Tritium Content of Precipitation and Groundwater at Yola, Nigeria". *Science world Journal*, vol. 4, no. 2, pp. 23 – 28.

Orlando, L. (2013) "Some considerations on electrical resistivity imaging for characterization of waterbed sediments". *Journal of Applied Geophysics*, vol. 95, pp. 77 – 89.

Orlando, L. and Pelliccioni, G. (2010) "P and PS data to reduce the uncertainty in the reconstruction of near-surface alluvial deposits (Case study – Central Italy)".*Journal of Applied Geophysics*, vol. 72, pp. 57 – 69.

Osazuwa, I.B. and Chii, E.C. (2010) "Two-dimensional electrical resistivity survey around the periphery of an artificial lake in the Precambrian basement complex of northern Nigeria". *International Journal of Physical Sciences*, vol. 5, no. 3, pp. 238 – 245.

Owais, S., Atal, S. and Sreendevi, P.D. (2007) "Groundwater flow and aquifer modelling using finite difference method. In: S. Ahmed, R. Jayakumar and A. Salih (Eds.), Groundwater dynamics in hard rock aquifer sustainable management and optimal monitoring network design". *Capital Publishing Co, India*, pp. 210 – 218.

Panagopoulos, G. (2012) "Application of MODFLOW for simulating groundwater flow in the Trifilia Karst aquifer, Greece". *Environment Earth Science,* vol. 67(3), pp. 1877 – 1889.

Park, Y.H., Doh, S.J. and Yun, S.T. (2007) "Geoelectric resistivity sounding of riverside alluvial aquifer in an agricultural area at Buyeo, Geum River watershed, Korea: an application to groundwater contamination study". *Environmental Geology*, vol. 53, pp. 849 – 859.

Parsad, R. and Khandelwal, M.K. (2010) "JMP statistical discovery software: an overview". pp. 1 – 81.

Passadore, G., Monego, M., Altissimo, L., Sottani, A., Putti, M. and Rinaldo, A. (2012) "Alternative conceptual models and the robustness of groundwater management scenarios in the multi-aquifer system of the Central Veneto Basin, Italy". *Hydrogeology Journal*, vol. 20, pp. 419 – 433.

Paul, C. (2007a) "Baptist Drilling". *RWSN documentation of cost effective boreholes*, pp. 1. Available online at www.rwsn.ch/documentatio. Last accessed on 25th November 2010.

Paul, C. (2007b) "EMAS Drilling". *RWSN documentation of cost effective boreholes*, pp. 1. Available online at www.rwsn.ch/documentatio. Last accessed on 25th November 2010.

Payne, S.M, Magruder, I.A. and Woessner, W.W. (2013) "Application of a groundwater classification system and GIS mapping system for the Lower Ruby Valley Watershed, Southwest Montana". *Journal of Water Resource and Protection*, vol. 5, pp. 775 – 791.

Peleg, N. and Gvirtzman, H. (2010) "Groundwater flow modelling of two-levels perched karstic leaking aquifers as a tool for estimating recharge and hydraulic parameters". *Journal of Hydrology*, vol.388, pp. 13 – 27.

Perttu, N., Wattanasen, K., Phommasone, K. and Elming, S. (2011) "Characterization of aquifers in the Vientiane Basin, Laos, using Magnetic Resonance Sounding and Vertical Electrical Sounding". *Journal of Applied Geophysics*, vol.73, pp. 207 – 220.

Petrovsky, E., Kapicka, A., Jordanova, N., Knab, N. and Hoffman, V. (2000) "Low-field magnetic susceptibility, a proxy method of estimating increased pollution of different environmental systems". *Environmental Geology*, vol. 39, pp. 312 – 318.

Polycarp, M.I. and Mustapha, A.R. (2001) "Adamawa State in Perspectives", pp. 1 – 49. Available online at http://www.Agric_Adamawa. Last accessed on 25th March 2011.

Popoff, M. (1988) "Du Gondwana àé Atlantique sud: les connexions du fossé de la Bénué avec les basins du Nord Est brésilien jusqúà é'ouverture du golfe de Guinée au Crétacé inférieur". *Journal of African Earth Science*, vol. 7, pp. 409 – 431.

Popoff, M., Wiedmann, J. and De Klasz, I. (1986) "The Upper Cretaceous and Gongola and Pindiga Formations, northern Nigeria: Subdivisions, age, stratigraphic correlations and paleogeographic implications". *Eclogae geol. Helv.*, vol. 79, pp. 343 – 363.

PRACTICA (2010) "Professionalizing the Manual Drilling Sector in Africa". A guide to Building Capacity to Increase Access to Safe Water in Rural Areas. *Designed by the United Nations, Outreach Division/DPT, New York*, pp. 1 – 38. Available online at http://www.unicef.org.Last accessed on 28th March 2011.

Pye, K. and Blott, S.J. (2004) "Particle size analysis of sediments, soils and related particulate materials for forensic purposes using laser granulometry". *Forensic Science International*, vol. 144, pp. 19 – 27. Available online at www.elsevier.com/locate/forsciint. Last accessed on 26thJuly 2011.

Quirez-Londono, O.M., Martinez, N. and Massone, H. (2012) "Estimating aquifer in plains environments based on groundwater level variations". *Technology Cicencias Del Agua*, vol. 3, no. 2, pp. 123 – 130.

Rai, S.N. and Manglik, A. (2012) "An analytical solution of Boussinesq Equation to predict water table fluctuations due to time varying recharge and withdrawal from multiple basins, wells and leakage sites". *Water Resources Management*, vol. 26, pp. 243 – 252.

Raimi, J., Abdulkarim, M.S., Hamidu, I. and Arabi, A.S. (2011) "Application of Shlumberger vertical electrical sounding for determination of suitable sites for construction of boreholes for irrigation scheme within a Basement complex". *International Journal of Multidisplinary Sciences and Engineering*, vol. 2, no. 6, pp. 81 – 84.

Ramsahoye, L.E. and Land, S.M. (1993) "A simple method for determining specific yield from pumpin tests". *Groundwater Hydraulics*, pp. 41 – 46.

Rassam, D.W. (2011) "A conceptual framework for incorporating surface–groundwater interactions into a river operation–planning model". *Environmental Modelling and Software*, vol. 26, pp. 1554 – 1567.

Rejani, R. Madan, K., Jha, M.K., Panda, S.N. and Mull, R. (2008) "Simulation modelling for efficient groundwater management in Balosore coastal basin, India". *Water Resources Management*, vol. 22, no. 1, pp. 23 – 50.

Rey, D., Lopez-Rodriguez, N., Rubio, B., Vilas, F., Mohamed, K., Pazos, O. and Bogalo, M.F. (2000) "Propiedades magneticas de los sedimentos e tipo estuarino.El caso de las Rias Baixas". *Journal of Iberian Geology*, vol. 26, pp. 151 – 169.

Reyment, R.A. (1956) "On the stratigraphy and Palaeontology of the Cretaceous of Nigeria and the Cameroon, British West Africa". *Geology Forensic Stockh Forth*, vol. 78, pp. 17 – 26.

Robbins, G.A., Aragon-Jose, A.T. and Romero, A. (2008) "Determining hydraulic conductivity using pumping data from low-flow sampling". *Ground Water*, vol. 47, pp. 271 – 276.

Robein, H., Descloitres, M., Ritz, M. and Atangana, Q.Y. (1996) "A multiscale electrical survey of a lateritic soil system in the rain forest of Cameroon". *Journal of Applied Geophysics*, vol. 34, pp. 237 – 253.

Robinson, B.A., Broxton, D.E. and Vaniman, D.T. (2005) "Observations and modelling of deep perched water beneath the Pajarito Plateau". *Vadose Zone Journal*, vol. 4, pp. 637 – 652.

Rodriguez, L.B., Cello, P.A. and Vionnet, C.A. (2005) "Modelling stream – aquifer interactions in a shallow aquifer, Choele Choel Island, Patagonia, Argentina". *Hydrogeology Journal*, vol. 14, pp. 591 – 602.

Rosenberry, D.O. (2000) "Unsaturated zone wedge beneath a large, natural lake". *Water Resources Research*, vol. 36, no. 12, pp. 3401 – 3409.

Rossi, G. and Cancelliere, A. (2002) "Early warning of drought: development of a drought bulletin for Sicily. Proc. 2nd international conference new trends in water and

environment engineering for safety and life: eco-compatible solutions foe aquatic environments". *Capri Italy*, June 24 – 28, 2002, pp. 1 – 12.

Rowell, D.L. (1994) "Soil science: methods and applications". *Wiley, Harlow, Essex*, pp. 1 – 350.

Rural Water Supply Network (RWSN) (2008) "Hand drilling". Available online at http://www.rwsn.ch/particle. Last accessed on 29th November 2010.

Rural Water Supply Network (RWSN) (2009) "Hand Drilling Directory". Available online at http://www.rwsn.ch/documentation/skatdocumentation. Last accessed on 14th December 2010.

Rural Water Supply Network (RWSN) (2012) "Supervising water well drilling: A guide for supervisors". Field Note No 2012-2, pp. 1 – 24. Available online at http://www.rural-water-supply.net/en/implementation/manual-drilling. Last accessed on 19th September 2013.

Rural Water Supply Network (RWSN) (2013) "An Introduction to Manually Drilled Wells". Available online at http://www.rural-water-supply.net/en/implementation/manual-drilling. Last accessed on 19thMay 2013.

Sabo, E. and Adeniji, O.T. (2007) "Studies on Awareness and Accessibility to Agricultural Technology Information by Dry Season Vegetable Farmers in Mubi, Nigeria". *Medwell Journal, Agricultural Journal*, vol. 2, no. 5, pp. 622 – 625.

Sainato, C.M., Losinno, B.N. and Malleville, H.J. (2012) "Assessment of contamination by intensive cattle activity through electrical resistivity tomography". *Journal of Applied Geophysics*, vol. 76, pp. 82 – 91.

Sander, G. (2001) "Ground water and river flow analysis". *Technical Report of the Platte River EIS Team U.S. Department of the Interior Bureau of Reclamation Fish and Wildlife Service*, pp. 1 – 26.

Sandgren, P. and Snowball, I. (2002) "Application of mineral magnetic techniques to Paleolimnology". pp. 1 – 22.

Sanford, W. (2002) "Recharge and groundwater models: an overview". *Hydrogeology Journal*, vol. 10, pp. 110 – 120.

Santisteban, J.I., Mediavilla, R., Lopez-Pamo, E., Dabrio, C.J., Zapata, M.B.R., Garcia, M.J.G., Castano, S. and Martinez-Alfaro, P.E. (2004) "Loss on ignition: a qualitative or quantitative method for organic matter and carbonate mineral content in sediments". *Journal of Paleolimnology*, vol. 32, pp. 287 – 299.

Sarch, M.T., Madakan, S.P. and Ladu, B.L. (2001) "Investigating systems of fisheries access along the River Benue in Nigeria". *PLA Notes CD-ROM*, pp. 1 – 5.

Scanlon, B.R., Healy, R.W. and Cook, P.G. (2002) "Choosing appropriate techniques for quantifying groundwater recharge". *Hydrogeology Journal*, vol. 10, pp. 18 – 39.

Scanlon, B.R., Keese, K.E., Flint, A.L., Flint, L.E., Gaye, C.B., Edmunds, W.M. and Simmers, I. (2006) "Global synthesis of groundwater recharge in semiarid and arid regions". *Hydrological Processes*, vol. 20, pp. 3335 – 3370.

Schjønning, P. (1986) "Shear strength determination in undisturbed soil at controlled water potential". *Soil Tillage Research*, vol. 8, pp. 171 – 179.

Schwertmann, C. (1985) "The effect of pedogenic environments on ion oxide minerals". *Advances in Soil Sciences*, vol. 1, pp. 172 – 200.

Scott, R.L., Cable, W.l. and Huxman, T.E. (2008) "Multiyear riparian evapotranspiration and groundwater use for a semiarid watershed.*Journal of Arid Environment*, vol. 72, no. 7, pp. 1232 – 1244.

Seaber, P.R. (1988) "Hydrostratigraphic Units: In Hydrogeology (W. Back, J.S. Rosenshein, and P.R. Seaber, eds.)" The Geology of North America, vol. 0-2, *Geological Society of America*, pp. 9 – 14.

Segalen, A.S., Pavlic, P. and Dillon, P. (2005) "Review of Drilling, Completion and Remediation Methods for ASR Wells in Unconsolidated Aquifers". *CSIRO Land and Water Technical Report*, vol. 5, pp. 1 – 22.

Servadio, P. and Bergonzoli, S. (2013) "Agricultural soil and water quality assessment and Co_2 storage on wetland reserve". *Journal of Environmental Protection*, vol. 4, pp. 20 – 26.

Shahin, M. (2002) "Hydrology and Water Resources of Africa". *ISBN: 978-1-4020-0866-5, Springer*, pp. 1 – 688.

Shamsudduha, M., Taylor, R.G., Ahmed, K.M. and Zahid, A. (2011) "The impact of intensive groundwater abstraction on recharge to a shallow regional aquifer system: evidence from Bangladesh". *Hydrogeology Journal*, vol. 19, pp. 901 – 916.

Sharp, J.M.Jr. (1988) "Alluvial aquifers along major rivers". *The Geology of North America, Hydrogeology*, vol. 0-2, pp. 273 – 282.

Shlens, J. (2009) "A Tutorial on Principal Component Analysis". *Centre for Neural Science, New York University*, pp. 1 – 12.

Shuman, B. (2003) "Controls on loss on ignition variation in cores from two shallow lakes in the northeastern Unites States. *Journal of Paleolimnology*, vol. 30, pp. 371 – 385.

Sikandar, P. and Christen, E.W. (2012) "Geoelectrical sounding for the estimation of hydraulic conductivity of alluvial aquifers". *Water Resources Management*, vol. 26, pp. 1201 – 1215.

Singh, K.P. (2005) "Nonlinear estimation of aquifer parameters from surficial resistivity measurements". *Hydrology Earth Sciences*, vol. 2, pp. 917 – 938.

Sinha, R. (1995) "Sedimentology of Quaternary Alluvial Deposits of the Gandak-Kosi interfan North Bihar Plains", *Journal Geological Society of India*, vol. 46, pp. 512 – 532.

Sirieix, C., Martinez, J.L.F., Riss, J. and Genelle, F. (2013) "Electrical resistivity characterization and defect detection on a geosynthetic clay liner (GCL) on an experimental site". *Journal of Applied Geophysics*, vol. 90, pp. 19 – 26.

Sissoko, K., Keulen, H.V., Verhagen, J., Tekken, V. and Battaglini, A. (2011) "Agriculture, livelihoods and climate change in the West African Sahel". *Regional Environmental Change*, vol. 11, pp. 119 – 125.

Sivakumar, M.V.K., Das, H.P. and Brunini, O. (2005) "Impacts of present and future climate variability and change on agriculture and forestry in the arid and semi-arid tropics". *Climate Change*, vol. 70, pp. 31 – 72.

Sjodin, A., Lewis, Jnr. W.A. and Saunders III, J.F. (2001) "Analysis of groundwater exchange for a large plains river in Colorado (USA)". *Hydrological Processes*, vol. 15, pp. 1 – 9.

Song, L., Zhu, J., Yan, Q. and Kang, H. (2012) "Estimation of groundwater levels with vertical electrical soundings in the semiarid area of South Keerqin sandy aquifer, China". *Journal of Applied Geophysics*, vol. 83, pp. 11 – 18.

Sonou, M. (2010) "Low-cost shallow tube well construction in West Africa". *FAO Regional Office, Accra, Ghana*, pp. 1 – 13. Available online at http://www/fao.org/docrep. Last accessed on 28th November 2010.

Sophocleous, M. (2002) "Interaction between groundwater and surface water: the state of the science". *Hydrogeology Journal*, vol. 10, no. 1, pp. 52 – 67.

Sophocleous, M., Townsend, M.A., Volgler, L.D., Mclain, T.J., Marks, E.T. and Coble, G.R. (1988) "Experimental studies in stream-aquifer interaction along the Arkansas River in Central Kansas – field testing and analysis". *Journal of Hydrology*, vol. 98, pp. 249 – 273.

Sperazza, M., Moore, J.N. and Hendrix, M.S. (2004) "High-resolution particle size analysis of naturally occurring very fine-grained sediment through laser diffractometry". *Journal of Sedimentary Research*, vol. 74, no. 5, pp. 736 – 743.

Storti, F. and Balsamo, F. (2010) "Particle size distributions by laser diffraction: sensitivity of granular matter strength to analytical operating procedures". *Solid Earth*, vol. 1, pp. 25 – 48. Available online at www.solid-earth.net. Last accessed on 19th February 2012.

Sugita, R. and Marumo, Y. (2001) "Screening of soil evidence by a combination of simple techniques: validity of particle size distribution". *Forensic Science International*, vol. 122, pp. 155 – 158.

Sun, Z., Huang, Q., Opp, C., Hennig, T. and Marold, U. (2012) "Impacts and implications of major changes caused by the three Gorges Dam in the middle reaches of the Yangtze River, China". *Water Resources Management*, vol. 26, pp. 3367 – 3378.

Sutton, I. (2007) "An Assessment of hand drilling potential in Upland and Lowland, Dambo environment of Malawi". *Unpublished M.Sc Thesis, school of Applied Science, Water Management. Cranfield University*, pp. 1 – 140.

Swiecki, R. (2011) "Banka hand drill". Available online at http://www.minelinks.com/tools/banka_hand.html. Last accessed on 29th July 2013.

Swinton, S.M. (1988) "Drought survival tactics of subsistence farmers in Niger", *Human Ecology*, vol. 16, no. 2, pp. 123 – 144.

Tahmiscioğlu, M.S., Anul, N., Ekmekç, F. and Durmuş, N. (2004) "Positive and negative impacts of dams on the environment". *International Congress on River Basin Management*, pp. 759 – 769.

Tallaksen, L.M. (1995) "A review of baseflow recession analysis: In Goswami, D., Kalita, P.K. and Mehnert, E., 2010". *Journal of Hydrology (Amsterdam)*, vol. 165, pp. 349 – 370.

Tamfuh, P.A., Woumfo, E.D., Bitom, D. and Njopwouo, D. (2011) "Petrological, Physio-Chemical and Mechanical Characterization of the Topomorphic Vertisols from the Sudano-Sahelian Region of North Cameroon". *The Open Geological Journal*, vol. 5, pp. 33 – 55.

Tanaka, H.H. and Hollowell, J.R. (1966) "Hydrology of the alluvium of the Arkansas River, Muskogee, Oklahoma, to Fort Smith, Arkansas, USGS". *Water Supply Paper 1809-T*, pp. 1 – 16.

Tarhule, A. and Lamb, P.J. (2003) "Climate research and seasonal forecasting for West Africans: Perceptions, Dissemination, and Use". *Bulletin American Meteorological Society*, vol. 84, pp. 1741 – 1759.

Tarhule, A. and Woo, M. (1997) "Characteristics and use of shallow wells in a stream fadama". *Applied Geography*, vol. 17, no. 1, pp. 29 – 42.

Taylor, C.J. and Allay, W.M. (2001) "Groundwater level monitoring and the importance of long term water level data". U.S. *Geological Survey Circular 12177*, pp. 1 – 74.

Taylor, R.G., Koussis, A.D. and Tindimugaya, C. (2009) "Groundwater and climate in Africa". *Hydrological Sciences Journal*, vol. 5, no. 4, pp. 655 – 664.

Taylor, R.G., Scanlon, B.R., Doell, P., Rodell, M., van Beek, L., Wada, Y., Longuevergne, L., LeBlanc, M., Famiglietti, J.S., Edmunds, M., Konikow, L., Green, T., Chen, J., Taniguchi, M., Bierkens, M.F.P., MacDonald, A., Fan, Y., Maxwell, R., Yechieli, Y., Gurdak, J., Allen, D., Shamsudduha, M., Hiscock, K., Yeh, P., Holman, I. and Treidel, H. (2013a) "Groundwater and climate change". *Nature Climate Change*, vol. 3, pp. 322 – 329.

Taylor, R.G., Todd, M., Kongola, L., Nahozya, E., Maurice, L., Sanga, H. and MacDonald, A. (2013b) "Evidence of the dependence of groundwater resources on extreme rainfall in East Africa". *Nature Climate Change*, vol. 3, pp. 374 – 378.

Taylor, S.R., Moltyaner, G.L., Howard, K.W.F. and Killey, R.W.D. (1987) "A comparison of field and laboratory methods for determining contaminant flow parameters". *Ground Water*, vol. 25, no. 3, pp. 321 – 330.

Tchotsoua, M., Moussa, A. and Fotsing, J.M. (2004) "The Socio-Economic Downstream Impact of Large Dams: A Case study from an Evaluation of Flooding Risks in the Benue River Basin Downstream of the Lagdo Dam (Cameroon)". *Ann Arbor, MI: scholarly publishing office, University of Michigan Library*. Available online at http://www.hdl.handle.net. Last accessed on 5th March 2011.

Tenzer, G.E., Meyers, P.A. and Knoop, P.A. (1997) "Sources and distribution of organic and carbonate carbon in surface sediments of Pyramid Lake, Nevada". *Journal of Science Research*, vol. 67, pp. 887 – 893.

Thompson, R. and Oldfield, F. (1986) "Environmental magnetism". *London: Allen and Unwin*, pp. 72 – 100.

Thompson, R., Batter, R.W., Osullivan, P.E. and Oldfield, F. (1975) "Magnetic susceptibility of Lake Sediments" .*Limnology and Oceanography*, vol. 20, pp. 1 – 5.

Tizro, A.T., Voudouris, K.S, Salehzade, M. and Mashayekhi, H. (2010) "Hydrogeological framework and estimation of aquifer hydraulic parameters using geoelectrical data: a case study from West Iran". *Hydrogeology Journal*, vol. 18, pp. 917 – 929.

Todd, D.K. (1995) "Groundwater Hydrology". *John Wiley and Sons Singapore*.

Toro, S.M. (1997) "Post-Construction Effects of the Cameroonian Lagdo Dam on the River Benue". *Journal of CIWEM*, vol. 11, pp. 109 – 113.

Townley, L.R. (1998) "Shallow groundwater systems: In: Dillon, P. and Simmers, I. (Eds.)". *International Contributions to Hydrogeology 18: Shallow Groundwater Systems. Balkema, Rotterdam*, pp. 3 – 12.

Tucker, G., Gasparini, N.M., Lancaster, S.T. and Bras, R.L. (1999) "Modelling Floodplain Dynamics and Stratigraphy: Implications for Geoarchaeology". *Part II-C of final technical report submitted to U.S. Army Corps of Engineers Construction Engineering Research Laboratory*, pp. 1 – 17.

Tukur, L.I. and Ray, H.H. (1994) "Flood management options spontaneous Government response versus community knowledge and interest. A case of Loko, Adamawa State; In Omuta, G.E.D, et al., (eds.)". *Geographical Association*.

Uma, K.O. and Leohnert, E.P. (1994) "Hydraulic conductivity of shallow sandy aquifers: Effects of sedimentologic and diagenetic differences". *Environmental Geology*, vol. 23, pp. 171 – 181.

Uma, K.O., Egboka, B.C.E. and Onuoha, K.M. (1989) "New statistical grain-size method of evaluating the hydraulic conductivity of sandy aquifers of Ajalli Sandstone Formation". *Journal of Hydrology,* vol. 108, pp. 343 – 366.

Upper Benue River Basin Development Authority (UBRBDA) (1980 – 2012) "Hydro meteorological Year Book. Yola, Nigeria".

Uyigue, E. (2006) "Dams are Unrenewable". *Community Research and Development Centre (CREDC), 90 Uselu – Lagos Road, Opposite Zenith Bank, P. O. Box 11011, Benin City Nigeria*, pp. 1 – 20. Available online at http://www.credcentre.org/publications. Last accessed on 27th March 2011.

Van der Wal, A., Carter, R.C., Fellinga, W.J., Labas, J., Mgina, W. and Nedrestight, F. (2010) "Understanding Groundwater and Wells in manual drilling" An instruction manual for manual drilling teams on hydro-geology for well drilling, well installation and well development. *NL-2628 RC Delft-Netherlands*, pp. 1 – 41. Available online at www.practicafoundation.nl. Last accessed on 15th December 2010.

Van der Wal, A., Carter, R.C., Labas, J. and Mgina, W. (2008) "Understanding Groundwater and Wells" An instruction manual for manual drilling teams on hydro-geology for well drilling teams on hydro-geology for well drilling, well installation and well development. *PRACTICA Foundation*, pp. 1 – 37. Available online at www.practicafoundation.nl. Last accessed on 15th December 2010.

Van Herwijnen, A. (2005) "Rota Sludge and Stone Hammer Drilling–part 1 Drilling Manual". *PRACTICA Foundation and ETC Energy. Maerten Tromspstraat31, 2628 RC Delft, the Netherlands*, pp. 1 – 37. Available online at http://www.practicafoundation.nl/. Last accessed on 7th March 2011.

Van Oel, P.R., Mulatu, D.W., Odongo, V.O., Meins, F.M., Hogeboom, R.J., Becht, R., Stein, A., Onyando, J.O. and Veen, A.V. (2013) "The effects of groundwater and surface water use on total water availability and implications for water management: the case of Lake Naivasha, Kenya". *Water Resources Management*, vol. 27, pp. 3477 – 3492.

Van Overmeeren, R.A. (1989) "Aquifer boundaries explored by geoelectrical measurements in the coastal plain of Yemen: A case equivalent". *Geophysics*, vol. 54, no. 1, pp. 38 – 48.

Vereş, D.Ş. (2002) "A comparative study between loss on ignition and total carbon analysis on minerogenic sediments". *Studia University Babes-Bolyai, Geologia, XLVII*, vol. 1, pp. 171 – 182.

Vincent, M., Andrew, W.R., Ward, M. and Ousamne, N. (2007) "Weather types and rainfall over Senegal, Part I. Observational analysis". *Journal of Climate*, vol. 21, pp. 266 – 287.

Virdi, M.L., Lee, T.M., Swancar, A. and Niswonger, R.G. (2013) "Simulating the effect of climate extremes on groundwater flow through a Lakebed". *Groundwater*, vol. 51, no. 2, pp. 203 – 218.

Volk, J.M. and Costa, O.S. (2010) "The influence of land – use and seasons on SOM distribution in headwaters of a central Ohio watershed". *Journal of Natural and Environmental Sciences*, vol.1, no. 2, pp. 66 – 74.

Von, E.H.W. (1988) "Instructions for Drilling Tube wells with the Vonder Rig". *V and W Engineering Ltd. Harare, Zimbabwe*.

Vrba, J. and Gun, J.V.D. (2004) "The World's Groundwater Resources". *International Groundwater Resources Assessment Centre, IP 2004-1*, pp. 1 – 10.

Vuik, R., Van der Wal, A., Cansdale, R., Stallen, M. and Labas, J. (2010) "Manual drilling series jetting. Technical training handbook on affordable manual well drilling". *Practica Foundation Oosteined 47-NL-3356 AB Popendrecht. The Netherlands*, pp. 1 – 60. Available online at www.practicafoundation.nl. Last accessed on 29th November 2010.

Wake, J.S. (2008) "Groundwater – surface water interaction modelling using visual MODFLOW and GIS". *Unpublished Masters Dissertation, University Ghent*, pp. 1 – 80.

Walling, D.E., Fang, D., Nicholas, A.P. and Sweet, R.J. (2004) "The grain size characteristics of overbank deposits on the flood plains of British lowland rivers". *Sediment Transfer through the Fluvila System (Proceedings of a Symposium held in Moscow, August 2004) IHAS Publication*, vol. 288, pp. 226 – 234.

Walling, D.E., Owens, P.N. and Leeks, G.J.L. (1997) "The characteristics of overbank deposits associated with a major flood event in the catchment of the River Ouse, Yorkshire, UK". *Catena*, vol. 31, pp. 53 – 75.

Wang, L., Dochartaigh, B.O. and Macdonald, D. (2010) "A literature reviews of recharge estimation and groundwater resource assessment in Africa". *Groundwater Resources Programme, British Geological Survey*, pp. 1 – 31.

Wanogho, S., Gettinby, G., Caddy, B. and Robertson, J. (1985) "Determination of particle size distribution of soil in forensic science using classical and modern instrumental methods". *Journal of Forensic Science*, vol. 34, pp. 823 – 835.

Water Surveys (1994) "River Yobe Fadama Study Report". *Consultants Report to North East Arid Zone Development Programme, PMB 18, Gashua, Yobe State, Nigeria.*

Watson, E.B., Pasternack, G.B., Goñi, M. and Woolfolk, A.M. (2013) "Particle size characterization of historic sediment deposition from a closed estuarine, lagoon, central, California". *Estuarine, Coastal and Shelf Science*, vol. 126, pp. 23 – 33.

Watts, K.R. (1989) "Potential hydrologic effects of groundwater withdrawals from the Dakota aquifer, south-western Kansas".*USGS, Water Supply Paper 2304*, pp. 1 – 47.

Weight, E., Yoder, R. and Keller, A. (2013) "Manual well drilling investment opportunity in Ethiopia". *Working Paper 155, AGWATER Solutions*, pp. 1 – 30.

White, I. (1988) "Comment on: A natural gradient experiment on solute transport in a sand aquifer: spatial variability of hydraulic conductivity and its role in the dispersion process by E.A. Sudicky". *Water Resources Research*, vol. 24, no. 6, pp. 892 – 894.

Wightman, W.E., Jalinoos, F., Sirles, P. and Hanna, K. (2003) "Application of Geophysical Methods to Highway Related Problems". *Federal Highway Administration, central Federal Highway Division, Lakewood, co. Publication* No. FHWA-IF-04-021. Available online at http://www.cflhd.gov/resources/agm/. Last accessed on 21st March 2012.

Winter, T.C. (1999) "Relations of stream, lakes and wetlands to groundwater flow system". *Hydrogeology Journal*, vol. 7, no. 1, pp. 28 – 45.

Winter, T.C., Havey, J.W., Franke, O.L. and Alley, W.M. (1998) "Groundwater and surface water: A single resource".*U.S. Geological Circular*, vol. 1139, pp. 1 – 87.

Wisser, D.S., Frolking, S., Douglas, E.M., Fekete, B.M., Vörösmarty, C.J. and Schumann A.H. (2008) "Global irrigation water demand: Variability and uncertainties arising from agricultural and climate data sets". *Geophysical Research Letters*, vol. 35, pp. 1 – 5.

Woessner, W.W. (2000) "Stream and fluvial plain groundwater interactions: rescaling hydrogeologic thought". *Ground Water*, vol. 38, pp. 423 – 429.

Xu, X., Huang, G.H. and Qu, Z.Y. (2009) "Integrating MODFLOW and GIS technologies for assessing impacts of irrigation management and groundwater use in the Hetao irrigation District, Yellow River basin". *Science China Series E-Technological Science*, vol.52, no. 11, pp. 3257 – 3263.

Xu, X., Huang, G.H., Qu, Z.Y. and Pereira, L.S. (2011) "Using MODFLOW and GIS to assess changes in groundwater dynamics in response to water saving measures in irrigation districts of the Upper Yellow River". *Water Resources Management*, vol. 25, pp. 2035 – 2059.

Yenika, M.E., Uma, K.O. and Obiefuna, G.I. (2003) "A case studies of shallow aquifer in Jimeta-Yola metropolis, north eastern Nigeria". *Water Resources Journal of the Nigerian Association of Hydrogeologists*, vol. 14, pp. 84 – 91.

Zaborski, P., Ugodulunwa, F., Idornigie, A., Nnbo, P. and Ibe, K. (1997) "Stratigraphy and structure of the Cretaceous Gongola Basin, Northeast Nigeria". *Elf exploration production, F-64018 Pau*.

Zume, J. and Tarhule, A. (2011) "Modelling the response of an alluvial aquifer to anthropogenic and recharge stresses in the United States Southern Great Plains". *Journal of Earth System Science*, vol. 120, no. 4, pp. 557 – 572.

APPENDIX A: Particle size distribution for the floodplain sediments obtained along River Benue outcrops and boreholes cores

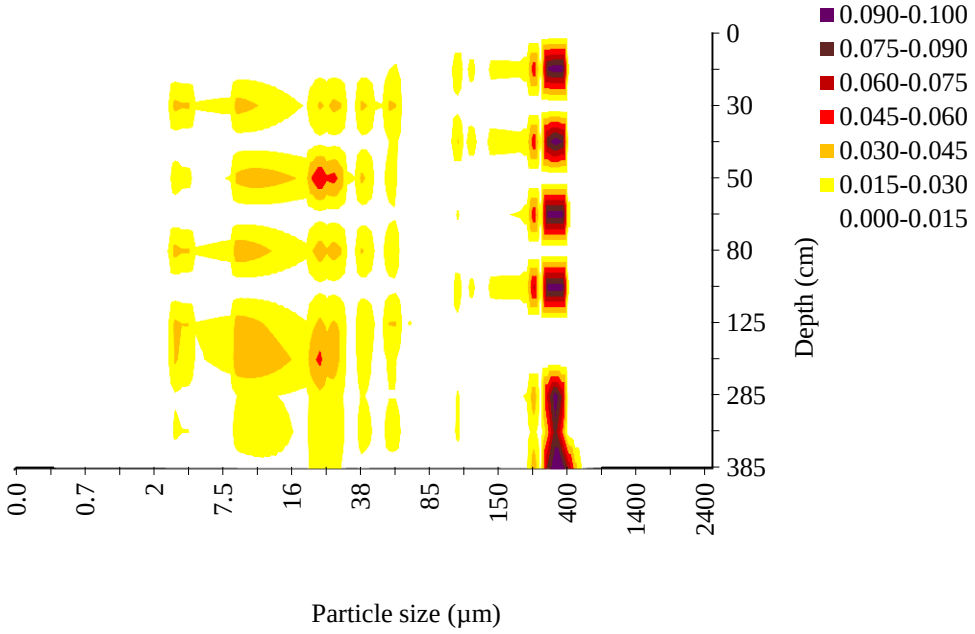

Figure A1: Particle size distribution surface plot for the outcrop sediment sample at location C along River Benue in Nigeria. For location of sample point see outcrop sampling along transect 1 Figure 5.30. The values 0.000 to 0.100 are percentage concentration of the sedimemts. Depth scale is not linear.

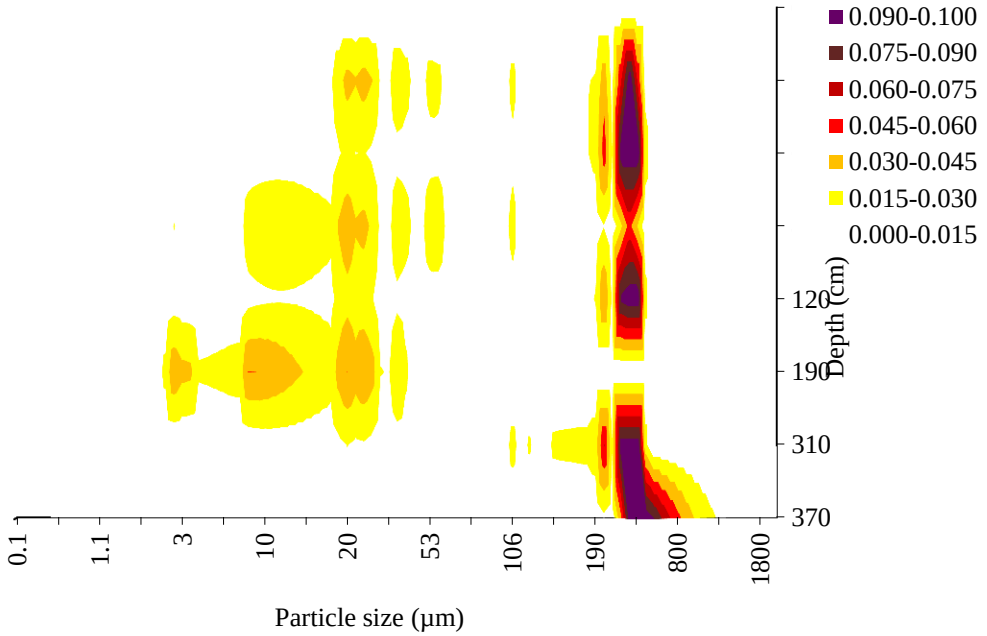

Figure A2: Particle size distribution surface plot for the outcrop sediment sample at location G along River Benue in Nigeria. For location of sample point see outcrop sampling along transect 2 Figure 5.30. The values 0.000 to 0.100 are percentage concentration of the sedimemts. Depth scale is not linear.

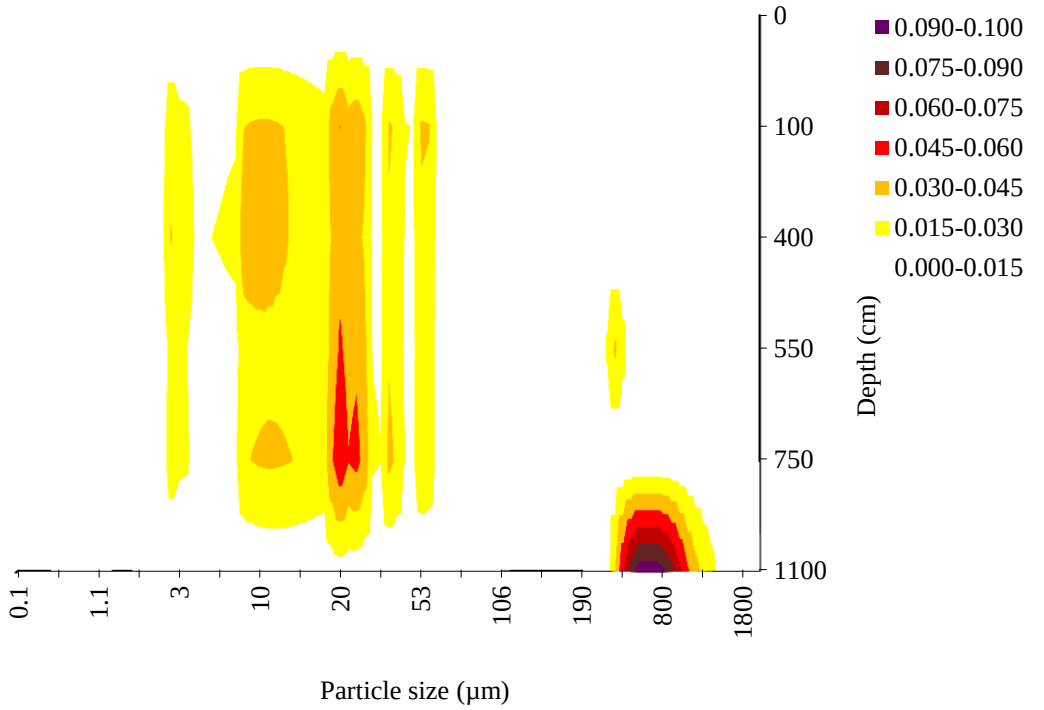

Figure A3: Particle size distribution surface plot for sediment sample at location borehole 4. For location of sample point see transect 2 (Figure 5.30). The values 0.000 to 0.100 are percentage concentration of the sediments. Depth scales are not liner.

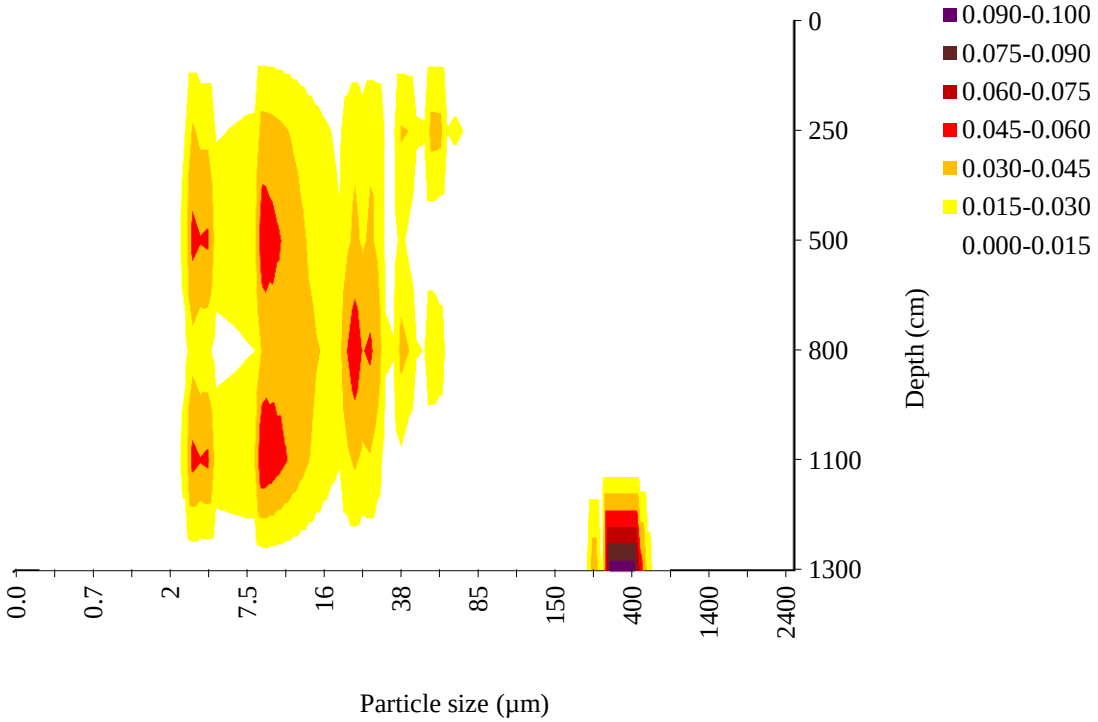

Figure A4: Particle size distribution surface plot for sediment sample at location borehole 7. For location of sample point see transect 4 (Figure 5.30). The values 0.000 to 0.100 are percentage concentration of the sediments. Depth scales are not liner.

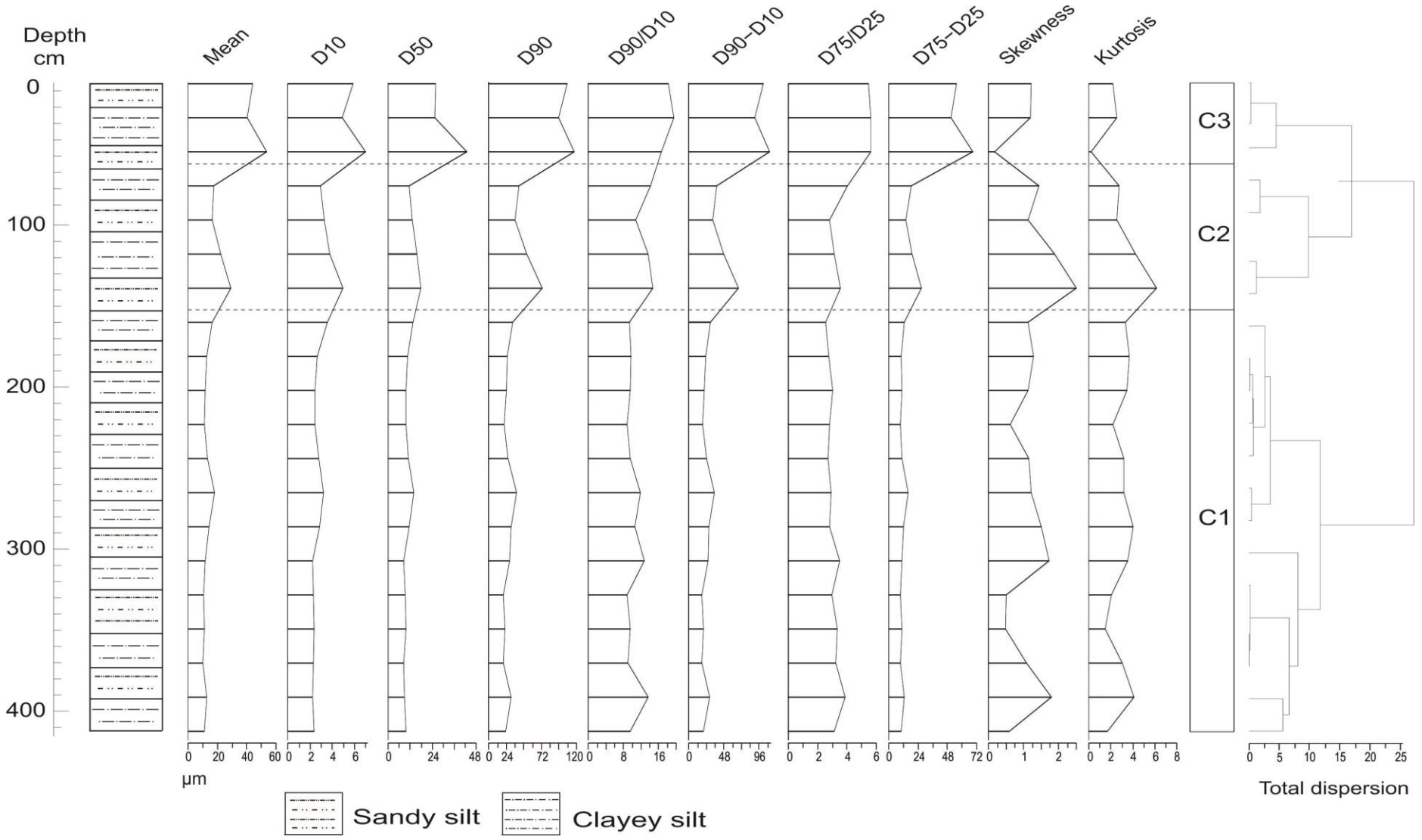

Figure A5: Summary statistics for grain size data for outcrop sediment sample on the River Benue in Cameroon. For location of sample point (see Figure 1.1).

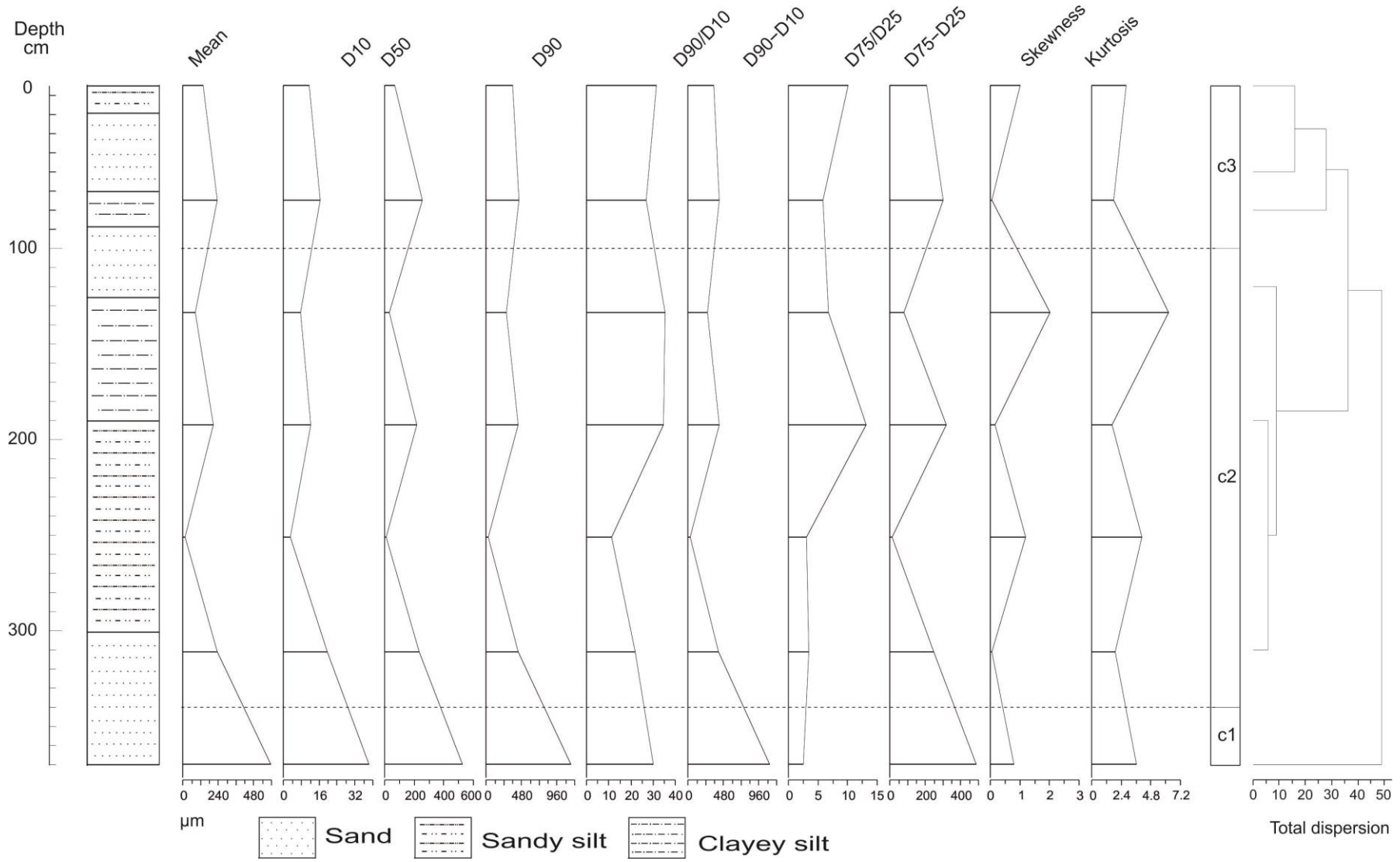

Figure A6: Summary statistics for grain size data for the outcrop sediment samples at location G on the River Benue in Nigeria. For location of sample point see outcrop sampling along transect 2 (see Figure 5.30).

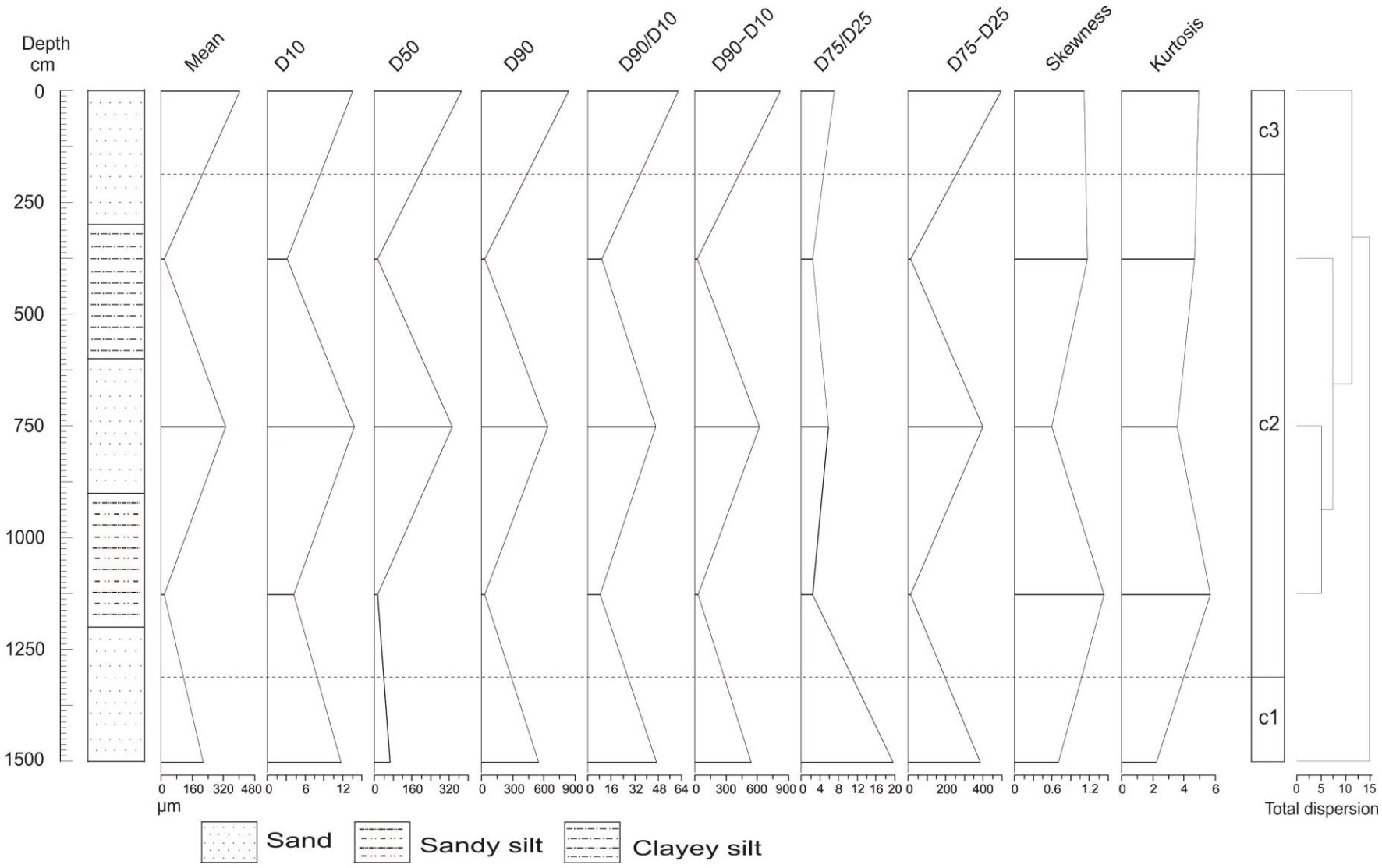

Figure A7: Summary statistics for grain size data for the coring on the floodplain sediment sample at location borehole 11. For location of sample point (see Figure 5.30).

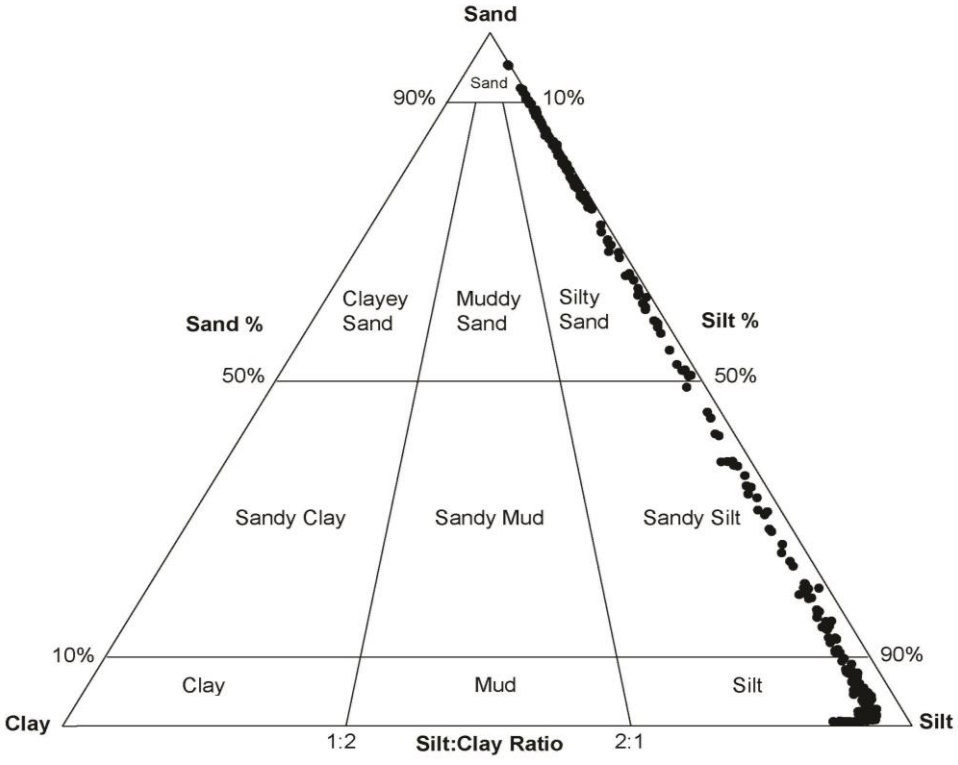

Figure A8: Particle size distribution for both outcrops and boreholes samples on sand-silt-clay triangular plot.

Table A: Particle size data for the two hundred and fifty six sediment samples collected. Cu – Coefficient of Uniformity; D – grain size diameter

Sample location A										
S/NO	Depth (cm)	D10 (µm)	D50 (µm)	D60 (µm)	D90 (µm)	(D90 / D10) (µm)	(D90 - D10) (µm)	(D75 / D25) (µm)	(D75 - D25) (µm)	Cu
1	15	5.92	26.12	32.04	107.60	18.18	101.70	5.49	55.66	5.41
2	40	4.91	25.30	30.21	95.47	19.44	90.56	5.62	50.86	6.15
3	55	7.03	42.72	49.75	117.00	16.66	110.00	5.64	68.62	7.08
4	75	2.93	11.61	14.54	41.32	14.11	38.40	4.02	18.44	4.97
5	95	3.32	13.12	16.44	35.83	10.78	32.50	2.81	14.16	4.95
6	125	3.79	15.58	19.37	51.65	13.63	47.86	3.13	19.35	5.11
7	145	4.98	18.05	23.03	73.42	14.74	68.44	3.54	26.74	4.62
8	165	3.55	13.78	17.33	33.20	9.35	29.65	2.54	13.04	4.88
9	185	2.65	10.53	13.18	25.76	9.72	23.11	2.76	10.47	4.98
10	205	2.49	9.95	12.43	23.93	9.63	21.45	3.03	10.60	5.00
11	225	2.45	9.64	12.09	21.48	8.78	19.03	2.79	9.47	4.94

S/NO	Depth (cm)	D10 (µm)	D50 (µm)	D60 (µm)	D90 (µm)	(D90 / D10) (µm)	(D90 - D10) (µm)	(D75 / D25) (µm)	(D75 - D25) (µm)	Cu
12	245	2.78	10.94	13.72	26.80	9.63	24.02	2.69	10.71	4.93
13	265	3.23	14.18	17.41	38.21	11.83	34.98	2.92	15.70	5.39
14	285	2.89	11.56	14.45	30.68	10.61	27.79	2.79	11.94	5.00
15	305	2.23	8.42	10.64	28.34	12.73	26.12	3.51	10.76	4.78
16	325	2.32	9.44	11.76	20.54	8.85	18.22	2.95	9.54	5.07
17	355	2.36	9.68	12.03	22.36	9.48	20.00	3.36	10.81	5.10
18	375	2.31	8.50	10.82	20.68	8.94	18.37	3.22	9.47	4.68
19	395	2.24	9.06	11.31	30.61	13.66	28.37	3.89	12.56	5.04
20	415	2.40	9.58	11.98	22.87	9.52	20.46	3.14	10.48	4.99
Sample location B										
1	15	4.50	16.37	20.87	42.56	9.46	38.06	2.75	17.41	4.64
2	30	3.73	14.80	18.53	39.10	10.49	35.37	2.87	16.43	4.97
3	45	4.08	16.00	20.08	44.65	10.94	40.57	2.95	18.45	4.92
4	55	12.91	97.63	110.55	333.65	25.84	320.73	6.01	161.35	8.56
5	60	4.78	18.57	23.35	60.15	12.58	55.37	3.11	22.89	4.88
6	75	19.50	125.66	145.16	331.77	17.01	312.27	3.03	133.57	7.44
7	95	4.95	19.16	24.11	58.53	11.83	53.59	3.33	24.81	4.87
8	105	12.29	63.28	75.57	205.08	16.69	192.79	4.33	87.17	6.15
9	110	3.38	14.31	17.69	48.77	14.42	45.39	3.65	20.67	5.23
10	115	34.30	265.32	299.63	443.80	12.94	409.49	2.41	212.54	8.73
11	120	4.87	21.09	25.96	77.09	15.82	72.21	4.47	36.75	5.33
12	125	21.84	168.39	190.23	377.89	17.30	356.05	2.66	165.42	8.71
13	150	9.79	102.33	112.12	379.30	38.75	369.51	11.06	232.05	11.46
14	165	22.04	326.92	348.96	611.78	27.76	589.74	3.15	319.83	15.83
15	170	3.20	11.68	14.89	35.63	11.12	32.43	2.92	12.92	4.65
16	180	34.04	198.13	232.17	404.31	11.88	370.27	2.49	183.90	6.82
17	195	9.73	66.74	76.47	304.58	31.31	294.86	8.15	136.71	7.86
18	215	6.21	23.33	29.53	90.51	14.59	84.31	4.29	40.68	4.76
19	230	14.54	117.94	132.49	365.85	25.16	351.31	6.81	200.37	9.11
20	260	4.44	16.68	21.12	56.03	12.62	51.59	3.36	22.69	4.76
21	280	3.75	14.63	18.38	55.80	14.90	52.05	3.62	21.78	4.91
22	300	17.37	200.69	218.06	415.09	23.90	397.72	4.92	256.71	12.55
23	315	9.01	66.43	75.44	361.18	40.11	352.17	11.63	188.57	8.38
24	345	34.13	335.75	369.88	679.36	19.91	645.23	2.76	310.76	10.84
Sample location C										
1	20	17.65	200.10	217.76	421.03	23.85	403.38	4.10	249.61	12.33
2	30	3.78	16.62	20.39	72.57	19.21	68.80	5.07	33.58	5.40
3	40	15.27	175.22	190.49	405.84	26.58	390.57	4.45	239.42	12.48

S/NO	Depth (cm)	D10 (µm)	D50 (µm)	D60 (µm)	D90 (µm)	(D90 / D10) (µm)	(D90 - D10) (µm)	(D75 / D25) (µm)	(D75 - D25) (µm)	Cu
4	50	5.14	17.44	22.58	46.87	9.11	41.73	2.78	18.82	4.39
5	65	20.73	258.95	279.68	442.35	21.34	421.62	3.48	257.35	13.49
6	80	3.57	14.73	18.30	55.07	15.42	51.50	3.90	23.26	5.13
7	95	20.21	220.70	240.91	425.86	21.07	405.65	3.38	237.64	11.92
8	125	3.87	16.56	20.43	76.69	19.83	72.83	4.96	33.81	5.28
9	165	3.85	14.75	18.60	44.91	11.67	41.06	2.84	16.17	4.83
10	285	8.57	88.92	97.49	387.87	45.24	379.30	14.92	254.95	11.37
11	315	6.45	41.21	47.66	348.03	53.97	341.58	11.92	147.12	7.39
12	385	14.66	264.09	278.75	538.31	36.71	523.65	13.03	376.20	19.01
Sample location D										
1	10	15.10	180.73	195.83	402.35	26.65	387.25	4.01	228.87	12.97
2	30	4.28	25.01	29.29	332.60	77.69	328.32	14.75	151.32	6.84
3	170	8.52	32.98	41.50	280.33	32.91	271.82	6.70	87.89	4.87
4	190	12.02	97.08	109.10	382.34	31.81	370.32	10.78	233.25	9.08
5	205	12.84	202.87	215.70	422.21	32.89	409.37	4.71	261.45	16.80
6	225	5.92	21.75	27.67	194.35	32.85	188.43	4.83	45.65	4.68
7	280	9.83	99.35	109.17	380.28	38.70	370.45	12.23	237.20	11.11
8	300	12.86	165.16	178.02	403.54	31.38	390.68	7.53	265.37	13.84
9	370	9.68	135.99	145.67	396.69	40.96	387.00	11.76	268.53	15.04
10	470	4.46	16.91	21.37	48.49	10.86	44.03	3.08	20.30	4.79
11	500	18.59	225.01	243.61	428.89	23.07	410.30	3.38	240.52	13.10
Sample location E										
1	10	16.92	131.49	148.40	377.50	22.32	360.59	4.63	199.93	8.77
2	30	16.17	239.83	256.00	433.80	26.83	417.64	3.27	242.12	15.84
3	110	14.09	162.26	176.35	394.16	27.97	380.07	4.23	220.74	12.51
4	260	3.92	15.58	19.51	44.77	11.41	40.85	2.83	16.87	4.97
5	320	14.90	222.77	237.67	429.06	28.80	414.16	4.15	259.36	15.95
6	350	3.95	14.97	18.92	42.64	10.79	38.69	2.76	15.75	4.79
7	365	3.10	11.80	14.90	43.72	14.09	40.62	3.31	15.27	4.80
8	395	15.25	229.66	244.92	430.13	28.20	414.88	3.67	250.03	16.06
9	415	5.89	22.09	27.99	322.90	54.80	317.01	9.12	94.99	4.75
10	475	6.07	24.86	30.93	355.66	58.63	349.59	15.39	173.80	5.10
11	505	3.96	14.48	18.44	36.49	9.21	32.53	2.62	14.35	4.66
12	515	18.83	370.73	389.55	771.48	40.98	752.65	2.75	347.95	20.69
Sample location F										
1	15	13.67	185.86	199.53	403.53	29.53	389.87	3.84	226.46	14.60
2	45	4.95	16.68	21.63	42.02	8.48	37.07	2.55	16.08	4.37
3	105	29.67	257.53	287.20	439.20	14.80	409.53	2.46	211.82	9.68

S/NO	Depth (cm)	D10 (µm)	D50 (µm)	D60 (µm)	D90 (µm)	(D90 / D10) (µm)	(D90 - D10) (µm)	(D75 / D25) (µm)	(D75 - D25) (µm)	Cu
4	175	2.80	12.10	14.89	28.25	10.10	25.45	2.87	12.45	5.33
5	235	10.04	23.84	33.87	271.19	27.02	261.15	2.98	29.98	3.38
6	385	8.46	49.36	57.82	127.23	15.04	118.77	4.95	71.77	6.83
7	415	23.11	381.44	404.55	698.81	30.24	675.70	2.19	288.60	17.51
8	585	4.42	16.55	20.97	51.41	11.63	46.99	2.98	19.62	4.74
9	600	17.65	233.07	250.72	433.88	24.58	416.23	4.20	265.65	14.21
Sample location G										
1	15	11.63	67.99	79.62	365.80	31.46	354.20	10.10	208.80	6.85
2	60	16.34	256.08	272.42	441.90	27.04	425.50	5.88	299.10	16.67
3	80	7.66	30.40	38.06	272.39	35.55	264.70	6.76	81.30	4.97
4	120	12.44	217.60	230.04	432.80	34.79	420.40	13.19	320.50	18.49
5	190	3.14	13.07	16.21	35.73	11.38	32.59	3.11	15.36	5.16
6	310	19.78	236.00	255.78	434.00	21.95	414.30	3.50	249.30	12.93
7	370	38.22	527.90	566.12	1145.30	29.97	1107.10	2.47	484.90	14.81
Sample location H										
1	15	4.69	16.74	21.43	49.52	10.56	44.83	2.88	18.96	4.57
2	30	8.92	30.53	39.45	68.77	7.71	59.84	3.27	36.34	4.42
3	50	4.25	16.47	20.71	53.89	12.69	49.65	3.39	22.79	4.88
4	65	311.54	664.80	976.34	1163.62	3.74	852.08	1.94	436.51	3.13
5	75	5.17	26.99	32.16	479.69	92.72	474.51	23.54	252.72	6.22
6	85	36.91	306.58	343.49	536.57	14.54	499.66	2.52	256.84	9.31
7	115	5.09	17.86	22.95	54.80	10.77	49.71	3.02	21.42	4.51
8	125	33.30	327.14	360.45	547.04	16.43	513.74	1.98	215.58	10.82
9	155	7.81	37.45	45.25	241.74	30.96	233.93	6.36	82.01	5.80
10	170	33.57	308.09	341.66	532.60	15.86	499.03	2.46	251.60	10.18
11	370	7.75	34.39	42.14	108.68	14.03	100.93	5.26	60.87	5.44
12	390	3.54	13.95	17.49	50.61	14.30	47.07	3.65	20.86	4.94
13	410	4.50	19.75	24.25	69.67	15.50	65.17	4.20	33.56	5.39
14	425	21.45	322.96	344.41	554.00	25.83	532.55	2.40	255.59	16.06
15	455	3.62	13.60	17.22	41.88	11.58	38.27	3.09	16.72	4.76
16	470	38.57	313.81	352.38	555.01	14.39	516.44	3.17	302.71	9.14
17	500	24.08	542.54	566.62	1153.43	47.90	1129.36	2.52	497.46	23.53
Sample location I										
1	45	12.70	139.15	151.86	369.00	29.04	356.29	6.18	207.74	11.95
2	65	9.81	85.10	94.90	265.94	27.12	256.13	5.24	119.31	9.68
3	115	16.24	229.75	245.99	429.17	26.43	412.93	4.85	271.66	15.15
4	120	6.12	38.22	44.34	307.74	50.31	301.62	7.66	86.83	7.25
5	320	22.41	312.85	335.26	520.93	23.24	498.52	2.14	222.81	14.96

S/NO	Depth (cm)	D10 (µm)	D50 (µm)	D60 (µm)	D90 (µm)	(D90 / D10) (µm)	(D90 - D10) (µm)	(D75 / D25) (µm)	(D75 - D25) (µm)	Cu
6	325	3.83	15.74	19.57	63.36	16.56	59.53	4.05	26.85	5.11
7	330	16.64	147.32	163.96	368.98	22.17	352.34	3.90	185.73	9.85
8	365	3.02	11.91	14.93	39.97	13.23	36.95	3.32	15.44	4.94
9	375	46.28	331.26	377.54	545.93	11.80	499.65	1.89	205.70	8.16
10	390	8.18	33.62	41.79	107.32	13.13	99.15	4.55	56.61	5.11
11	410	16.79	301.38	318.17	524.05	31.21	507.26	4.48	320.80	18.95
12	420	14.52	84.92	99.44	221.39	15.25	206.87	3.14	89.93	6.85
13	425	4.68	18.38	23.07	67.82	14.48	63.13	3.74	28.53	4.92
14	495	17.34	358.17	375.51	732.01	42.20	714.66	8.40	474.43	21.65
15	525	3.67	13.96	17.63	35.32	9.61	31.64	2.66	14.09	4.80
16	585	12.93	248.09	261.03	519.54	40.17	506.61	16.67	371.84	20.18
Sample location J										
1	15	12.86	111.66	124.52	329.86	25.66	317.01	7.05	173.37	9.69
2	85	17.18	247.39	264.57	436.35	25.40	419.16	3.42	249.55	15.40
3	160	5.58	24.80	30.38	89.50	16.03	83.91	4.90	46.71	5.44
4	175	22.57	250.87	273.44	439.52	19.47	416.95	2.98	237.26	12.12
5	205	20.03	149.85	169.87	377.90	18.87	357.87	3.35	181.84	8.48
6	225	3.77	15.41	19.18	57.18	15.17	53.41	4.17	26.75	5.09
7	235	28.95	229.49	258.44	430.08	14.86	401.13	2.91	225.28	8.93
8	285	3.92	15.92	19.83	55.31	14.12	51.39	3.47	22.47	5.06
9	400	34.14	322.46	356.61	541.77	15.87	507.63	2.15	231.54	10.44
Sample location K										
1	90	11.31	90.61	101.93	349.72	30.91	338.40	8.67	183.10	9.01
2	240	5.21	19.71	24.91	73.06	14.04	67.86	3.69	29.90	4.79
3	240	5.57	23.93	29.50	84.73	15.21	79.16	4.31	40.38	5.30
4	640	19.31	150.74	170.05	353.85	18.32	334.53	2.69	146.47	8.80
5	840	54.27	296.99	351.25	454.10	8.37	399.83	1.84	172.70	6.47
Sample location L										
1	45	4.61	16.52	21.14	54.56	11.83	49.95	3.30	22.36	4.58
2	165	21.39	211.33	232.72	416.57	19.47	395.18	2.91	212.87	10.88
3	215	16.63	186.03	202.66	407.79	24.52	391.16	3.63	225.87	12.19
4	235	120.51	454.34	574.85	775.44	6.43	654.94	1.82	272.60	4.77
5	255	15.00	114.25	129.25	354.20	23.61	339.20	4.34	163.03	8.62
6	455	104.07	440.52	544.58	783.16	7.53	679.10	1.90	282.33	5.23
Sample location M										
1	15	10.85	77.77	88.62	202.08	18.62	191.23	4.79	100.06	8.17
2	45	30.42	258.00	288.42	439.00	14.43	408.58	2.30	201.69	9.48
3	75	3.78	16.73	20.51	62.79	16.61	59.01	4.18	28.34	5.43

S/NO	Depth (cm)	D10 (µm)	D50 (µm)	D60 (µm)	D90 (µm)	(D90 / D10) (µm)	(D90 - D10) (µm)	(D75 / D25) (µm)	(D75 - D25) (µm)	Cu
4	115	30.08	590.67	620.75	1105.61	36.76	1075.53	2.37	489.32	20.64
5	120	3.79	15.63	19.42	59.46	15.70	55.67	3.82	24.55	5.13
6	170	28.73	263.46	292.20	444.16	15.46	415.43	2.82	234.90	10.17
7	175	4.10	16.73	20.83	56.52	13.78	52.41	3.67	25.12	5.08
8	265	28.72	341.05	369.77	569.90	19.84	541.18	1.98	225.75	12.88
9	270	8.59	67.05	75.64	278.77	32.45	270.18	7.09	115.33	8.80
10	570	21.75	318.69	340.43	554.02	25.47	532.27	2.95	289.85	15.65
Sample location N										
1	50	26.22	263.79	290.02	443.54	16.91	417.32	2.60	223.32	11.06
2	65	14.32	179.84	194.17	398.31	27.81	383.99	4.10	225.46	13.56
3	125	19.98	197.56	217.54	411.30	20.58	391.32	4.06	239.14	10.89
4	225	4.98	22.02	27.00	81.68	16.40	76.70	4.32	38.18	5.42
5	235	29.87	309.80	339.68	548.24	18.35	518.36	2.85	280.91	11.37
6	245	3.43	13.88	17.31	46.58	13.58	43.15	3.58	20.15	5.05
7	255	48.99	379.95	428.94	741.30	15.13	692.31	2.13	284.67	8.76
8	265	5.74	59.19	64.92	493.44	86.03	487.71	26.22	336.55	11.32
9	345	72.19	344.67	416.86	575.04	7.97	502.85	1.86	211.18	5.77
10	360	5.26	20.56	25.81	74.40	14.15	69.15	3.87	32.26	4.91
11	600	67.76	345.26	413.02	599.45	8.85	531.69	1.95	228.83	6.10
12	610	10.24	95.96	106.20	375.00	36.63	364.76	8.99	213.65	10.37
Sample location O										
1	100	13.40	114.50	127.91	332.63	24.82	319.23	4.31	151.34	9.54
2	130	26.70	263.43	290.13	441.39	16.53	414.70	2.24	199.38	10.87
3	330	9.15	101.25	110.41	380.72	41.60	371.56	12.02	231.30	12.06
4	345	30.93	393.55	424.48	705.69	22.81	674.76	2.01	270.92	13.72
5	365	10.24	94.32	104.56	328.61	32.09	318.37	6.75	157.71	10.21
6	375	3.42	13.11	16.53	34.78	10.17	31.36	2.67	13.16	4.83
7	575	15.04	225.22	240.26	532.35	35.40	517.31	6.59	352.00	15.98
8	675	244.50	513.77	758.27	889.17	3.64	644.68	1.84	316.59	3.10
Sample location P										
1	30	4.45	17.70	22.15	62.62	14.08	58.17	3.70	26.72	4.98
2	70	64.97	323.36	388.33	534.20	8.22	469.23	1.95	208.47	5.98
3	80	11.80	254.71	266.52	536.81	45.48	525.01	9.35	372.59	22.58
4	100	46.68	389.80	436.49	815.59	17.47	768.91	2.36	327.72	9.35
5	105	22.43	225.31	247.74	428.22	19.09	405.79	3.01	227.63	11.04
6	605	32.00	336.66	368.66	533.60	16.68	501.60	1.74	184.25	11.52
Sample location Q										
1	40	5.29	20.28	25.57	82.45	15.58	77.16	4.61	38.75	4.83

S/NO	Depth (cm)	D10 (µm)	D50 (µm)	D60 (µm)	D90 (µm)	(D90 / D10) (µm)	(D90 - D10) (µm)	(D75 / D25) (µm)	(D75 - D25) (µm)	Cu
2	50	41.39	213.32	254.71	425.62	10.28	384.23	3.21	231.77	6.15
3	170	41.89	286.45	328.34	451.44	10.78	409.55	2.21	205.50	7.84
4	175	4.72	23.61	28.33	83.19	17.63	78.47	5.12	43.38	6.00
5	235	18.28	182.36	200.64	420.69	23.01	402.40	4.19	250.18	10.97
6	245	19.78	162.08	181.87	409.41	20.69	389.63	3.69	227.48	9.19
7	545	93.02	351.76	444.77	584.82	6.29	491.80	1.84	213.32	4.78
Sample borehole 1										
1	100	45.00	320.34	365.34	546.40	12.14	501.40	2.15	231.95	8.12
2	400	29.83	296.47	326.31	454.21	15.23	424.38	1.95	185.10	10.94
3	500	4.20	16.77	20.97	67.95	16.20	63.75	3.89	27.43	5.00
4	600	24.42	259.54	283.96	441.15	18.07	416.74	2.64	223.62	11.63
5	650	3.51	13.62	17.13	40.53	11.54	37.02	2.91	15.29	4.88
6	800	48.39	438.29	486.68	815.43	16.85	767.04	2.04	312.53	10.06
Sample borehole 2										
1	200	5.18	17.67	22.85	46.42	8.96	41.24	2.63	17.83	4.41
2	300	9.03	46.87	55.90	383.00	42.42	373.97	14.96	241.16	6.19
3	500	3.80	15.77	19.57	38.43	10.12	34.63	2.77	16.29	5.15
4	650	17.19	267.93	285.12	445.72	25.92	428.53	4.73	288.82	16.58
Sample borehole 3										
1	100	9.74	106.91	116.65	508.56	52.19	498.82	18.89	355.74	11.97
2	250	21.28	255.78	277.06	439.64	20.66	418.36	2.67	223.65	13.02
3	550	3.09	13.11	16.21	36.88	11.92	33.78	3.11	15.63	5.24
4	750	80.41	359.23	439.65	672.47	8.36	592.06	2.24	275.61	5.47
5	800	2.70	10.75	13.45	34.65	12.84	31.96	3.34	13.35	4.98
6	1100	20.31	362.77	383.08	680.95	33.53	660.64	2.60	315.21	18.86
Sample borehole 4										
1	100	4.75	19.89	24.65	79.26	16.68	74.51	4.07	33.49	5.19
2	400	3.94	16.32	20.25	69.32	17.61	65.39	4.03	27.52	5.14
3	550	6.31	25.12	31.43	180.83	28.66	174.52	4.99	52.19	4.98
4	750	5.35	20.13	25.48	68.78	12.85	63.43	3.30	26.53	4.76
5	1100	45.62	797.17	842.79	1332.99	29.22	1287.36	1.96	521.73	18.47
Sample borehole 5										
1	150	3.40	13.59	16.99	40.00	11.75	36.60	2.86	14.88	4.99
2	300	13.27	111.64	124.91	349.31	26.32	336.03	5.12	170.29	9.41
3	600	4.42	16.24	20.66	50.70	11.48	46.28	3.14	20.60	4.68
4	750	40.75	388.90	429.65	669.67	16.43	628.92	2.05	269.09	10.54
5	850	4.97	19.25	24.22	83.10	16.72	78.13	3.98	32.23	4.87
6	950	5.24	30.51	35.76	346.17	66.02	340.92	12.94	133.11	6.82

S/NO	Depth (cm)	D10 (µm)	D50 (µm)	D60 (µm)	D90 (µm)	(D90 / D10) (µm)	(D90 - D10) (µm)	(D75 / D25) (µm)	(D75 - D25) (µm)	Cu
7	1050	30.74	195.58	226.32	406.12	13.21	375.38	2.74	196.86	7.36
Sample borehole 6										
1	200	4.73	21.08	25.81	96.93	20.48	92.19	4.15	35.70	5.45
2	500	3.75	15.75	19.50	53.25	14.19	49.50	3.14	19.33	5.20
3	700	6.29	23.96	30.25	93.29	14.84	87.00	4.12	39.75	4.81
4	1000	5.71	25.34	31.05	154.86	27.14	149.16	5.85	59.49	5.44
5	1200	165.64	473.81	639.45	940.68	5.68	775.04	2.11	361.15	3.86
Sample borehole 7										
1	250	3.70	17.62	21.32	84.83	22.91	81.13	5.75	41.71	5.76
2	500	2.79	10.65	13.44	30.76	11.02	27.97	3.02	11.92	4.82
3	800	4.89	18.20	23.09	54.54	11.15	49.65	3.09	22.34	4.72
4	1100	2.77	10.29	13.07	26.46	9.54	23.69	2.77	10.36	4.71
5	1300	71.88	346.87	418.75	584.96	8.14	513.08	1.95	227.37	5.83
Sample borehole 8										
1	40	3.81	17.14	20.95	66.05	17.32	62.24	4.26	30.23	5.49
2	150	35.59	313.64	349.23	534.57	15.02	498.98	2.21	232.51	9.81
3	170	3.44	13.92	17.36	41.97	12.20	38.53	2.89	15.41	5.05
4	210	36.62	204.38	241.00	405.74	11.08	369.12	2.46	183.82	6.58
5	215	4.16	17.17	21.33	56.64	13.61	52.47	3.55	24.67	5.13
6	615	18.69	293.10	311.80	541.68	28.98	522.99	3.80	312.66	16.68
Sample borehole 9										
1	50	8.16	47.46	55.62	240.22	29.43	232.06	7.96	109.77	6.81
2	200	64.87	379.32	444.19	685.88	10.57	621.02	1.96	254.32	6.85
3	250	3.77	14.59	18.36	40.98	10.87	37.21	2.81	15.59	4.87
4	500	27.08	314.58	341.66	461.85	17.06	434.78	1.88	183.27	12.62
Sample borehole 10										
1	300	3.11	13.08	16.20	32.43	10.42	29.32	2.83	13.58	5.20
2	500	8.75	248.39	257.14	439.56	50.22	430.80	15.19	333.45	29.38
3	700	3.14	13.15	16.29	31.69	10.10	28.55	2.67	12.91	5.19
4	1000	2.90	12.09	14.99	31.56	10.88	28.66	2.75	12.12	5.17
5	1300	5.55	25.17	30.72	319.27	57.49	313.72	7.42	74.04	5.53
6	1500	4.40	18.83	23.24	63.69	14.47	59.29	3.78	29.00	5.28
Sample borehole 11										
1	300	13.58	372.73	386.31	836.05	61.57	822.47	7.11	493.53	28.45
2	600	3.21	13.70	16.90	30.70	9.57	27.49	2.53	12.65	5.27
3	900	13.81	334.41	348.23	638.56	46.23	624.74	5.82	396.58	25.21
4	1200	4.24	15.31	19.55	35.50	8.37	31.26	2.48	14.13	4.61
5	1500	11.71	66.12	77.83	550.62	47.03	538.91	19.66	386.94	6.65

S/NO	Depth (cm)	D10 (µm)	D50 (µm)	D60 (µm)	D90 (µm)	(D90 / D10) (µm)	(D90 - D10) (µm)	(D75 / D25) (µm)	(D75 - D25) (µm)	Cu
Sample borehole 12										
1	300	2.07	9.37	11.44	21.93	10.60	19.87	3.78	10.98	5.53
2	600	3.17	13.58	16.75	34.23	10.79	31.06	2.86	14.36	5.28
3	900	2.05	9.15	11.20	20.34	9.94	18.30	3.26	9.67	5.47
4	1200	3.50	14.35	17.84	59.71	17.08	56.21	3.91	23.34	5.10
5	1500	2.37	11.19	13.56	21.61	9.11	19.23	2.66	10.22	5.72
6	1800	6.77	76.24	83.01	531.24	78.47	524.47	26.63	374.67	12.26

APPENDIX B: Procedures followed to obtain loss on ignition

The procedures followed to obtain loss on ignition as proposed by Bengtsson and Enell (1986).

i. The ceramic crucibles were cleaned with water dried in an oven to remove moisture and weighed after cooling to room temperature using a Mettler AE160 balance. The weight of the crucibles was determined.

ii. Fresh samples of 10 to 15 g were place to the crucibles and the weights of samples plus crucibles were determined. The samples plus crucibles were then placed in an oven at 105 $^{\circ}$C and were dry to constant weight overnight for 36 hours.

iii. The crucibles and samples were cool to room temperature and the weight of the dry samples plus crucibles was determined.

iv. The crucibles with the dry samples were then placed in a muffle furnace for 2 hours at 550 $^{\circ}$C. The crucibles and sediment ash were placed in a dessicator again until cool and then weighed.

v. The crucibles with the ignited samples were cool to room temperature and the weights of ashes plus crucibles were determined.

vi. The crucibles with the ignited samples were further placed in a muffle furnace for 4 hours at 950 $^{\circ}$C.

vii. The crucibles with the ignited samples were cool to room temperature and the weights of ashes plus crucibles were determined.

Equations (1, 2 and 3) were used to estimate the Water content (θ), LOI at 550 ˚C and LOI at 950 ˚C in percentage for the sediment samples. Volk and Costa (2010) have shown that values less than 5% in the sediments might be a function of clay dewatering and thus, anything less than 5% is interpreted to have essentially zero LOI at 950 ˚C. When the LOI is very low, it may be lost of moisture bond within a clayey silt of the sediments.

After oven-drying of the sediment samples for thirty six hours at 105 ˚C, moisture content of the sediment samples can be calculated by the formula as follow:

$$\theta = \frac{W_{wet} - W_{dry}}{W_{wet}} \text{ X } 100 \qquad 1$$

where θ is the moisture content (%); W_{wet} is the sample weight (g) and W_{dry} is the sample dry wet (g).

After the moisture content determination, the LOI at 550 ˚C and LOI at 950 ˚C can be determined as follows. The loss on ignition at 550 ˚C is used to estimate the percentage loss of LOI at 550 ˚C and the loss on ignition at 950 ˚C is used to estimate the percentage loss of LOI at 950 ˚C in the sediment samples, using the equation as follows:

$$\text{LOI at } 550\ ^{\circ}\text{C} = \left[\frac{DW_{105} - DW_{550}}{DW_{105}}\right] \text{ X } 100 \qquad 2$$

where DW_{105} is the dry weight of the sample (g) and DW_{550} is the dry weight of the sample after heating to 550 ˚C (g).

$$\text{LOI at } 950\ ^{\circ}\text{C} = \left[\frac{DW_{550} - DW_{950}}{DW_{105}}\right] \text{ X } 100 \qquad 3$$

where DW_{950} is the dry weight of the sample after heating to 950 ˚C (g).

Table B: Sediment colour by Munsell chart, and loss on ignition (LOI) data for the two hundred and fifty six sediment samples collected. MC – moisture content

Sample location A						
S/No	Depth (cm)	Colour code	Colour	MC (%)	LOI at 550 ˚C	LOI at 950 ˚C
1	15	2.5Y 5/4	Reddish brown	1.15	2.64	0.69
2	40	2YR 7/1	Light gray	1.49	2.97	0.58
3	55	7.5YR 8/2	Pinkish white	1.30	2.85	0.64
4	75	2.5YR 7/2	Pale red	2.83	5.65	1.22
5	95	10R 8/2	Very pinkish white	3.16	6.01	1.12
6	125	GLEY1 7/10Y	Light greenish gray	2.24	4.02	0.87
7	145	7.5YR 8/2	Pinkish white	1.57	3.43	0.70
8	165	5YR 5/2	Reddish gray	2.24	6.56	1.23
9	185	2.5YR 7/2	Pale red	2.65	7.28	1.32
10	205	2.5YR 5/2	Weak red	3.53	8.02	1.45
11	225	5YR 5/2	Reddish gray	2.38	8.08	1.49
12	245	2.5YR 5/2	Weak red	2.88	7.48	1.29
13	265	2.5YR 6/3	Light reddish brown	2.61	4.97	1.01
14	285	2.5YR 6/3	Light reddish brown	2.75	6.14	1.28
15	305	5YR 6/2	Pinkish gray	3.03	7.19	1.34
16	325	5YR 6/2	Pinkish gray	2.28	8.28	1.51
17	355	2.5YR 5/2	Weak red	3.28	7.76	1.28
18	375	2.5YR 6/3	Light reddish brown	3.75	6.55	1.71
19	395	2.5YR 4/1	Dark reddish gray	18.50	6.74	1.56
20	415	2.5YR 4/1	Dark reddish gray	23.39	7.18	1.11
Sample location B						
1	15	2.5YR 5/2	Weak red	1.72	5.60	0.77
2	30	2.5YR 4/3	Reddish brown	1.76	5.85	0.91
3	45	2.5YR 4/3	Reddish brown	1.77	5.83	1.00
4	55	2.5YR 6/3	Light reddish brown	1.60	2.03	0.54
5	60	2.5YR 4/3	Reddish brown	1.65	4.81	0.92
6	75	2.5YR 4/3	Reddish brown	1.11	1.58	0.38
7	95	2.5YR 5/2	Weak red	1.94	6.90	1.03
8	105	5YR 5/2	Reddish gray	1.27	2.72	0.69
9	110	2.5YR 5/2	Weak red	2.69	5.29	1.08
10	115	2.5YR 8/4	Pink	2.72	0.61	0.20
11	120	2.5YR 6/6	Light red	2.72	4.99	0.98
12	125	2.5YR 8/4	Pink	2.74	0.83	0.27

S/No	Depth (cm)	Colour code	Colour	MC (%)	LOI at 550 ˚C	LOI at 950 ˚C
13	150	2.5YR 6/6	Light red	2.78	2.26	0.56
14	165	2.5YR 6/6	Light red	2.96	1.01	0.15
15	170	2.5YR 4/1	Dark reddish gray	5.62	4.00	0.90
16	180	2.5YR 6/6	Light red	5.81	0.50	0.23
17	195	10R 2.5/1	Reddish black	7.47	2.16	0.57
18	215	10R 3/2	Dusty red	9.45	2.34	0.73
19	230	2.5YR 6/6	Light red	9.91	1.59	0.49
20	260	2.5YR 7/2	Pale red	12.38	2.06	0.57
21	280	2.5YR 4/3	Reddish brown	18.53	2.67	0.69
22	300	2.5YR 5/8	Red	18.58	0.81	0.30
23	315	2.5YR 2.5/4	Dark reddish brown	20.45	2.08	0.57
24	345	2.5YR 5/8	Red	21.54	0.38	0.14
Sample location C						
1	20	10YR 7/4	Very pale brown	1.04	0.87	0.27
2	30	10YR 5/2	Grayish brown	3.24	4.65	0.90
3	40	2.5YR 8/4	Pink	3.98	0.74	0.25
4	50	7.5YR 4/6	Strong brown	4.47	4.53	1.03
5	65	10YR 7/4	Very pale brown	4.67	1.06	0.32
6	80	7.5YR 4/6	Strong brown	5.04	4.91	0.98
7	95	10YR 7/4	Very pale brown	6.01	0.67	0.22
8	125	7.5YR 4/6	Strong brown	6.34	4.27	0.88
9	165	5YR 5/2	Reddish gray	7.06	4.42	0.97
10	285	7.5YR 5/3	Brown	10.27	0.41	0.34
11	315	7.5YR 4/1	Dark gray	20.80	3.06	0.73
12	385	5Y 4/2	Olive gray	21.23	2.23	0.35
Sample location D						
1	10	7.5YR 5/3	Brown	1.19	2.10	0.39
2	30	10YR 6/1	Gray	1.45	1.90	0.45
3	170	2.5Y 6/4	Light yellowish brown	1.65	3.03	0.72
4	190	2.5Y 6/4	Light yellowish brown	2.26	2.50	0.60
5	205	2.5Y 3/1	Very dark gray	2.45	1.10	0.34
6	225	2.5Y 6/4	Light yellowish brown	2.75	2.72	0.68
7	280	10YR 7/4	Very pale brown	2.86	2.36	0.52
8	300	10YR 5/8	Yellowish brown	2.95	2.06	0.47
9	370	2.5Y 6/4	Light yellowish brown	6.69	2.79	0.48
10	470	5YR 4/6	Yellowish red	10.09	7.11	1.01
11	500	10YR 7/4	Very pale brown	17.12	0.82	0.26

S/No	Depth (cm)	Colour code	Colour	MC (%)	LOI at 550 ˚C	LOI at 950 ˚C
Sample location E						
1	10	2.5Y 5/4	Light olive brown	1.54	1.35	0.41
2	30	2.5Y 6/4	Light yellowish brown	1.92	1.02	0.31
3	110	10YR 5/8	Yellowish brown	1.94	1.54	0.46
4	260	10YR 6/3	Pale brown	3.28	3.44	0.85
5	320	7.5YR 6/3	Light brown	3.50	0.91	0.24
6	350	10YR 7/4	Very pale brown	3.91	3.82	0.76
7	365	7.5YR 4/6	Strong brown	5.78	5.54	1.02
8	395	10YR 6/3	Pale brown	6.80	0.95	0.28
9	415	2.5Y 6/4	Light yellowish brown	7.13	1.93	0.48
10	475	7.5YR 5/3	Brown	8.50	1.80	0.51
11	505	7.5YR 4/1	Dark gray	17.02	4.92	0.84
12	515	5YR 4/6	Yellowish red	17.49	0.79	0.26
Sample location F						
1	15	2.5YR 7/2	Pale red	1.07	0.88	0.25
2	45	2.5YR 5/2	Weak red	2.87	2.24	0.58
3	105	2.5YR 6/3	Light reddish brown	2.98	0.34	0.23
4	175	2.5YR 4/3	Reddish brown	9.04	5.13	1.29
5	235	2.5YR 8/4	Pink	9.30	0.25	0.15
6	385	10YR 4/4	Dark yellowish brown	11.01	1.25	0.50
7	415	2.5YR 7/2	Pale red	13.45	0.41	0.13
8	585	GLEY 4/10BG	Dark greenish gray	25.80	3.67	0.86
9	600	2.5YR 4/3	Reddish brown	26.93	1.15	0.36
Sample location G						
1	15	2.5YR 8/4	Pink	1.75	1.40	0.45
2	60	10YR 7/4	Very pale brown	2.51	0.43	0.21
3	80	2.5YR 7/2	Pale red	2.82	2.22	0.64
4	120	2.5YR 8/4	Pink	3.02	0.77	0.27
5	190	7.5YR 5/3	Brown	7.12	4.80	1.33
6	310	2.5YR 8/4	Pink	11.17	0.34	0.17
7	370	5YR 7/2	Pinkish gray	16.49	0.17	0.10
Sample location H						
1	15	2.5YR 7/2	Pale red	4.35	3.55	0.86
2	30	2.5YR 6/3	Light reddish brown	1.09	0.70	0.31
3	50	2.5YR 7/2	Pale red	4.13	3.41	0.83
4	65	2.5YR 6/3	Light reddish brown	0.32	0.23	0.10
5	75	10YR 5/8	Yellowish brown	2.32	3.22	0.59

S/No	Depth (cm)	Colour code	Colour	MC (%)	LOI at 550 ˚C	LOI at 950 ˚C
6	85	5YR 8/2	Pinkisk white	0.39	0.40	0.16
7	115	2.5YR 7/2	Pale red	3.08	4.12	0.86
8	125	5YR 8/2	Pinkish white	0.30	0.37	0.15
9	155	2.5YR 6/3	Light reddish brown	2.91	2.75	0.65
10	170	2.5YR 7/2	Pale red	0.43	0.47	0.20
11	370	10YR 5/8	Yellowish brown	4.70	2.95	0.73
12	390	2.5YR 5/2	Weak red	9.25	6.78	1.07
13	410	2.5YR 4/3	Reddish brown	11.88	4.32	2.30
14	425	5YR 7/2	Pinkish gray	12.43	0.35	0.13
15	455	2.5YR 4/3	Reddish brown	15.43	6.62	1.13
16	470	10YR 4/4	Dark yellowish brown	18.77	0.55	0.19
17	500	10YR 6/1	Gray	19.08	0.28	0.08
Sample location I						
1	45	5YR 7/2	Pinkish gray	1.37	0.98	0.28
2	65	7.5YR 5/3	Brown	1.50	2.03	0.45
3	115	5YR 7/2	Pinkish gray	1.87	0.52	0.20
4	120	2.5YR 8/4	Pink	2.87	3.42	0.74
5	320	5YR 8/2	Pinkish white	2.89	0.30	0.14
6	325	2YR 7/1	Light gray	2.90	4.44	0.81
7	330	5YR 7/2	Pinkish gray	3.03	0.75	0.26
8	365	5YR 4/6	Yellowish red	3.04	6.66	1.15
9	375	2.5YR 8/4	Pink	3.25	0.37	0.11
10	390	2.5YR 5/2	Weak red	3.37	2.74	0.63
11	410	2.5YR 6/3	Light reddish brown	3.38	0.30	0.17
12	420	5YR 7/2	Pinkish gray	3.81	2.68	0.67
13	425	5YR 6/6	Reddish yellow	3.99	3.15	0.73
14	495	2.5YR 4/3	Reddish brown	9.50	0.64	0.23
15	525	2.5YR 4/1	Dark reddish gray	15.24	6.52	1.09
16	585	2.5YR 8/4	Pink	16.86	0.43	0.15
Sample location J						
1	15	2.5Y 8/3	Pale yellow	1.04	1.03	0.34
2	85	10YR 8/6	Yellow	1.06	0.44	0.21
3	160	2.5YR 8/4	Pink	2.68	3.39	0.81
4	175	2.5YR 7/2	Pale red	3.41	0.59	0.14
5	205	2.5Y 8/3	Pale yellow	4.17	0.96	0.35
6	225	7.5YR 4/6	Strong brown	4.59	4.59	0.88
7	235	10YR 6/6	Brownish yellow	10.19	0.56	0.18

S/No	Depth (cm)	Colour code	Colour	MC (%)	LOI at 550 ˚C	LOI at 950 ˚C
8	285	5YR 5/2	Reddish gray	16.55	5.58	0.98
9	400	10YR 7/4	Very pale brown	16.94	0.37	0.11
Sample location K						
1	90	7.5YR 5/3	Brown	1.18	1.71	0.34
2	240	5Y 5/3	Olive	2.96	4.42	0.65
3	240	10YR 6/1	Gray	2.31	4.16	0.75
4	640	2.5YR 6/3	Light reddish brown	9.15	0.82	0.23
5	840	2.5YR 7/2	Pale red	19.84	0.33	0.11
Sample location L						
1	45	2.5YR 5/2	Weak red	1.47	6.35	0.86
2	165	2.5YR 7/2	Pale red	1.59	0.56	0.18
3	215	2.5YR 2.5/4	Dark reddish brown	3.19	1.60	1.39
4	235	2.5YR 6/3	Light reddish brown	3.35	0.27	0.13
5	255	2.5YR 5/2	Weak red	10.08	1.57	0.41
6	455	2.5YR 4/1	Dark reddish gray	16.65	0.29	0.11
Sample location M						
1	15	10YR 6/1	Gray	1.75	2.39	0.53
2	45	2.5YR 6/3	Light reddish brown	1.99	0.49	0.17
3	75	5YR 5/2	Reddish gray	2.40	3.49	0.70
4	115	2.5YR 6/3	Light reddish brown	2.41	0.69	0.19
5	120	7.5YR 5/3	Brown	2.49	3.40	0.69
6	170	2.5YR 6/3	Light reddish brown	2.62	0.48	0.19
7	175	2.5YR 4/3	Reddish brown	3.08	3.41	0.75
8	265	2.5YR 8/4	Pink	7.04	0.35	0.13
9	270	10YR 6/1	Gray	10.64	2.80	0.64
10	570	2.5YR 5/2	Weak red	16.54	4.75	1.64
Sample location N						
1	50	10YR 8/6	Yellow	1.04	0.56	0.19
2	65	2.5YR 7/2	Pale red	1.67	1.47	0.42
3	125	2.5YR 8/4	Pink	2.43	0.67	0.23
4	225	2.5YR 6/6	Light red	2.94	4.58	0.81
5	235	2.5YR 6/6	Light red	3.01	0.45	0.13
6	245	2.5YR 4/3	Reddish brown	3.55	5.95	0.95
7	255	2.5YR 8/4	Pink	3.59	0.41	0.13
8	265	2.5YR 4/3	Reddish brown	3.62	3.05	0.58
9	345	5YR 6/6	Reddish yellow	3.68	0.29	0.13
10	360	5YR 5/2	Reddish gray	4.68	4.27	0.84

S/No	Depth (cm)	Colour code	Colour	MC (%)	LOI at 550 ˚C	LOI at 950 ˚C
11	600	10YR 7/4	Very pale brown	10.01	0.35	0.11
12	610	GLEY 4/10BG	Dark greenish gray	17.39	2.02	0.42
Sample location O						
1	100	2.5YR 4/3	Reddish brown	1.35	2.24	0.46
2	130	2.5YR 6/3	Light reddish brown	1.44	0.48	0.17
3	330	10YR 5/8	Yellowish brown	2.11	4.15	0.76
4	345	2.5YR 8/4	Pink	2.19	0.78	0.23
5	365	7.5YR 4/1	Dark gray	2.23	2.38	0.61
6	375	2.5YR 5/2	Weak red	5.47	5.83	1.21
7	575	2YR 7/1	Light gray	10.52	2.52	0.69
8	675	2.5YR 6/3	Light reddish brown	15.25	0.49	0.14
Sample location P						
1	30	5YR 5/2	Reddish gray	1.99	4.96	0.85
2	70	2.5YR 6/6	Light red	2.16	0.39	0.15
3	80	2.5YR 5/2	Weak red	5.11	2.08	0.71
4	100	2.5YR 6/3	Light reddish brown	5.46	0.35	0.17
5	105	2.5YR 4/3	Reddish brown	9.69	0.58	0.22
6	605	2.5YR 6/3	Light reddish brown	16.43	0.25	0.13
Sample location Q						
1	40	7.5YR 4/6	Strong brown	2.45	4.76	0.77
2	50	5YR 6/6	Reddish yellow	4.06	1.08	0.33
3	170	10YR 8/6	Yellow	4.13	0.42	0.19
4	175	10YR 3/3	Dark brown	6.03	3.15	0.75
5	235	2.5Y 6/4	Light yellowish brown	7.00	0.65	0.23
6	245	10YR 5/8	Yellowish brown	9.91	0.70	0.27
7	545	7.5YR 4/6	Strong brown	17.00	0.43	0.11
Sample BH 1						
1	100	2.5YR 4/1	Dark reddish gray	5.54	0.99	0.22
2	400	2.5YR 7/2	Pale red	1.73	0.40	0.16
3	500	2.5YR 4/1	Dark reddish gray	3.12	3.79	0.57
4	600	2.5YR 5/2	Weak red	3.16	0.56	0.25
5	650	2YR 7/1	Light gray	14.66	8.26	1.09
6	800	2.5YR 6/3	Light reddish brown	16.07	0.55	0.14
Sample BH 2						
1	200	2.5YR 4/1	Dark reddish gray	3.88	3.63	0.66
2	300	2.5YR 8/4	Pink	3.94	1.70	0.44
3	500	GLEY 4/10BG	Dark greenish gray	15.15	7.63	1.21

S/No	Depth (cm)	Colour code	Colour	MC (%)	LOI at 550 ˚C	LOI at 950 ˚C
4	650	2.5YR 8/4	Pink	19.25	0.97	0.26
Sample BH 3						
1	100	7.5YR 5/3	Brown	4.69	1.95	0.36
2	250	10YR 7/4	Very pale brown	4.52	0.66	0.21
3	550	2.5YR 4/3	Reddish brown	13.31	6.48	0.94
4	750	10YR 7/4	Very pale brown	13.53	0.64	0.19
5	800	2.5YR 4/3	Reddish brown	16.30	5.80	1.09
6	1100	2.5YR 7/2	Pale red	17.53	0.61	0.18
Sample BH 4						
1	100	7.5YR 5/3	Brown	2.55	3.16	0.68
2	400	2.5Y 6/4	Light yellowish brown	3.54	4.07	0.81
3	550	7.5YR 5/3	Brown	4.88	3.62	0.62
4	750	10YR 6/1	Gray	10.20	2.91	0.64
5	1100	2.5YR 6/3	Light reddish brown	16.31	0.42	0.10
Sample BH 5						
1	150	2.5YR 4/1	Dark reddish gray	4.19	6.60	1.08
2	300	2.5YR 4/3	Reddish brown	4.62	1.57	0.33
3	600	2.5YR 4/1	Dark reddish gray	5.49	6.23	0.95
4	750	2.5YR 6/3	Light reddish brown	7.01	0.40	0.15
5	850	2.5YR 4/3	Reddish brown	8.78	3.30	0.60
6	950	GLEY2 4/5PB	Dark bluish gray	17.32	2.76	0.43
7	1050	2.5Y 6/4	Light yellowish brown	18.50	0.56	0.19
Sample BH 6						
1	200	7.5YR 5/3	Brown	3.77	2.68	0.72
2	500	2.5Y 3/1	Very dark gray	4.64	5.24	0.67
3	700	2.5YR 5/2	Weak red	10.29	2.61	0.70
4	1000	5YR 5/2	Reddish gray	14.74	1.99	0.48
5	1200	2.5YR 5/2	Weak red	15.33	0.32	0.13
Sample BH 7						
1	250	2.5YR 4/1	Dark reddish gray	3.78	2.66	0.75
2	500	2.5YR 2.5/1	Reddish black	6.40	7.02	1.17
3	800	2.5Y 5/2	Grayish brown	8.79	4.10	0.82
4	1100	10YR 4/2	Dark grayish brown	15.17	8.79	2.07
5	1300	7.5YR 5/3	Brown	17.95	0.49	0.13
Sample BH 8						
1	40	2.5YR 5/2	Weak red	2.62	3.68	0.80
2	150	2.5YR 8/4	Pink	3.21	5.89	0.15

S/No	Depth (cm)	Colour code	Colour	MC (%)	LOI at 550 ˚C	LOI at 950 ˚C
3	170	2.5YR 5/2	Weak red	3.48	4.95	0.92
4	210	2.5YR 8/4	Pink	4.27	0.54	0.22
5	215	2.5YR 7/2	Pale red	10.22	3.87	0.93
6	615	2.5Y 3/1	Very dark gray	16.26	0.78	0.22
Sample BH 9						
1	50	2.5YR 5/2	Weak red	1.36	1.92	0.44
2	200	5YR 6/6	Reddish yellow	5.92	0.32	0.13
3	250	5YR 4/6	Yellowish red	10.04	7.09	0.92
4	500	2.5YR 6/6	Light red	15.73	0.40	0.16
Sample BH 10						
1	300	10R 3/2	Dusty red	4.71	5.89	1.07
2	500	10YR 4/4	Dark yellowish brown	6.50	3.25	0.57
3	700	10R 3/2	Dusty red	7.74	6.33	1.13
4	1000	7.5YR 5/3	Brown	14.51	3.45	0.67
5	1300	10YR 4/4	Dark yellowish brown	16.14	3.77	0.79
6	1500	2.5Y 4/4	Olive brown	19.32	3.05	0.86
Sample BH 11						
1	300	2.5YR 4/1	Dark reddish gray	3.61	0.83	0.16
2	600	2.5YR 4/1	Dark reddish gray	7.06	4.20	0.86
3	900	2.5YR 5/2	Weak red	7.55	2.13	0.36
4	1200	5YR 2.5/1	Black	13.37	4.71	0.83
5	1500	2.5YR 4/1	Dark reddish gray	16.67	1.47	0.23
Sample BH 12						
1	300	GLEY 4/10BG	Dark greenish gray	7.83	8.27	1.34
2	600	5YR 5/2	Reddish gray	7.64	7.27	1.00
3	900	GLEY 4/10BG	Dark greenish gray	9.90	5.02	1.29
4	1200	5YR 5/2	Reddish gray	14.74	4.43	0.94
5	1500	GLEY1 3/10Y	Very dark greenish gray	19.04	5.87	1.62
6	1800	2.5YR 5/2	Weak red	20.71	3.07	0.61

APPENDIX C: Magnetic susceptibility data for the floodplain sediment samples.

Table C: Magnetic susceptibility (MS) data for the two hundred and fifty six sediment samples collected

Sample location A							
S/No	Depth (cm)	1st Reading	2nd Reading	3rd Reading	4th Reading	5th Reading	Mean MS (10^{-6} m^3 kg)
1	15	0.39	0.38	0.38	0.38	0.37	0.38
2	40	0.35	0.35	0.36	0.38	0.37	0.36
3	55	0.39	0.38	0.38	0.38	0.39	0.38
4	75	0.25	0.26	0.26	0.26	0.25	0.26
5	95	0.27	0.27	0.28	0.28	0.29	0.28
6	125	0.32	0.32	0.31	0.33	0.33	0.32
7	145	0.39	0.39	0.4	0.38	0.39	0.39
8	165	0.25	0.24	0.25	0.25	0.25	0.25
9	185	0.25	0.26	0.27	0.27	0.25	0.26
10	205	0.25	0.27	0.26	0.26	0.26	0.26
11	225	0.26	0.25	0.25	0.26	0.26	0.26
12	245	0.27	0.27	0.27	0.28	0.28	0.27
13	265	0.28	0.29	0.29	0.28	0.29	0.29
14	285	0.35	0.35	0.35	0.34	0.34	0.35
15	305	0.36	0.37	0.36	0.35	0.34	0.36
16	325	0.28	0.27	0.3	0.29	0.29	0.29
17	355	0.25	0.23	0.24	0.23	0.26	0.24
18	375	0.31	0.31	0.31	0.31	0.3	0.31
19	395	0.29	0.29	0.29	0.29	0.3	0.29
20	415	0.3	0.31	0.31	0.32	0.32	0.31
Sample location B							
1	15	0.59	0.59	0.6	0.6	0.61	0.6
2	30	0.55	0.54	0.55	0.56	0.54	0.55
3	45	0.41	0.41	0.4	0.41	0.41	0.41
4	55	0.59	0.6	0.59	0.6	0.6	0.6
5	60	0.46	0.45	0.45	0.45	0.45	0.45
6	75	1.04	1.05	1.04	1.03	1.04	1.04
7	95	0.76	0.77	0.77	0.77	0.77	0.77
8	105	0.64	0.64	0.64	0.65	0.63	0.64
9	110	0.42	0.43	0.44	0.46	0.44	0.44
10	115	0.43	0.41	0.4	0.4	0.4	0.41

S/No	Depth (cm)	1st Reading	2nd Reading	3rd Reading	4th Reading	5th Reading	Mean MS (10^{-6} m^3 kg)
11	120	0.73	0.73	0.73	0.72	0.73	0.73
12	125	1.3	1.3	1.3	1.3	1.3	1.3
13	150	0.97	0.97	0.96	0.96	0.96	0.96
14	165	1.73	1.73	1.74	1.73	1.74	1.73
15	170	0.91	0.92	0.92	0.92	0.91	0.92
16	180	0.88	0.89	0.89	0.89	0.89	0.89
17	195	1.28	1.29	1.29	1.3	1.3	1.29
18	215	0.54	0.54	0.53	0.54	0.55	0.54
19	230	1.36	1.38	1.38	1.38	1.39	1.38
20	260	0.77	0.78	0.78	0.79	0.78	0.78
21	280	0.8	0.8	0.81	0.81	0.81	0.81
22	300	1.31	1.3	1.31	1.31	1.3	1.31
23	315	1.05	1.06	1.06	1.07	1.06	1.06
24	345	0.46	0.46	0.47	0.46	0.48	0.47
Sample location C							
1	20	0.92	0.91	0.93	0.93	0.94	0.93
2	30	0.93	0.95	0.94	0.94	0.94	0.94
3	40	1.28	1.3	1.3	1.3	1.29	1.29
4	50	0.81	0.83	0.81	0.84	0.84	0.83
5	65	0.69	0.7	0.68	0.71	0.7	0.7
6	80	0.88	0.87	0.86	0.87	0.85	0.87
7	95	4.03	4.03	3.97	4.08	4.02	4.03
8	125	1.01	1.01	1.02	1.01	1	1.01
9	165	1.03	1.03	1.01	1.02	1.02	1.02
10	285	2.31	2.31	2.31	2.32	2.32	2.31
11	315	1.31	1.3	1.31	1.3	1.3	1.3
12	385	1.74	1.74	1.74	1.78	1.74	1.75
Sample location D							
1	10	0.92	0.9	0.92	0.92	0.91	0.91
2	30	1.71	1.7	1.72	1.7	1.7	1.71
3	170	1.12	1.12	1.15	1.12	1.12	1.13
4	190	1.69	1.69	1.72	1.7	1.69	1.7
5	205	1.61	1.61	1.6	1.59	1.59	1.6
6	225	1.18	1.18	1.18	1.19	1.18	1.18
7	280	1.77	1.77	1.79	1.78	1.77	1.78
8	300	1.81	1.79	1.8	1.8	1.84	1.81
9	370	1.97	1.97	1.98	1.98	1.98	1.98

S/No	Depth (cm)	1st Reading	2nd Reading	3rd Reading	4th Reading	5th Reading	Mean MS (10^{-6} m^3 kg)
10	470	0.68	0.68	0.68	0.68	0.68	0.68
11	500	0.95	0.95	0.96	0.95	0.97	0.96
Sample location E							
1	10	0.74	0.75	0.73	0.74	0.75	0.74
2	30	0.87	0.85	0.85	0.88	0.75	0.84
3	110	0.67	0.67	0.68	0.68	0.68	0.68
4	260	0.54	0.53	0.55	0.54	0.56	0.54
5	320	0.66	0.69	0.68	0.67	0.67	0.67
6	350	0.84	0.84	0.85	0.83	0.83	0.84
7	365	0.86	0.9	0.85	0.88	0.88	0.87
8	395	0.84	0.83	0.82	0.84	0.82	0.83
9	415	0.8	0.8	0.79	0.77	0.81	0.79
10	475	0.78	0.77	0.77	0.78	0.78	0.78
11	505	0.88	0.88	0.87	0.87	0.88	0.88
12	515	0.66	0.66	0.66	0.67	0.67	0.66
Sample location F							
1	15	1.6	1.61	1.63	1.6	1.62	1.61
2	45	0.72	0.7	0.73	0.7	0.7	0.71
3	105	0.67	0.66	0.67	0.68	0.68	0.67
4	175	0.64	0.64	0.65	0.67	0.64	0.65
5	235	1.11	1.09	1.09	1.09	1.09	1.09
6	385	0.86	0.86	0.85	0.84	0.87	0.86
7	415	0.51	0.52	0.5	0.52	0.52	0.51
8	585	0.41	0.41	0.4	0.42	0.41	0.41
9	600	1.46	1.46	1.49	1.47	1.46	1.47
Sample location G							
1	15	1.23	1.19	1.21	1.21	1.23	1.21
2	60	0.64	0.68	0.64	0.69	0.68	0.67
3	80	0.7	0.72	0.7	0.7	0.72	0.71
4	120	2.28	2.3	2.27	2.28	2.28	2.28
5	190	0.71	0.7	0.72	0.74	0.73	0.72
6	310	1.02	1.03	1.03	1.04	1.04	1.03
7	370	2.05	2.05	2.05	2.04	2.06	2.05
Sample location H							
1	15	0.88	0.87	0.88	0.87	0.88	0.88
2	30	1.01	1	1.01	0.99	0.99	1
3	50	1.03	1.06	1.08	1.07	1.05	1.06

S/No	Depth (cm)	1st Reading	2nd Reading	3rd Reading	4th Reading	5th Reading	Mean MS (10^{-6} m^3 kg)
4	65	0.22	0.18	0.22	0.22	0.23	0.21
5	75	0.67	0.66	0.69	0.69	0.69	0.68
6	85	0.6	0.63	0.6	0.59	0.61	0.61
7	115	0.75	0.76	0.77	0.79	0.79	0.77
8	125	0.45	0.48	0.51	0.49	0.47	0.48
9	155	0.99	0.98	0.97	0.97	0.97	0.98
10	170	1.2	1.21	1.21	1.19	1.2	1.2
11	370	0.89	0.86	0.89	0.87	0.88	0.88
12	390	0.76	0.79	0.77	0.77	0.78	0.77
13	410	0.78	0.81	0.81	0.78	0.78	0.79
14	425	1.34	1.32	1.35	1.35	1.34	1.34
15	455	0.83	0.85	0.81	0.83	0.83	0.83
16	470	0.85	0.83	0.83	0.82	0.84	0.83
17	500	0.48	0.5	0.51	0.49	0.48	0.49
Sample location I							
1	45	1.26	1.23	1.23	1.22	1.22	1.23
2	65	1.09	1.04	1.07	1.08	1.1	1.08
3	115	1.09	1.07	1.07	1.06	1.06	1.07
4	120	1.24	1.22	1.27	1.22	1.22	1.23
5	320	1.61	1.6	1.6	1.61	1.61	1.61
6	325	0.63	0.65	0.64	0.65	0.64	0.64
7	330	1.65	1.68	1.67	1.68	1.68	1.67
8	365	0.56	0.59	0.57	0.57	0.59	0.58
9	375	0.88	0.89	0.88	0.88	0.88	0.88
10	390	0.67	0.68	0.69	0.65	0.67	0.67
11	410	1.25	1.25	1.27	1.26	1.27	1.26
12	420	0.72	0.74	0.71	0.73	0.72	0.72
13	425	0.8	0.8	0.81	0.81	0.8	0.8
14	495	0.52	0.5	0.49	0.49	0.49	0.5
15	525	0.71	0.7	0.72	0.72	0.72	0.71
16	585	1.75	1.75	1.74	1.75	1.76	1.75
Sample location J							
1	15	0.65	0.64	0.65	0.65	0.64	0.65
2	85	1.01	1	0.99	1.01	0.99	1
3	160	0.87	0.88	0.87	0.87	0.87	0.87
4	175	0.61	0.61	0.62	0.6	0.6	0.61
5	205	1.31	1.32	1.31	1.32	1.33	1.32

S/No	Depth (cm)	1st Reading	2nd Reading	3rd Reading	4th Reading	5th Reading	Mean MS (10^{-6} m^3 kg)
6	225	0.84	0.84	0.87	0.84	0.87	0.85
7	235	0.8	0.8	0.81	0.8	0.8	0.8
8	285	0.62	0.61	0.6	0.61	0.61	0.61
9	400	4.14	4.22	4.16	4.14	4.15	4.16
Sample Location K							
1	90	1.73	1.74	1.73	1.73	1.73	1.73
2	240	1.14	1.17	1.18	1.15	1.17	1.16
3	240	0.91	0.91	0.9	0.9	0.91	0.91
4	640	1.91	1.93	1.98	1.96	1.94	1.94
5	840	1.09	1.09	1.08	1.08	1.08	1.08
Sample location L							
1	45	0.69	0.69	0.69	0.67	0.69	0.69
2	165	1.11	1.11	1.09	1.13	1.1	1.11
3	215	1.43	1.45	1.47	1.45	1.47	1.45
4	235	0.21	0.21	0.22	0.22	0.21	0.21
5	255	1.19	1.18	1.17	1.19	0.18	0.98
6	455	0.35	0.37	0.36	0.35	0.37	0.36
Sample location M							
1	15	1	1	0.98	0.99	0.98	0.99
2	45	0.49	0.48	0.47	0.46	0.47	0.47
3	75	0.81	0.8	0.8	0.79	0.81	0.8
4	115	0.48	0.47	0.49	0.48	0.47	0.48
5	120	1.07	1.05	1.04	1.06	1.05	1.05
6	170	0.31	0.31	0.32	0.32	0.3	0.31
7	175	0.85	0.84	0.85	0.86	0.87	0.85
8	265	0.76	0.76	0.76	0.75	0.76	0.76
9	270	1	1	1	1.01	1.02	1.01
10	570	1.25	1.26	1.28	1.27	1.28	1.27
Sample location N							
1	50	0.54	0.56	0.55	0.56	0.55	0.55
2	65	0.69	0.69	0.69	0.69	0.71	0.69
3	125	0.81	0.81	0.8	0.83	0.8	0.81
4	225	0.76	0.75	0.76	0.75	0.76	0.76
5	235	1.06	1.07	1.07	1.06	1.06	1.06
6	245	0.81	0.8	0.8	0.79	0.8	0.8
7	255	1.72	1.72	1.71	1.71	1.71	1.71
8	265	0.75	0.73	0.72	0.73	0.75	0.74

S/No	Depth (cm)	1st Reading	2nd Reading	3rd Reading	4th Reading	5th Reading	Mean MS (10^{-6} m^3 kg)
9	345	0.32	0.29	0.32	0.31	0.31	0.31
10	360	0.93	0.93	0.93	0.92	0.92	0.93
11	600	2.45	2.48	2.45	2.46	2.45	2.46
12	610	1.1	1.1	1.12	1.09	1.11	1.1
Sample location O							
1	100	13.40	1.36	1.36	1.37	1.36	1.36
2	130	26.70	1.16	1.17	1.17	1.15	1.16
3	330	9.152	2.16	2.16	2.16	2.16	2.16
4	345	30.93	0.8	0.8	0.8	0.82	0.8
5	365	10.24	0.86	0.87	0.85	0.87	0.86
6	375	3.420	0.49	0.48	0.5	0.47	0.49
7	575	15.04	1.21	1.21	1.22	1.2	1.21
8	675	244.5	0.95	0.94	0.94	0.97	0.95
Sample location P							
1	30	0.98	0.97	0.98	0.98	0.99	0.98
2	70	0.65	0.64	0.67	0.66	0.66	0.66
3	80	1.74	1.74	1.75	1.75	1.73	1.74
4	100	0.48	0.48	0.5	0.5	0.49	0.49
5	105	1.12	1.13	1.13	1.12	1.13	1.13
6	605	0.84	0.85	0.86	0.84	0.83	0.84
Sample location Q							
1	40	0.87	0.88	0.87	0.87	0.89	0.88
2	50	2.26	2.26	2.24	2.25	2.27	2.26
3	170	0.87	0.86	0.86	0.88	0.86	0.87
4	175	0.72	0.72	0.72	0.72	0.73	0.72
5	235	0.57	0.57	0.56	0.57	0.57	0.57
6	245	0.84	0.84	0.83	0.85	0.86	0.84
7	545	1.51	1.49	1.5	1.49	1.48	1.49
Sample borehole 1							
1	100	0.98	0.98	0.98	0.97	0.98	0.98
2	400	0.59	0.58	0.6	0.6	0.59	0.59
3	500	2.17	2.18	2.18	2.19	2.19	2.18
4	600	1.75	1.76	1.79	1.77	1.75	1.76
5	650	0.89	0.88	0.89	0.89	0.89	0.89
6	800	0.25	0.25	0.25	0.26	0.25	0.25
Sample borehole 2							
1	200	0.37	0.39	0.37	0.37	0.36	0.37

S/No	Depth (cm)	1st Reading	2nd Reading	3rd Reading	4th Reading	5th Reading	Mean MS (10^{-6} m^3 kg)
2	300	0.38	0.4	0.38	0.39	0.39	0.39
3	500	0.31	0.31	0.32	0.33	0.32	0.32
4	650	0.47	0.48	0.46	0.47	0.48	0.47
Sample borehole 3							
1	100	1.12	1.07	1.07	1.08	1.07	1.08
2	250	0.42	0.41	0.42	0.43	0.41	0.42
3	550	0.87	0.88	0.88	0.88	0.89	0.88
4	750	0.81	0.83	0.82	0.81	0.81	0.82
5	800	0.79	0.8	0.8	0.81	0.81	0.80
6	1100	0.74	0.76	0.76	0.75	0.76	0.76
Sample borehole 4							
1	100	0.59	0.58	0.59	0.59	0.59	0.59
2	400	0.66	0.66	0.66	0.67	0.67	0.66
3	550	0.76	0.77	0.76	0.77	0.76	0.76
4	750	0.55	0.55	0.56	0.56	0.56	0.56
5	1100	0.27	0.24	0.24	0.24	0.25	0.25
Sample borehole 5							
1	150	0.85	0.85	0.86	0.84	0.86	0.85
2	300	1.01	0.99	1.01	1.01	0.99	1
3	600	0.82	0.83	0.84	0.83	0.82	0.83
4	750	0.24	0.23	0.25	0.25	0.24	0.24
5	850	1.1	1.11	1.11	1.12	1.11	1.11
6	950	1.72	1.74	1.72	1.76	1.73	1.73
7	1050	1.99	1.97	1.98	2	1.99	1.99
Sample borehole 6							
1	200	1	1	0.97	0.99	1	0.99
2	500	0.72	0.75	0.74	0.75	0.74	0.74
3	700	1.08	1.08	1.1	1.1	1.08	1.09
4	1000	1.02	1.05	1.03	1.04	1.02	1.03
5	1200	0.53	0.52	0.53	0.55	0.53	0.53
Sample borehole 7							
1	250	0.74	0.7	0.73	0.72	0.72	0.72
2	500	0.37	0.37	0.36	0.37	0.37	0.37
3	800	0.65	0.65	0.66	0.65	0.66	0.65
4	1100	0.55	0.54	0.55	0.55	0.56	0.55
5	1300	1.92	1.93	1.95	1.94	1.93	1.93
Sample borehole 8							

S/No	Depth (cm)	1st Reading	2nd Reading	3rd Reading	4th Reading	5th Reading	Mean MS (10^{-6} m^3 kg)
1	40	0.84	0.84	0.83	0.82	0.82	0.83
2	150	0.61	0.62	0.64	0.64	0.65	0.63
3	170	0.84	0.85	0.85	0.85	0.86	0.85
4	210	1.03	1.03	1.03	1.04	1.04	1.03
5	215	0.87	0.87	0.86	0.87	0.87	0.87
6	615	1.17	1.17	1.17	1.18	1.18	1.17
Sample borehole 9							
1	50	0.88	0.88	0.9	0.91	0.91	0.9
2	200	0.22	0.23	0.23	0.23	0.23	0.23
3	250	0.78	0.79	0.79	0.8	0.8	0.79
4	500	0.27	0.28	0.28	0.27	0.27	0.27
Sample borehole 10							
1	300	0.38	0.4	0.39	0.38	0.39	0.39
2	500	0.57	0.57	0.55	0.55	0.54	0.56
3	700	0.4	0.4	0.4	0.39	0.41	0.4
4	1000	0.42	0.43	0.42	0.42	0.41	0.42
5	1300	0.27	0.26	0.26	0.27	0.27	0.27
6	1500	0.35	0.38	0.36	0.36	0.37	0.36
Sample borehole 11							
1	300	0.95	0.96	0.92	0.96	0.91	0.94
2	600	0.15	0.16	0.14	0.15	0.16	0.15
3	900	0.23	0.24	0.23	0.23	0.23	0.23
4	1200	0.13	0.12	0.14	0.14	0.13	0.13
5	1500	0.19	0.2	0.21	0.18	0.18	0.19
Sample borehole 12							
1	300	0.25	0.26	0.25	0.24	0.27	0.25
2	600	0.69	0.68	0.68	0.67	0.69	0.68
3	900	0.29	0.28	0.28	0.28	0.29	0.28
4	1200	0.95	0.93	0.94	0.93	0.94	0.94
5	1500	0.22	0.21	0.21	0.21	0.21	0.21
6	1800	1.11	1.11	1.11	1.12	1.13	1.12

APPENDIX D: Shear strength forces on sediments across the floodplain obtained at twelve different locations

Table D: Shear strength forces on sediment across the floodplain. BH – borehole

Depth (cm)	BH 1	BH 2	BH 3	BH 4	BH 5	BH 6	BH 7	BH 8	BH 9	BH 10	BH 11	BH 12
	kPa											
15	15	40	50	130	120	100	42	41	102	103	45	90
30	17	70	52	130	115	118	45	45	100	100	50	85
50	19	118	63	105	116	102	50	30	95	101	53	84
75	16	82	65	110	130	120	49	35	50	95	55	80
100	19	90	69	90	125	140	52	36	45	96	67	82
130	20	80	41	80	110	130	55	34	43	94	60	83
170	22	85	40	100	100	112	53	46	39	90	59	90
210	18	70	42	74	102	150	60	37	35	90	51	92
250	19	50	41	73	105	156	61	25	35	89	50	93
300	19	40	43	100	105	152	80	25	34	89	50	95

APPENDIX E: Resistivity results of the twenty four vertical electrical soundings

Table E: Results obtained from the computer output of the twenty four vertical electrical sounding point stations

Location	Thickness of Layer (m)				Resistivity (Ωm)					Resistance (Ωm)				Conductivity (Sm^{-1})				Elevation (depth) (m)				Fitting Error (%)
	H_1	H_2	H_3	H_4	ρ_1	ρ_2	ρ_3	ρ_4	ρ_5	R_1	R_2	R_3	R_4	δ_1	δ_2	δ_3	δ_4	E_1	E_2	E_3	E_4	
VES 1	0.66	5.98	13.8	-	156.8	68.65	21.38	135.4	-	103.5	410.6	295.9	-	0.042	0.0871	0.646	-	0.66	6.64	20.47	-	1.85
VES 2	1.65	26.16	-	-	10.72	16.02	279.2	-	-	17.77	419.3	-	-	0.154	1.63	-	-	1.65	27.8	-	-	2.49
VES 3	1.64	2.14	48.1	-	735.5	3600.4	128.2	186.1	-	1206.6	7735.5	6167.9	-	0.0022	5.967	0.375	-	1.64	3.78	51.89	-	1.72
VES 4	2.41	11.59	3.44	-	27.48	18.9	4001.6	1.47	-	66.32	219.2	13773.3	-	0.087	0.613	8.601	-	2.41	14	17.45	-	3.73
VES 5	1.52	13.65	6.01	16.28	17.26	20.13	49.39	112	283.1	56.72	274.8	297.2	4.3	0.0408	0.678	0.121	0.145	1.52	15.2	21.19	37.5	3.72
VES 6	3.25	2.77	-	-	116.5	3252.7	105.8	-	-	378.8	9016.7	-	-	0.0278	8.522	-	-	3.25	6.02	-	-	2.6
VES 7	4.21	3.10	-	-	36.58	3.95	318.8	-	-	15.4	12.31	-	-	0.115	0.785	-	-	4.21	7.32	-	-	1.35
VES 8	1.59	11.61	-	-	508.8	937.3	108.7	-	-	812.2	10887	-	-	0.0031	0.0123	-	-	1.59	13.2	-	-	2.41
VES 9	0.259	6.14	85.2	-	193.7	492.1	144.1	391.1	-	50.27	3024.4	12278.7	-	0.0013	0.0124	0.591	-	0.25	6.4	91.6	-	3.81
VES 10	3.06	10.23	-	-	1800.1	179.4	102	-	-	5512.6	1836.8	-	-	0.0017	0.057	-	-	3.06	13.3	-	-	0.9
VES 11	0.49	6.17	3.45	-	260.7	60.08	8.34	119	-	128.1	420	28.77	-	0.0018	0.0906	0.413	-	0.49	6.66	10.11	-	1.66
VES 12	0.2	1.98	7.27	5.55	432.2	36.42	22.52	14.02	152	86.44	72.12	163.7	77.81	0.00046	0.0543	0.322	0.395	0.2	2.18	9.45	15	1.1
VES 13	1.5	1.58	33.2	-	23.89	90.76	59.09	128.5	-	36.04	143.4	196.9	-	0.6631	0.0174	0.562	-	1.5	3.08	36.33	-	2.03
VES 14	10.13	5.13	13.1	-	27.12	2.16	99.01	0.146	-	274.8	11.14	1301.5	-	0.373	2.36	0.132	-	10.13	15.27	28.41	-	3.05
VES 15	0.506	0.675	3.08	26.5	28.93	4324	75.71	397.4	118.4	14.56	2920.6	233.5	10548.3	0.0175	0.000156	0.0407	0.0667	0.506	1.18	4.26	30.8	3.76
VES 16	7.5	5.29	-	-	50.86	8.01	456	-	-	381.6	42.44	-	-	0.147	0.661	-	-	7.5	12.8	-	-	2.92
VES 17	1.36	2.71	-	-	43.17	1003.7	133	-	-	59.1	2722.9	-	-	0.0317	0.0027	-	-	1.36	4.08	-	-	2.98
VES 18	1.32	1.72	4.6	-	61.65	255	6.14	400.8	-	81.86	440.8	28.26	-	0.0215	0.00678	0.749	-	1.32	3.05	7.65	-	3.34
VES 19	1.28	6.71	20.1	-	869.5	1664.4	372.9	73.77	-	1121.1	11174.7	7480.3	-	0.00148	0.00403	0.0537	-	1.28	8	28.06	-	4.2
VES 20	1.45	5.89	-	-	373.6	888.2	132.2	-	-	542.2	5232.7	-	-	0.00388	0.00663	-	-	1.45	7.34	-	-	2.94
VES 21	0.577	1.18	5.14	-	100.5	9873.6	26.37	216.3	-	58.04	11717.5	135.6	-	0.00574	0.00012	0.195	-	0.577	1.76	6.9	-	3.92
VES 22	1.38	5.78	4.89	-	491.2	701.6	24.28	187.4	-	678	4062.1	118.3	-	0.00281	0.00825	0.201	-	1.38	7.17	12.06	-	2.98
VES 23	5.54	36.80	-	-	8.91	29.02	3270.5	-	-	49.42	1053.5	-	-	0.521	1.25	-	-	5.54	41.84	-	-	2.06
VES 24	1.12	3.91	33.3	-	6.23	1.43	749.4	14.56	-	7.04	5.62	24924.3	-	0.18	2.72	0.0443	-	1.12	5.04	38.3	-	3.99
Mean Value	2.275	7.45	18.98	16.12	265.91	1147.00	445.61	158.53	184.5	489.10	3077.34	4494.94	3543.47	0.102	1.06	0.87	0.20223	2.275	9.71	25.61	27.77	2.730

APPENDIX F: Hydraulic conductivity values for the floodplain alluvial sediments obtained from both laboratory and pumping tests in the field.

Table F1: Laboratory permeability values for sediment samples at twelve boreholes (BH) on the floodplain

Location	Sand	Sandy silt	Clayey silt
BH 1	3.02×10^{-02}	1.96×10^{-07}	4.50×10^{-08}
BH 2	4.10×10^{-02}	1.17×10^{-07}	3.71×10^{-08}
BH 3	$3.10x\ 10^{-02}$	1.30×10^{-07}	3.54×10^{-08}
BH 4	1.13×10^{-02}	$1.12x\ 10^{-07}$	2.86×10^{-08}
BH 5	2.68×10^{-02}	2.03×10^{-07}	5.24×10^{-08}
BH 6	2.93×10^{-02}	$1.61x\ 10^{-07}$	5.54×10^{-08}
BH 7	1.85×10^{-02}	1.14×10^{-07}	5.60×10^{-08}
BH 8	2.64×10^{-02}	1.39×10^{-07}	3.58×10^{-08}
BH 9	$2.74x\ 10^{-02}$	1.37×10^{-07}	5.73×10^{-08}
BH 10	2.04×10^{-02}	1.64×10^{-07}	4.36×10^{-08}
BH 11	2.80×10^{-02}	1.51×10^{-07}	3.22×10^{-08}
BH 12	1.08×10^{-02}	1.83×10^{-07}	4.52×10^{-08}
Mean	2.51×10^{-02}	1.51×10^{-07}	4.37×10^{-08}

Table F2: Laboratory permeability values for sediment samples outcrops (C to Q) along the Nigerian position of River Benue Yola region and the 2 main rivers in Cameroon.

Location	Sand	Sandy silt	Clayey silt
River Benue Cameroon	8.76×10^{-04}	4.35×10^{-07}	6.79×10^{-10}
River Faro Cameroon	2.49×10^{-03}	4.77×10^{-07}	1.52×10^{-09}
C	5.66×10^{-02}	5.33×10^{-07}	4.20×10^{-09}
D	5.41×10^{-02}	5.77×10^{-07}	4.33×10^{-09}
E	6.81×10^{-02}	8.49×10^{-07}	2.89×10^{-08}
F	2.69×10^{-02}	1.73×10^{-07}	1.63×10^{-08}
G	1.93×10^{-02}	7.91×10^{-07}	7.94×10^{-10}
H	8.52×10^{-02}	6.23×10^{-07}	3.32×10^{-10}
I	2.28×10^{-02}	4.94×10^{-07}	5.38×10^{-09}
J	1.45×10^{-02}	4.17×10^{-07}	4.48×10^{-09}
K	1.26×10^{-02}	1.13×10^{-07}	6.17×10^{-09}
L	7.96×10^{-03}	2.92×10^{-07}	9.88×10^{-09}
M	3.41×10^{-03}	1.83×10^{-07}	1.78×10^{-09}
N	2.79×10^{-02}	2.40×10^{-07}	5.52×10^{-09}
O	3.66×10^{-03}	1.22×10^{-07}	4.03×10^{-08}
P	1.65×10^{-03}	1.12×10^{-07}	2.19×10^{-09}
Q	2.32×10^{-03}	1.06×10^{-07}	3.71×10^{-10}
Mean	2.41×10^{-02}	3.85×10^{-07}	7.83×10^{-09}

APPENDIX G: Groundwater level measurements across the floodplain obtained from both manual and automatic piezometer

Table G1: Weekly groundwater measurement data at piezometers for the period April 2012 to April 2013

S/No	Weekly	Piezometer 1	Piezometer 2
1	07/04/2012	174.19	172.87
2	14/04/2012	174.09	172.88
3	21/04/2012	174.09	172.94
4	28/04/2012	174.06	172.89
5	05/05/2012	174.04	172.97
6	12/05/2012	174.18	173.07
7	19/05/2012	174.19	173.12
8	26/05/2012	174.03	173.24
9	02/06/2012	173.93	173.37
10	09/06/2012	173.93	173.27
11	16/06/2012	173.86	173.26
12	23/06/2012	174.21	173.62
13	30/06/2012	174.29	173.77
14	07/07/2012	174.48	174.78
15	14/07/2012	174.84	174.92
16	21/07/2012	174.84	175.05
17	28/07/2012	175.01	175.13
18	04/08/2012	175.43	175.37
19	11/08/2012	175.49	175.80
20	18/08/2012	175.55	176.06
21	25/08/2012	176.59	176.97
22	01/09/2012	176.59	176.97
23	08/09/2012	176.59	176.97
24	15/09/2012	176.59	176.97
25	22/09/2012	176.59	176.97
26	29/09/2012	176.59	176.97
27	06/10/2012	176.59	176.97
28	13/10/2012	176.59	176.97
29	20/10/2012	176.05	176.48
30	27/10/2012	176.00	176.32
31	03/11/2012	175.94	176.27
32	10/11/2012	175.96	176.28
33	17/11/2012	175.84	176.17
34	24/11/2012	175.74	176.12

S/No	Weekly	Piezometer 1	Piezometer 2
35	01/12/2012	175.54	175.97
36	08/12/2012	175.44	175.82
37	15/12/2012	175.36	175.77
38	22/12/2012	175.34	175.67
39	29/12/2012	175.24	175.57
40	05/01/2013	175.19	175.47
41	12/01/2013	175.14	175.40
42	19/01/2013	175.04	175.27
43	26/01/2013	174.96	175.17
44	02/02/2013	174.84	175.07
45	09/02/2013	174.79	174.90
46	16/02/2013	174.74	174.87
47	23/02/2013	174.69	174.80
48	02/03/2013	174.64	174.67
49	09/03/2013	174.59	174.57
50	16/03/2013	174.54	174.52
51	23/03/2013	174.54	174.37
52	30/03/2013	174.49	174.27
53	06/04/2013	174.34	174.17
54	13/04/2013	174.34	174.17
55	20/04/2013	174.29	174.17
56	27/04/2013	174.29	174.17
57	04/05/2013	174.25	174.10

Table G2: Manual daily groundwater level measurement data from twelve different wells along the floodplain

S/No	Daily	Well 1	Well 2	Well 3	Well 4	Well 5	Well 6	Well 7	Well 8	Well 9	Well 10	Well 11	Well 12
1	01/04/2012	174.12	172.80	172.41	172.25	172.27	172.24	172.30	171.73	172.01	171.97	170.95	172.47
2	02/04/2012	174.12	172.80	172.42	172.24	172.25	172.23	172.28	171.72	171.99	171.95	170.96	172.46
3	03/04/2012	174.16	172.80	172.43	172.25	172.27	172.24	172.29	171.71	172.00	171.96	170.94	172.43
4	04/04/2012	174.01	172.85	172.42	172.24	172.26	172.25	172.30	171.70	172.01	171.95	170.93	172.47
5	05/04/2012	174.12	172.80	172.43	172.19	172.27	172.23	172.27	171.69	172.00	171.97	170.95	172.46
6	06/04/2012	174.13	172.84	172.41	172.25	172.26	172.23	172.28	171.70	172.01	171.96	170.94	172.43
7	07/04/2012	174.16	172.81	172.39	172.26	172.27	172.22	172.29	171.71	172.02	171.95	170.96	172.47
8	08/04/2012	174.16	172.85	172.40	172.25	172.28	172.25	172.30	171.72	172.04	171.93	170.98	172.48
9	09/04/2012	174.10	172.90	172.41	172.44	172.24	172.24	172.29	171.66	172.03	171.94	170.97	172.48
10	10/04/2012	174.12	172.84	172.42	172.22	172.25	172.23	172.28	171.65	171.99	171.95	170.95	172.47
11	11/04/2012	174.13	172.82	172.40	172.20	172.23	172.22	172.27	171.71	172.01	171.93	170.96	172.44
12	12/04/2012	174.11	172.70	172.34	172.15	172.25	172.19	172.26	171.69	171.98	171.97	170.93	172.45
13	13/04/2012	174.13	172.90	172.34	172.17	172.20	172.20	172.25	171.68	171.97	171.95	170.92	172.46
14	14/04/2012	174.06	172.84	172.33	172.16	172.22	172.15	172.25	171.71	172.00	171.96	170.96	172.47
15	15/04/2012	174.13	172.83	172.34	172.20	172.28	172.21	172.23	171.70	172.02	171.96	170.95	172.48
16	16/04/2012	174.12	172.81	172.34	172.21	172.18	172.24	172.13	171.65	172.01	171.95	170.97	172.43
17	17/04/2012	174.15	172.80	172.32	172.22	172.29	172.23	172.24	171.71	172.03	171.93	170.95	172.47
18	18/04/2012	174.11	172.88	172.36	172.25	172.29	172.24	172.28	171.70	172.02	171.94	170.95	172.45
19	19/04/2012	174.10	172.90	172.37	172.21	172.28	172.25	172.30	171.71	172.03	171.95	170.96	172.43
20	20/04/2012	174.01	172.90	172.33	172.16	172.27	172.24	172.29	171.72	172.04	171.97	170.97	172.45
21	21/04/2012	174.06	172.92	172.32	172.15	172.29	172.26	172.31	171.74	172.03	171.98	170.97	172.43
22	22/04/2012	174.12	172.75	172.34	172.20	172.28	172.21	172.14	171.78	171.97	171.97	171.00	172.45
23	23/04/2012	174.11	172.86	172.35	172.22	172.25	172.23	172.26	171.77	172.00	171.99	170.97	172.47
24	24/04/2012	174.12	172.89	172.34	172.24	172.26	172.25	172.25	171.79	171.93	171.95	170.98	172.43
25	25/04/2012	174.14	172.84	172.36	172.25	172.28	172.24	172.28	171.78	171.96	171.98	170.99	172.48
26	26/04/2012	174.11	172.80	172.32	172.30	172.20	172.26	172.29	171.78	171.92	171.94	171.01	172.47
27	27/04/2012	174.00	172.88	172.33	172.31	172.24	172.27	172.30	171.80	171.86	171.92	171.01	172.46

S/No	Daily	Well 1	Well 2	Well 3	Well 4	Well 5	Well 6	Well 7	Well 8	Well 9	Well 10	Well 11	Well 12
28	28/04/2012	174.02	172.86	172.34	172.33	172.27	172.27	172.31	171.82	171.78	172.00	171.02	172.47
29	29/04/2012	174.11	172.89	172.32	172.35	172.23	172.28	172.32	171.81	171.82	171.95	170.97	172.49
30	30/04/2012	174.11	172.89	172.41	172.36	172.27	172.28	172.30	171.81	171.84	171.97	170.98	172.50
31	01/05/2012	174.01	172.90	172.32	172.36	172.28	172.29	172.33	171.83	171.82	171.95	171.02	172.51
32	02/05/2012	174.05	172.91	172.23	172.37	172.27	172.27	172.32	171.84	171.77	171.93	171.01	172.50
33	03/05/2012	174.06	172.90	172.28	172.39	172.29	172.29	172.32	171.85	171.81	171.92	171.03	172.51
34	04/05/2012	174.10	172.92	172.26	172.37	172.28	172.28	172.38	171.84	171.77	172.00	171.03	172.51
35	05/05/2012	174.02	172.94	172.22	172.23	172.27	172.27	172.42	171.84	171.74	172.01	171.03	172.51
36	06/05/2012	174.05	173.00	172.33	172.36	172.28	172.29	172.40	171.83	171.74	172.01	171.03	172.52
37	07/05/2012	174.08	172.95	172.32	172.24	172.28	172.29	172.38	171.84	171.73	172.03	171.04	172.53
38	08/05/2012	174.11	172.96	172.34	172.35	172.28	172.28	172.37	171.83	171.73	172.05	171.04	172.53
39	09/05/2012	174.13	172.94	172.32	172.33	172.28	172.29	172.35	171.83	171.73	172.05	171.04	172.56
40	10/05/2012	174.11	172.96	172.11	172.42	172.29	172.29	172.39	171.85	171.74	172.01	171.06	172.59
41	11/05/2012	174.15	173.00	172.29	172.44	172.29	172.30	172.38	171.86	171.77	171.99	171.07	172.58
42	12/05/2012	174.14	173.03	172.30	172.56	172.32	172.25	172.40	171.84	171.78	172.04	171.04	172.60
43	13/05/2012	174.20	173.03	172.33	172.63	172.33	172.27	172.37	171.83	171.78	172.05	171.02	172.60
44	14/05/2012	174.20	173.05	172.35	172.65	172.34	172.24	172.36	171.80	171.77	172.05	171.04	172.61
45	15/05/2012	174.40	173.15	172.32	172.37	172.29	172.28	172.43	171.76	171.81	171.99	171.08	172.61
46	16/05/2012	174.33	173.20	172.30	172.50	172.28	172.29	172.45	171.83	171.76	172.00	171.07	172.59
47	17/05/2012	174.23	173.15	172.28	172.60	172.26	172.27	172.44	171.84	171.74	171.97	171.06	172.58
48	18/05/2012	174.20	173.10	172.27	172.55	172.27	172.23	172.37	171.85	171.77	172.02	171.05	172.60
49	19/05/2012	174.13	173.10	172.24	172.56	172.27	172.30	172.38	171.85	171.79	172.03	171.03	172.57
50	20/05/2012	174.12	173.12	172.26	172.53	172.29	172.28	172.40	171.84	171.80	172.05	171.07	172.61
51	21/05/2012	174.10	173.13	172.23	172.55	172.30	172.26	172.45	171.82	171.81	171.96	171.09	172.59
52	22/05/2012	174.08	173.12	172.32	172.58	172.28	172.24	172.46	171.78	171.77	171.97	171.08	172.59
53	23/05/2012	174.05	173.14	172.33	172.56	172.27	172.25	172.46	171.76	171.80	172.01	171.07	172.60
54	24/05/2012	174.02	173.15	172.35	172.61	172.27	172.25	172.45	171.75	171.77	172.02	171.07	172.61
55	25/05/2012	174.00	173.20	172.35	172.62	172.26	172.27	172.46	171.78	171.78	172.02	171.08	172.60